Seismic Hazard and Risk Assessment Groningen Field update for Production Profile GTS - raming 2020

March 2020

By Jan van Elk, Anke Jannie Landman, Jeroen Uilenreef and Dirk Doornhof

Errata:

On 13th March NAM submitted the report “Seismic Hazard and Risk Assessment Groningen Field update for Production Profile GTS - raming 2020” to the Minister of Economic Affairs and Climate Policy. The report was shared by the Minister with SodM for an initial check. In particular, SodM checked whether the assessment report was complete and all tables, graphs and figures requested in the expectation letter (verwachtingenbrief) had been included. SodM identified a number of sections in the report that lacked clarity and requested a number of additional tables and graphs to be added.

As a result, the following amendments were made to the report:

- The tables with the annual probabilities for occurrence of earthquakes exceeding a set magnitude (Tab. 5.2a and 5.2b) were further refined.
- The tables with the annual probabilities for occurrence of earthquakes exceeding a set magnitude (Tab. 5.2a and 5.2b) provided these probabilities for gas-years. Similar tables for calendar years have been added in appendix H.
- Reconciliation of the number of buildings in the different safety groups relative to the norm between HRA2019 and HRA2020 has in the main text been presented in Sanky diagrams (Fig. 7.12, 7.13 and 7.14). The information contained in these figures is also presented in tables (for both operational strategies) in Appendix J.
- Text in chapter 7 on risk metrics has been edited to improve clarity. A reference to the report on the fragility and consequence model (v7 and v6) has been added.

The minor changes made in tables 5.2a and 5.2b (top bullet) were initially not implemented in the text of the Hazard and Risk Assessment and Operational Strategy documents in a consistent manner. In this version of the report the resulting inconsistences have been resolved.

Contents

Samenvatting

Deze Nederlandstalige samenvatting van dit rapport met de dreigings- en risicoinschatting is opgenomen in de Operationele Strategie. Deze is hier herhaald zodat dit rapport ook als een zelfstandig rapport gelezen kan worden.

In de Mijnbouwwet Artikel 52c is vastgelegd dat de NAM elk jaar op verzoek van de Minister van Economische Zaken en Klimaat (hierna: minister) één of meerdere operationele strategieën moet indienen bij de minister. Voor dit jaar heeft de minister door middel van een verwachtingenbrief (ref DGKE / 20018021, hierna: "de Verwachtingenbrief") de NAM verzocht om twee operationele strategieën uit te werken en in te dienen. Het verschil tussen deze twee strategieën is de manier waarop de Groningenveld productie over de verschillende clusters wordt verdeeld. De clusters zijn verspreid over het veld, en afhankelijk van welke clusters wanneer worden ingezet, wordt er meer of minder gas uit een bepaald deel van het Groningenveld geproduceerd. Dat is van belang omdat dit effect heeft op de seismiciteit.

Voor Operationele Strategie 1 worden de productievolumes verdeeld over de clusters Zuidoost, Zuidwest, Centraal-Oost en Bierum. Als basis voor de productie wordt cluster Bierum ingezet. Op momenten van hoge vraag worden achtereenvolgens de clusters Zuidoost, Zuidwest en tot slot Centraal-Oost ingezet. Als gevolg van de lagere capaciteitsbehoefte op het Groningenveld zal cluster Eemskanaal in tegenstelling tot voorgaande jaren niet meer noodzakelijk zijn om momenten van uitzonderlijk hoge piekvraag af te dekken. Voor Operationele Strategie 2 worden de productievolumes verdeeld over de clusters Zuidoost en Zuidwest en zal het clusters Centraal-Oost alleen gebruikt worden op momenten van hoge vraag. Cluster Bierum zal onder deze operationele strategie net als cluster Eemskanaal niet meer nodig zijn om de piekcapaciteitsvraag op het Groningenveld af te dekken. Onderstaande figuur geeft een overzicht van de clusters op het Groningenveld. Het cluster Loppersum is sinds februari 2018 definitief ingesloten en wordt niet meer ingezet in deze operationele strategieën.

Operationele Strategie 1

Clusters	Productielocatie volgorde
Bierum	BIR
Zuidoost	ZPD EKR SZW
Zuidwest	ZVN SPI TUS KPD SLO
Centraal-Oost	OWG SCB AMR (TJM) (SDB)
Eemskanaal	(EKL)

Operationele Strategie 2

Clusters	Productielocatie volgorde
Zuidoost	ZPD EKR SZW
Zuidwest	ZVN SPI TUS KPD SLO
Centraal-Oost	OWG SCB AMR TJM (SDB)
Bierum	(BIR)
Eemskanaal	(EKL)

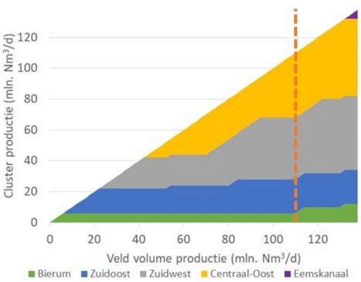

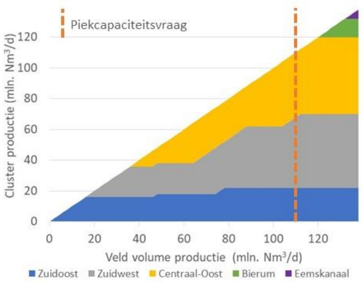

De minister zal besluiten op welke wijze het Groningenveld moet worden geopereerd in het gasjaar 2020-2021. Om te zorgen dat de minister een goed afgewogen besluit kan nemen, staat in dit document beschreven wat de consequenties van de twee operationele strategieën zijn. Welke consequenties de NAM precies inzichtelijk moet maken staat beschreven in de Mijnbouwwet, de Mijnbouwregeling en de Verwachtingenbrief. De belangrijkste conclusies uit de door de NAM gemaakte analyse van de twee operationele strategieën worden hieronder gegeven.

Volume: Onder beide operationele strategieën wordt relatief gezien het meeste volume onttrokken uit het zuidoosten van het Groningenveld. Voor een gemiddeld jaar wordt ongeveer de helft van het totale volume uit cluster Zuidoost geproduceerd. Onder Operationele Strategie 1 zal het cluster Bierum nog aanzienlijke productievolumes laten zien terwijl onder Operationele Strategie 2 er helemaal geen productie meer uit Bierum wordt verwacht. De volumes die onder Operationele Strategie 1 uit cluster Bierum worden geproduceerd zullen onder Strategie 2 over de clusters Zuidoost, Zuidwest en Centraal-Oost worden verdeeld. Beide strategieën laten voor het cluster Eemskanaal geen volume bijdrage meer zien.

De gevolgen van de productie uit het Groningenveld op bodembeweging zijn door middel van een dreigings- en risicoanalyse bepaald. Deze modelmatige berekeningen combineren de hele oorzaak-gevolg keten, beginnend met de gasproductie en eindigend met schade en risico. De modellen zijn gevoed met de meest recente stand van de wetenschap rond seismiciteit in het Groningenveld en nemen alle relevante onzekerheden op een wetenschappelijk verantwoorde wijze mee.

Dreiging of "hazard": Dreiging en risico zijn twee termen die in het dagelijkse spraakgebruik vaak door elkaar heen worden gebruikt, maar een andere betekenis hebben. De dreiging wordt door de NAM inzichtelijk gemaakt met de zogenaamde "hazard kaarten". Op deze kaarten is te zien welke maximale grondversnelling er op basis van modellering te verwachten is boven het Groningenveld. Het risico bestaat uit de kans dat de dreiging en het gevolg hiervan werkelijkheid wordt.

De hazard kaarten die gemaakt zijn laten zien dat Operationele Strategie 1 minder dreiging in het zuiden tot gevolg heeft in vergelijking met Operationele Strategie 2. De verschillen zijn echter klein. Een andere manier om de dreiging te duiden is door inzichtelijk te maken wat het verwachte aantal bevingen is en wat de mogelijke sterkte van de bevingen is die verwacht kunnen worden bij elk van de twee operationele strategieën. De volgende tabel laat de resultaten van deze analyse zien met daarin de jaarlijkse kans op bevingen boven een bepaalde magnitude. De verschillen zijn hier ook klein. Door de verminderde gaswinning neemt de dreiging de komende jaren verder af.

Gasjaar 2020-2021	**M > 3.6**	**M > 4.0**	**M > 4.5**	**M > 5.0**
Operationele Strategie 1	4.73%	1.29%	0.16%	0.02%
Operationele Strategie 2	4.88%	1.30%	0.17%	0.02%

Schade: Schade als gevolg van bodembeweging wordt gedefinieerd als de nadelige en zichtbare gevolgen die de bodembeweging heeft op gebouwen zonder dat de aanwezigheid in dit gebouw extra persoonlijk risico's met zich mee brengt. Om inzichtelijk te maken hoeveel schade wordt verwacht door de gasproductie uit het Groningenveld, is gemodelleerd hoeveel DS1, DS2 en DS3 schade er bij de uitvoering van de beide operationele strategieën is te verwachten. Het blijkt dat dit nagenoeg gelijk is voor de beide strategieën (verschillen < 1%). Gevolgen van bodembeweging voor gebouwen die wel persoonlijk risico met zich mee brengen worden gecategoriseerd als risico.

Risico: De bovengenoemde dreiging krijgt betekenis als deze gecombineerd wordt met de kwetsbaarheid van woningen wat uitgedrukt wordt in het risico. Een nieuwe woning die gebouwd is volgens de laatste bouwnormen zal bij een blootstelling aan eenzelfde dreiging een ander risico hebben dan een oude boerderij.

Er zijn verschillende manieren om risico te definiëren. De minister heeft aan de NAM gevraagd om het risico te berekenen waarbij er van uit wordt gegaan dat de mensen 100% van de tijd aanwezig zijn in hun huis[1]; het zogenoemde plaatsgebonden persoonlijk risico of "LPR".

De belangrijkste uitkomsten van de HRA 2020 ten opzichte van de HRA 2019 zijn:

De kans op aardbevingen en daaropvolgende schade is afgenomen als gevolg van de dalende gaswinning;

Er zijn geen gebouwen meer in deze modelmatige berekening die niet aan de Meijdamnorm voldoen.

Fluctuaties: De wijze waarop de productievolumes verdeeld worden over het Groningenveld heeft ook invloed op de grootte van de regionale productiefluctuaties. Bij een sterke voorkeursonttrekking uit bepaalde clusters, bijvoorbeeld uit cluster Zuidoost, zullen op momenten van hoge vraag overige clusters moeten worden opgeregeld. Aangezien deze clusters op andere momenten van lage vraag weinig of niets produceren leidt dit tot grotere en frequentere variaties in de desbetreffende productievolumes. Door de lagere productieniveaus op het Groningenveld en de gewijzigde inzet van UGS Norg zijn deze variaties frequenter en relatief groter dan in voorgaande jaren. Voor Operationele Strategie 1 worden hierbij meer overschrijdingen van de fluctuatie bandbreedtebeperking verwacht ten opzichte van Operationele Strategie 2. Dit is een gevolg van de inzet van cluster Bierum dat niet meer zal produceren onder Operationele Strategie 2 en hiermee ook geen fluctuaties kan veroorzaken.

Onderstaande tabel geeft op kwalitatieve wijze op een aantal hoofdcriteria een vergelijking tussen de twee uitgewerkte operationele strategieën.

	Operationele Strategie 1	**Operationele Strategie 2**
Schade (DS1, DS2, DS3)	+/-	+/-
Aantal gebouwen LPR > 10^{-5}	0	0
Aantal overschrijdingen fluctuatiebandbreedte minimaal	41 % (-)	32 % (+/-)
Aantal in te sluiten productielocaties	3	3
Operationele uitvoerbaarheid	+/-	+/-
Laagste energieverbruik / CO_2 emissie	+	-

[1] De definitie waarbij uitgegaan wordt van een meer realistische aanwezigheidstijd (OIA) is opgenomen in de HRA 2020 documentatie (Appendix A).

Executive Summary

In this executive summary the main conclusions from the hazard and risk assessment for production profile GTS-raming 2020 are listed:

Introduction

- The Hazard and Risk Assessment for production profile GTS raming-2020 is the tenth since 2012 and last assessment prepared by NAM on instruction of the Minister of Economic Affairs and Climate Policy.
- TNO has developed an own seismic risk assessment tool (modellentrein) and will from 2021 onwards prepare the annual Hazard and Risk Assessment.

HRA-Model improvements since HRA GTS-raming 2019

- Since the previous Hazard and Risk Assessment was submitted in March 2019, the HRA-tool has been further developed with focus on the dynamic reservoir model, the seismological model and ground motion prediction.
- Enhancement of the exposure database was modest due to limited additional data availability to NAM. Focus was on farm houses and barns. Additional modelling was done for different farm houses. Fragility and consequence models were developed for the house and barn section of these buildings separately.

Reservoir and Pressure Modelling

- Two Operational Strategies (OS) have been proposed. Main difference is the role of the Bierum production cluster, located north of Delfzijl. In OS2 the Bierum cluster is effectively closed-in.
- The difference in pressure between the two OS shows for OS1 a slightly lower pressure north of Delfzijl and higher pressure near Hoogezand. After 2022 the pressure differences are very small.

Subsidence

- The compaction/subsidence model was calibrated using results from 16 levelling campaigns spanning from 1964 to 2018.
- Subsidence forecasts were made for 2025 and 2030 based on OS1.
- In 2030 some 40 cm of surface subsidence (since start of production) is expected in the deepest point of the subsidence bowl, with a P95 uncertainty range estimated at about 15%.

Seismic Event Rate

- The number of earthquakes with magnitude larger than M=1.5 declines. By gas-year 2025/2026 the expected number of earthquakes has declined to three per year with an uncertainty of between 0 and 9 per year.
- Comparison with a case where the field is closed in on 1st October 2020 (start gas-year 2020/2021) shows that the seismicity in later years is primarily caused by equilibration of the current pressure differences in the field. The low production levels in the remaining years have limited impact on the seismic event rate, regardless of which the Operating Strategy is employed.
- The effect of a warm or cold gas-year 2020/2021 and the operational strategy on the seismic event rate is much smaller than the uncertainty.
- Probability of an earthquake with magnitude larger than the Huizinge earthquake (M=3.6) has reduced to 4.73% for gas-year 2020/2021. In the HRA GTS-raming 2019, submitted March 2019, this probability was estimated at 9.3% for the same gas-year.

Seismic Hazard Assessment

- The hazard shows a declining trend. Although the hazard declines in the whole Groningen area, the decline is fastest in the south-east of the field. As a result, the remaining hazard after 2024 is concentrated to north-west of the village of Loppersum.

Seismic Risk Assessment

- As a consequence of the reduced gas production, seismic risk is also declining.
- The assessment shows that all buildings in the Groningen field area meet the life safety risk of LPR< 10^{-5}/year (Meijdam-norm).
- For a limited number of buildings there is a 10% probability that the building does not meet the life safety risk of LPR< 10^{-5}/year. These are buildings in the P90-group.
    - For Operating Strategy 2, 82 buildings have been evaluated to belong to the P90 group in gas-year 2020/2021. After four years no buildings are left in the P90 group.
    - For Operating Strategy 1, 162 buildings have been evaluated to belong to the P90 group in gas-year 2020/2021. After three years no buildings are left in the P90 group.
- The buildings in the P90 group all belong to the same typology: barns of farmhouses. This means there are no dwellings in the P90 group. There is a debate whether barns should be assigned occupancy and therefore whether they need to comply with the life safety norm. In this seismic risk assessment cautiously the position is taken that, based on the available knowledge, occupancy should be assigned to barns as well, and that these should therefore comply with the safety norm.
- All barns in the P90 group are located around the village of Loppersum, west of Appingedam.

Structural Upgrading Plan

- The HRA is a probabilistic assessment of the number of buildings that do not meet the Meijdam-norm. This does not immediately translate into an estimate of the structural upgrading scope. The involvement of the Minister of EZK over the past years with the structural upgrading has been formally implemented in the Mining law in December 2019.

Building Damage

- With declining seismic hazard, damage caused to primary (occupied) buildings will decline as well. The assessment for gas-year 2020/2021 shows the chance that more than 1,000 buildings will receive DS1 damage is below 10%. This result is for both operational strategies.

1 Introduction

1.1 Previous Hazard and Risk Assessment Reports

Since 2012 NAM has prepared hazard and risk assessments (HRA) for different production scenarios. Table 1.1 provides an overview of these HRA reports. The first calibrated and fully probabilistic HRA was submitted to SodM and the Ministry of Economic Affairs in November 2015 (Ref. 7). This was followed by Winningsplan 2016 (Ref. 8 to Ref. 14). The Mining Law requires that Winningsplannen are approved by the Minister of Economic Affairs and Climate Policy (Minister). The approval was granted in the Instemmingsbesluit Winningsplan Groningenveld, issued on the 30th of September 2016 (Ref. 27).

In response to the specific instruction in the Instemmingsbesluit, NAM prepared the report "Assessment of Hazard Building Damage and Risk for Induced Seismicity in Groningen – November 2017" (Ref. 15), which was submitted to the Minister of Economic Affairs and Climate Policy and to SodM on 1st November 2017. The Wijzigingsbesluit of 24th May 2017 (Ref. 22) limited the production in an average temperature year to 21.6 Bcm/year. Due to the fact that in the Wijzigingsbesluit special circumstances were identified that could require an increase in the production from the field, the Hazard and Risk Assessment of November 2017 (Ref. 15) was prudently based on an average annual gas production level of 24 Bcm/year, which also covered these eventualities.

To assess the effect of different production profiles on seismic risk, a complementary set of production profiles covering a wide range of production levels was presented in the addendum to the November 2017 Hazard and Risk Assessment (Ref. 15), The report was issued March 2018. The set of production profiles analysed included the production aspirations as outlined in the Coalition Agreement (Regeerakkoord of 10/10/2017) (Fig. 1.1) and several production profiles included in reports by GTS, which were based on different utilisation of the existing nitrogen blending plant and the option of the construction of an additional nitrogen blending plant.

The letter sent by the Minister of Economic Affairs and Climate Policy to Parliament (Kamerbrief) on 29th March 2018 (Ref. 23) announced the ambition of the cabinet to reduce the production from the Groningen field as soon as possible, leading to cessation of production around 2030. It contained annual production volumes for the period 2018-2031, which was labelled "Basispad Kabinet" (Fig. 1.1). Different production profiles were presented for cold, average and warm temperature years.

An Expectation Letter (verwachtingenbrief) was sent to NAM on 2nd May 2018 (Ref. 25) by the Minister of Economic Affairs and Climate Policy. It detailed the expectations for further NAM technical studies in preparation of a new Winningsplan decision (due by 15th November 2018 latest). NAM was requested to perform a Hazard and Risk Assessment for the "Basispad Kabinet" production profile, to indicate the impact of the strong reduction of production on safety risk and the scope of the structural upgrading needed to comply with the Meijdam-norm (Ref. 28 to Ref. 30). With the Expectation Letter the Minister of Economic Affairs and Climate Policy provided the demand and production profile for Groningen quality gas (Fig. 1.3) to NAM, which served as the basis for the Hazard and Risk Assessment for the production profile "Basispad Kabinet" (Ref. 17).

On 6th June 2018, the Minister of Economic Affairs and Climate Policy sent a letter to Parliament on the progress of the measures to end production from the Groningen field (Ref. 24). In this letter, a number of additional measures are referenced that were not yet incorporated in the "Basispad Kabinet" as presented on 29th March 2018. The risk impact of a profile based on the maturation of these additional measures to reduce Groningen gas demand was not assessed, but this would directionally have reduced the risk further as compared to the Hazard and Risk Assessment based on the production profile “Basispad Kabinet” (Ref. 17 and Ref. 18).

On 12th February 2019, NAM received the Expectation Letter with the updated production profile prepared by GTS: “GTS-raming 2019” (Ref. 19). Actual production realised in gas-year 2018-2019 was 18.8 Bcm compared to 19.4 Bcm in the production profile of “Basispad Kabinet”. This 0.6 Bcm lower production has been included in this Hazard and Risk Assessment. In figure 1.1 the annual production rates for the five production profiles; (1) Coalition Agreement, (2) Basispad Kabinet March 2018 Letter, (3) Basispad Kabinet Expectation May 2018 Letter, (4) Expectation Letter February 2019 and (5) Expectation Letter February 2020 are compared. The comparison is shown in this figure for cold, average and warm year gas demand.

1.2 Expectation Letter (verwachtingenbrief) 2020

In accordance with article 52c of the Mining Law, NAM proposes two operational strategies based on the premises for these strategies contained in the expectation letter (Ref. 31). In this report the subsidence, seismic event rate, hazard, risk and building damage consequences of these operational strategies will be presented. The expectation letter has been attached to this report as Appendix A.

On 21st February, the Minister of Economic Affairs and Climate Policy sent a letter to parliament on the production profile GTS-raming 2020 (Ref. 32). In his letter the Minister also announced a reduction in the gas production for the current gas-year (2019/2020) from 11.8 Bcm/year to 10 Bcm/year. In this report this reduction in production for the current gas-year has not been taken into account. The production for gas-year 2019/2020 used in this report is based on the actual production from 1st October 2019 until 1st January 2020 and the prognosed production of GTS-raming 2019 for the remainder of this gas-year.

Apart from the premises for the operational strategies, the expectation letter also describes the maps, graphs and tables to be included in the current report. In order to present a clear analysis additional maps, graphs and tables have been included in this report when required for clarity. The hazard, building damage and risk assessment has been requested to be presented based on gas-years. Gas-years are the 12-month period starting at 1st October. The gas-year 2020/2021 is the period from 1st October 2020 up to and including 30st September 2021. Gas-years are used to avoid the high gas demand winter period to be split over two reporting periods. To avoid confusion and very long sections of tables, the main document will present the analysis in gas-years, while the tables for calendar years are presented in Appendix E. The assessment of subsidence included in this report uses calendar years to be in line with other subsidence reports.

1.3 TNO Hazard and Risk Assessment

TNO has built their own modelling tool for assessment of hazard and risk in Groningen (de TNO Modellentrein). Using this modelling tool, TNO will take over the preparation of the hazard and risk assessment from NAM, starting with the HRA 2021.

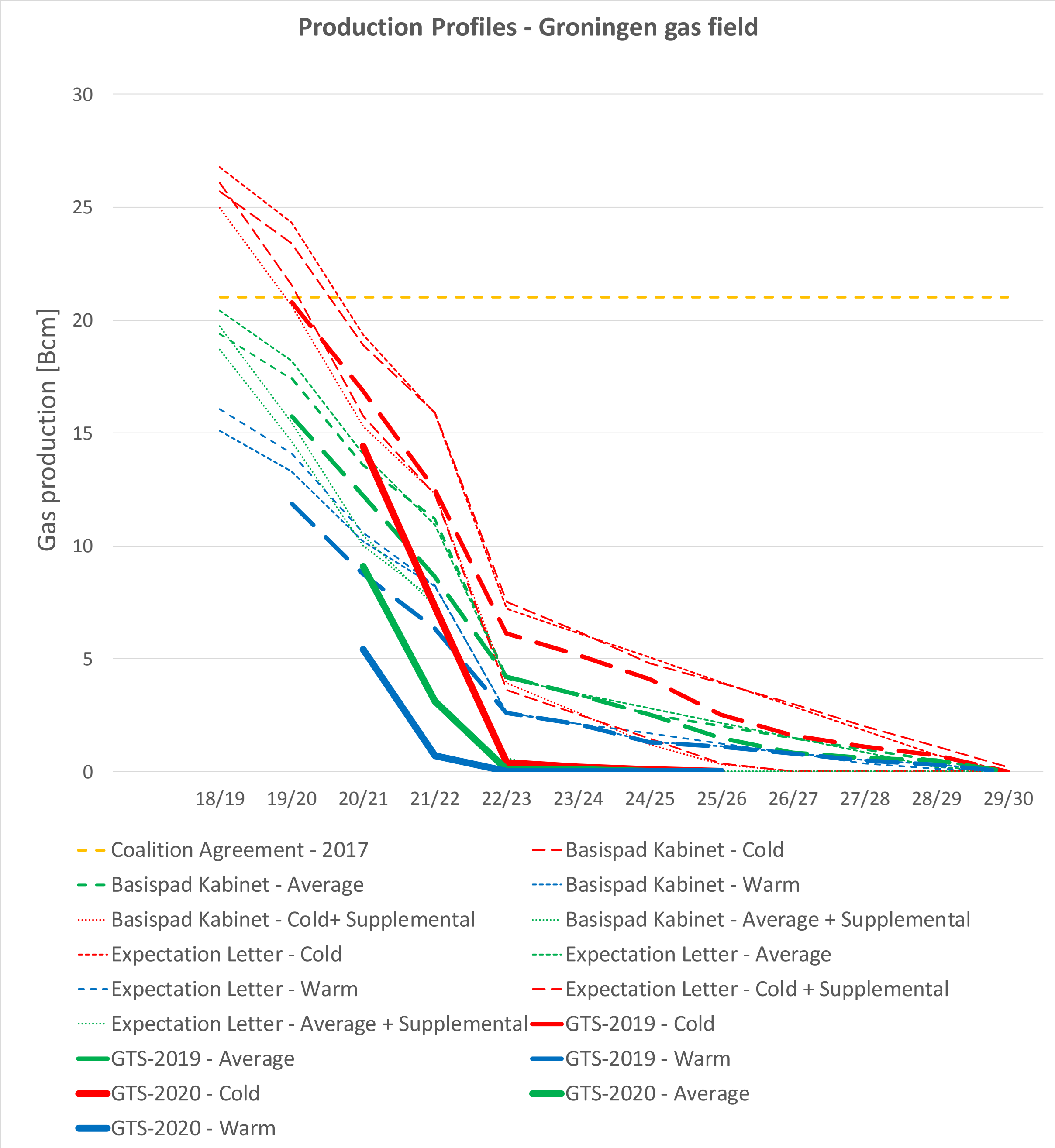

Figure 1.1 *Comparison of the production profiles:*

1. *Coalition Agreement (Regeerakkoord) (10/10/2017),*
2. *"Basispad Kabinet" from Kamerbrief (29/3/2018) in blue (Ref. 23),*
3. *"Basispad Kabinet" from the Expectation Letter (verwachtingenbrief) (2/5/2018) in red (Ref. 25)*
4. *Production profile GTS-raming 2019 in green (Ref. 19) and*
5. *Production profile GTS-raming 2020 in green (Ref. 31) and*

Production profiles for a warm gas-year are shown in blue. Those for average and cold temperature gas-year in green and red respectively.

Hazard and Risk Assessment	Ref	Submitted to EZK & SodM	Production profile	Ref	Comment
Winningsplan 2013 and Technical Addendum to Winningsplan 2013	1, 2	November 2013	In the Technical Addendum to the Winningsplan hazard for several production scenarios were assessed.		Probabilistic hazard assessment combined with a scenario based risk assessment.
Supplementary Information to Technical Addendum to Winningsplan 2013	2	December 2013	Letter to NAM: Mijnbouwwet instemmingsbesluit winningsplan Groningenveld; aanvullingsverzoek, 20-12-2013.	20	Two production scenarios were requested: (1) 'market demand' scenario and (2) 'market demand' scenario with closing in five clusters around Loppersum (LRM, OVS, PAU, POS and ZND).
Hazard Assessment Eemskanaal Region and Addendum to: Hazard Assessment for the Eemskanaal area of the Groningen field	3, 4	May 2014	Requested by SodM.		Additional hazard assessment for production from the cluster located close to the city of Groningen.
Dreigings- en risicoanalyse voor geïnduceerde seismiciteit Groningen - Onderzoek 1 dreigingsanalyse and Onderzoek 2 risicoanalyse	5, 6	May 2015	Requested by Scientific Advisory Committee and SodM.		Uncalibrated probabilistic hazard and risk assessment.
Hazard and Risk Assessment for Induced Seismicity in Groningen	7	November 2015	Requested by Scientific Advisory Committee and SodM.		First calibrated probabilistic hazard and risk assessment. This was also the first HRA where LPR results could be compared to the Meijdam-norm (Ref. 28 to Ref. 30).
Winningsplan 2016, Technical Addendum to Winningsplan Groningen 2016	8 – 14	April 2016	Verwachtingen brief	21	
HRA 2017 - Addendum to WP 2016	15	November 2017	Wijzigingsbesluit of 24th May 2017.	22	Production scenario with 24 Bcm/year plateau was prudently used.
HRA for a selection of production profiles	16	March 2018	Assessments were prepared for a wide range of production profiles.		Report was prepared to inform decision on the future production from the Groningen gas field.
HRA Basispad Kabinet	17, 18	August 2018	Letter to parliament 29 March 2018 en 6 Juni 2018 Verwachtingenbrief of 2nd May 2018	23, 24 and 25	
HRA GTS-raming 2019	19	March 2019	Verwachtingenbrief of 12th February 2019	25	
HRA GTS-raming 2020		March 2020	Verwachtingenbrief of 1st February 2020		This report.

Table 1.1 Overview of the Hazard and Risk Assessments prepared by NAM.

2 HRA-Model improvements since HRA GTS-raming 2019

2.1 Introduction

A number of improvements and changes have been implemented in this Hazard and Risk Assessment since the HRA-model was used in the preparation of the HRA for GTS-raming 2019, which was submitted in March 2019. The regulator, SodM, has reviewed these updates of the Hazard and Risk Model (Ref. 33). Their preliminary assessment of the update of the HRA model has been included in this report in Appendix A (Relevant correspondence).

The main improvements and changes implemented in the HRA-tool since the previous HRA (HRA GTS-raming 2019) issued at 1st March 2019 are:

- The dynamic model of the Groningen gas field has been updated (Ref. 34 and Ref. 35). The prime objective of the update was to improve the predictive ability for the long-term pressure development in the reservoir following cessation of production from the gas field. Focus of the update was therefore on the lateral aquifers connected to the field and low-saturation gas in the aquifer below the gas-water-contact (Ref. 36 and Ref. 37). The impact of these changes will be limited in the central area of the field and therefore not significantly impact seismicity. The impact is expected to be primarily on subsidence in the outer regions of the field and areas outside the field boundary.
- A number of improvements were incorporated in the development of the ground motion model (Ref. 38 and Ref. 39). The most important change is the switch from using the G4 geophones recordings acquired at 200 m depth to the G0-station accelerograms acquired at surface. This change was made possible by the expansion of the database of ground motion recordings.
- Previous investigations into the seismological model focussed on the temporal and spatial distribution of induced earthquakes in the Groningen area (Ref. 40 and Ref. 41). The update of the seismological model addresses the occurrence of larger magnitude earthquakes relative to smaller magnitude earthquakes (Ref. 42 and Ref. 43).
- In 2018, the exposure database was updated with the results from 189,126 documents retrieved from municipality archives during 353 visits. With this extended update implemented in HRA GTS-raming 2019, nearly all information publicly available and to which NAM has access had been incorporated in the exposure database. The update since the previous HRA (GTS-raming 2019) is therefore relatively modest and focussing primarily on farm houses.
- The fragility of several building typologies was further investigated.

These improvements of the HRA-model have been documented extensively (Ref. 34 to Ref. 43) in reports available at the research report page (onderzoeksrapporten pagina) of www.nam.nl. Improvements that are of direct interest for the hazard and risk assessment and the reconciliation of risk at building level will be further described in this section.

2.2 Exposure Database

To be able to assess the risk for the buildings and community in Groningen resulting from induced earthquakes, knowledge of the occupied building stock in the region of the Groningen field is required. To assign a unique building typology to each individual building in the earthquake area, a program of building inspections was initiated in 2013. The program consists of the collection of building data from existing databases and data sources. This is supplemented by building data gathered from public sources (e.g. observation from public areas (street level) and Google Street View) and engineering drawings of buildings, publicly available at the municipality office. The taxonomy of building typologies of GEM (Global Earthquake Model) is used to assign typologies, based on the structural system of each building.

For practical reasons the Groningen field area has been divided in two areas[2]. The core area consists of the seismically most active area and contains some 20,000 buildings. Additionally, data on the use of the buildings and occupancy are collected. The data on the buildings in the Groningen field area are stored in the exposure database (EDB). An earlier version of this database (V2) was used for the Hazard and Risk Assessment of November 2015 (Ref. 7) and Hazard and Risk Assessment for Winningsplan 2016 (Ref. 8 to Ref. 14). Early 2017 and mid-2018, updated versions of the database were issued (Ref. 45, Ref. 46 and Ref. 47). The exposure database of mid-2018 (Ref. 47) was used in the Hazard and Risk Assessment for the production profile "Basispad Kabinet", which was issued June 2018.

The exposure database combines many data sources (BAG, AHN, Deltares top soil, etc.) together with inference rules to assign typologies to individual buildings. The datasets used for the EDB are categorised as follows:

- **Source data** Datasets which have been received and maintained by external sources such as government departments.
- **Project data** Datasets which have been produced within the project such as inspection datasets and desktop studies. This includes project information produced by ARUP and external consultants.
- **Processed data** Datasets which ARUP has created utilising source datasets, assumptions and analysis to provide information that is not available from external sources.

For many buildings this leads to a non-unique typology description. In the core area, almost every building has a unique typology assigned, but away from this area, the typology of many buildings is based on inference rules, reflecting the experience of local engineers with knowledge of the development of local building methods. These inference rules are also updated in light of the on-going building data gathered. The Hazard and Risk (HRA) model applies the assessed earthquake hazard to the buildings and the population in the exposure database to assess the earthquake risk. The inference rules will in most cases not be able to establish the building typology uniquely and will assign a number of typologies to the building, each with a probability. On a regional level this provides a reliable assessment of the number of buildings where the safety-norm is exceeded and a risk-based ranking of all building in the Groningen field area.

2.2.1 Recent activities to improve the expose database

The development of EDB V7 included the update of several datasets. The source datasets used in EDB V7 are described in Table 2.1. Most of these datasets are inputs into algorithms which generate process datasets that provide the classification parameters required for the assignment of the appropriate Structural System(s) to each building in the database.

[2] These areas have been introduced by the NCG based on a hazard map of KNMI. The 0.2 g contour of the 2015 KNMI hazard map was chosen as the boundary between these areas.

Dataset	**Data source**	**Date**	**Notes**
Apartment Dataset	Arup	2017	Included as part of the drawing data.
Opening Percentage and Storey Count	Ticinum Aerospace (TA)	2019	Data as delivered on September 2019. Updated from V6.
Drawing Data	Arup	2019	Included information collected up to December 2019 from other inspection activities.
Data Collection	Arup	2019	Included information collected up to December 2019. Incorporates the information collected as part of the forgotten building lists.
Extended Visual Screening (EVS)	Arup	2015	No update. Included as per V5.
Rapid Visual Screening (RVS)	Arup	2015	No update. Included as per V5.
Desktop Visual Inspections (Streetview)	Arup	2019	Included information collected as part of the ‘WBH’ visual inspections and sample checking exercises.
Desktop Visual Inspections (Streetview)	JBG	2019	No update. Included as per V5.
Strengthened buildings	NCG	-	No update provided since 28 January 2019 by CVW. Any progress in structural upgrading is not considered in this report.
BAG (Buildings, Addresses and Occupancy)	Basisregistratie Adressen en Gebouwen (BAG)	2019	Data as per August 2019. Updated from V6.
Lidar data (height map)	Actueel Hoogtebestand Nederland (AHN)	2009	No update. Included as per V5.
Architectural and building descriptions	Dataland	2018	Data as per 26th September 2018. Included as per V6.
Educational buildings (for building use and population analysis)	Dienst Uitvoering Onderwijs (DUO), Basisregister Instellingen	2019	Data as per January 2019. Included as per V6.
Hospitals (for building use and population analysis)	Rijksinstituut voor Volksgezondheid en Milieu, Nationale Atlas Volksgezondheid	2019	Data as per January 2019. Included as per V6.
Inhabitant and Employee population (for population analysis)	NCG	2018	Data as per April 2018 (provided by NAM December 2018). Included as per V6.
Footfall data (for population analysis)	Tony Taig	2015	No updates. Included as per V5.
CBS Buurten, Wijken and Gementee data (for community and population analysis)	CBS	2018	No update. Included as per V6.

Table 2.1 Source datasets in EDB V7.

The process datasets used in EDB V7 are described in Table 2.2. All the datasets below are calculated by Arup.

Dataset	Notes	Data input
Adjacency calculation	Algorithm has been updated and improved. Includes also latest BAG data.	BAG
Building Use analysis	Updated with latest BAG data.	BAG
Exposed Footprint Length	Updated with latest BAG data.	BAG
Usable Area	Updated with latest BAG data.	BAG
Footprint Area	Updated with latest BAG data.	BAG
Storey count proxy	Updated with latest BAG data.	BAG
Geometric parameters	Updated additional buildings identified in latest BAG data.	BAG, AHN

Table 2.2 Main processed datasets in EDB V7.

Aside from data updates and new parameters, the EDB V7 also features several methodology updates in comparison to the ones described in EDB V6. Since the list of buildings above the norm in previous HRA was dominated by farmhouses the main focus has been to improve the identification of different types of farmhouses.

An overview of the methodology updates is found in Table 2.3.

Structural Layout	Updates around the WB / WBH identification including revised Dataland flag and visual inspections.
Farmhouse subtypes	Identification of WBH (farmhouse) subtypes of 'Aggregate' and 'Continuous'.
Inspection data for structural system	Additional project data incorporated including inspections around V6's 'Forgotten buildings' and any additional inspections undertaken by Arup.
Blockpart uniformity	Revised adjacency algorithm to better identify uniform blockparts. Results have been used to review assignment of structural layout and irregularity
Irregularity	Opening percentage cut off has been adjusted to 85%. Updates also include removal of TA data and revised building year inferences.

Table 2.3 Overview of methodology updates in EDB V7.

The sub-typologies have been defined making use of the analysis results generated within the fragility function modelling developments for several farmhouses. Two farmhouse subtypes have been identified. This includes:

- Subtype A – characterised by a connection (either direct or via a narrow 'neck') between the house and barn but without the continuity of the roof ridge.
- Subtype C - characterised by a continuous roof structure from the house to the barn.

The defining characteristic for the sub-typologies is therefore based on the geometric relationship within the farmhouse between the house and the barn geometry parts.

2.3 Fragility and Consequence Models for building typologies

In 2019 the effort to update and refine fragility and consequence models has focussed on buildings with relatively high risk. Figure 2.1 below illustrates that farmhouses, masonry terraced houses and masonry apartment buildings received most attention.

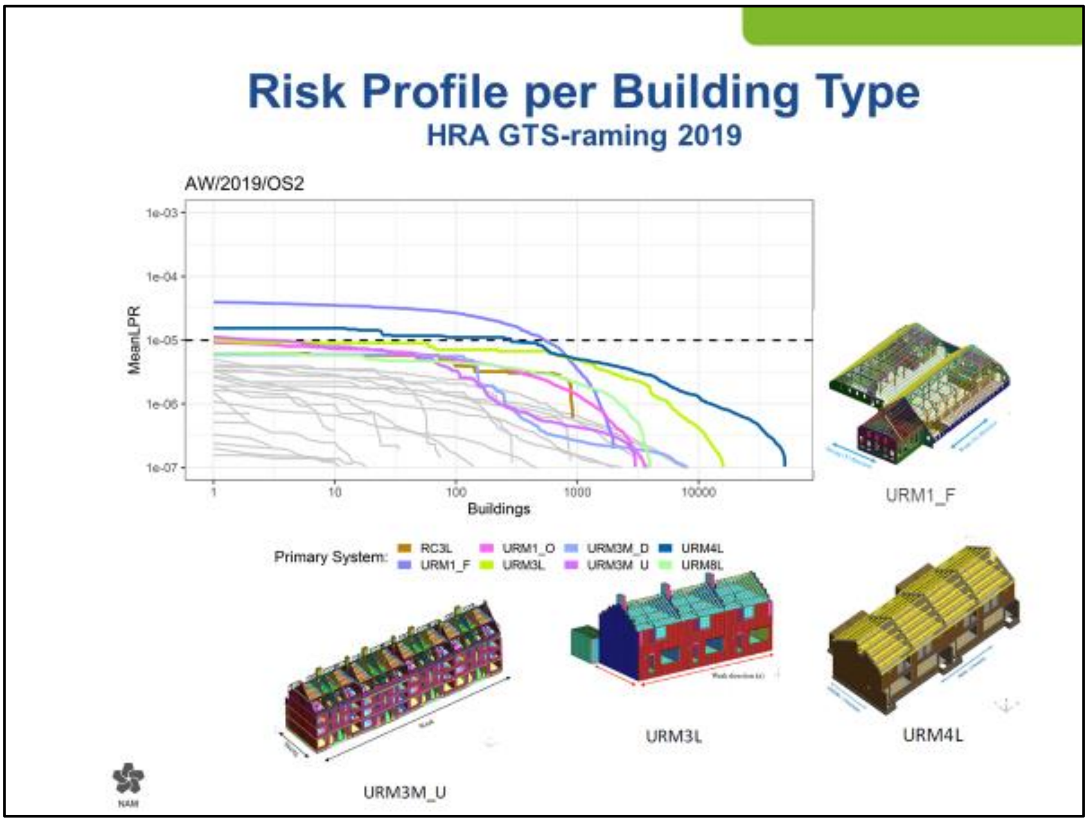

Figure 2.1: Risk profile per building type as per GTS-raming 2019, Operational Strategy 2 and average temperature demand.

2.4 Farmhouses (URM1F_HA, URM1F_HC and URM1F_B)

Typical farmhouses in Groningen consist of a relatively small residential part and a barn with large span. It has become clear that seismic behaviour of the house differs from the barn leading to significantly different risk profiles for the people inside the house and the barn.

While the 4 farmhouse index buildings were modelled entirely to include interaction between the 2 parts, fragility and consequence models were developed separately:

- URM1F_HA and URM1F_HC representing the house part depending on the subtype A or C.
- URM1F_B representing the Barn part.

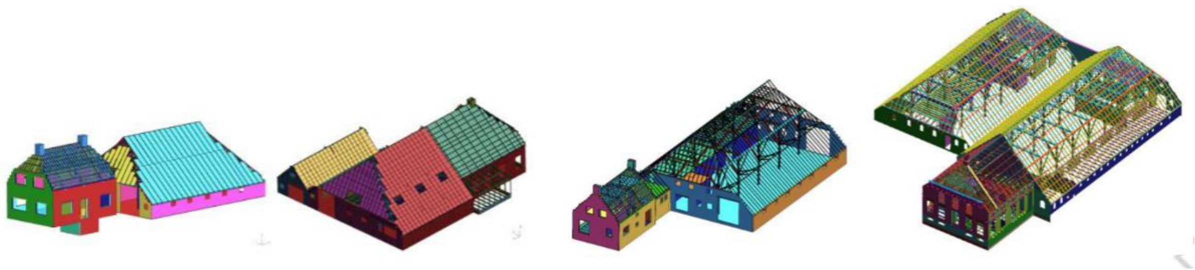

Figure 2.2: These 4 index buildings form the basis of Farmhouse fragility and consequence models

This will also facilitate addressing TNO’s suggestion to re-evaluate farmhouse building risk profiles based on inspection visits. In Advies vaststellingsbesluit Groningen gasveld 2019/2020 of 7 May 2019 (Ref. 54) TNO advised the Minister that in the event a barn has storage function, there is no occupancy, and there is no need to include them the risk assessment. In the meantime, NAM have cautiously assumed that all these barns do have occupancy.

2.5 Terraced masonry houses (URM3L and URM4L)

Another update relates to typology URM3L and URM4L. These represent the terraced masonry houses with cavity walls and concrete floors that are widespread across the Groningen region. The difference between the types relates to the percentage of ground floor openings in the façade walls, with URM4L having the larger openings and being the more vulnerable type.

For both types additional index buildings have been modelled and SDOF model results were calibrated to MDOF results (assurance panel recommendation). URM3L is now based on 4, and URM4L on 2 index buildings.

2.6 Masonry apartment buildings (URM3M_B and URM3M_U)

Following shake table test results late 2018 and early 2019, the LS-Dyna constitutive model was recalibrated to more accurately predict the behaviour of heavy loaded walls. Both index buildings representing URM3M_B and URM3M_U have been reanalysed, and the fragility functions updated.

For a more detailed description of V7 Fragility and Consequence models please refer to Ref. 55

3 Reservoir and Pressure Modelling

Modelling the pressure in the Groningen gas reservoir forms the starting point for both the seismic hazard and risk assessment as well as the subsidence forecast. The future pressure distribution in the reservoir depends on the amount of gas produced and on how this production is regionally distributed.

3.1 Production: Demand profiles GTS-raming 2020

The Ministry of Economic Affairs and Climate Policy provided demand profiles for Groningen gas with the Expectation Letter (Verwachtingenbrief, Ref. 31) sent to NAM on the 31st of January 2020. The demand for Groningen-quality gas has been determined by GTS. For gas-year 2020/2021 30 daily demand profiles are provided based on temperature profiles of the last 30 gas-years. Three reference years were chosen, for which longer term daily and monthly demand profiles have been supplied. These reference years correspond to the temperature profiles of gas-years 1996 (cold year), 2012 (average year), and 2007 (warm year). For the reservoir pressure modelling monthly production profiles are used.

The GTS demand profiles assume 100% utilisation of the GTS nitrogen plants Ommen, Wieringermeer and Zuidbroek (once available in 2022) to produce pseudo-G gas. Further processing of the datasets has been done by GasTerra to account for the contributions of UGS Norg and PGI Alkmaar, resulting in net Groningen production profiles.

As requested in the Expectation Letter (Verwachtingenbrief, Ref. 31), the HRA is performed for three temperature scenarios for gas year 2020/2021 (cold, average, warm), with subsequent gas years based on average temperature. These three production profiles are given in Figure 3-1.

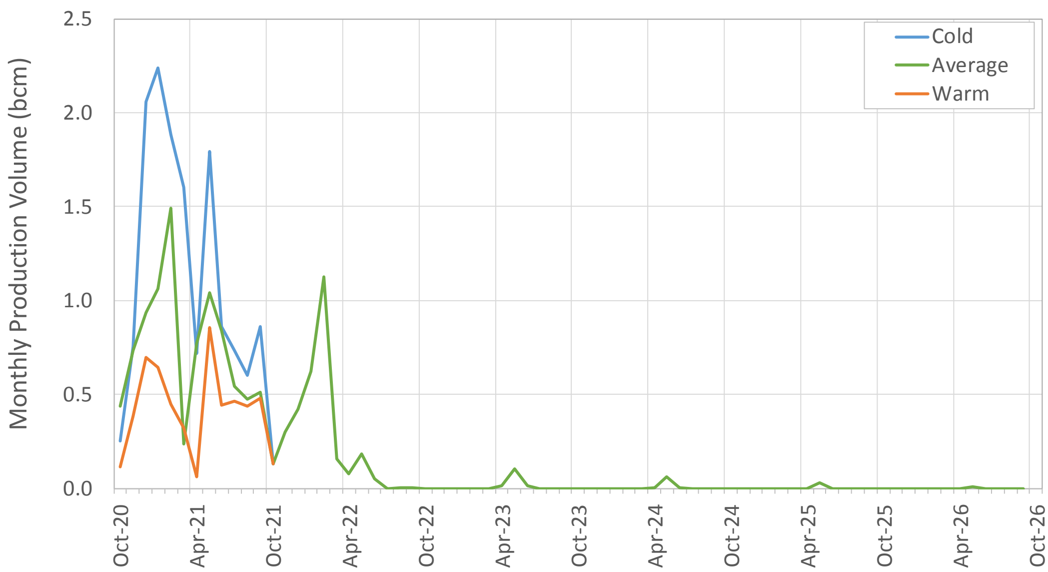

Figure 3-1: Groningen field monthly gas production according to GTS-raming 2020. The warm and cold scenarios are applied to gas-year 2020/2021 only.

3.2 Spatial distribution of production (Operational Strategy)

3.2.1 Production regions

In Article 1.3a.1 of the Mining Regulations ("Mijnbouwregeling"), the Groningen production regions ("clusters") are defined as follows:

a) Bierum: production location Bierum
b) Eemskanaal: production location Eemskanaal
c) East-Central ("Centraal-Oost"): production locations Amsweer, Schaapbulten, Oudeweg, Siddeburen, and Tjuchem
d) South-East ("Zuidoost"): production locations De Eeker, Scheemderzwaag, and Zuiderpolder
e) South-West ("Zuidwest"): production locations Kooipolder, Slochteren including Froombosch, Spitsbergen, Tusschenklappen including Sappemeer, and Zuiderveen
f) Loppersum: production locations De Paauwen, Leermens, Overschild, 't Zandt, and Ten Post

Use of the Loppersum cluster stopped in February 2018 following the instruction from the Minister of Economic Affairs and Climate Policy.

3.2.2 Operational Strategies

In the 2018 Production Optimisation study (Ref. 56) NAM investigated whether the seismic hazard and risk in Groningen could be influenced by the way the production volume was distributed over the various production locations and for which distribution the seismic risks would be minimized as much as possible. In a letter to the Ministry of Economic Affairs on 16/10/2018, SodM advised the Minister to use NAM's 2018 optimisation study to steer the production distribution in the field (Ref. 57). Production distribution as calculated for the optimisation metric "population weighted Peak Ground Velocity" was judged to minimize the seismic risks over the entire Groningen gas field in a socially responsible manner. This distribution resembles "Operational Strategy 1" in NAM's 2018 "Bouwstenen document", the document which outlines options for the Operational Strategy of gas-year 2018/2019 (Ref. 58). Operational Strategy 1 was adopted as the operational strategy of choice in the 14/11/2018 Ministerial Instemmingsbesluit (Ref. 59) and has been applied in the field since. In the Vaststellingbesluit for gas-year 2019/2020 (Ref. 60) the Minister instructed NAM again to adopt Operational Strategy 1.

For this 2020 HRA update, the Ministry of Economic Affairs and Climate Policy requested NAM to propose two Operational Strategies. The first is Operational Strategy 1 as currently in use. In the second Operational Strategy the same order of cluster priorities is to be followed with the exception of the Bierum cluster. Rather than utilising Bierum at a constant rate like in Operational Strategy 1 (OS1), in Operational Strategy 2 (OS2) Bierum will only be utilised when demand requires this, similar to (but prioritised before) the Eemskanaal cluster.

- **Operational Strategy 1 (OS1)**
  Gas is produced preferentially from the South-East. If more production is required, production locations in the South-West and Central-East regions are added. Cluster Bierum is kept at a constant rate whereas cluster Eemskanaal is only utilised to provide additional capacity when required.
- **Operational Strategy 2 (OS2)**
  Gas is produced preferentially from the South-East. If more production is required production locations in the South-West and Central-East regions are added. The clusters Bierum and Eemskanaal are only utilised in periods of high demand if their capacity is required.

3.2.3 Start-up sequence

To implement the Operational Strategies in the Integrated Production System Model, the production regions are further divided into control groups (Figure 3-2). In the model forecast, the production wells within these control groups are opened in order of their control group priority until the required production level is reached.

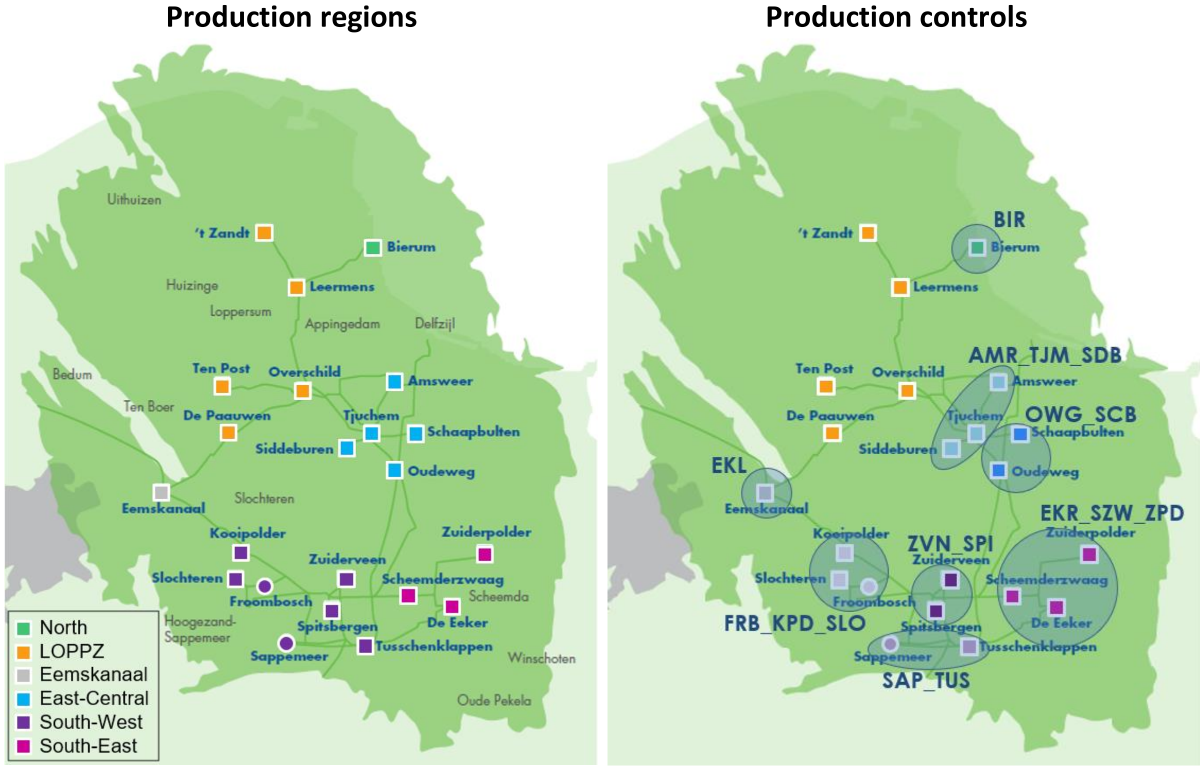

Figure 3-2: Production regions and control groups as used in the start-up sequence

The start-up sequence for the two Operational Strategies is given in Table 3-1.

Control Group	OS1	Control Group	OS2
BIR	Constant rate		
EKR/SZW/ZPD	1	EKR/SZW/ZPD	1
SPI/ZVN	2	SPI/ZVN	2
SAP/TUS	3	SAP/TUS	3
SCB/OWG	4	SCB/OWG	4
FRB/KPD/SLO	5	FRB/KPD/SLO	5
AMR/SDB/TJM	6	AMR/SDB/TJM	6
EKL	7	BIR	7
		EKL	8

Table 3-1: Production start-up list for OS1 and OS2. Starting from the top, groups of production locations are sequentially opened-up by the surface network model until the total required production is achieved.

In OS1, a constant rate is set for the Bierum cluster. This rate is 6 mln Nm^3/d until 1-4-2021 in line with the current operational strategy. Since gas demand decreases over time, the fixed rate for Bierum is also stepped down: to 4 mln Nm^3/d on 1-4-2021 and 2 mln Nm^3/d on 1-10-2021 (start of next gas year). It is assumed Bierum is closed in from 1-4-2022 onwards. In months where gas demand is lower than the Bierum rate (which happens only in the warm temperature scenario) the Bierum rate is scaled down to match the total demand which is then provided by Bierum alone.

3.2.4 Load Factor

The load factor represents the ratio of cluster production to cluster capacity. A maximum value for the load factor can be set as a constraint in the surface network model. This is needed to correctly reflect the distribution of production volume over the clusters. The model uses monthly volumes and time-steps, in which daily fluctuations are averaged out. The maximum load factors have been decreased compared to the values used in the HRA 2019 analysis, to bring the model results better in line with operational reality. The maximum load factor for gas year 2020/2021 ranges between 50% and 65% and is set to 40% for subsequent gas years.

3.3 Modelling setup

An Integrated Production System Model is used for forecasting. In this set-up, the dynamic reservoir model in MoReS is coupled to the surface network model in Genrem. Dynamic reservoir model V6 is used (Ref. 35). The V6 model includes several additional features compared to model V5 (used in the 2019 HRA):

- Gas-in-aquifer (Slochteren formation)
- Carboniferous formation (both gas and water bearing)
- Depletion in the Lauwerszee aquifer resulting from the fields Roden, Vries, Pasop and Faan

The inclusion of gas-in-aquifer improves the subsidence match and GWC rise in the North-West compared to model V5. The overall model match to measured pressures (SPG data) in V6 is slightly improved from V5, with an RMSE of around 2 bar with all pressure data up to 1-1-2020 included.

The history-match period was run in (stand-alone) MoReS until the end of calendar year 2019. Genrem-MoReS forecasting starts from 1-1-2020 onwards, where the Latest Estimate (LE) is used to constrain production up to 1-10-2020. This LE is in accordance with the graaddagen formula of the Vaststellingsbesluit for gas-year 2019/2020. The various pressure forecast scenarios therefore have a common starting point at the start of gas-year 2020/2021.

3.4 Forecast Scenarios

As requested in the Expectation Letter ("verwachtingenbrief", Ref. 31), seismic hazard and risk calculations are performed for 6 scenarios: 3 temperature scenarios 2 operational strategies. The distribution of production volume over the regions and the forecasted pressure distributions are discussed below. For each temperature scenario results for Operational Strategy 1 and 2 are compared.

3.4.1 Average temperature

Figure 3-1 shows the required monthly production volume for each temperature scenario. The average scenario is based on a temperature profile like in gas-year 2012. Figure 3-3 compares the distribution of production volume over the regions for the two Operational Strategies. Figure 3-4 shows these distributions for each of the next 6 gas-years. The key difference is that in OS2, cluster Bierum does not produce since it is low in the start-up sequence (Table 3-1) and it is not required in order to satisfy the demand. As Ref. 56 shows, there is sufficient excess capacity.

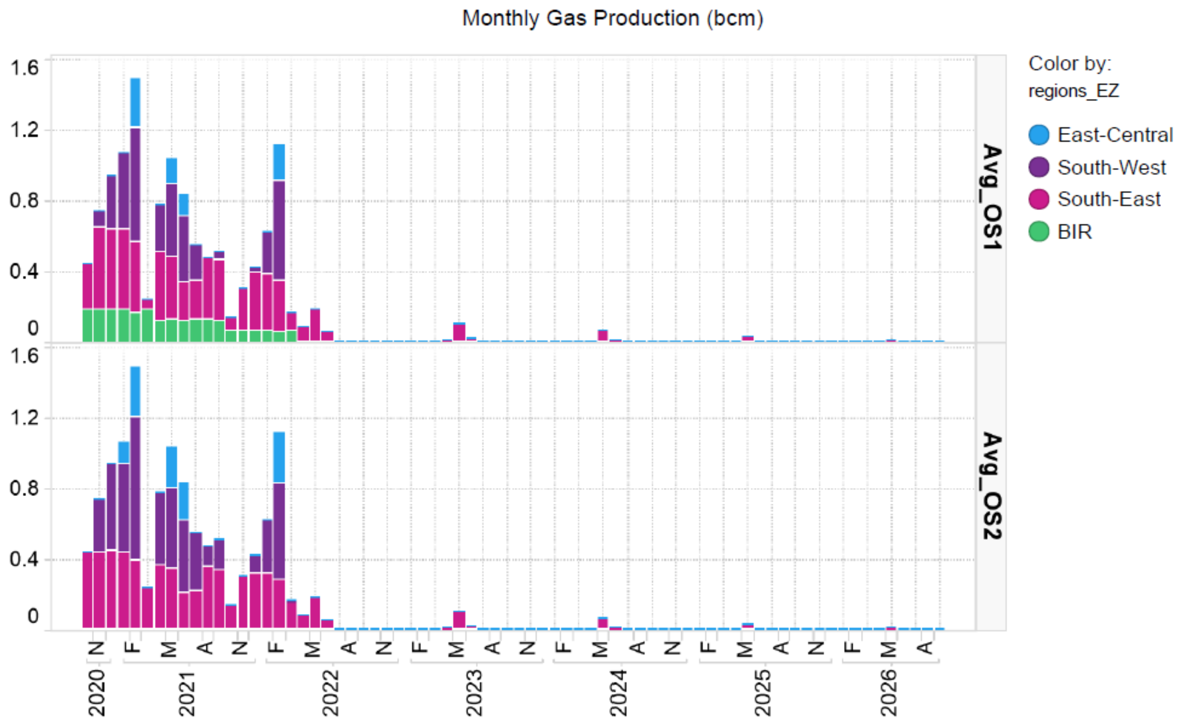

Figure 3-3: Monthly production volume per region for the next 6 gas-years for OS1 (top) and OS2 (bottom) in the average temperature scenario. Note the Bierum production cluster (BIR) is indicated in green.

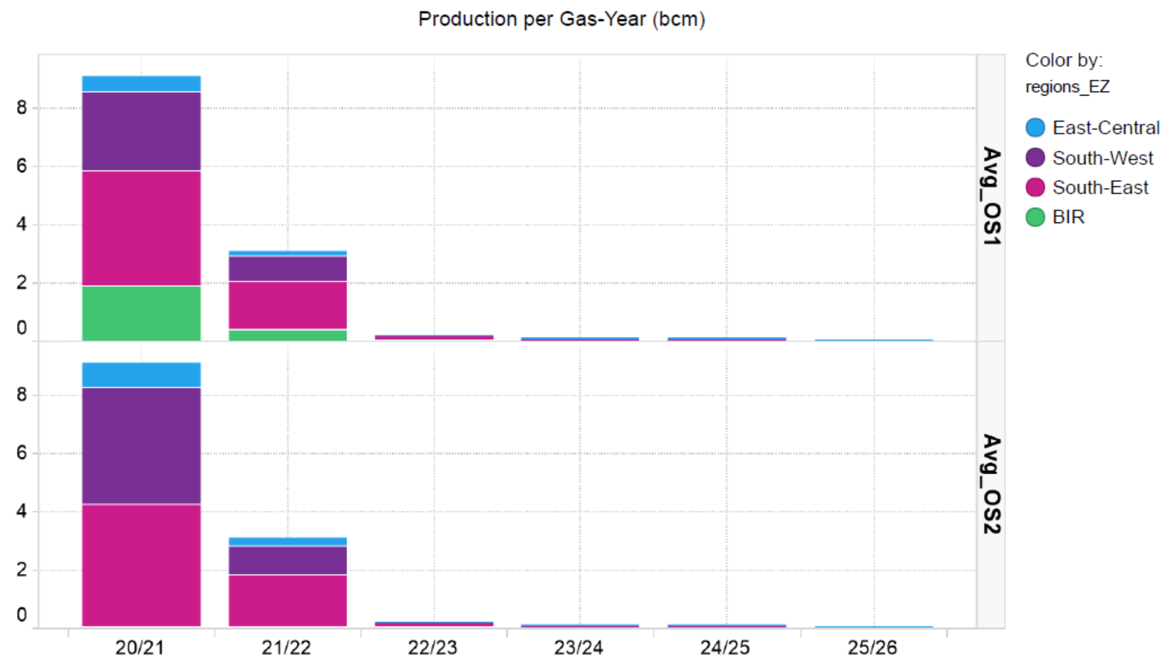

Figure 3-4: Regional distribution of production volume per gas-year for OS1 (top) and OS2 (bottom) in the average temperature scenario. Note the Bierum production cluster (BIR) is indicated in green.

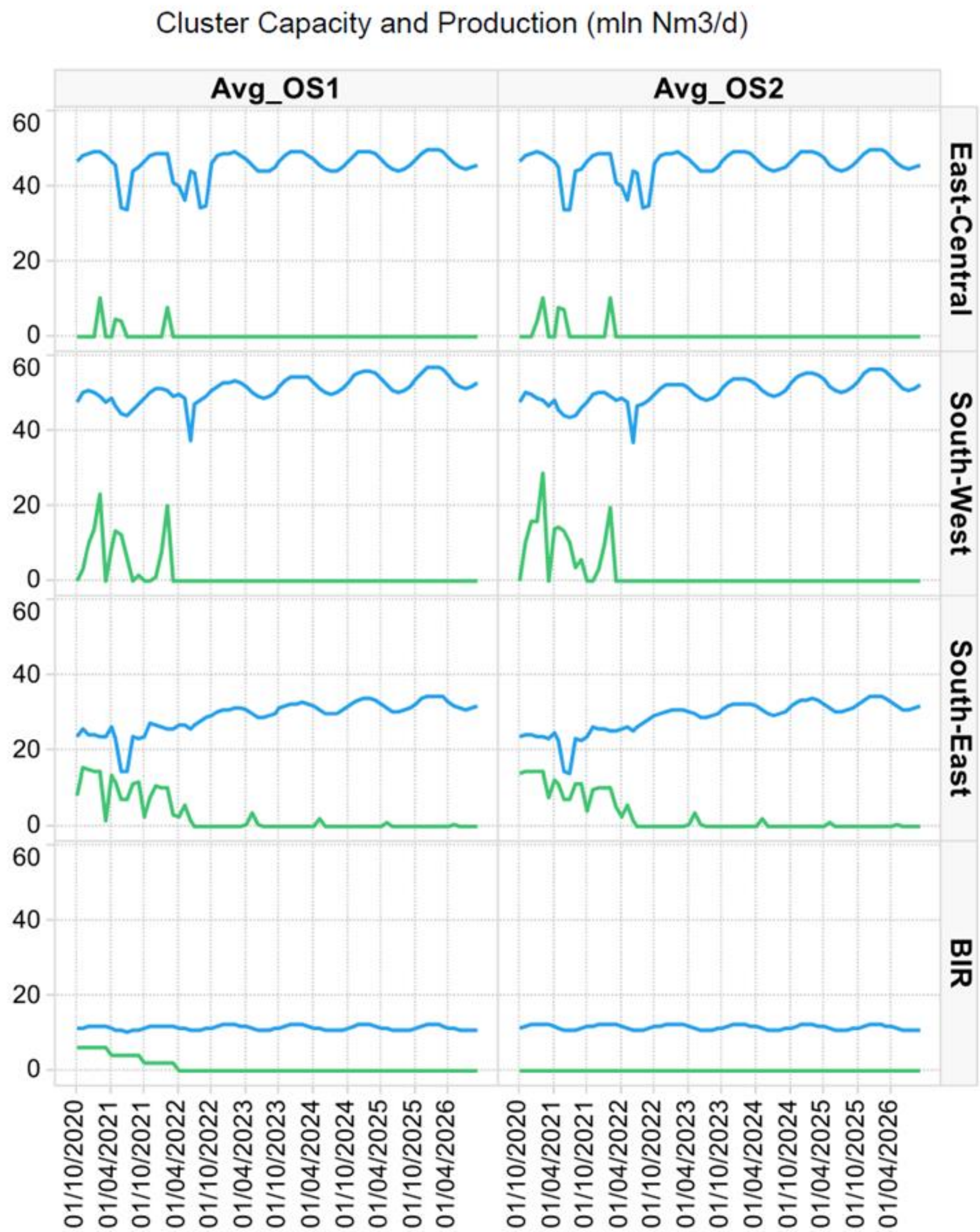

Figure 3-5: Cluster capacity (blue) and production rate (green) for OS1 (left) and OS2 (right) in the average temperature scenario

Figure 3-6 shows the modelled reservoir pressure distribution on 1-10-2020, which is the start of gas-year 2020/2021. This distribution is the common starting point for the 6 forecast scenarios. Figure 3-7 plots the difference in pressure between OS2 and OS1 at the end of an average gas-year 2020/2021. The maximum absolute local pressure differences between the Operational Strategies are around 2.5 bar. Figure 3-8 to Figure 3-12 show similar pressure maps and pressure difference maps for each gas-year up to 1-10-2030. Appendix F contains additional maps up to 1-10-2051. The same colour scales are used for the pressure and pressure difference maps throughout this document.

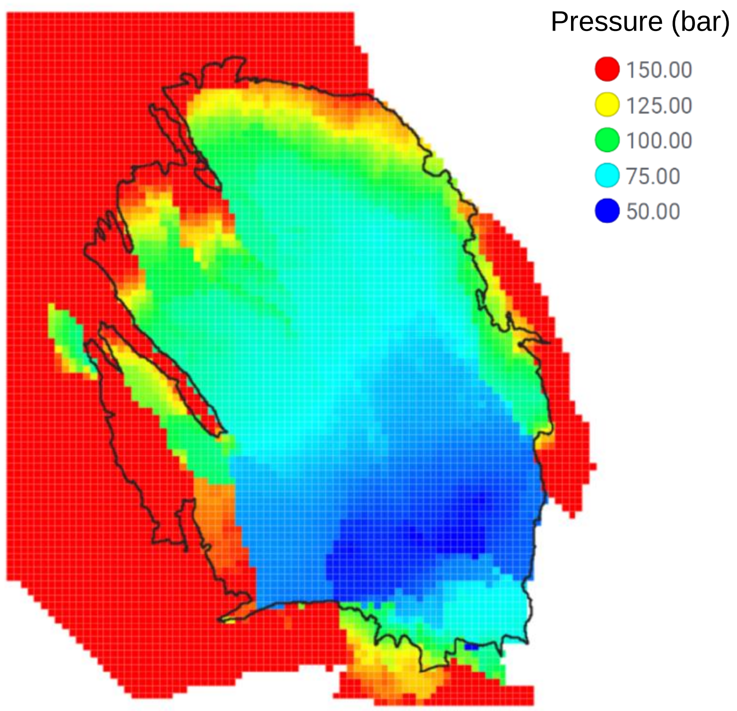

Figure 3-6 Modelled reservoir pressure at the start of gas-year 2020/2021

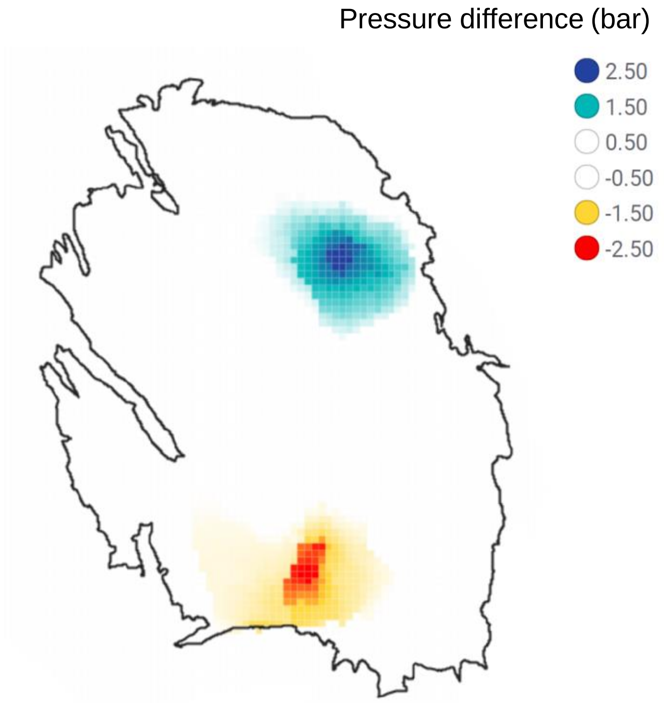

Figure 3-7 Pressure difference between the two Operational Strategies (pressure OS2 – pressure OS1) at the end of an average gas-year 2020/2021

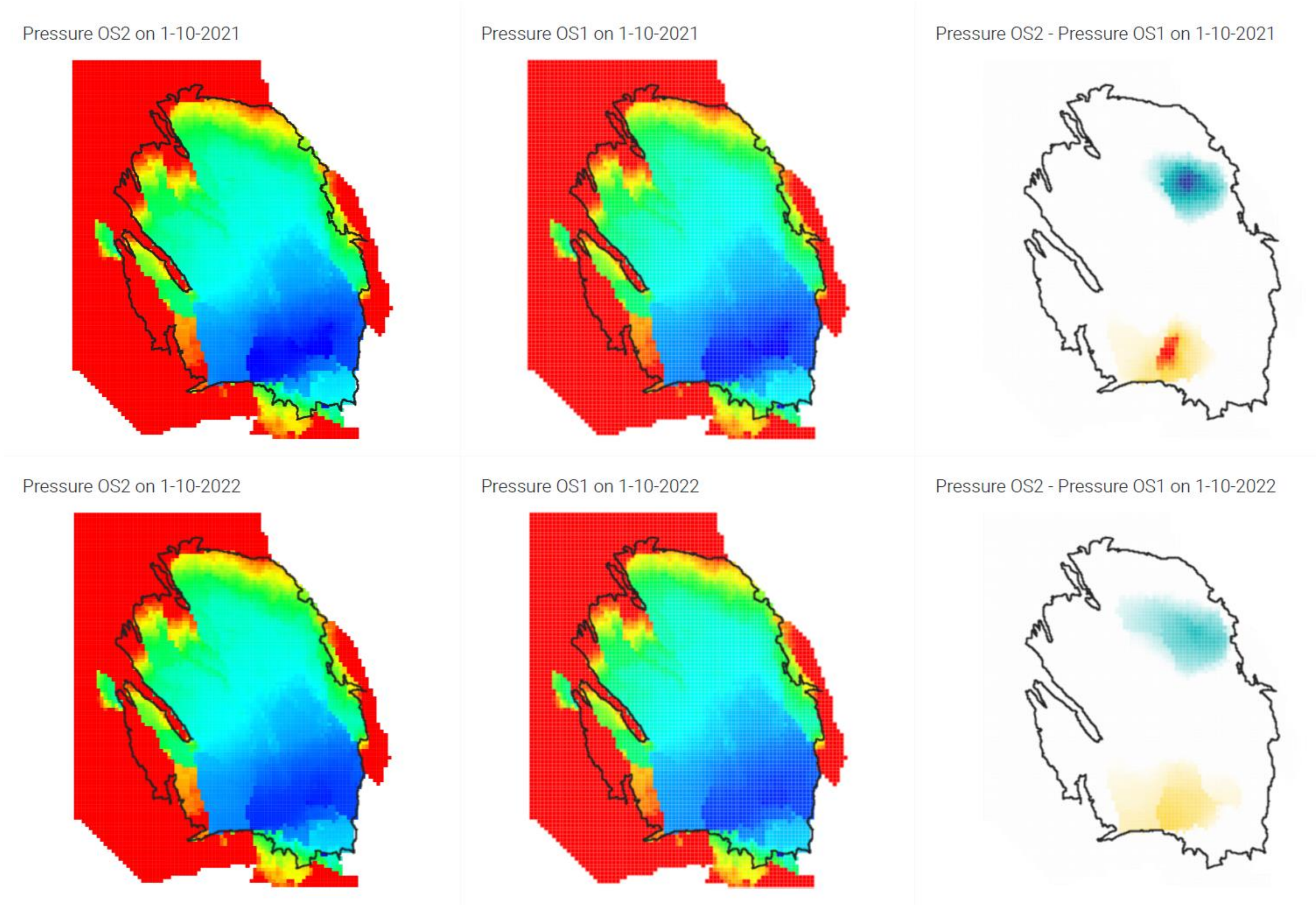

Figure 3-8 *Pressure and pressure difference maps for average temperature scenario: start (top) and end (bottom) of gas year 2021/2022. See for colour scales Figure 3-6 and Figure 3-7.*

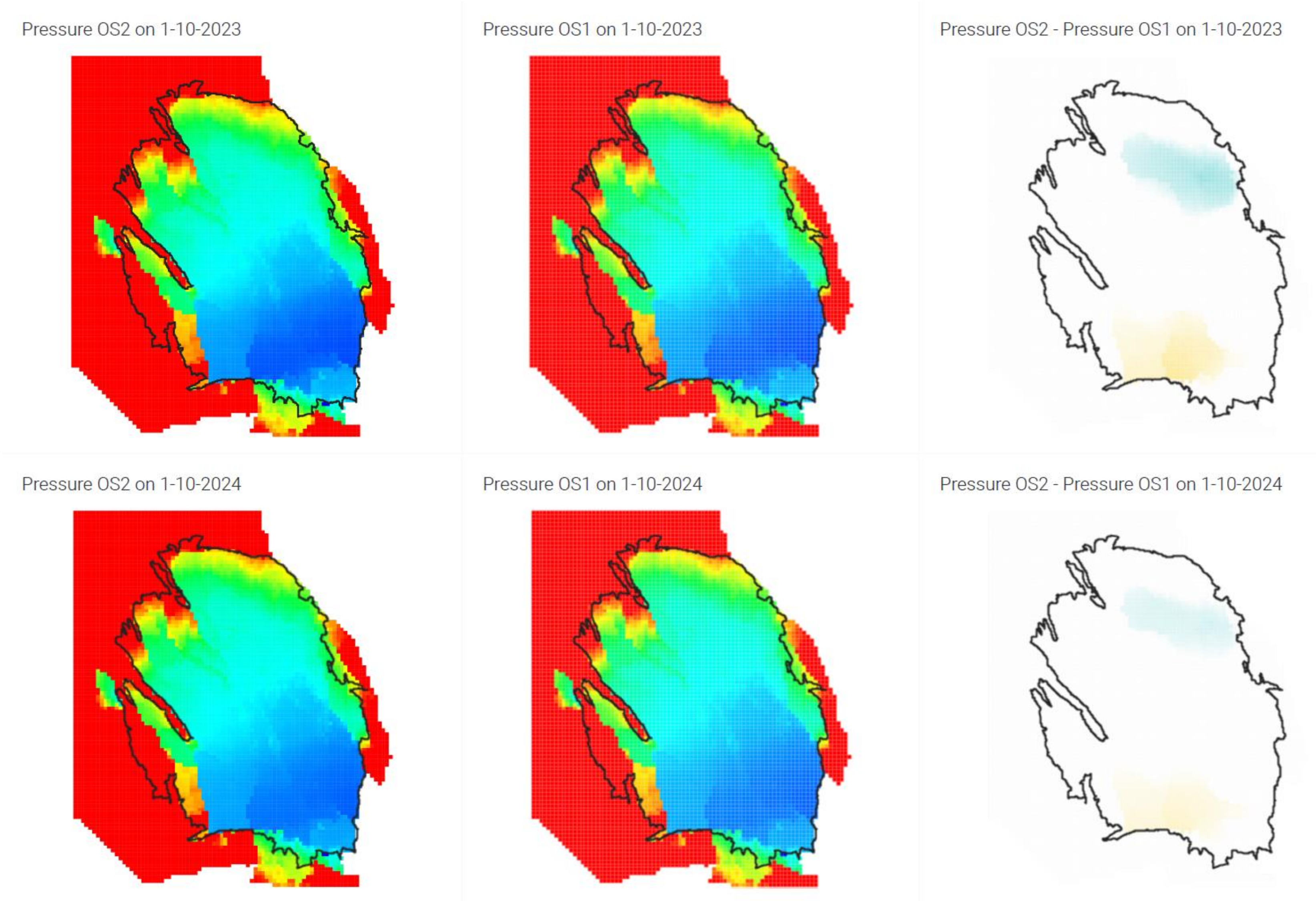

Figure 3-9 Pressure and pressure difference maps for average temperature scenario: start (top) and end (bottom) of gas year 2023/2024. See for colour scales Figure 3-6 and Figure 3-7.

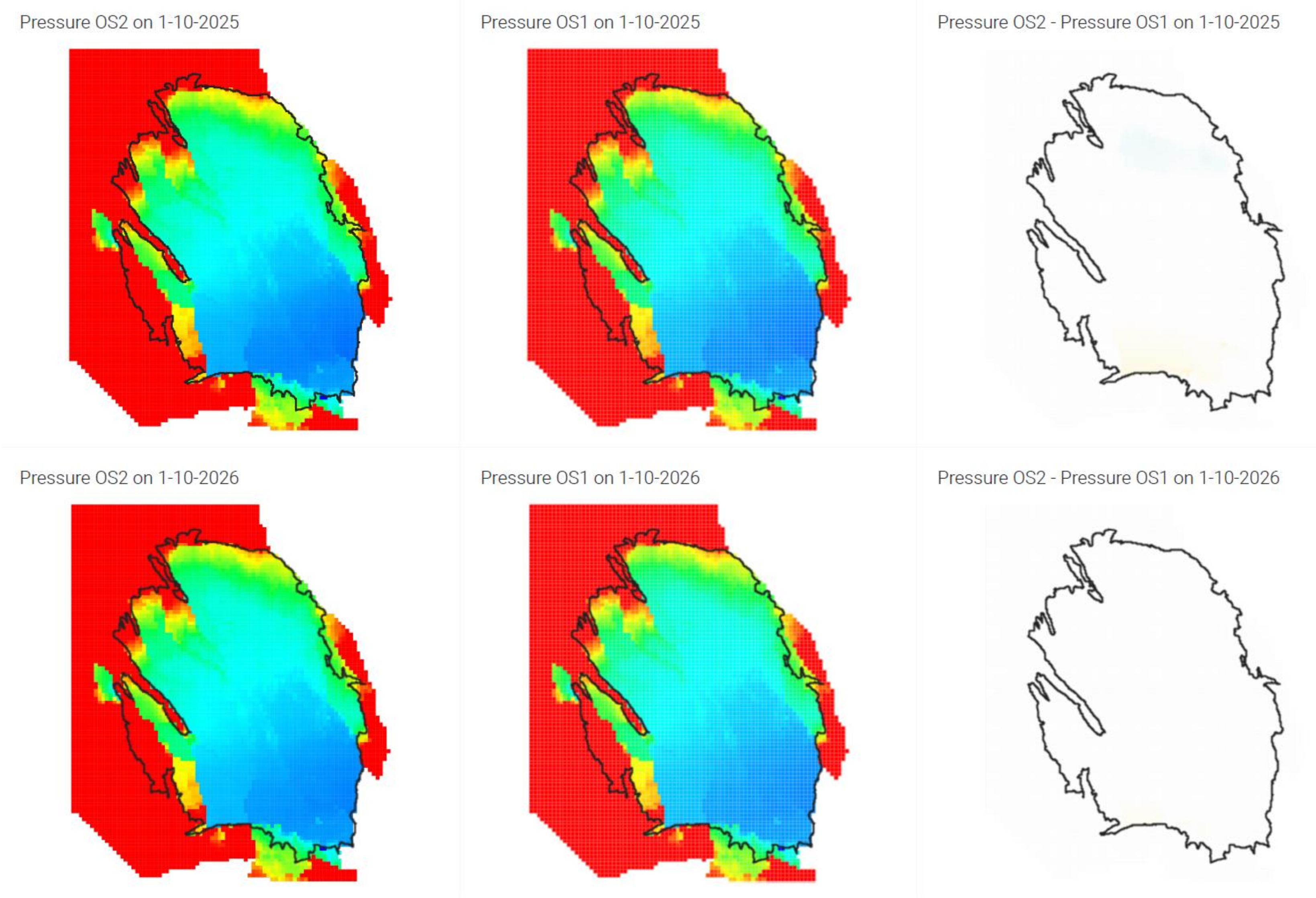

Figure 3-10: Pressure and pressure difference maps for average temperature scenario: start (top) and end (bottom) of gas year 2025/2026. See for colour scales Figure 3-6 and Figure 3-7.

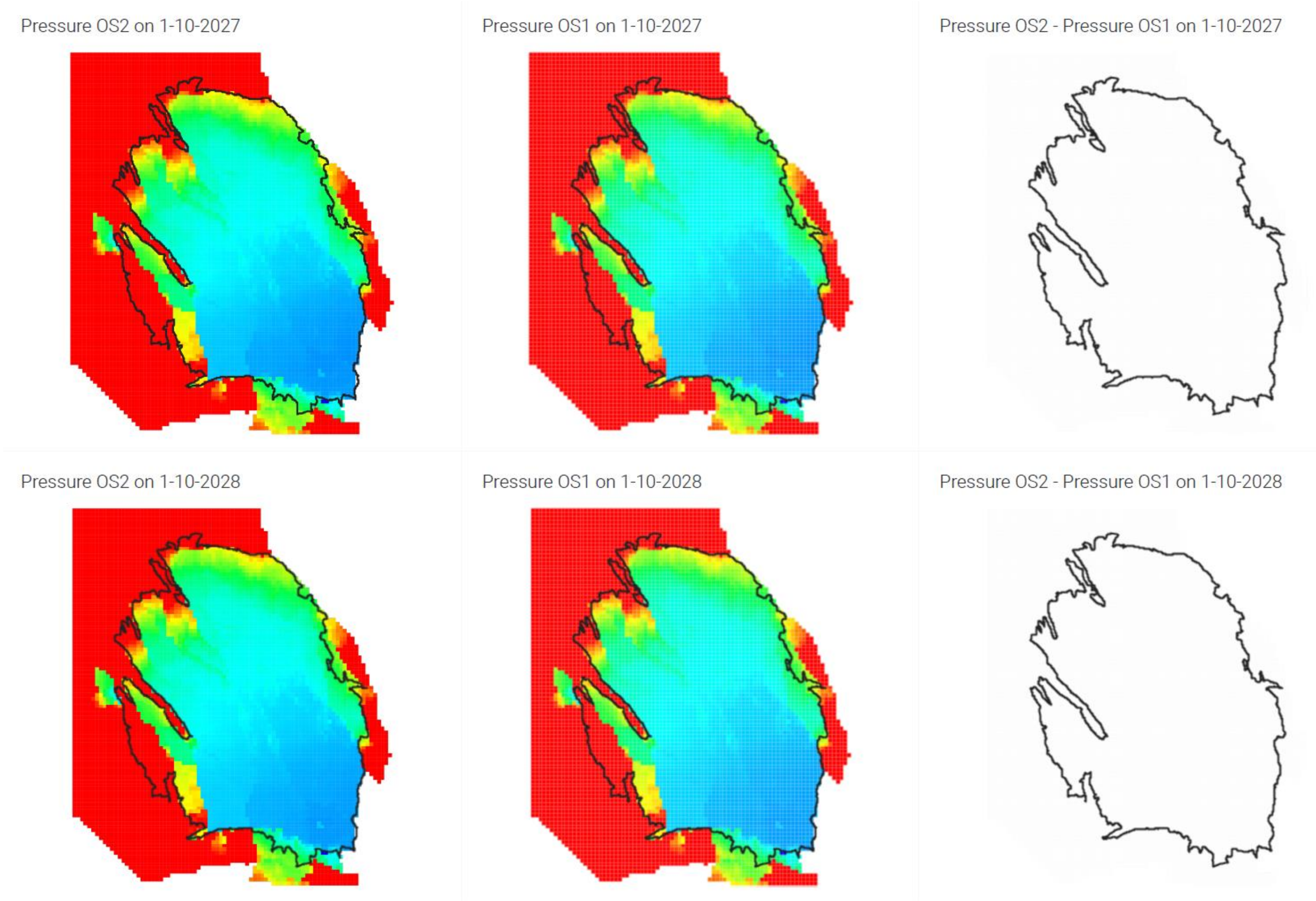

Figure 3-11: Pressure and pressure difference maps for average temperature scenario: start (top) and end (bottom) of gas year 2027/2028. See for colour scales Figure 3-6 and Figure 3-7.

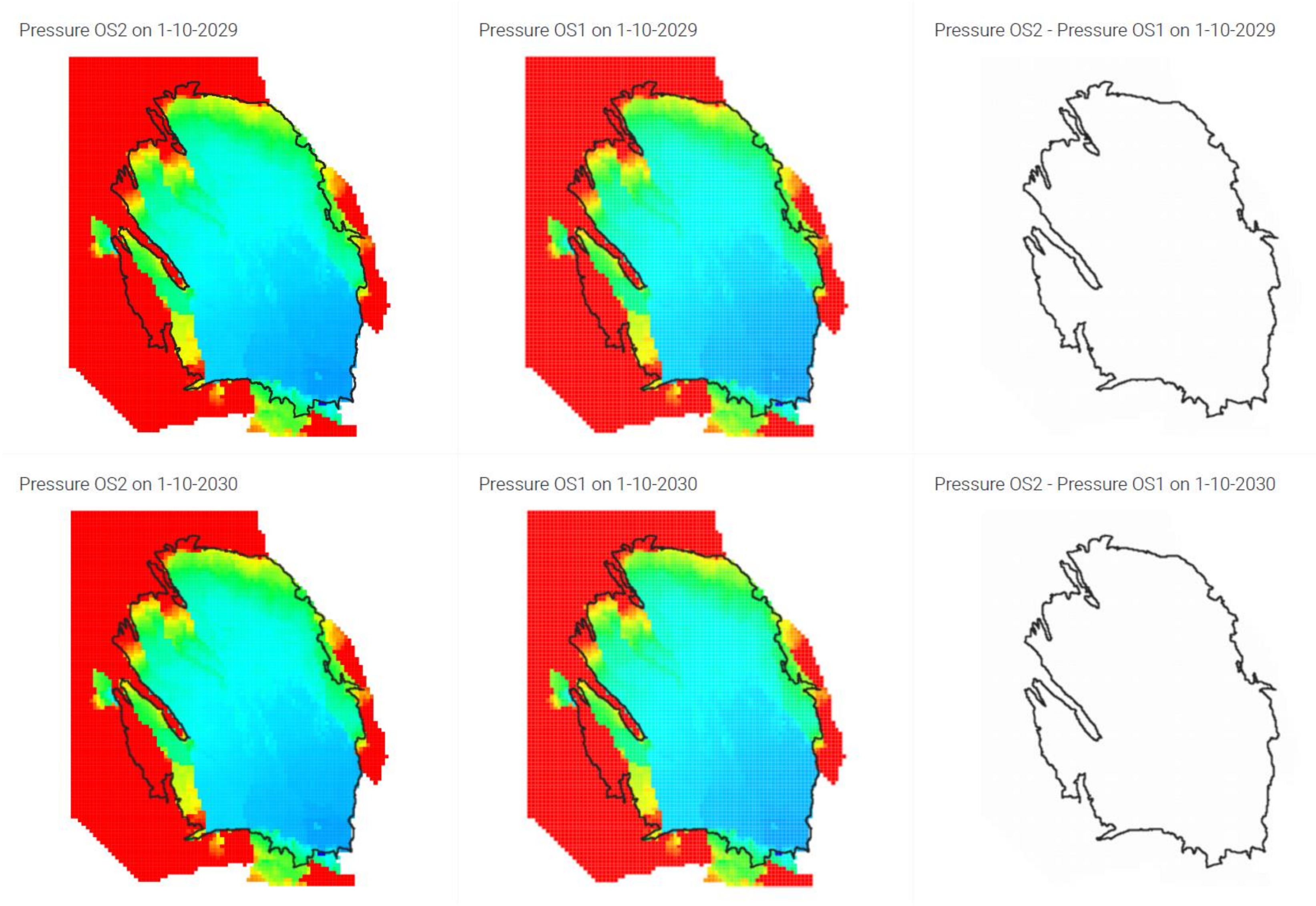

Figure 3-12: Pressure and pressure difference maps for average temperature scenario: start (top) and end (bottom) of gas year 2029/2030. See for colour scales Figure 3-6 and Figure 3-7.

3.4.2 Cold gas-year 2020/2021

Figure 3-13 and Figure 3-14 show the distribution over the regions in the case of a cold gas-year 2020/2021 followed by average years. Again production from Bierum is not required in OS2. Figure 3-15 shows production compared to capacity for each region in the two Operational Strategies.

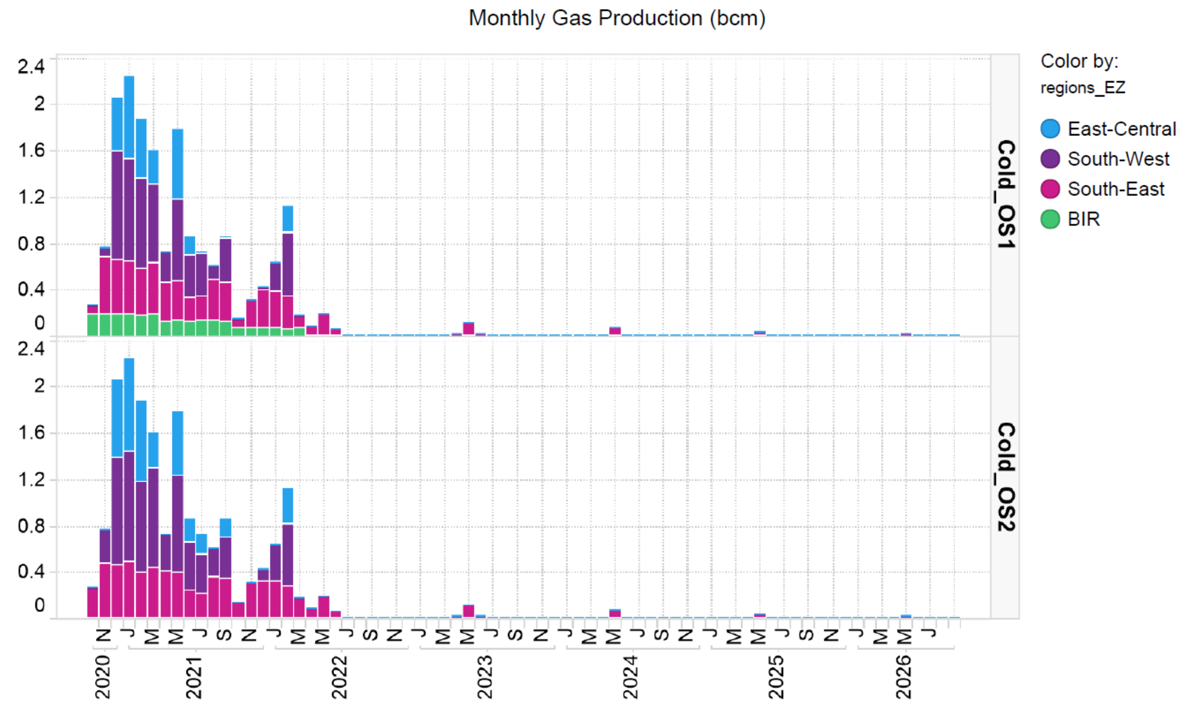

Figure 3-13: Monthly production volume per region for the next 6 gas-years for OS1 (top) and OS2 (bottom) in the cold gas-year scenario. Note the Bierum production cluster (BIR) is indicated in green.

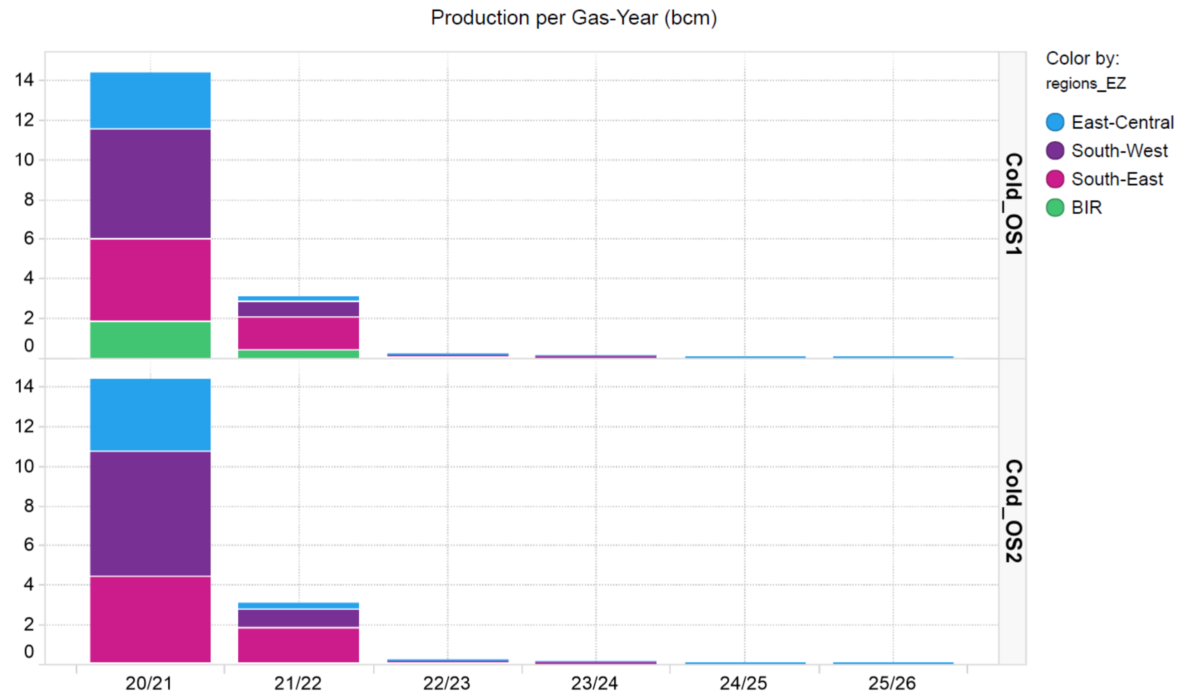

Figure 3-14: Regional distribution of production volume per gas-year for OS1 (top) and OS2 (bottom) in the cold gas-year scenario

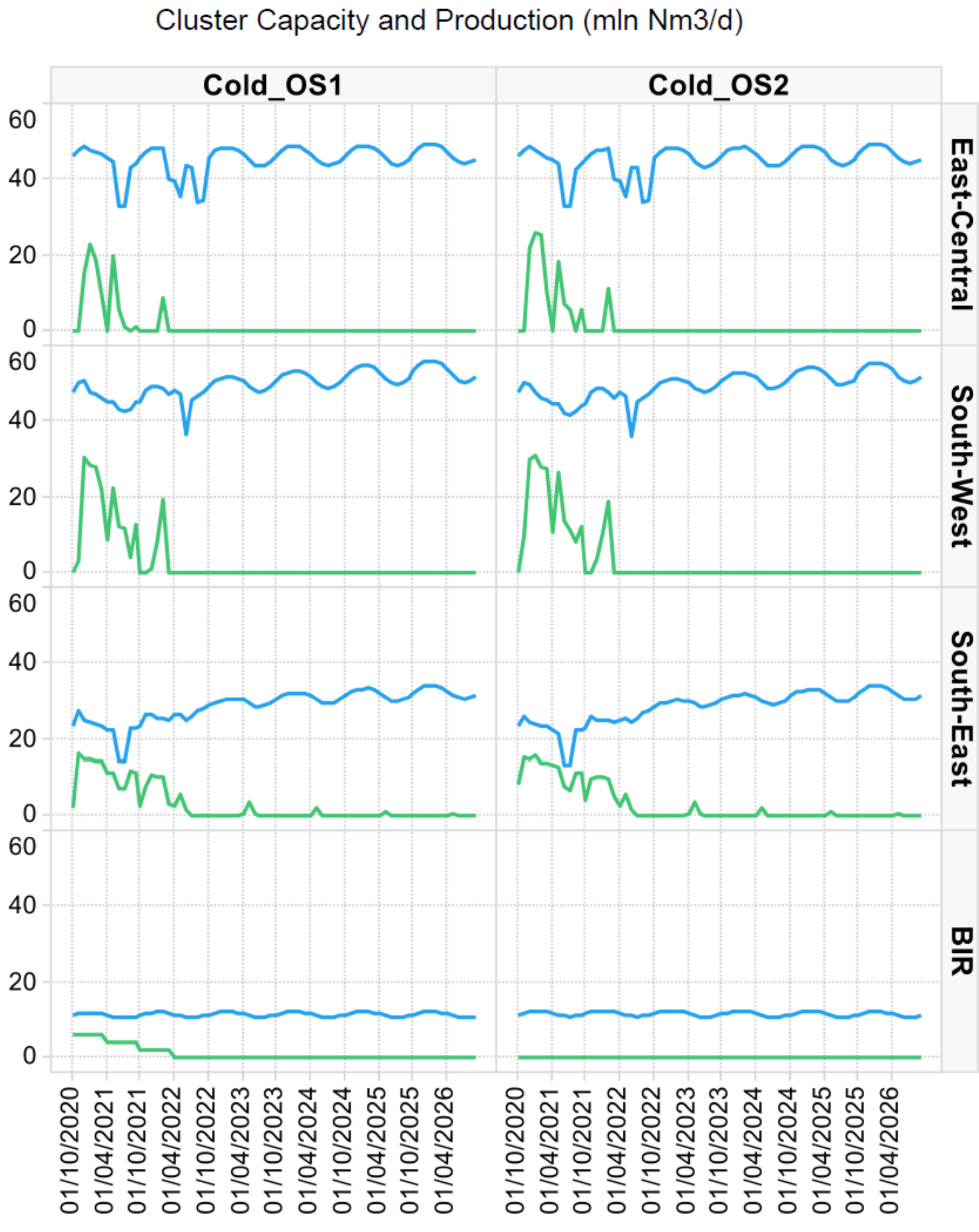

Figure 3-15: Cluster capacity (blue) and production rate (green) for OS1 (left) and OS2 (right) in the cold gas-year scenario

Figure 3-16 shows the pressure distribution at the end of a cold gas-year for the two Operational Strategies and their difference map.

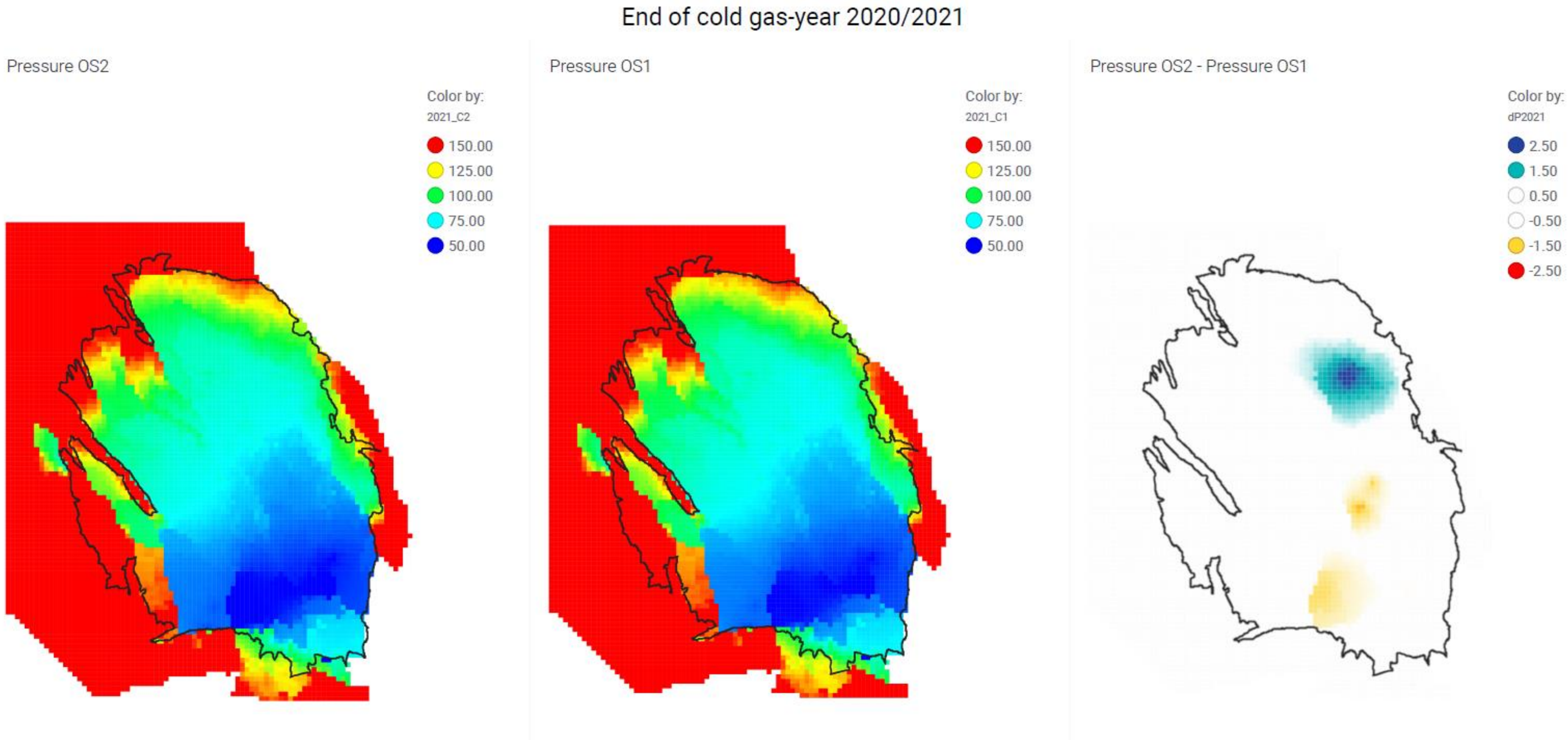

Figure 3-16: Pressure maps for the two Operational Strategies and pressure difference map at the end of a cold gas-year 2020/2021

3.4.3 Warm gas-year 2020/2021

Figure 3-17 and Figure 3-18 show the distribution over the regions in the case of a warm gas-year 2020/2021 followed by average years. Figure 3-19 shows production compared to capacity for each region in the two Operational Strategies.

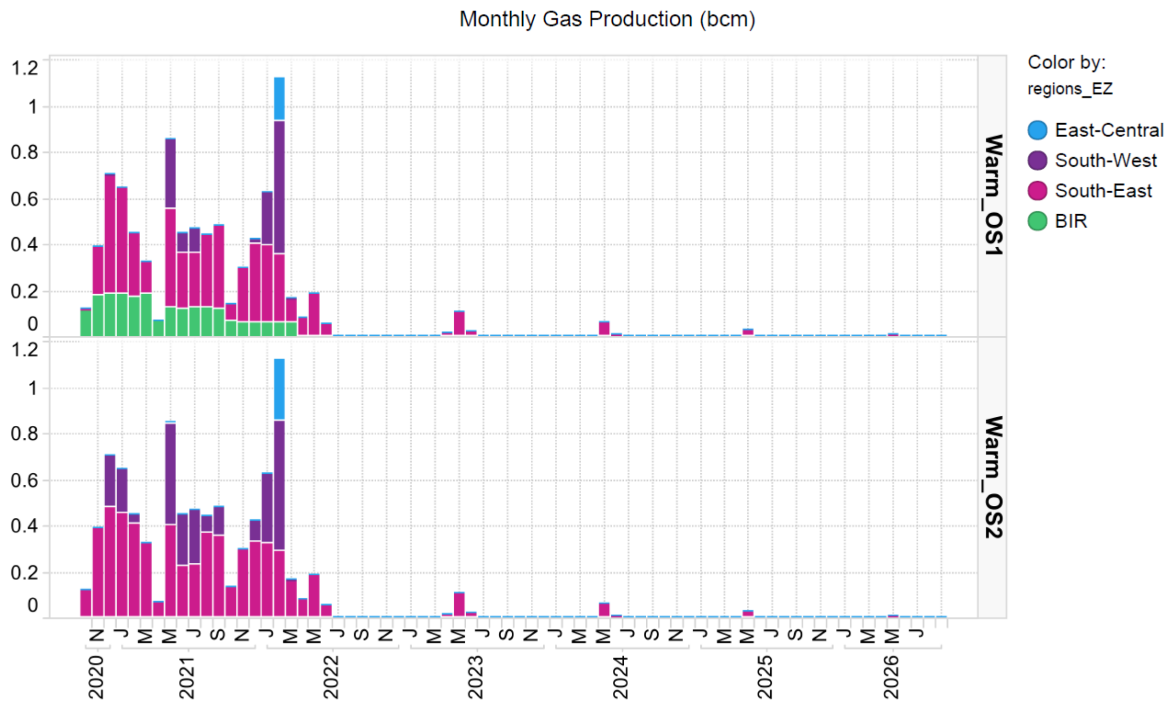

Figure 3-17: Monthly production volume per region for the next 6 gas-years for OS1 (top) and OS2 (bottom) in the warm gas-year scenario. Note the Bierum production cluster (BIR) is indicated in green.

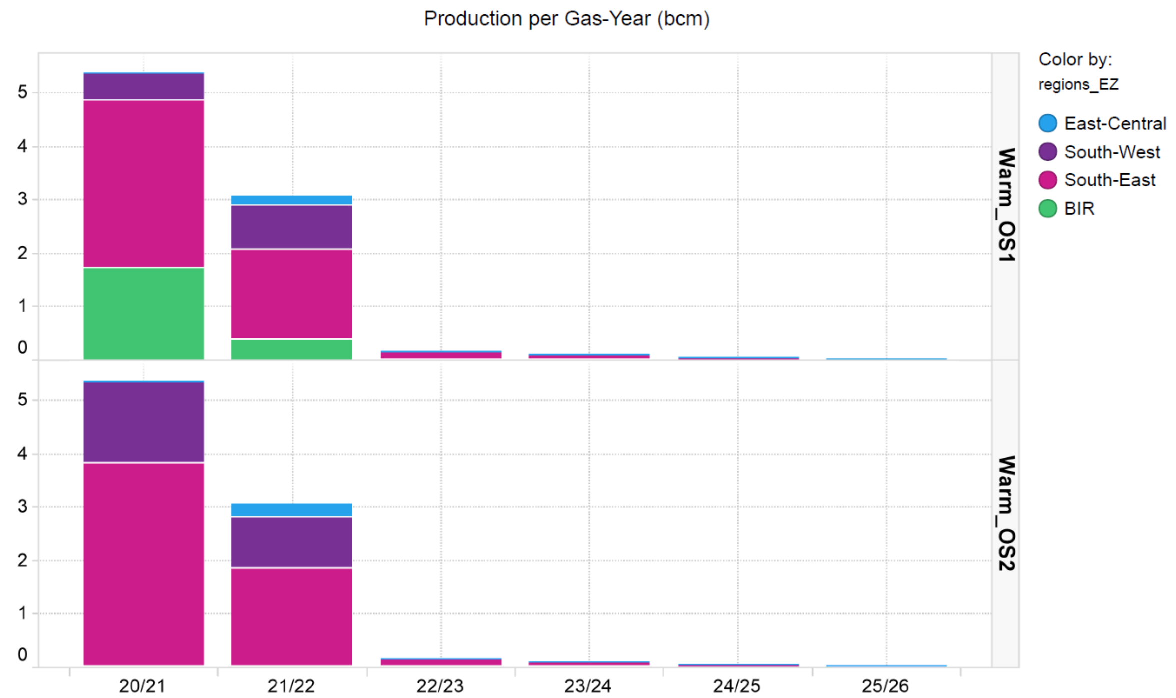

Figure 3-18: Regional distribution of production volume per gas-year for OS1 (top) and OS2 (bottom) in the warm gas-year scenario

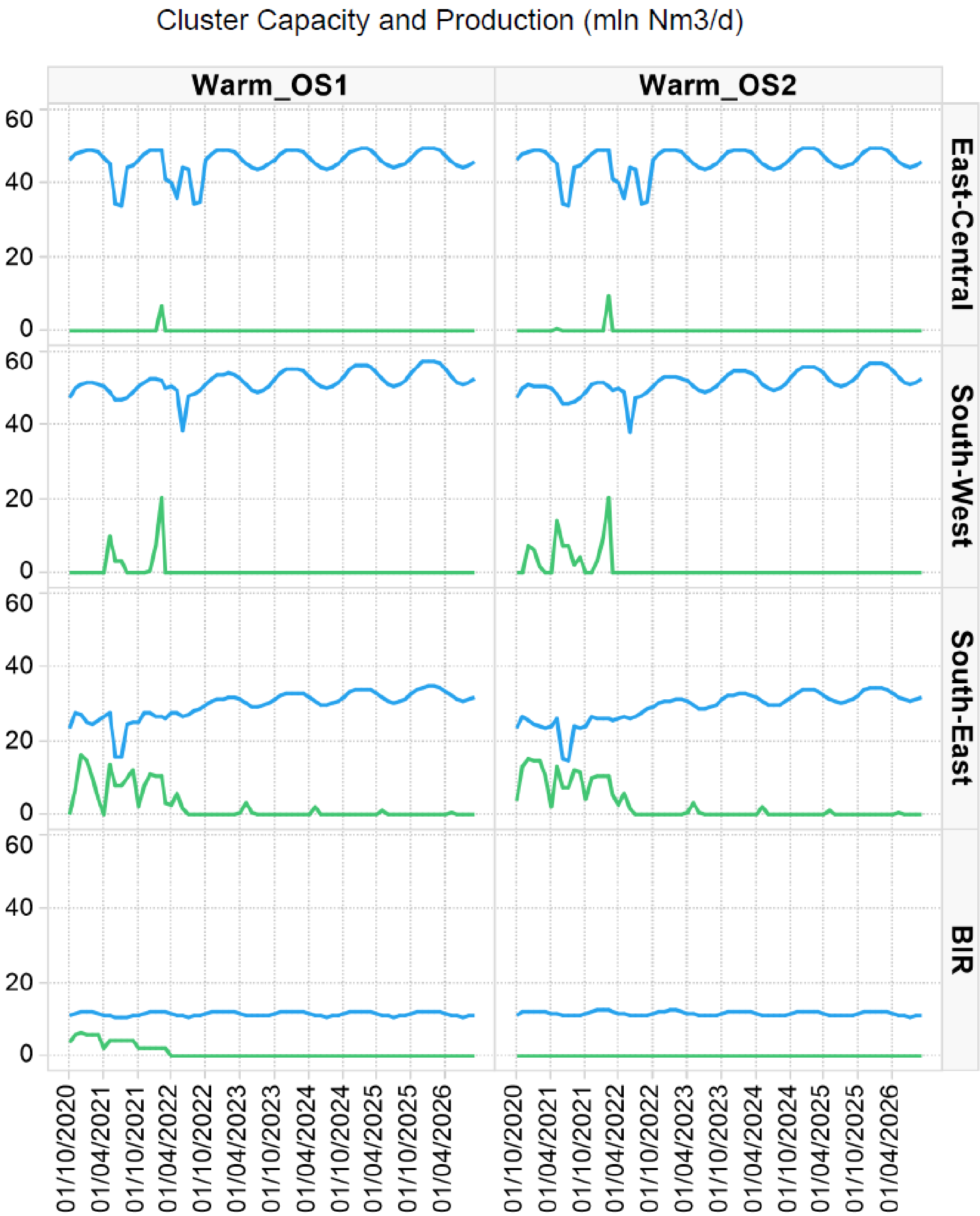

Figure 3-19: Cluster capacity (blue) and production rate (green) for OS1 (left) and OS2 (right) in the warm gas-year scenario

Figure 3-20 shows the pressure distribution at the end of a warm gas-year for the two Operational Strategies and their difference map.

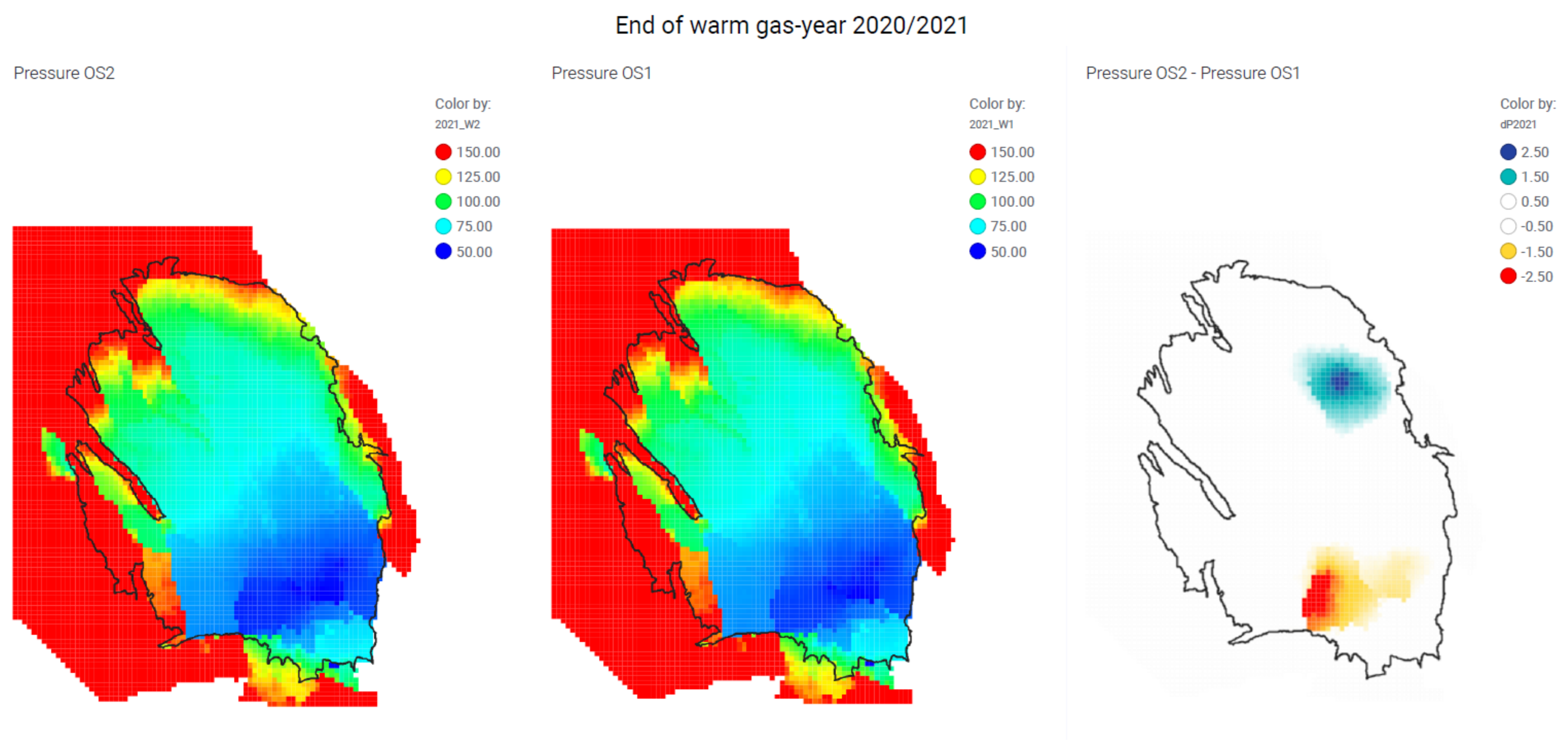

Figure 3-20: Pressure maps for the two Operational Strategies and pressure difference map at the end of a warm gas-year 2020/2021

4 Subsidence

In this HRA report for Groningen, subsidence is assessed for the period 2020-2030 for both the gas field and connected aquifers. Ongoing pressure depletion of these reservoirs is driving the subsidence. This chapter presents the forecast of surface subsidence based on "GTS-raming 2020", average temperature and Operational Strategy 1 as described in Chapter 3 of this report. In a series of updates of the Winningsplan Groningen 2016 (Ref. 8 to Ref. 14), this chapter is an updated version of relevant paragraphs on subsidence. As the subsidence and its effects will be less than assessed in Winningsplan 2016, only significant changes are presented.

The study area is defined by the Groningen gas field and the most important connected aquifers surrounding the field (Figure 4-1). These aquifers are:

- The "Southern Lauwerszee Trough (Zuidelijke Lauwerszee Trog)" aquifer located between the Groningen field and the smaller fields of Vries and Roden.
- In the north, the "Mowensteert" aquifer is connected to the Groningen gas field causing possible subsidence in the Waddenzee.
- The Rysum aquifer is connected to the eastern part of the field.
- In the south, an aquifer between Annerveen and Groningen is connected to the Groningen field.

The white coloured aquifers in Figure 4-1, e.g. the Goldhoorn aquifer to the east of the Groningen, have no connection to the gas field due to large offset faults blocking lateral fluid flow and hence preventing pressure communication. The "Noordelijke Lauwerszee trog" is mainly connected to the Bedum and Warffum fields.

The subsidence model consists of a compaction model that is described in section 4.1 and an influence model that translates the compaction in the subsurface to the earth's surface. The influence model is described in section 4.2.

Calibration of the model, the uncertainty estimation and the resulting subsidence forecast are presented respectively in sections 4.3, 4.4 and 4.5.

Figure 4-1 *Overview of the most important lateral aquifers attached to the Groningen field. In red the field names that are mentioned in the text.*

4.1 Compaction model

For the subsidence forecast the RTCiM model (Ref. 48) was used, as it gives the best match to core deformation experiments when compared to any of the other compaction models. Another advantage of the RTCiM model is that it spans a wide range of temporal behaviours to reflect the possible visco-plastic behaviour of the sandstone. The RTCiM model can behave more linear with depletion or exhibit time decay and temporal characteristics. None of the other models is as versatile. This choice concurs as well with the findings of the LTS-II research (Ref. 49).

4.1.1 Input to compaction model

Reservoir compaction is mainly dependent on pressure depletion, reservoir thickness and rock compressibility. These parameters will be described in the following sections.

4.1.1.1 Pressure scenario for the reservoir and laterally connected aquifers

The basis for the pressure scenario is the V6 reservoir model which includes a depleting Carboniferous as a separate layer (Chapter 3).

In Operational Strategy 1 cluster Bierum is kept at a constant rate, while most of the volume is produced from the South-East and South-West regions. When demand is high, production locations in the Central-East region are added. In this report subsidence is modelled using the pressure results of the Genrem-MoReS simulation using Operational Strategy 1 (base case).

For both the history-match and forecast period, annual reservoir pressure grids are exported from the reservoir model to be used in the subsidence model. Dynamic reservoir model V6 is used (Ref. 35). The V6 model includes several additional features compared to model V5, which provided the pressures for the winningsplan 2016 and 2018 update calculations (Ref. 8 to Ref. 14, Ref. 56), e.g.:

- Gas-in-aquifer (Slochteren formation)
- Carboniferous formation (both gas and water bearing)
- Additional depletion in the Lauwerszee aquifer resulting from the fields Roden, Vries, Pasop and Faan

The inclusion of gas-in-aquifer improves the subsidence match and GWC rise in the north-western area compared to model V5. The overall model match to measured reservoir pressures (SPG data) in V6 is slightly improved from V5, with a Root Mean Square Error of around 2 bar when all pressure data up to 1-1-2020 is included.

While there is ample pressure data available across the Groningen gas field, pressures in the surrounding aquifers are much more uncertain due to lack of pressure data. The connected aquifers (see Figure 4-1) are taken into account by the Groningen reservoir model and the V6 model gives a pressure realisation constrained by measured subsidence data and pressures in the gas field. The V6 model includes pseudo-aquifer wells to mimic aquifer depletion in the Lauwerszee aquifer due to the gas fields to the west (Roden, Vries, Pasop and Faan).

4.1.1.2 Reservoir Thickness

A reservoir thickness map from the V6 reservoir model reflecting the net thickness was used as input for the compaction model (Figure 4-2). Net thickness is specified for both the ROSL and DC.

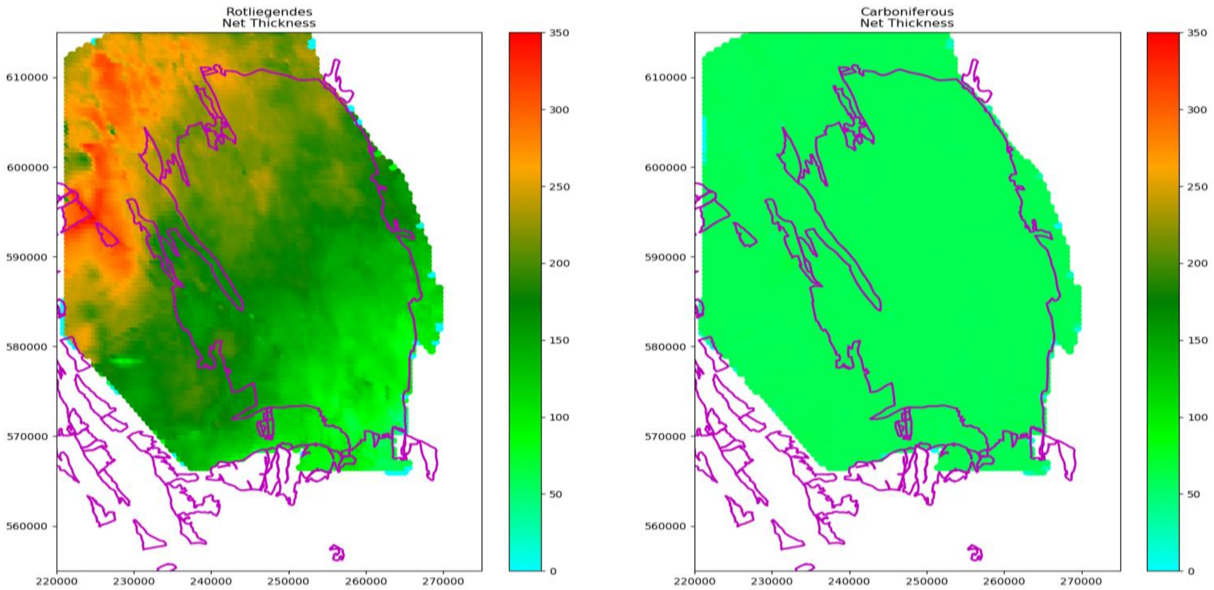

Figure 4-2 Net reservoir thickness [m] of the V6 reservoir model. Left: Net thickness for ROSL. Right: Net thickness for DC.

4.1.1.3 Rock compressibility

In previous subsidence studies a relationship was used between the porosity and the compressibility (Cm) of the rock. A recent study (Ref. 51), comparing Cm core plug measurements, in-situ strain/compaction data (DSS) and sonic velocity, all acquired in the ZRP-3 well, showed that the correlation of (DSS derived) Cm with sonic velocity is better than with porosity. The relation between the compressional slowness (DTC) and the compressibility (C_m) estimated from the strain measurements (assuming uniform depletion), derived by linear regression is:

$$C_m = 0.42 * DTC - 24.33$$

with DTC in µs/ft and C_m in µm/m/bar.

Figure 4-3 shows a comparison of the Cm core plug measurements, DSS estimated Cm values and Cm derived from the compressional sonic velocity. A velocity map was derived from the Groningen seismic cube and translated into a prior Cm grid for the ROSL applying the equation above. This ROSL Cm grid is presented in Figure 4-4 (left).

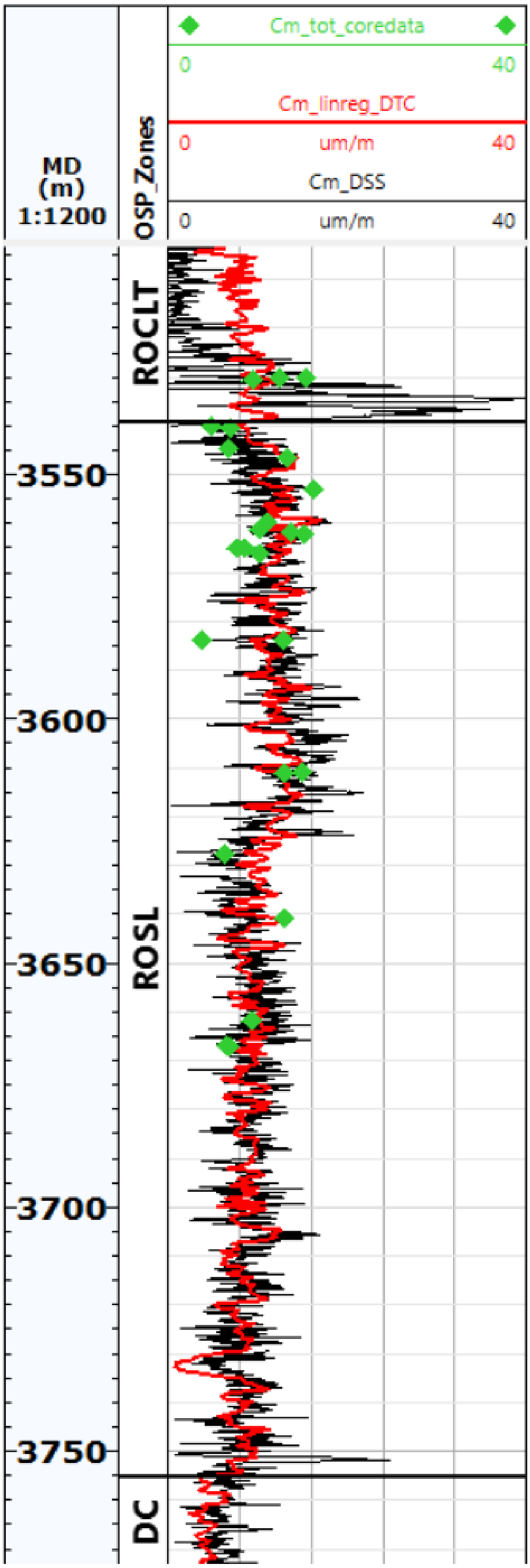

Figure 4-3 *Comparison of Cm values from core data (green markers), Cm values estimated from DSS (black), and Cm derived from the compressional sonic, using the suggested linear regression (red line). Units used for Cm are µm/m/bar for all three data sets.*

The value for the DC Cm value was deduced from recent core experiments. These experiments show a range of Cm values from 0.1 to 0.6 $10^{-5}bar^{-1}$. As no clear relation between compressibility and e.g. the porosity of the samples was observed, we assumed a constant (average) value of 0.3 $10^{-5}bar^{-1}$ for the DC (Figure 4-4, right).

These Cm maps for ROSL and DC were used as prior information into an inversion scheme, using the geodetic data to derive the final Cm grids.

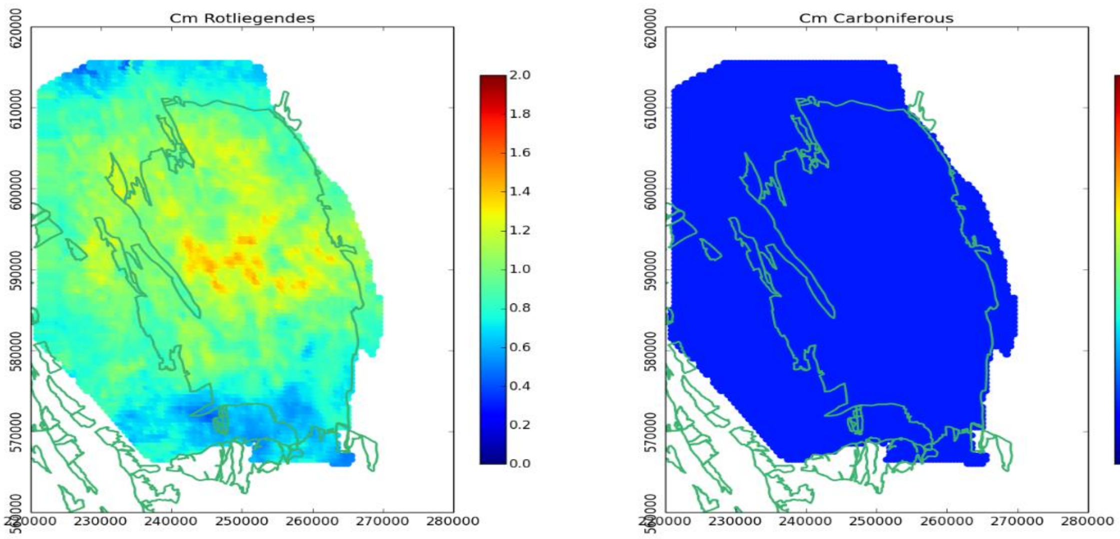

Figure 4-4 Input (prior) grid of Cm [10^{-5} bar^{-1}] for the ROSL (left) and DC (right)

4.2 Influence model

The influence model translates the compaction of the reservoir into surface subsidence. In Ref. 50 on subsidence above the Ameland field, it was concluded that a thick salt layer above the reservoir significantly impacts the temporal behaviour of the subsidence. Compared to the Groningen field, the Ameland field is relatively small, where compaction leads to stress arching in the overburden, changing the shear stress above the reservoir. These shear stresses cause creep deformation in the salt resulting in a narrower and more profound subsidence bowl. Due to its large size, stress arching is nearly absent above the Groningen field and therefore it is assumed in this study to neglect salt creep. Still the salt can result in a steeper edge of the subsidence bowl, a phenomenon that already was recognised and described earlier (Ref. 52). We adopted therefore the influence model as described in Ref. 52, that combines a half-space model with a rigid basement using a value of 7 km for the rigid basement and a Poisson’s ratio of 0.2. The effect of this model results in a change of the bowl shape that is time independent.

4.3 Calibration of compaction model parameters

Following a similar methodology as described in Ref. 50, the input data described above was combined with surface deformation measurements to calibrate the compaction model parameters, i.e. optical spirit-levelling data was used for inversion to compaction and calibration of the compaction model. Measurement results from 16 levelling campaigns spanning from 1964 to 2018 were used. After network adjustment of the individual campaigns, spatio-temporal double-differences were derived to serve as input to the modelling/inversion workflow. Only stable benchmarks (Ref. 53) were used in the calibration, providing a selection of some 10000 double differences.

New items in the inversion workflow are the application of strain data and the V6 reservoir model pressure data for both the ROSL and DC reservoirs. The inversion was carried out for both the ROSL and DC. Figure 4-5 shows the results for the (final) ROSL and DC C_m maps.

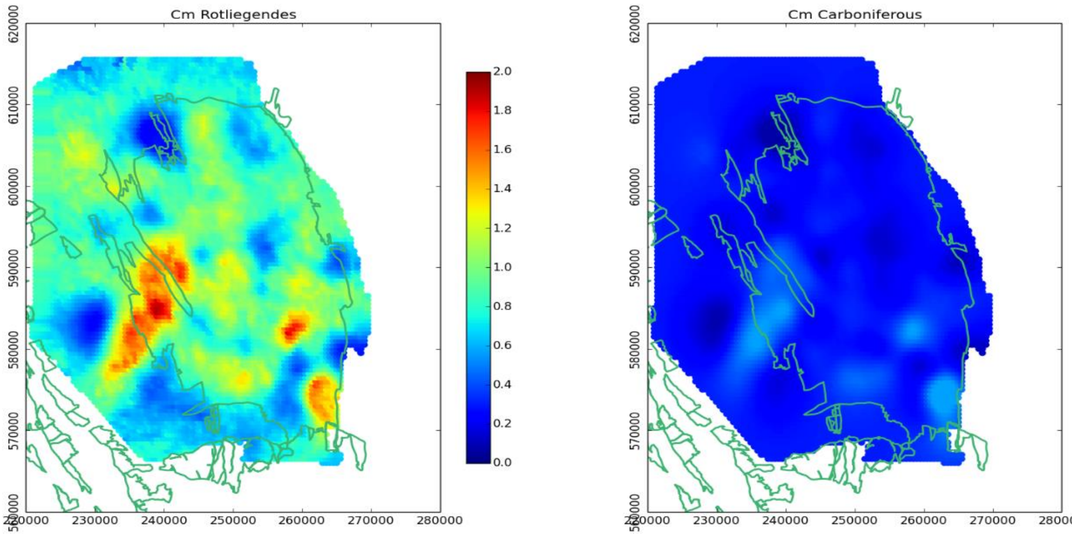

Figure 4-5 *Left: Cm of the ROSL after the inversion using both velocity data and geodetic data. Right: Cm for the DC (carboniferous). (Cm in $10^{-5}bar^{-1}$)*

4.4 Uncertainty estimation

A new approach was adopted to quantify the uncertainty of the model results. The objective of the approach is to define a 95% prediction interval, i.e. 95% of the measured double differences should fall within this interval/range around the modelled values. It is likely that the absolute difference between the modelled and measured values increases with magnitude and the simplest implementation is to adopt an uncertainty that is a linear function of the double difference value. To define this relation an intercept value and a slope need to be assessed. We therefore sort the modelled double differences from low to high values and split them up in 30 bins (Figure 4-6). Per bin we choose the uncertainty such that 95% of the data falls within the range. This way each bin produces a point that represents the uncertainty value per bin. Next a linear regression line is calculated through all points (Figure 4-7).

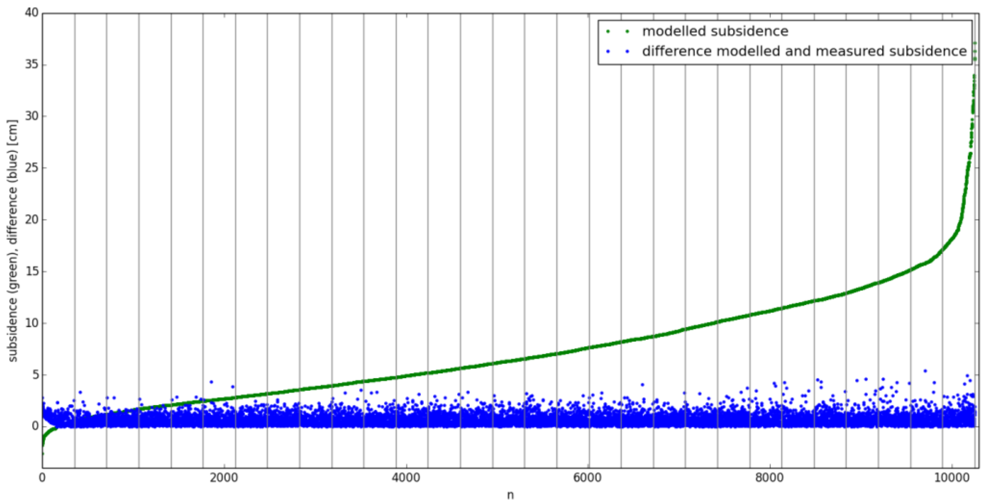

Figure 4-6 Modelled double differences (green) and their (absolute) difference with the measured subsidence

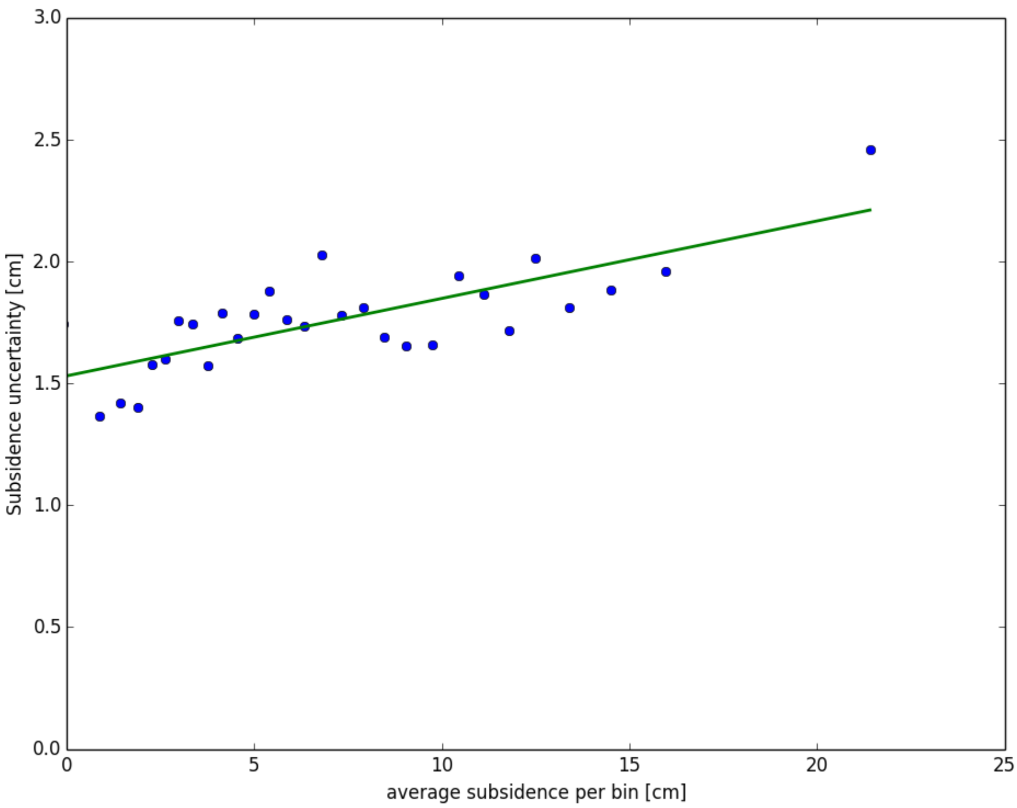

Figure 4-7 Uncertainty per bin with linear regression.

The following linear expression was found to obtain the P95 uncertainty:

$$P95\ uncertainty = 1.53\ (cm) + modelled\ subsidence * 0.032\ (cm)$$

With this equation the boundaries of the prediction interval were calculated.

4.5 Subsidence forecast

In this section the current status and expected development of subsidence up to 2030 is presented. Subsidence caused by gas production and aquifer depletion from the Groningen field is combined with the effects from ongoing gas production from neighbouring fields as published in the "winningsplannen" for these fields. Most of the expected subsidence has already occurred over the last 60 years.

The forecast uncertainty is a combination of uncertainties of the various model components. The measured subsidence since the start of production and all available intermediate measurement intervals were used to calibrate the model parameters as accurately as possible by means of inversion, explained in section 4.3.

Figure 4-8 shows the results of the subsidence model in comparison with the measured subsidence in benchmark locations across the gas field for the period 1972-2018.

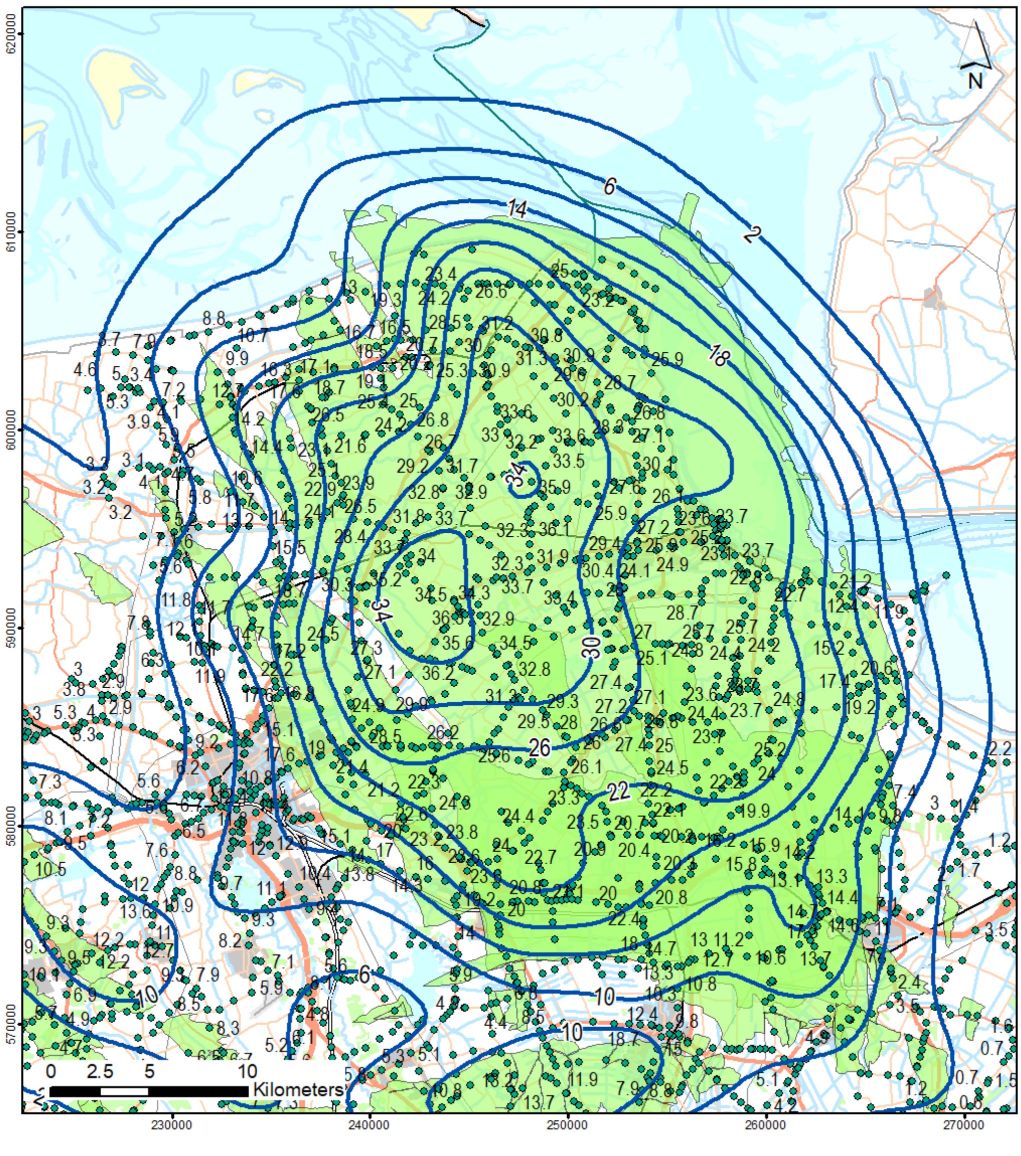

Figure 4-8 *Contours (solid blue lines) of the modelled subsidence between 1972 and 2018 compared to the measurements (green dots with value label) spanning the same period. All values are in cm.*

Subsidence forecasts for the years 2025 and 2030 are presented in respectively Figure 4-9 and Figure 4-10. The base case is presented by the contour lines while the P95 uncertainty is visualized by the coloured overlay. Note that the uncertainty is valid only for Groningen, i.e. the uncertainty shown above the neighbouring fields like Annerveen and Vries is the uncertainty in subsidence caused only by gas production from Groningen. Uncertainty for the other fields is not calculated here.

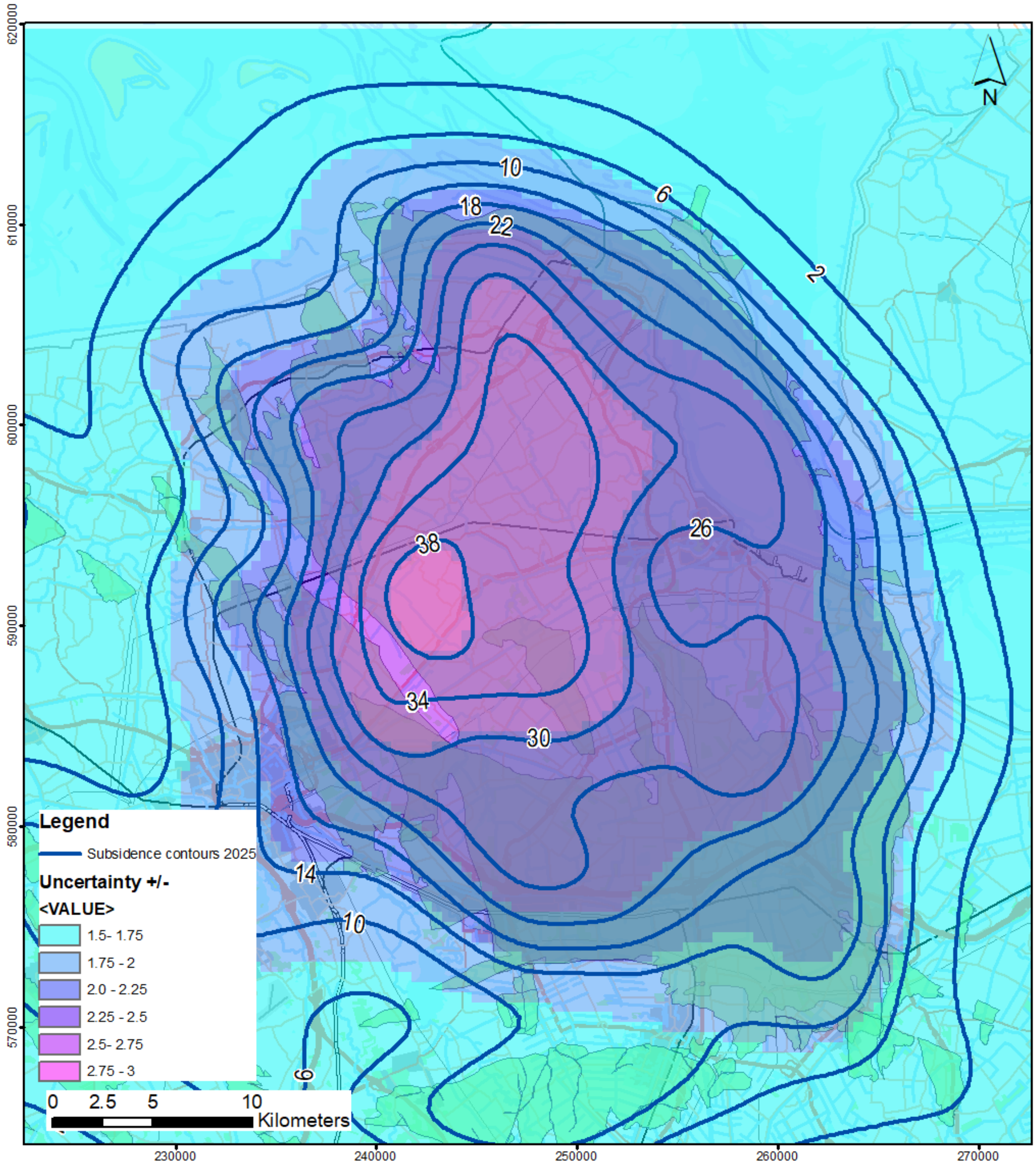

Figure 4-9 Subsidence in cm for 2025 (contours). The colours indicate the P95 uncertainty in the subsidence.

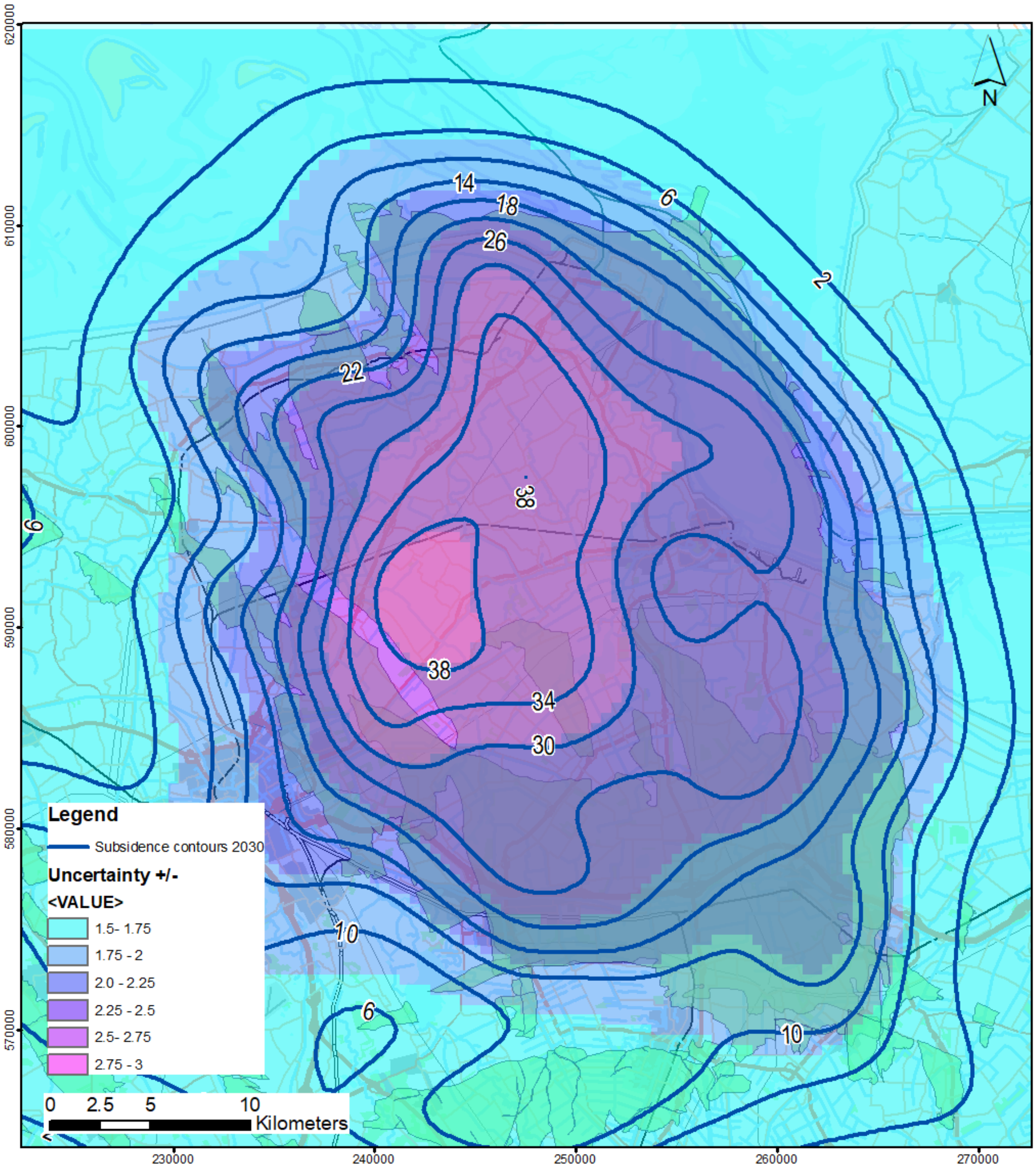

Figure 4-10 Subsidence in cm for 2030 (contours). The colours indicate the P95 uncertainty in the subsidence.

Figure 4-11 shows a comparison of the current subsidence forecast for 2030 with the previous forecast presented in the 2018 report “Assessment of Subsidence based on Production Scenario ‘Basispad Kabinet’ for the Groningen field” (Ref. 18).

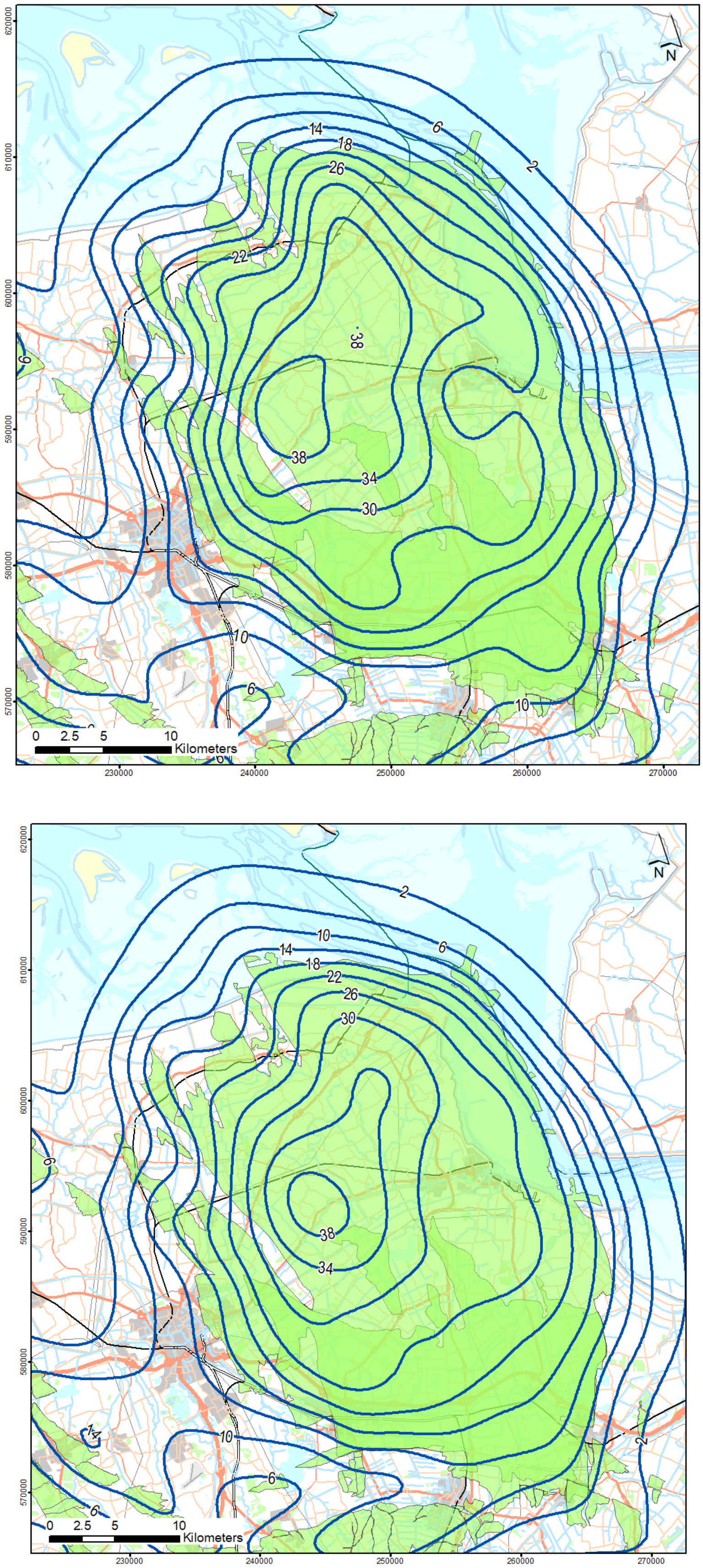

Figure 4-11 Comparison of current subsidence forecast for 2030 with forecast of “Basispad Kabinet” (issued in 2018). Top: Current forecast. Bottom: “Basispad Kabinet”. All contours in cm.

To visualise the match between modelled and measured subsidence over time since the first levelling surveys, a number of plots are presented in Figure 4-12, showing modelled and measured subsidence at various benchmark locations over the Groningen field.

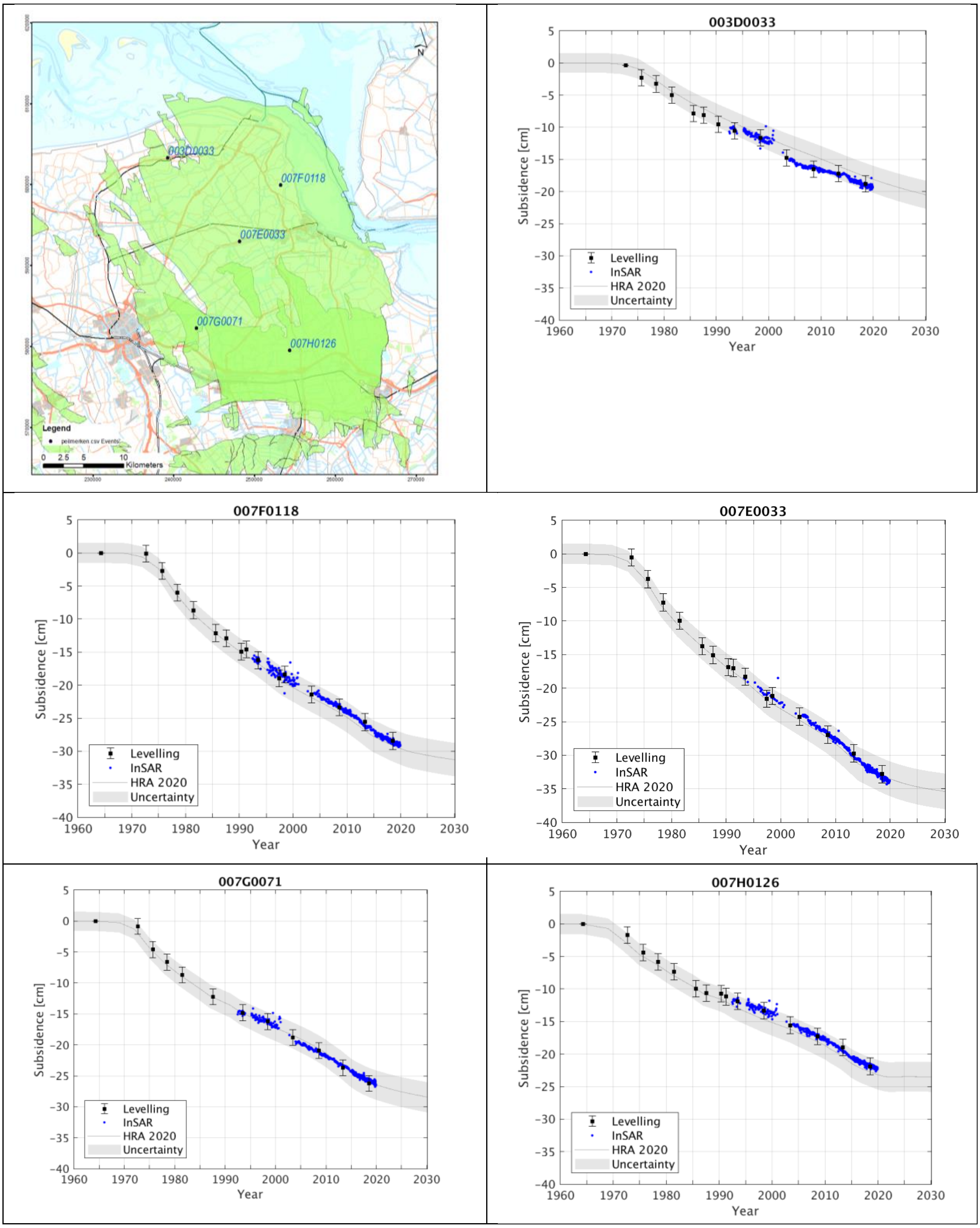

Figure 4-12 Subsidence at benchmark locations: dark grey line is the predicted subsidence, grey is the P95 uncertainty interval, black dots are levelling measurements plus uncertainty, the blue dots are the InSAR measurements.

5 Seismic Event Rate

5.1 Event Rate forecast

Based on the production profiles GTS-raming 2020, the number of earthquakes with a magnitude larger than or equal to M=1.5 have been forecasted. Figure 5.1 shows the annual number of earthquakes forecasted until gas-year 2033/2034 for Groningen field volume production for the "GTS-raming 2020" and average temperature profile. The number of earthquakes shows a declining trend. In gas-year 2018/2019, 11 earthquakes were recorded with a magnitude larger than M=1.5. Table 5.1 shows the recorded earthquakes for recent gas-years and calendar years. The decline in recorded earthquakes is a consequence of the decreasing gas production. Production from the field ceases, when the new nitrogen blending plant comes on stream in April 2022.

Starting year	Ending year	Gas-year	Calendar year
2012	**2013**	21	16
2013	**2014**	19	25
2014	**2015**	18	18
2015	**2016**	12	20
2016	**2017**	16	12
2017	**2018**	17	16
2018	**2019**	11	14
2019	**2020**	3 *	11
2020	**2021**		1 *

*Table 5.1 Number of observed earthquakes with a magnitude larger or equal to M=1.5 for both gas-years and calendar years. The gas-year is the one year period from 1st October in the starting year to 1st October in the ending year. The calendar year is the one year period 1st January in the starting year to 1st January ending year. Number of earthquakes indicated with an * are not for a full year, but up to 24th February 2020.*

The seismic activity rate declines to an expected 4 earthquakes per year in gas-year 2023/2024, with an uncertainty range of 1 to 10 earthquakes per year. The seismic activity rate beyond 2020 is primarily driven by the pressure equilibration in the field, between the high-pressure area North-West of Loppersum and the lower-pressure area South-East of the field (Ref. 16).

To further illustrate this, the event rate for a production profile (labelled Reference) based on cessation of production at the end of the current gas-year (2019/2020) is also shown in figure 5.1. The prognosed seismic event rate for this profile is very close to that for the GTS-raming 2020 profile. This sensitivity shows that the prognosed earthquakes are primarily the result of the pressure equilibration in the reservoir, between the low pressure south-east and the high pressure Loppersum region. This comparison demonstrates the impact of the gas production after 1st October 2020 on the seismicity is very limited.

Because the impact of future gas production on the seismic event rate is very limited, it is expected the impact of the operational strategy for the production of this gas will be even smaller. This can be seen by comparing both sides of figure 5.4.

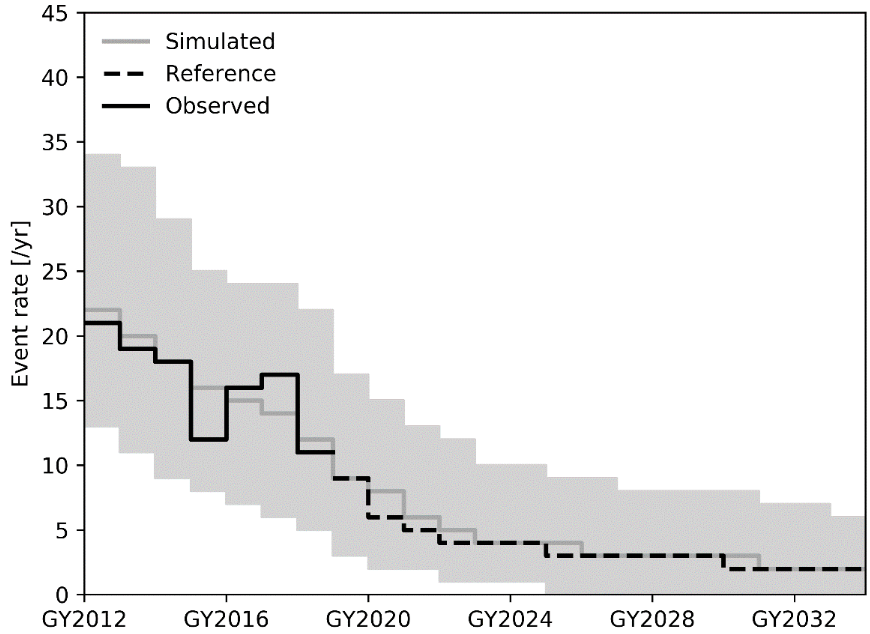

Figure 5.1 *Seismic Activity Rate of earthquakes for the period gas-years 2012/2013 to 2034/2035 based on production profile GTS-raming 2020 for the average weather temperature gas-year and production profile for operational strategy 1. The dark grey line indicates the expected number of earthquakes in each gas-year and the grey area the uncertainty band. The solid black line indicated the historical event rate. The dashed black line indicates the expected number of earthquakes when the field is closed in at the end of the current gas-year 2019/2020 (1st October 2020). GY2012 refers to gas-year 2012/2013.*

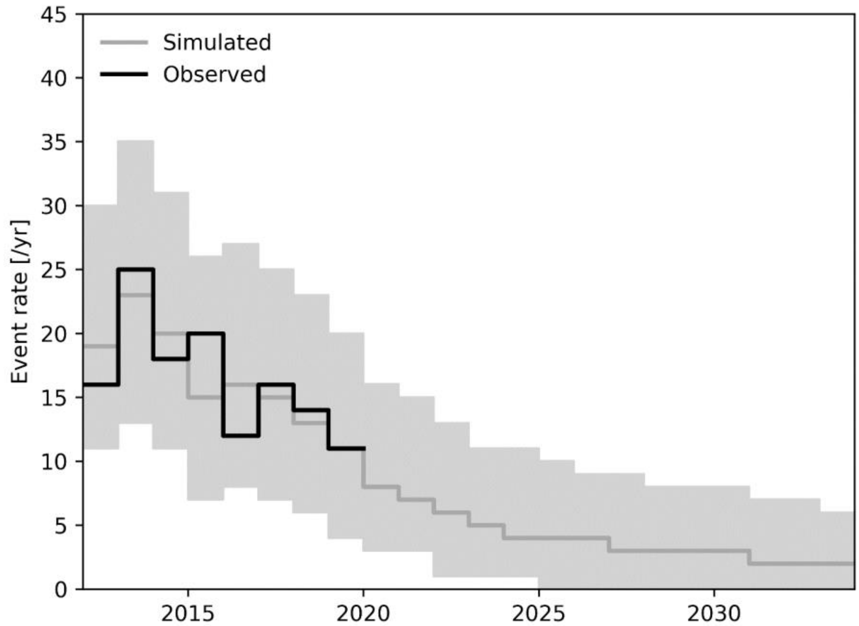

Figure 5.2 *Seismic Activity Rate of earthquakes for the period 2012 to 2033 (production profile GTS-raming 2020 for the average weather temperature calendar-year and production profile for operational strategy 1. The dark grey line indicates the expected number of earthquakes in each calendar-year and the grey area the uncertainty band.*

The expected impact of weather temperature uncertainty is within the uncertainty band for event rate of the average temperature profile. In figure 5.3 the seismic activity rate for three profiles is shown; the average temperature profile, an average temperature profile when gas-year 2020/2021 is a cold gas-year and an average temperature profile when gas-year 2020/2021 is a warm year and the later years with average temperature weather. Especially in year 2021 the activity rate is higher for the cold year profile (11 earthquakes at mean) than for the average temperature profile (8 earthquakes at mean) and lower for the warm year profile (7 earthquakes at mean).

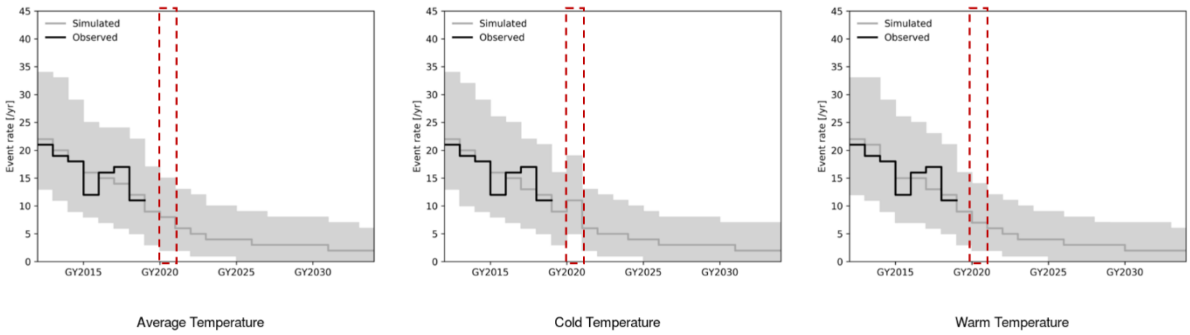

Figure 5.3 *Seismic Activity Rate of earthquakes for the period gas-years 2012/2013 to 2034/2035 based on production profile GTS-raming 2020 for operational strategy 1 for average temperature profile, cold temperature profile and warm temperature profile. For the cold temperature profile gas-year 2020/2021 is a cold year (with higher gas demand) and all following years are again an average year.*

The event rate for both operational strategies are compared in figure 5.4. The mean event rate is very similar for both operational strategies. Only the uncertainty band around the mean event rate shows very slight differences.

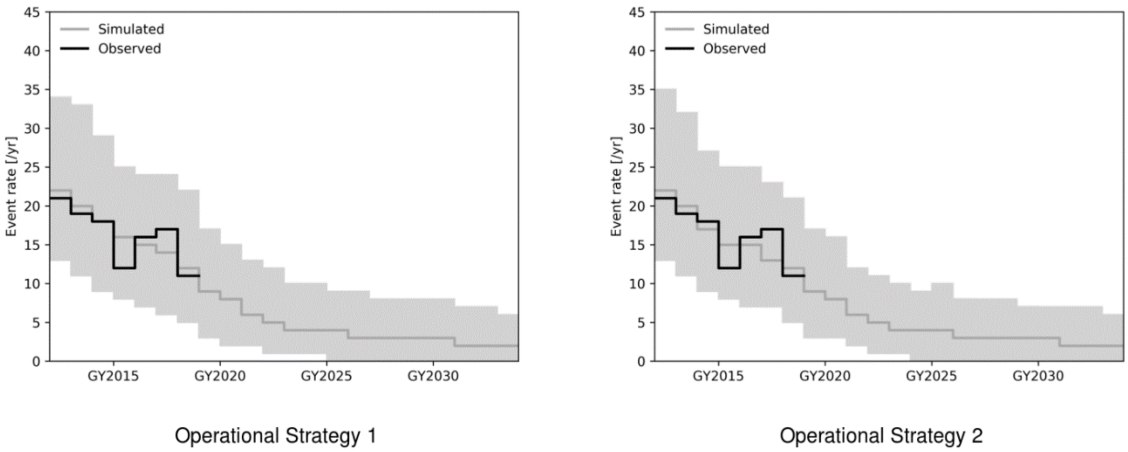

Figure 5.4 *The seismic event rate for the average temperature profile gas-year of GTS-raming 2020 for both operational strategies.*

5.2 Exceedance Probabilities

The probability of an earthquake with a magnitude exceeding a given magnitude can be assessed using the seismological model (Ref. 40 to Ref. 43). In table 5.2a and 5.2b the annual probability of an earthquake occurring with a magnitude exceeding the specified magnitude is given. For instance, the probability of an earthquake occurring in gas-year 2020/2021 with a magnitude exceeding M_L=3.6 (the magnitude of the Huizinge earthquake) is equal to 4.73%. In the HRA for GTS-raming 2019, this probability was close to 9.3%. The probability of an earthquake occurring in gas-year 2020/2021 with a magnitude exceeding M_L=3.6 has almost halved between these two assessments (HRA GTS-raming 2019 and HRA GTS-raming 2020). For larger exceedance magnitudes the reduction between these two HRA versions is even larger.

Gas-year	P(M>=3.6)	P(M>=4.0)	P(M>=4.5)	P(M>=5.0)
2020/2021	4.73%	1.29%	0.16%	0.02%
2021/2022	3.64%	0.97%	0.12%	0.02%
2022/2023	3.09%	0.83%	0.11%	0.02%
2023/2024	2.78%	0.74%	0.09%	0.01%
2024/2025	2.43%	0.64%	0.08%	0.01%
2025/2026	2.20%	0.57%	0.08%	0.01%
2026/2027	2.10%	0.55%	0.07%	0.01%
2027/2028	1.93%	0.50%	0.07%	0.01%
2028/2029	1.80%	0.46%	0.06%	0.01%
2029/2030	1.67%	0.43%	0.06%	0.01%
2030/2031	1.54%	0.40%	0.06%	0.01%

Table 5.2a Table with annual probabilities for occurrence of earthquakes exceeding a set magnitude. This table is for production profile GTS-raming 2020, average temperature gas-year and operational strategy 1.

Gas-year	P(M>=3.6)	P(M>=4.0)	P(M>=4.5)	P(M>=5.0)
2020/2021	4.88%	1.30%	0.17%	0.02%
2021/2022	3.58%	0.94%	0.12%	0.02%
2022/2023	3.03%	0.84%	0.10%	0.01%
2023/2024	2.74%	0.74%	0.09%	0.02%
2024/2025	2.47%	0.68%	0.09%	0.01%
2025/2026	2.31%	0.60%	0.08%	0.01%
2026/2027	2.09%	0.56%	0.07%	0.01%
2027/2028	1.91%	0.52%	0.07%	0.01%
2028/2029	1.84%	0.48%	0.06%	0.01%
2029/2030	1.67%	0.45%	0.06%	0.01%
2030/2031	1.49%	0.42%	0.06%	0.01%

Table 5.2b Table with annual probabilities for occurrence of earthquakes exceeding a set magnitude. This table is for production profile GTS-raming 2020, average temperature gas-year and operational strategy 2.

5.3 Event Density Maps

Annual event density maps for the two optimised Operational Strategies are compared in figure 5.5. These maps are based on the production profile "GTS-raming 2020" for an average temperature year. The scale for the comparison plot has been chosen at 0.01 earthquake/km^2 to highlight the small differences resulting from the operational strategies in gas-year 2020/2021. Even with this very sensitive scale the differences fade away in later years, especially after production from the field has been terminated.

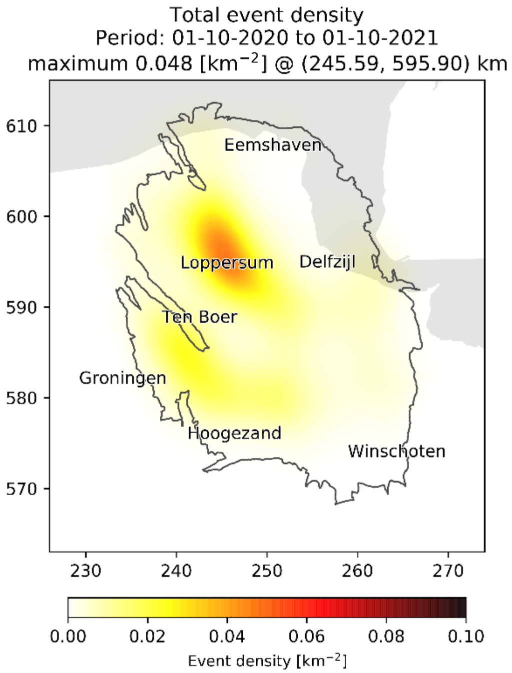

Operational Strategy 2

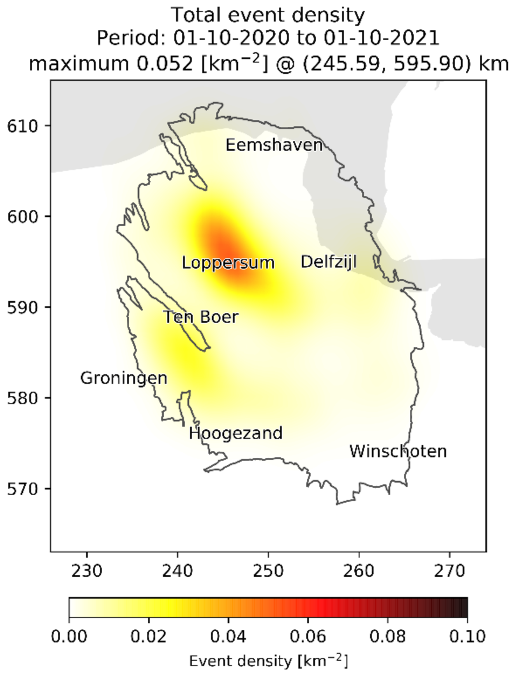

Operational Strategy 1

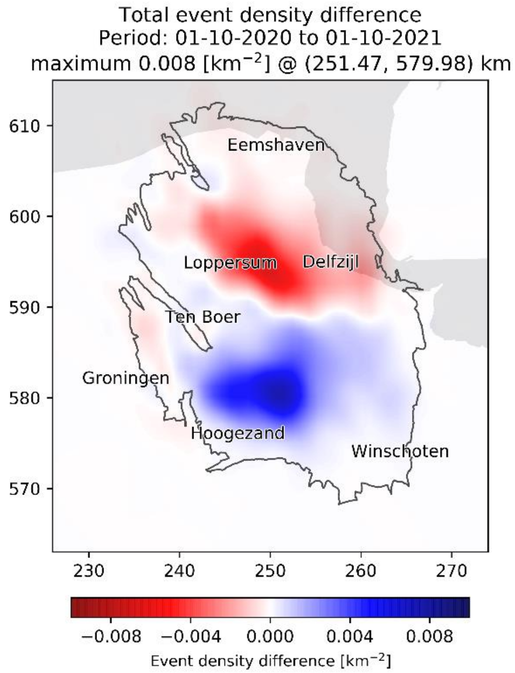

Difference

(Operational Strategy 2 – Operational Strategy 1)

2020/2021

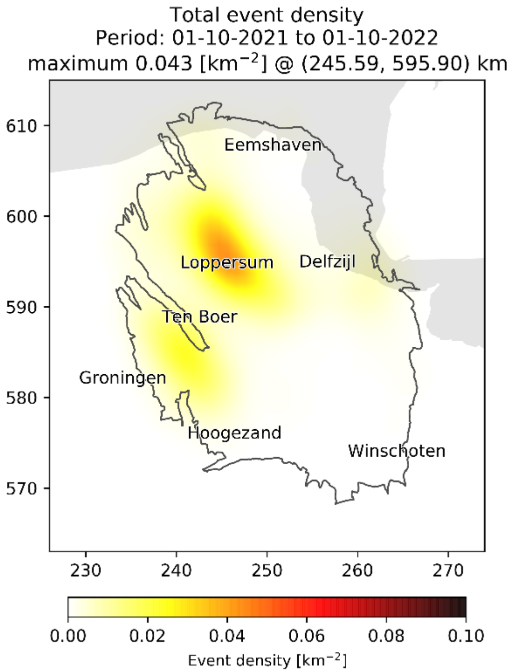

Operational Strategy 2

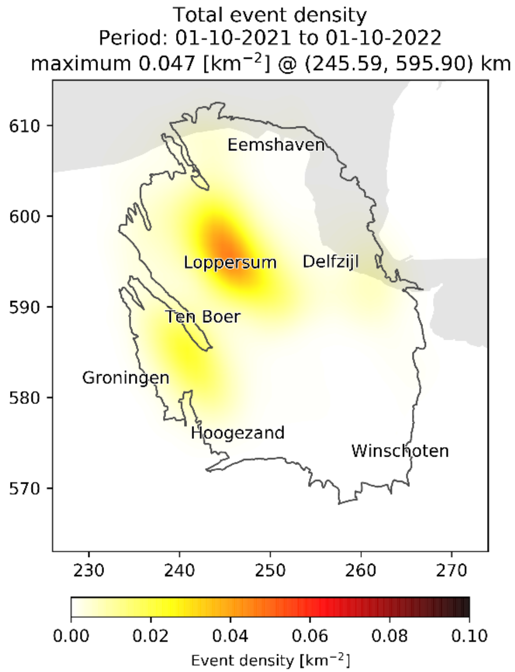

Operational Strategy 1

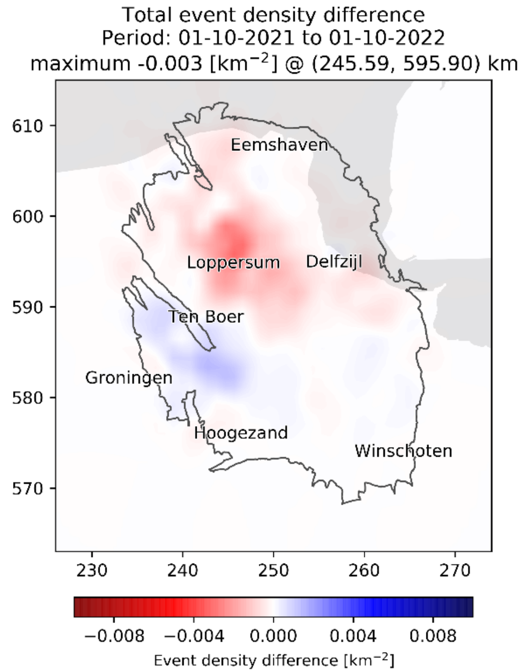

Difference
(Operational Strategy 2 – Operational Strategy 1)

2021/2022

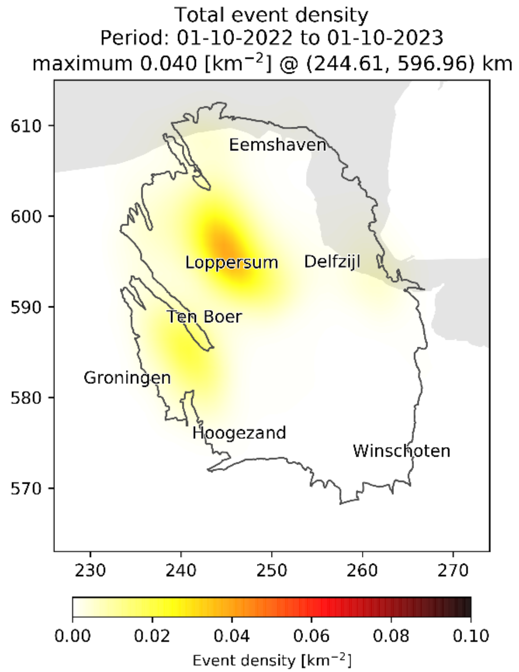

Operational Strategy 2

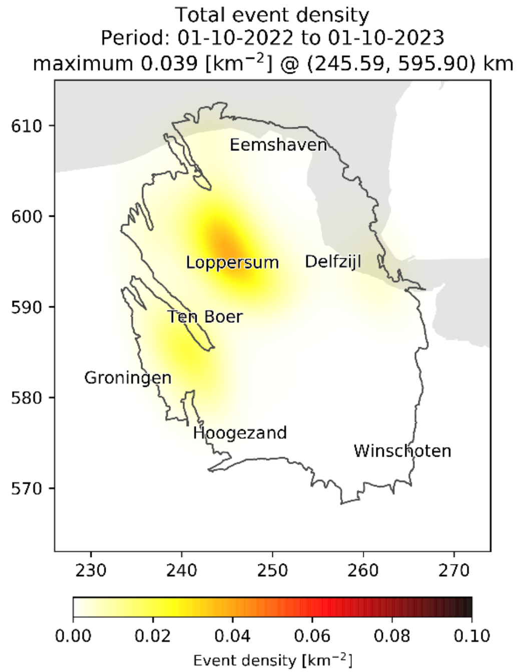

Operational Strategy 1

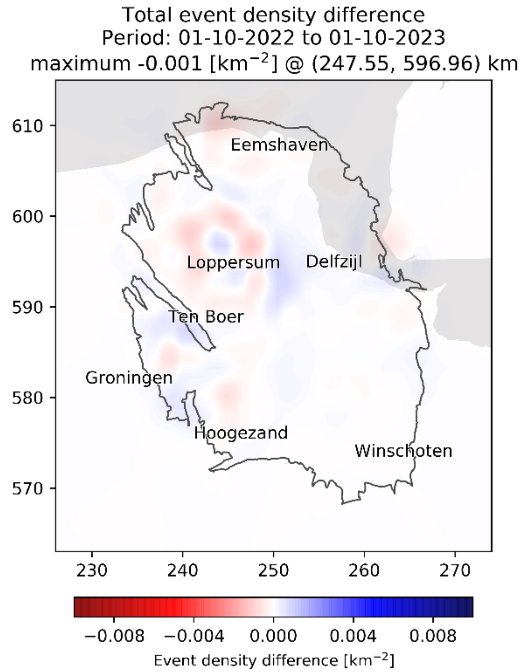

Difference

(Operational Strategy 2 – Operational Strategy 1)

2022/2023

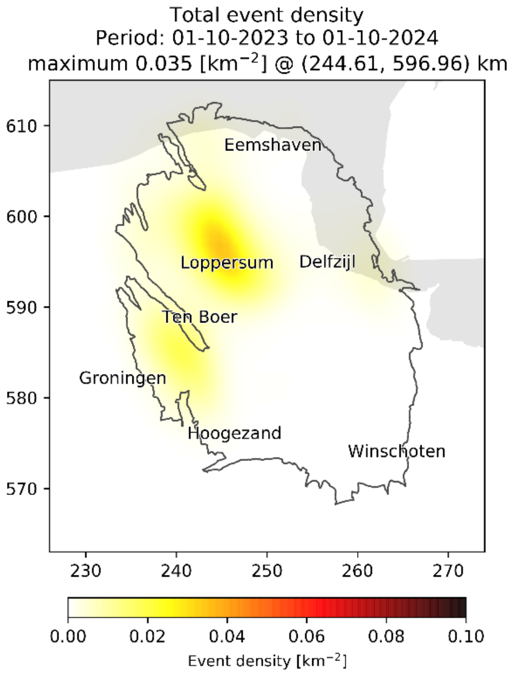

Operational Strategy 2

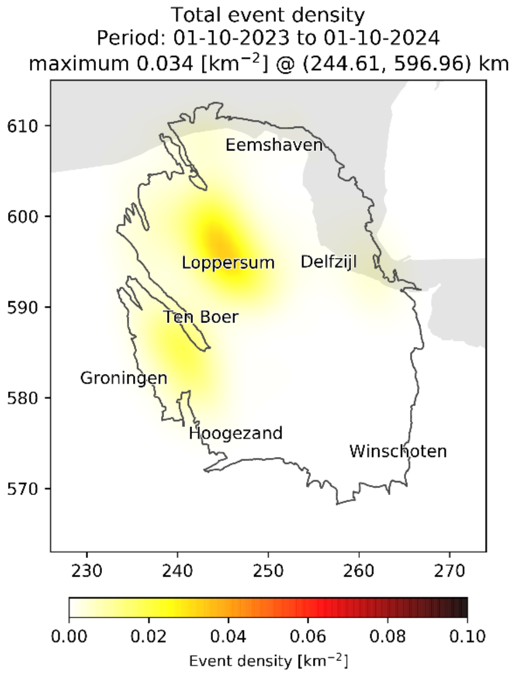

Operational Strategy 1

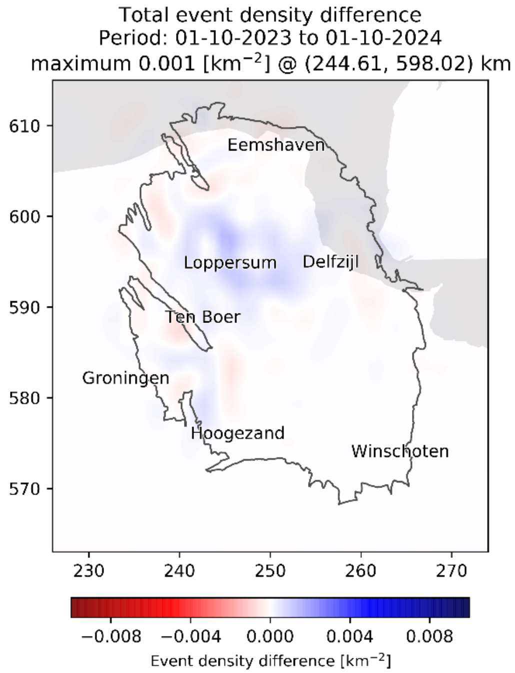

Difference

(Operational Strategy 2 – Operational Strategy 1)

2023/2024

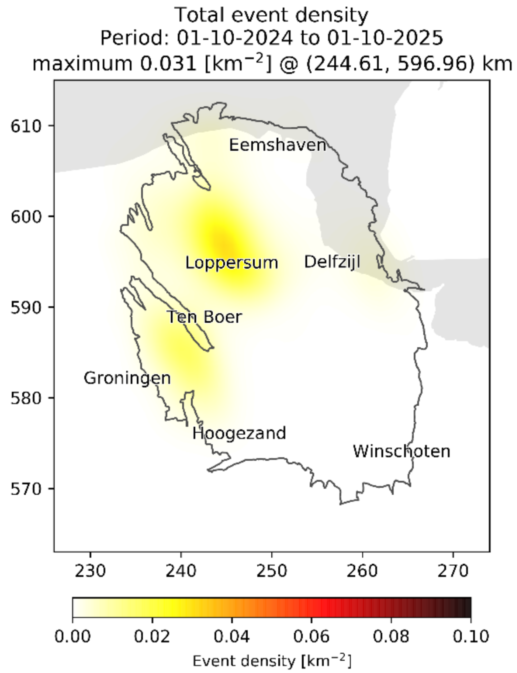

Operational Strategy 2

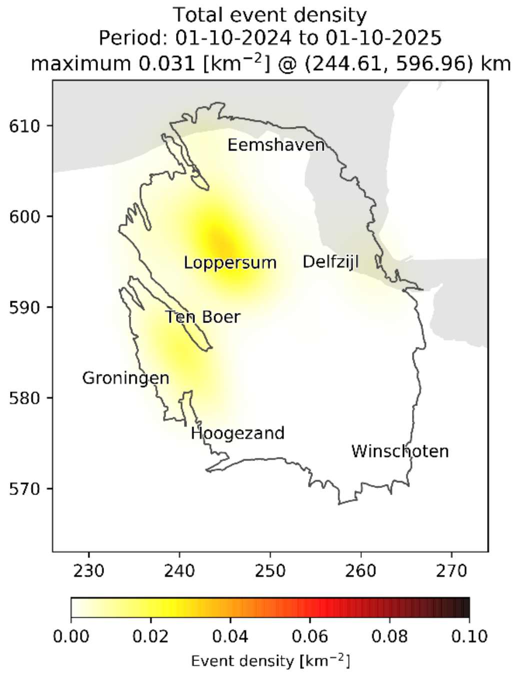

Operational Strategy 1

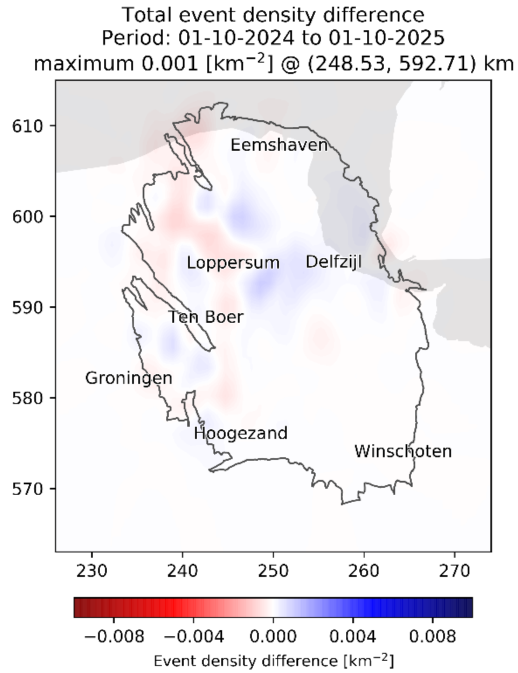

Difference

(Operational Strategy 2 – Operational Strategy 1)

2024/2025

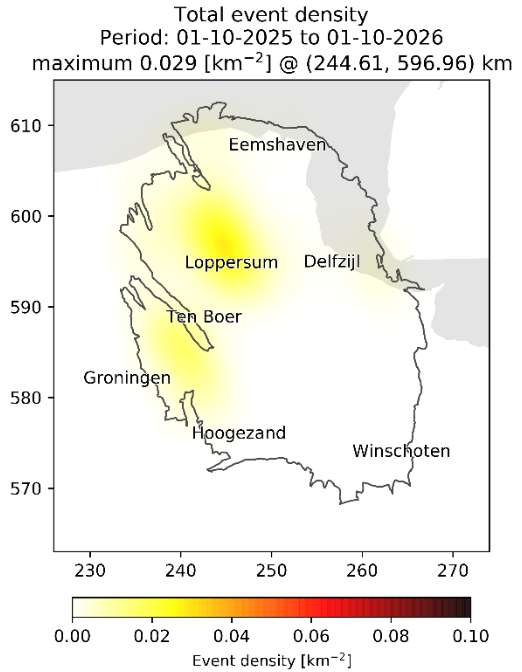

Operational Strategy 2

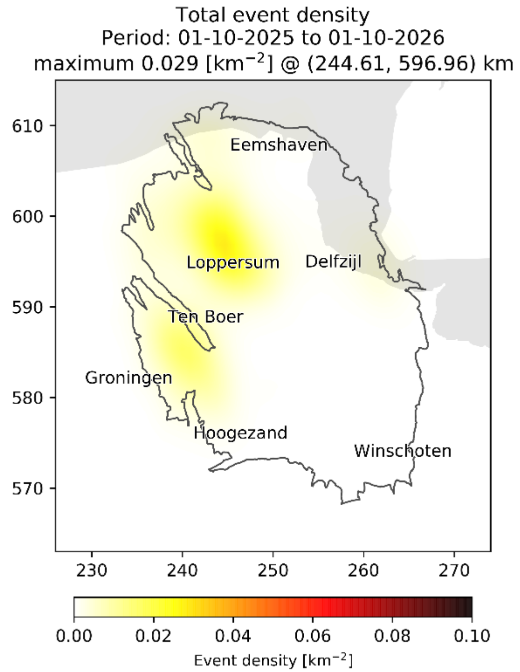

Operational Strategy 1

2025/2026

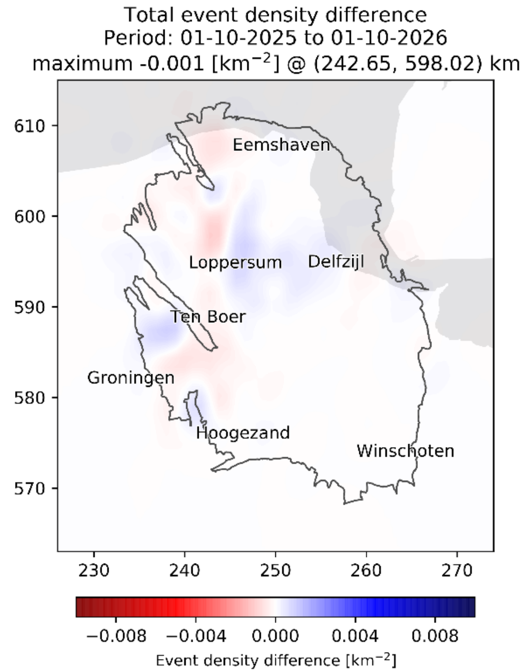

Difference

(Operational Strategy 2 – Operational Strategy 1)

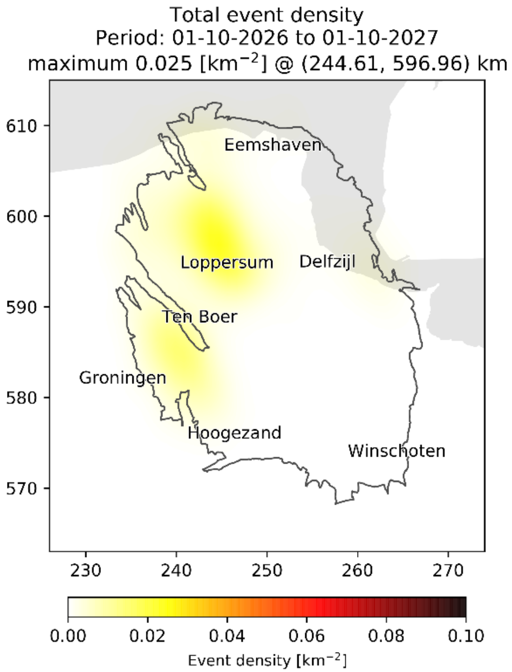

Operational Strategy 2

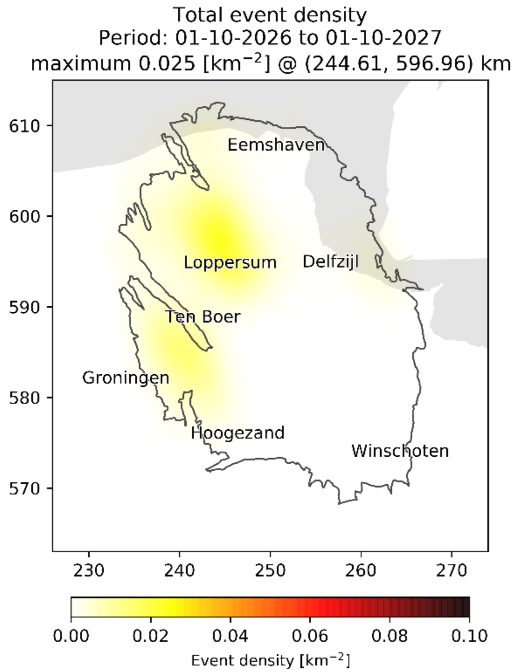

Operational Strategy 1

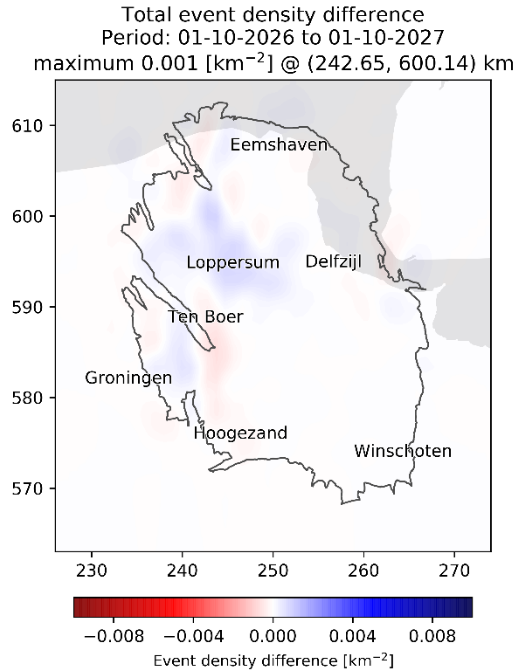

Difference

(Operational Strategy 2 – Operational Strategy 1)

2026/2027

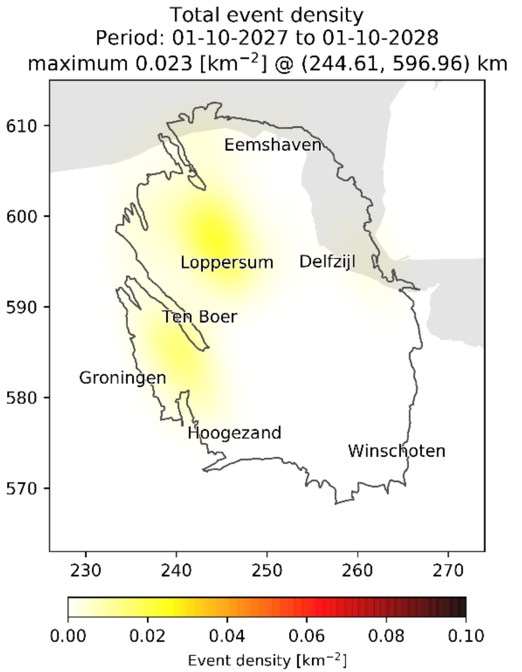

Operational Strategy 2

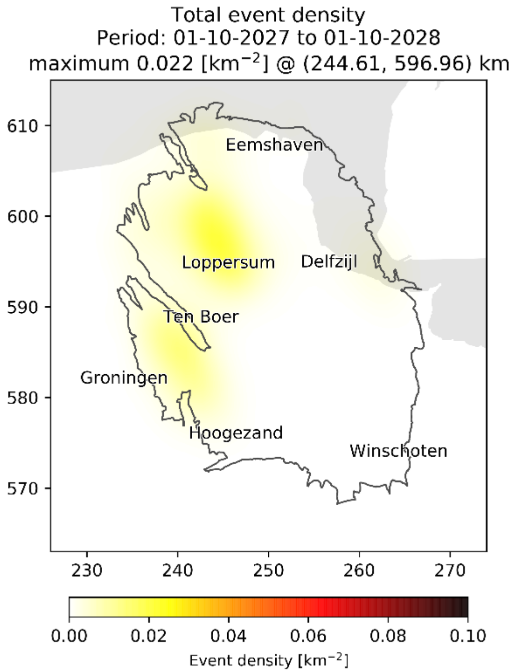

Operational Strategy 1

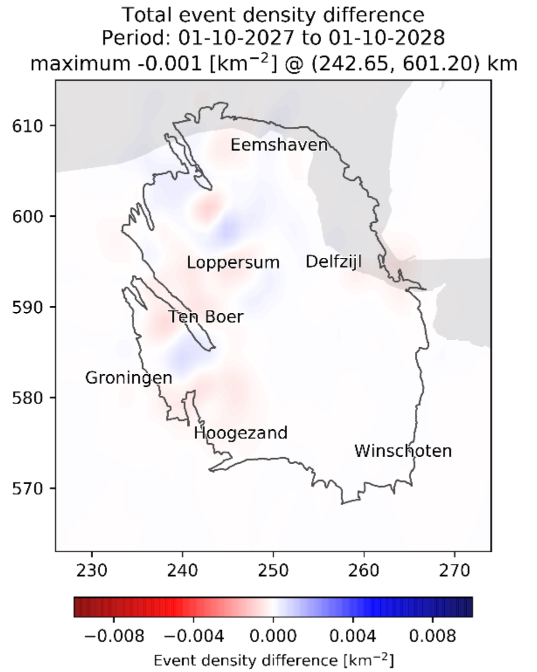

Difference
(Operational Strategy 2 – Operational Strategy 1)

2027/2028

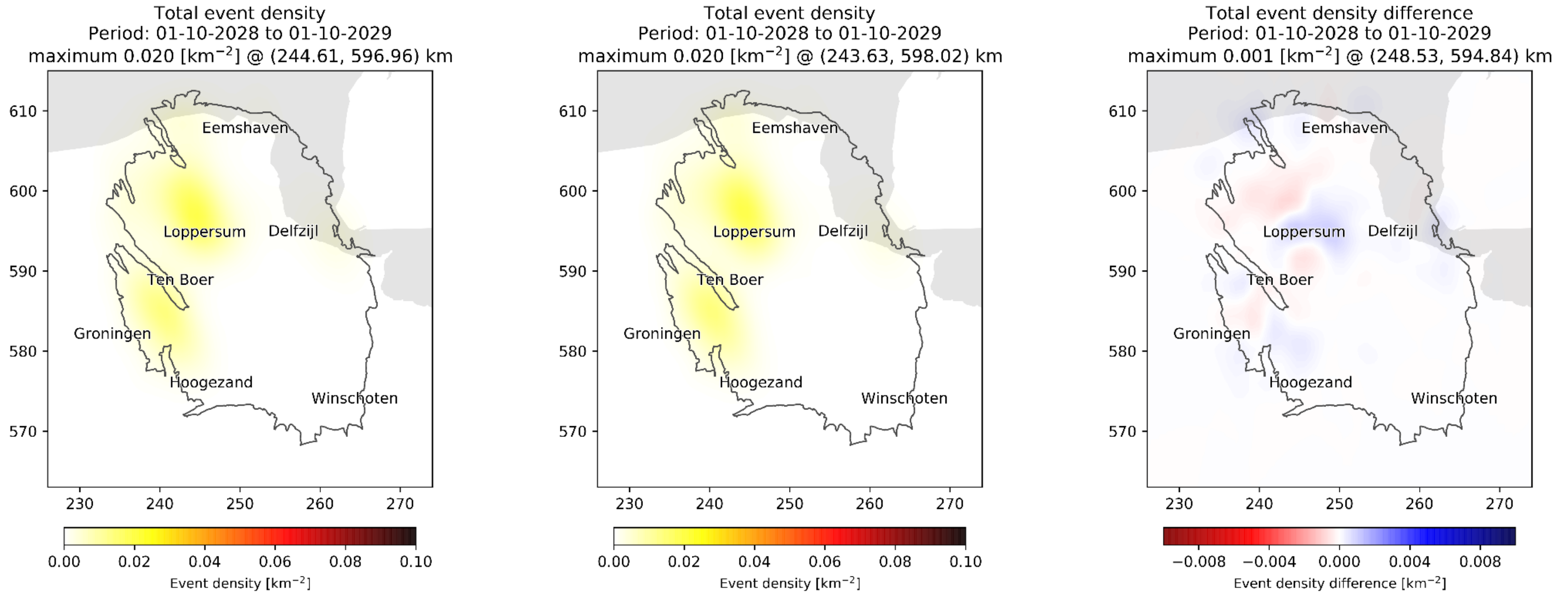

Operational Strategy 2

Operational Strategy 1

Difference

(Operational Strategy 2 – Operational Strategy 1)

2028/2029

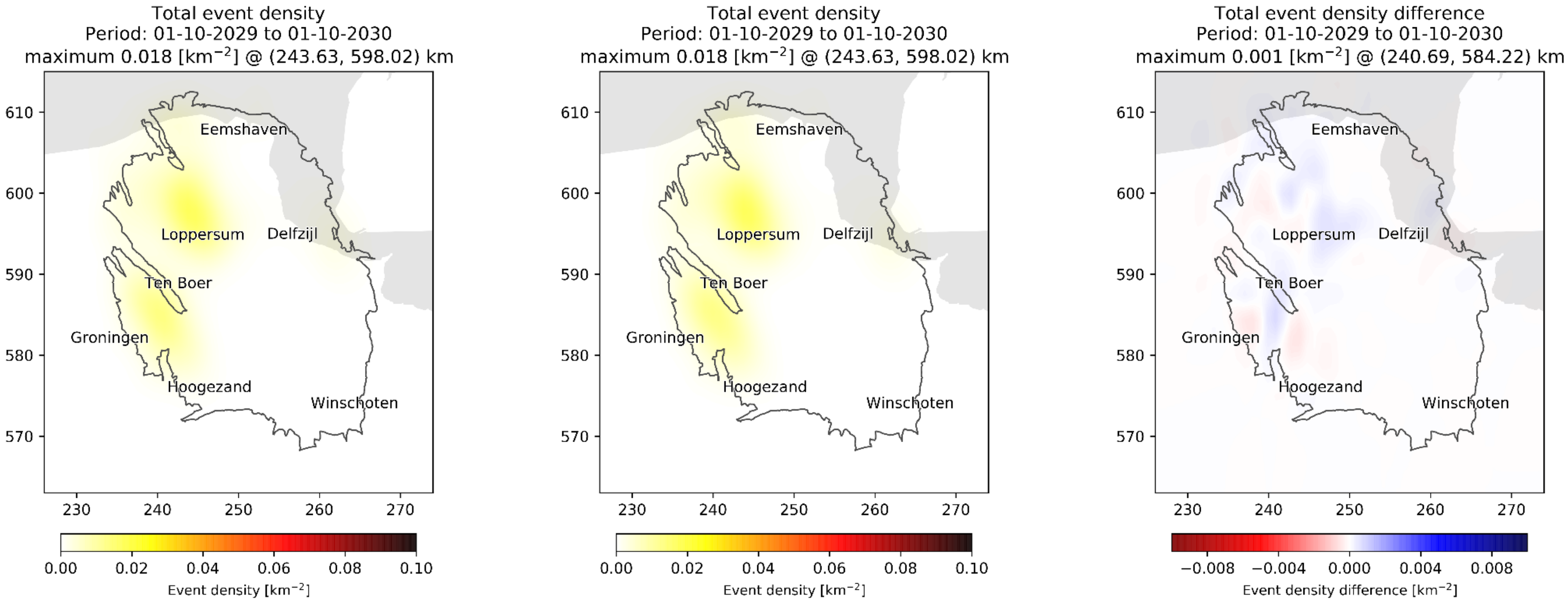

Operational Strategy 2 | **Operational Strategy 1** | **Difference** (Operational Strategy 2 – Operational Strategy 1)

2029/2030

Figure 5.5 Annual event density maps for the two optimised Operational Strategies compared. These maps are based on the production profile “GTS-raming 2020” for an average temperature year.

6 Seismic Hazard Assessment

6.1 Hazard metrics

Different metrics have been proposed to describe the hazard resulting from seismic activity. Most commonly used are the peak ground velocity (PGV) and peak ground acceleration (PGA). In the current report, the hazard assessment is based on Ground Motion Prediction Methodology (GMM) Version 6 (Ref. 38 and Ref. 39).

6.1.1 Risk Assessment

Peak Ground Acceleration (PGA) is a widely used metric for ground shaking intensity and was chosen as the most appropriate hazard metric for the seismic hazard assessment in support of the assessment of risk. Figure 6.1 shows the measured acceleration near the epicentre during the Huizinge earthquake of 16th August 2012. For the assessment of the response of a building to ground shaking average spectral acceleration (AvgSa) is used. It is the mean of the sum of the natural logarithms of spectral acceleration at 10 different periods of vibration. Ground Motion Prediction methods have therefore focused on prediction of PGA and spectral acceleration at several periods. These are the most important hazard parameters for the prediction of full or partial building collapse, failure of building elements and hence for personal risk.

6.1.2 Building Damage Assessment

For the assessment of the potential to cause building damage at lower damage states (see section 8 of this report), velocity-based hazard metrics such as PGV (Peak Ground Velocity) are also important. Empirical evidence elsewhere has shown that building damage at lower damage states (damage states DS1 and DS2) correlates strongly with PGV. A Groningen-specific (induced) ground motion prediction method to estimate the value of PGV at specific locations has therefore been developed as part of the Ground Motion Prediction Methodology since version 4. The assessment of PGV is primarily in support of assessment of building damage due to historical earthquakes and expected future damage.

The official Dutch guidelines for assessing the impact of vibrations on buildings, as presented in the document "Building Damage: Measurement and Assessment" by the SBR (Ref. 61), are based on the ground velocity metric V_{TOP}. To ensure consistency with the SBR Guidelines, apart from the geometric mean velocity also a ground motion prediction method for the V_{TOP} parameter (the 'maximum' value of PGV in any direction) was developed.

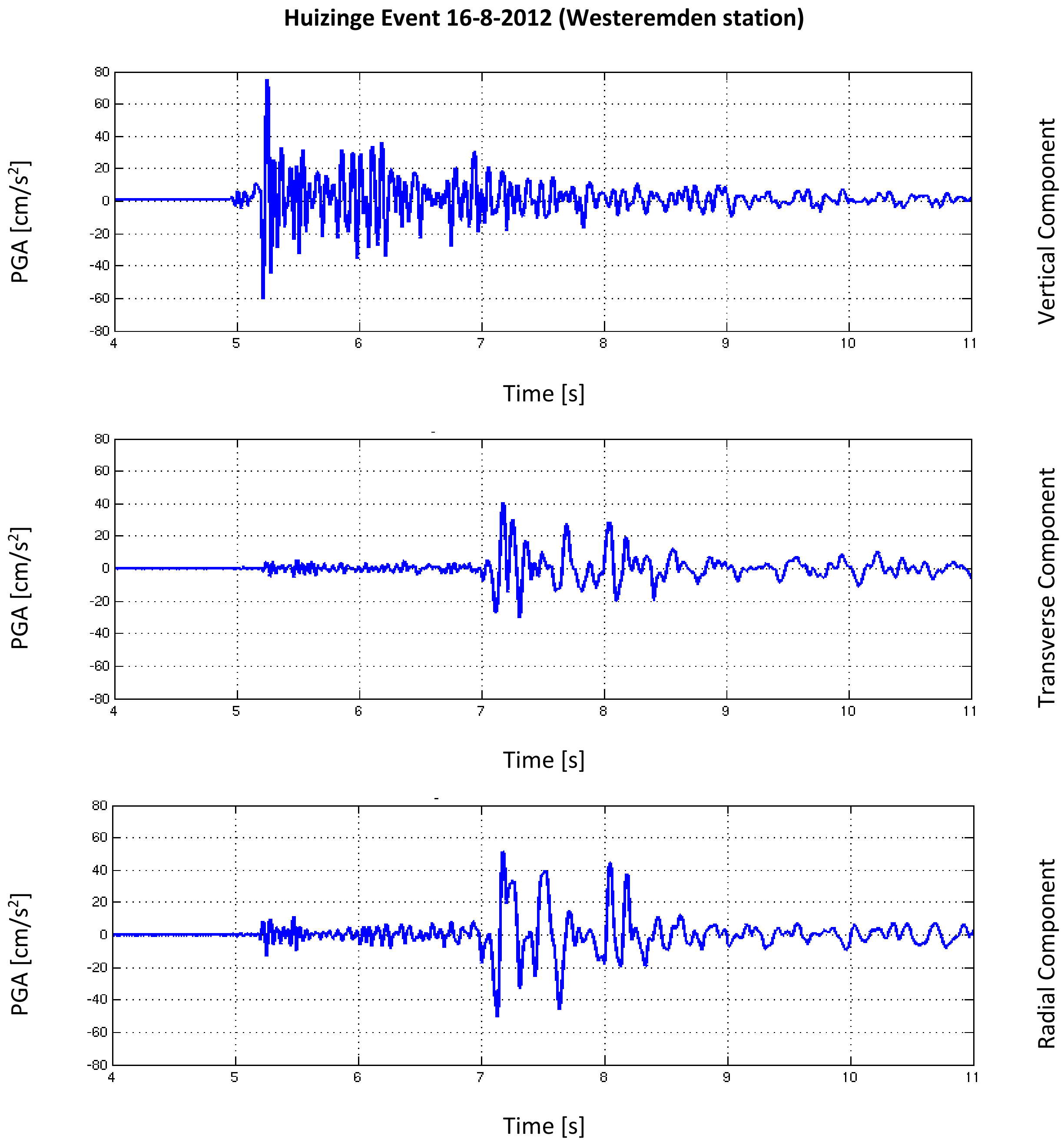

Figure 6.1 *Accelerogram of the earthquake near Huizinge recorded at the 16th August 2012 by the accelerometer located near Westeremden (near the epicentre).*

6.1.3 Hazard Map for Peak Ground Acceleration

For the probabilistic description of the ground accelerations (PGA, or generalised to Pseudo Spectral Acceleration, PSA), a hazard map is used. On this map for each location the acceleration is plotted that could occur, with a prescribed annualised probability of exceedance (exceedance level), during a prescribed analysis period. Hazard levels are shown using a gradual colour scale.

The hazard maps shown in this document were constructed according to the following procedure. Each location in the analysis area during the analysis period is subjected to ground motion accelerations resulting from induced earthquakes. At some locations at the centre of the field, e.g. near Loppersum, the chance of exceeding a given peak ground acceleration threshold is higher than at the periphery of the field, e.g. in Groningen city (Fig. 6.2).

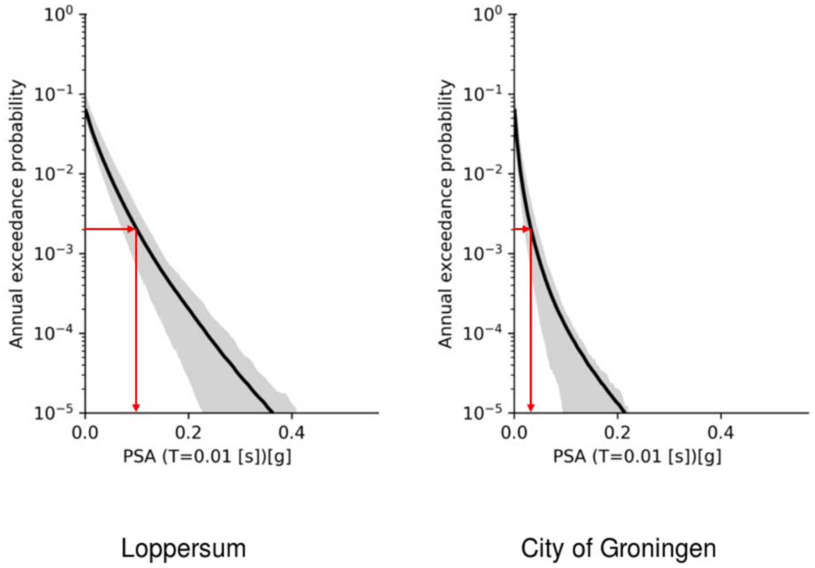

Figure 6.2 *Hazard curves for the average temperature profile gas-year 2020/2021 of GTS-raming 2020 for operational strategy 1 for two different locations in the Groningen area. Left for the village of Loppersum. Here the probability of being exposed to an acceleration exceeding larger than 0.09 g is 0.2% per year. On the right the hazard curve for the city of Groningen, the acceleration with an exposure of 0.2% per year is lower at 0.03 g. The black line notes the mean hazard curve, whereas the grey area notes the 80% prediction interval.*

Equally, at any one location, the chance of exceeding some value of peak ground acceleration decreases with increasing peak ground acceleration. A set of hazard curves is shown for a number of locations in figure 6.3. Each declining line indicates the hazard curve for a single location in the field.

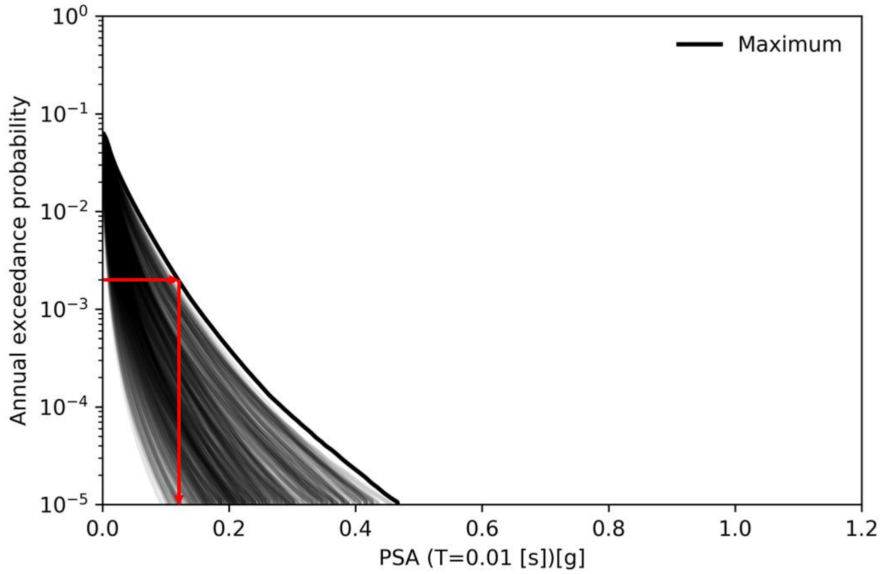

Figure 6.3 *A set of hazard curves showing average annual exceedance rate for peak ground acceleration at different locations in the field. Each line corresponds to a location in the field. The bold line indicates the maximum PGA anywhere within the field for a given exceedance level (bounding envelope). In this figure, the red line indicates that for an exceedance level of 0.2%/year the highest PGA in the field is 0.119 g. This plot was prepared based on the average temperature production profile of GTS-raming 2020 for Operational Strategy 1.*

To prepare a hazard map, an exceedance level needs to be chosen. This is not a purely technical choice. However, inspired by Eurocode 8, part of the current technical standards for structural design in Europe, it has become common practice to prepare hazard maps for an exceedance level of 0.2%/year. This exceedance level is equivalent to a 475-year return period for stationary seismicity. The same exceedance level is also used by KNMI for their hazard maps, which allows for comparison of these hazard maps. The choice of the exceedance levels (or return period) is only for the representation of the hazard. This choice of exceedance level does not affect the subsequent assessment of risk. Hazard maps can also be prepared for spectral acceleration at a specified period. The standard PGA hazard map is the same as the spectral acceleration hazard map at shortest period, which for this assessment was chosen at 0.01 s.

6.2 Hazard Assessment

Hazard maps have been prepared for the next ten gas-years starting at 1st October and running to 1st October a year later. Separate hazard maps are available for the production profile “GTS-raming 2020” at average temperature profile, cold temperature profile and warm temperature profile for gas-year 2020/2021.

The hazard map for the average temperature profile for each gas-year of the period 2020/2021 to 2029/2030 is shown in figure 6.4 a, b, c. The hazard is, as expected based on the declining gas production profile, also decreasing over this period. The trend in the largest PGA in these annual hazard maps is shown in figure 6.5. After gas-year 2021/2022, the differences between the largest PGA for the different temperatures profiles and operations strategies are very small (within 0.003 g from the case of average temperature and operations strategy 1).

However, this reduction in PGA is not evenly spread over all areas of the field. In the later years, the hazard is primarily located in the area North-West of Loppersum. This is consistent with the equilibration of reservoir pressures during these later years. The gas from the higher-pressure area to the North-West of Loppersum will continue to flow to the lower pressure South-Eastern area, causing a continued decrease of pressure in the former area. This effect of gas flow within the reservoir due to equilibration of pressure differences is referred to as the “remweg effect”. In theoretical remweg production profiles this effect has been demonstrated (Ref. 16). The hazard map for year 2020/2021 for production profile GTS-raming 2020, an average temperature year and operational strategy 1 is shown in large format in figure 6.6.

Figure 6.7 shows the impact of the operational strategy. Hazard maps for both operational strategies are shown for each year from 2020/2021 to 2029/2030, together with a difference map. The scales of the difference maps are set to +/- 1% of g. The impact of low and high temperature weather in 2020/2021 is shown in figure 6.8.

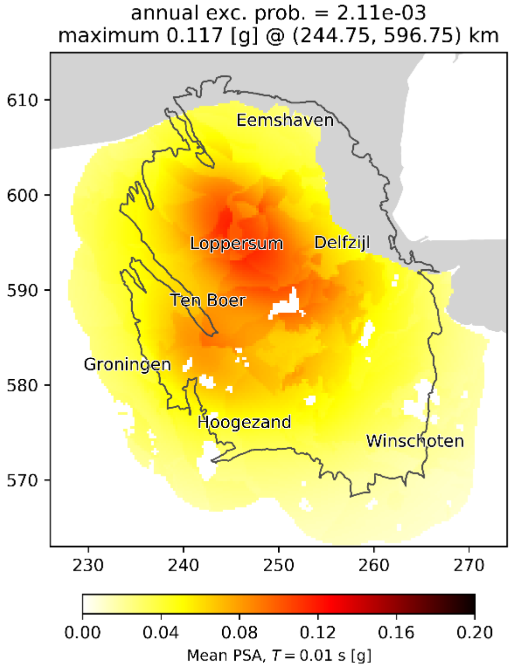

2020/2021

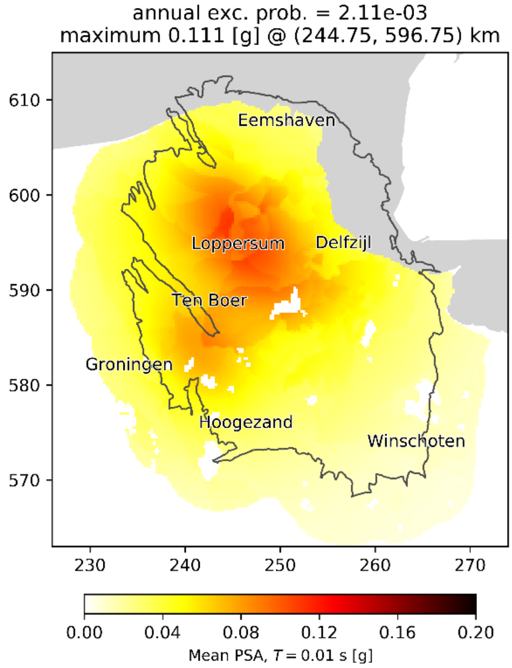

2021/2022

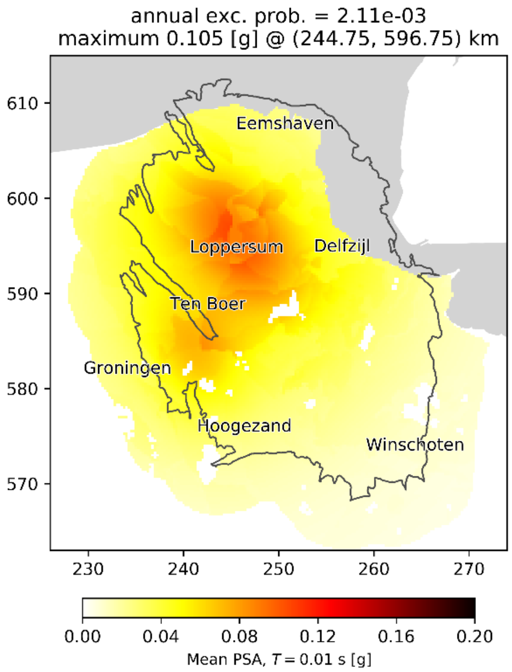

2022/2023

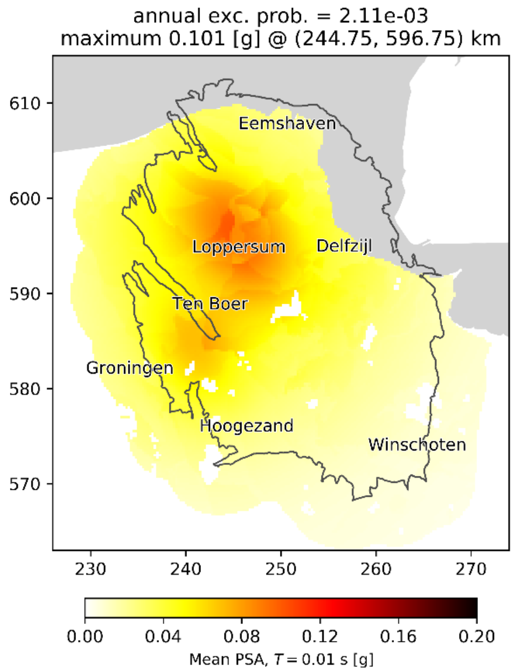

2023/2024

Figure 6.4a *Hazard Maps for the average temperature weather profile for the gas-years 2020/2021 (top – left), 2021/2022 (top – right), 2022/2023, (bottom – left) and 2023/2024 (bottom – right). The production profile for these hazard maps is “GTS-raming 2020, for an average temperature year and Operational Strategy 1. Note that water-bodies, such as the Schildmeer, are masked in these hazard maps.*

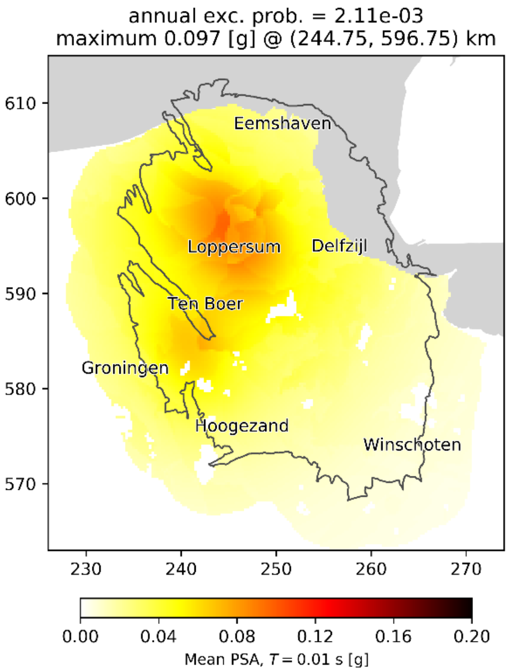

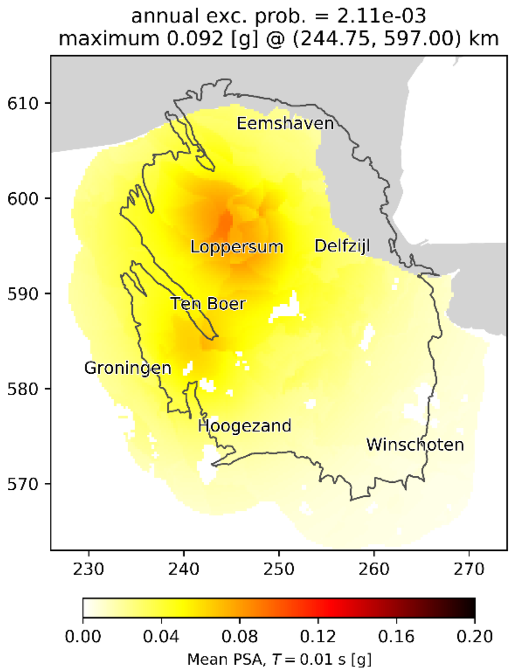

2024/2025

2025/2026

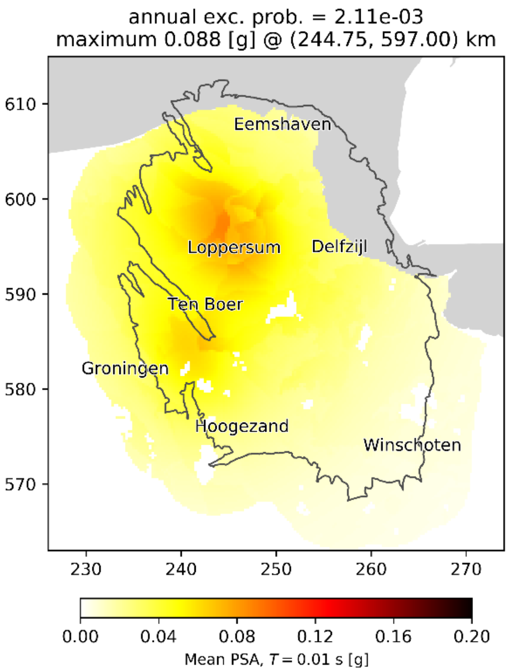

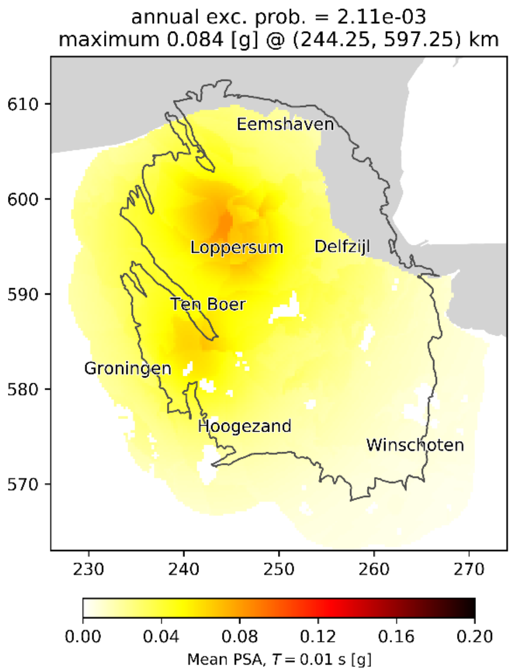

2026/2027

2027/2028

Figure 6.4b *Hazard Maps for the average temperature weather profile for the gas-years 2024/2025 (top – left), 2025/2026 (top – right), 2026/2027, (bottom – left) and 2027/2028 (bottom – right). The production profile for these hazard maps is "GTS-raming 2020, for an average temperature year and Operational Strategy 1.*

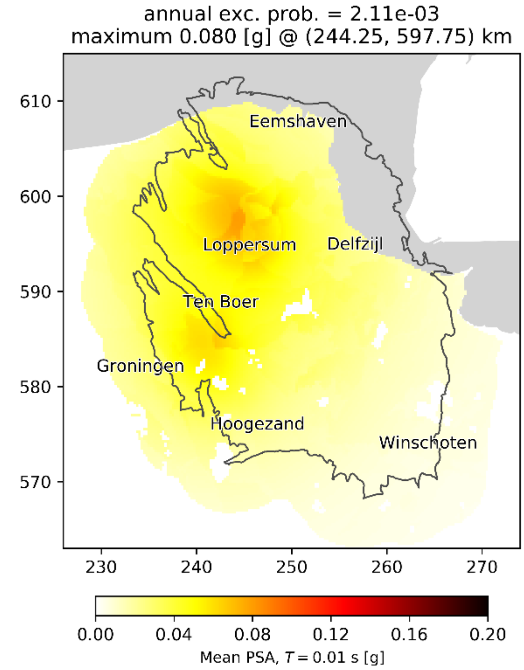

2028/2029

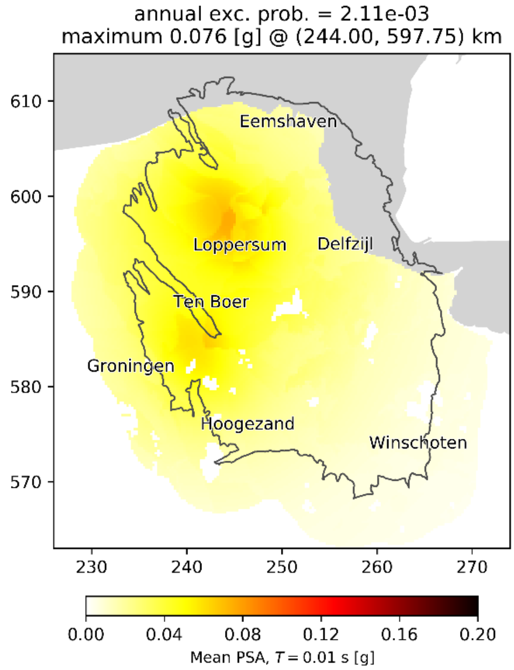

2029/2030

Figure 6.4c *Hazard Maps for the average temperature profile for the gas-years 2028/2029 (left), 2029/2030 (right). The production profile for these hazard maps is “GTS-raming 2020”, for an average temperature year and Operational Strategy 1.*

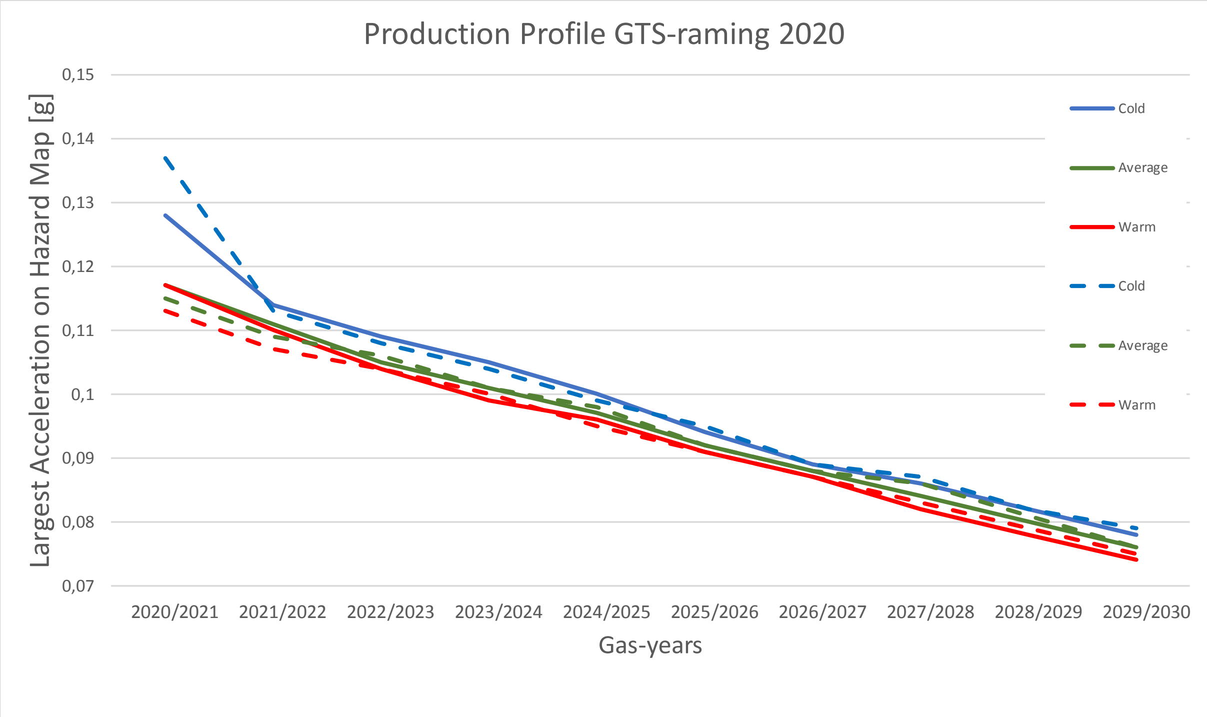

Figure 6.5 *Development over time of the largest PGA in the hazard maps. The largest PGA for each year in the hazard map for production profile “GTS-raming 2020 is plotted. Solid lines are for operational strategy 1 and dashed lines for operational strategy 2.*
The blue lines denotes the largest PGA for each year in the hazard map for the GTS-raming 2020 cold temperature profile.
The green lines denotes the largest PGA for each year in the hazard map for the GTS-raming 2020 average temperature profile.
The red lines denotes the largest PGA for each year in the hazard map for the GTS-raming 2020 warm temperature profile .

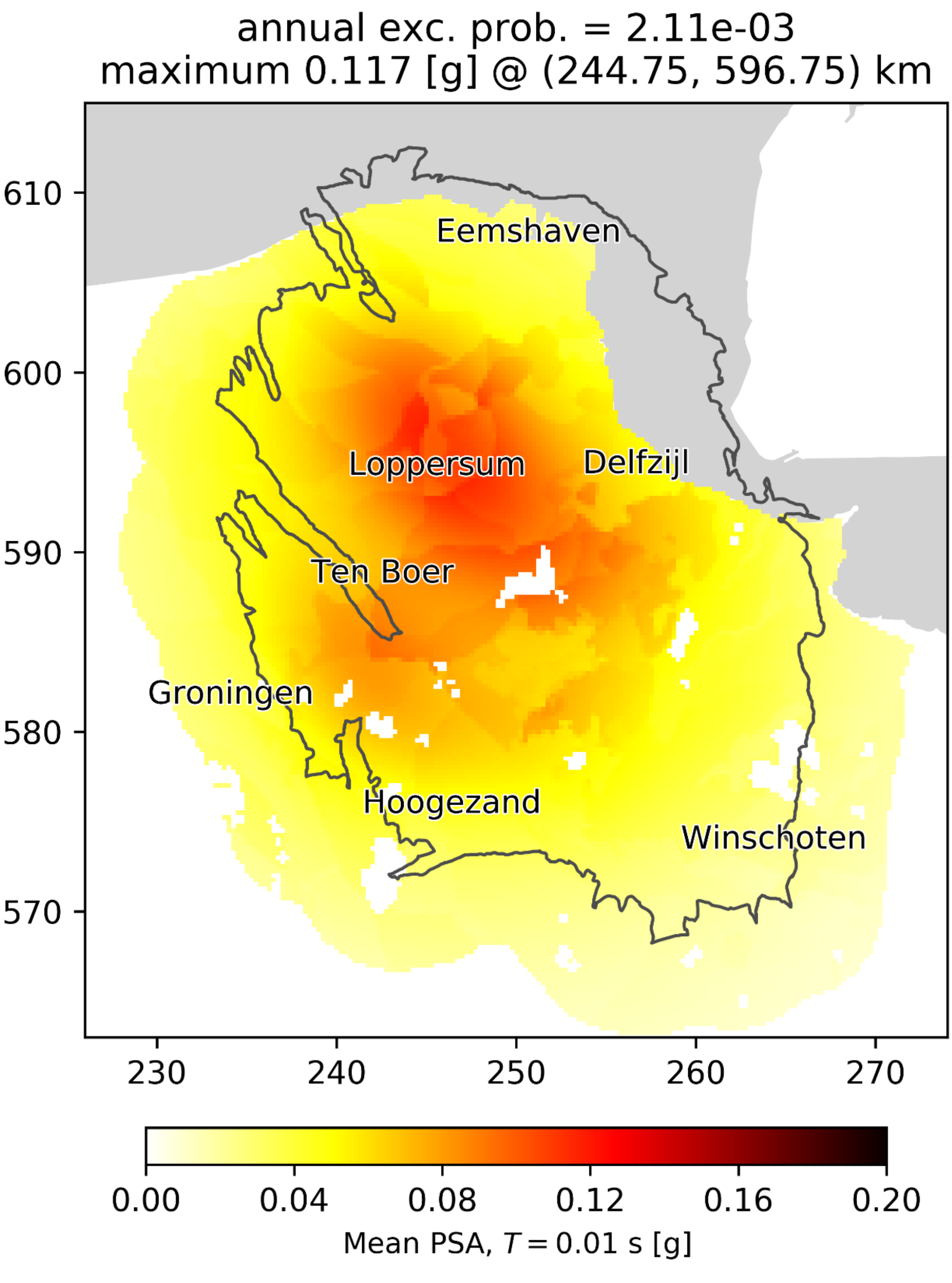

Figure 6.6 *Hazard Map for the average temperature weather profile for the gas-year 2020/2021. This is the same map as figure 6.4a (top-left) shown in a larger format. The production profile for these hazard maps is "GTS-raming 2020, for an average temperature year and Operational Strategy 1. Note that waterbodies, such as the Schildmeer, are masked in these hazard maps.*

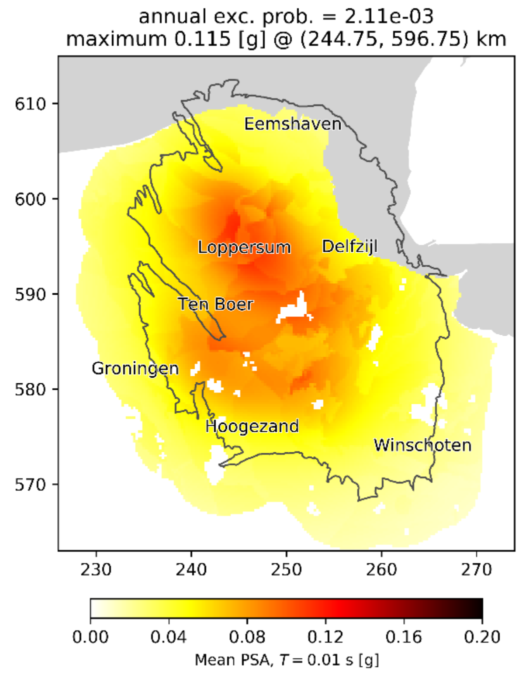

Operational Strategy 2

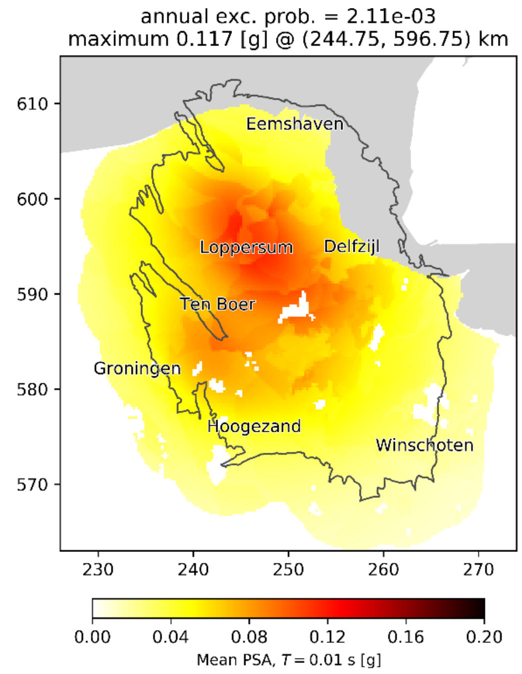

Operational Strategy 1

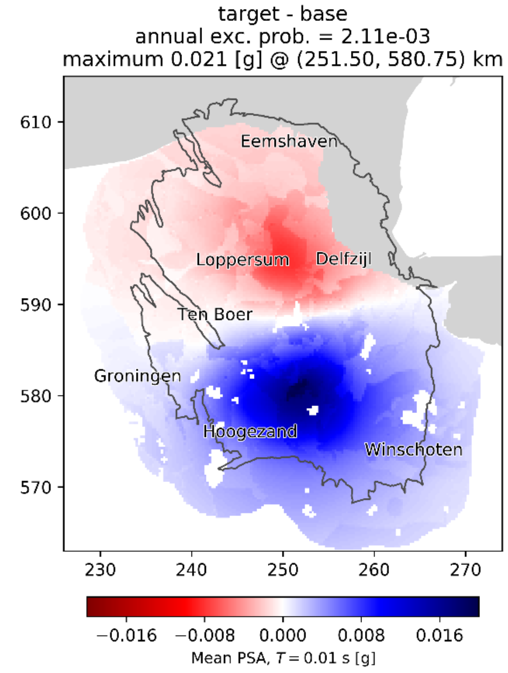

Difference

(Operational Strategy 2 – Operational Strategy 1)

2020/2021

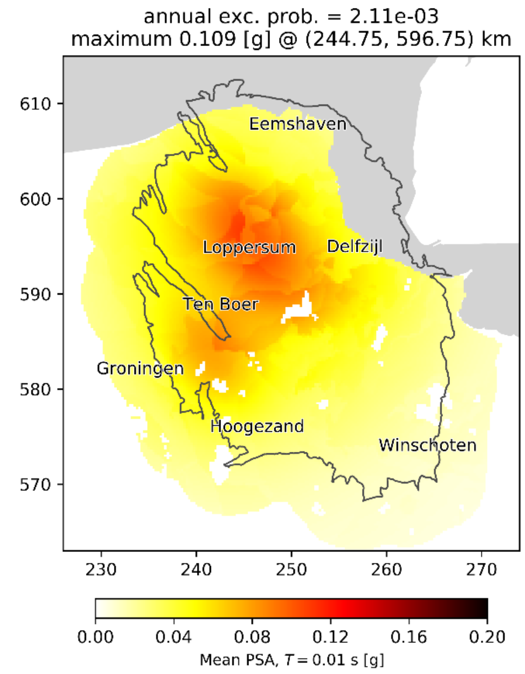

Operational Strategy 2

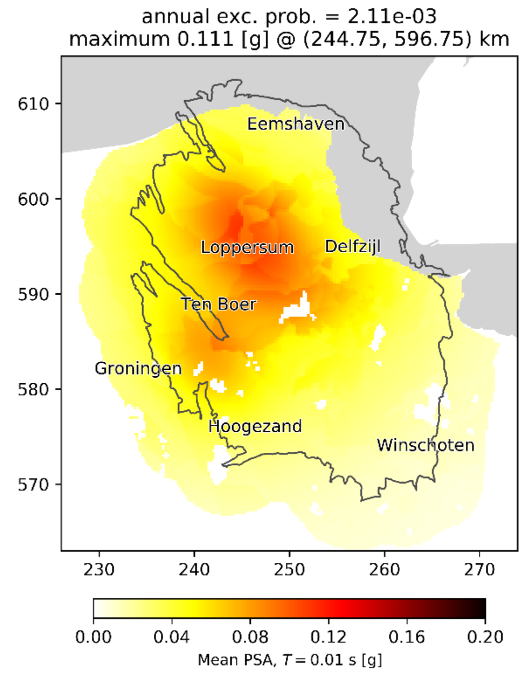

Operational Strategy 1

2021/2022

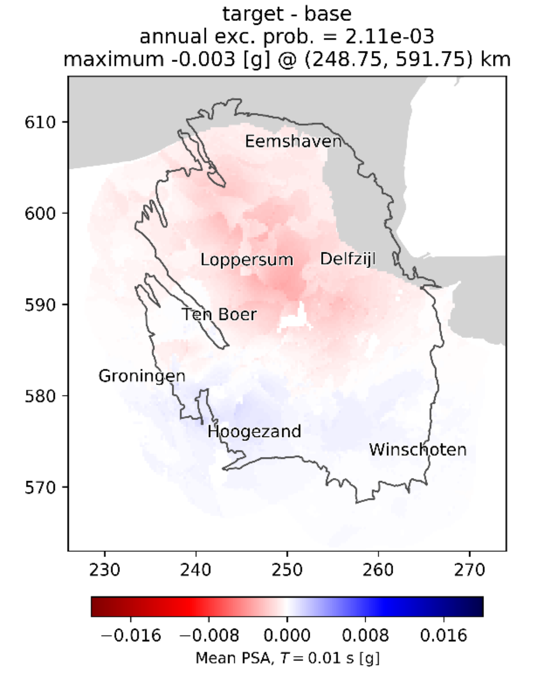

Difference

(Operational Strategy 2 – Operational Strategy 1)

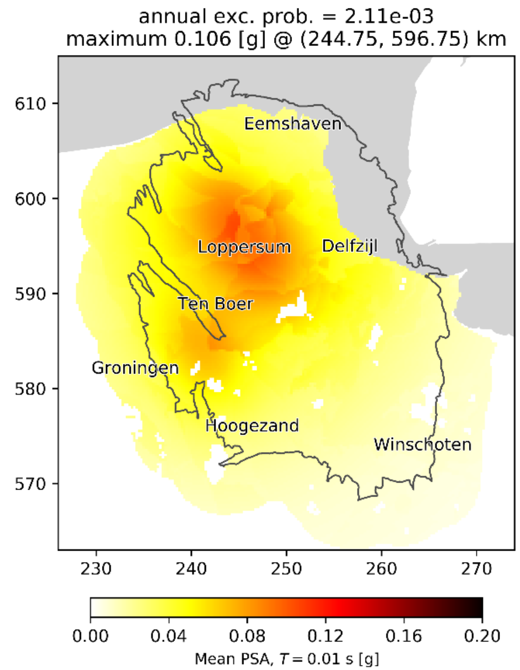

Operational Strategy 2

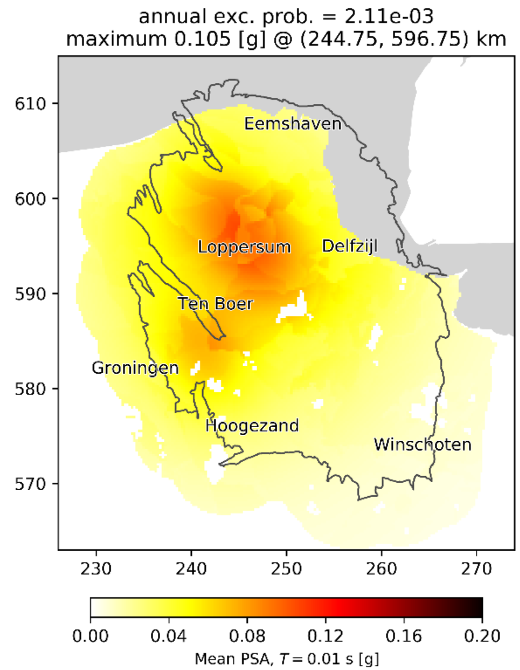

Operational Strategy 1

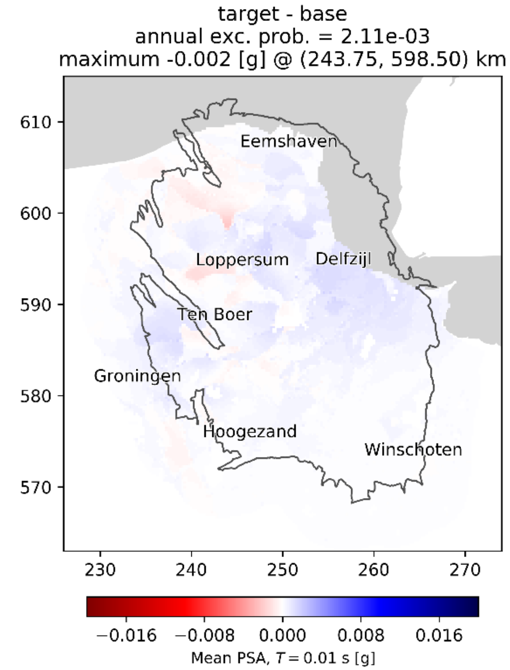

Difference

(Operational Strategy 2 – Operational Strategy 1)

2022/2023

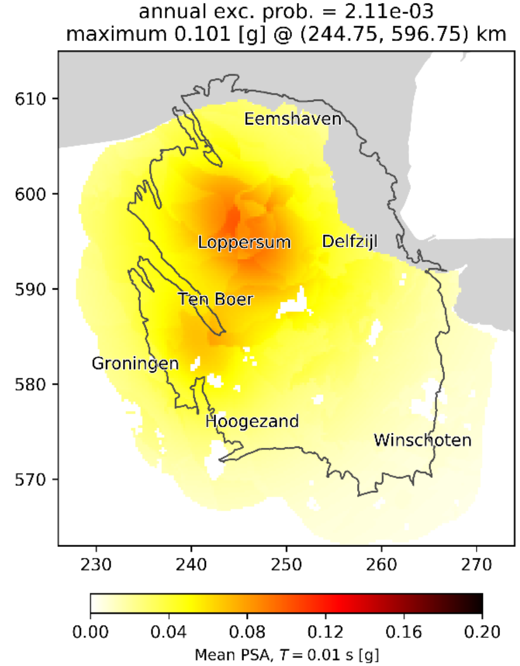

Operational Strategy 2

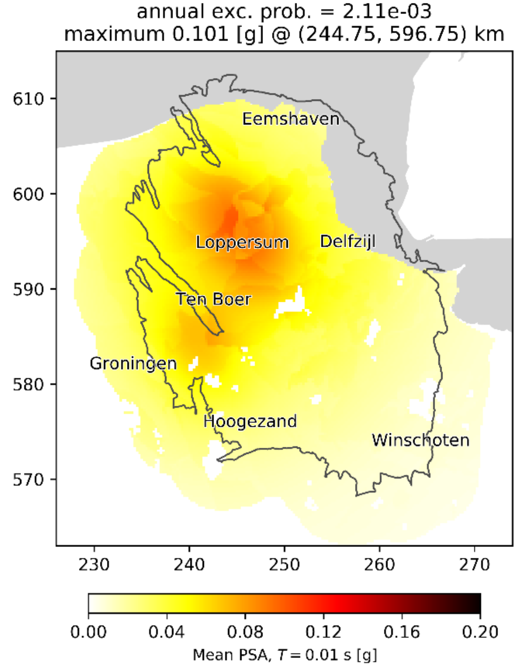

Operational Strategy 1

2023/2024

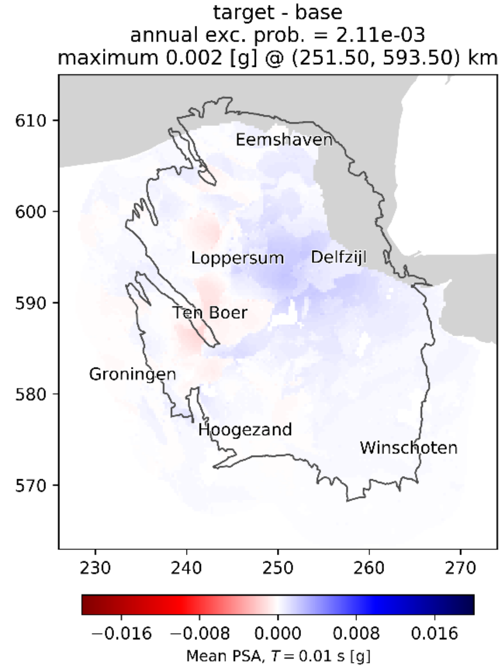

Difference

(Operational Strategy 2 – Operational Strategy 1)

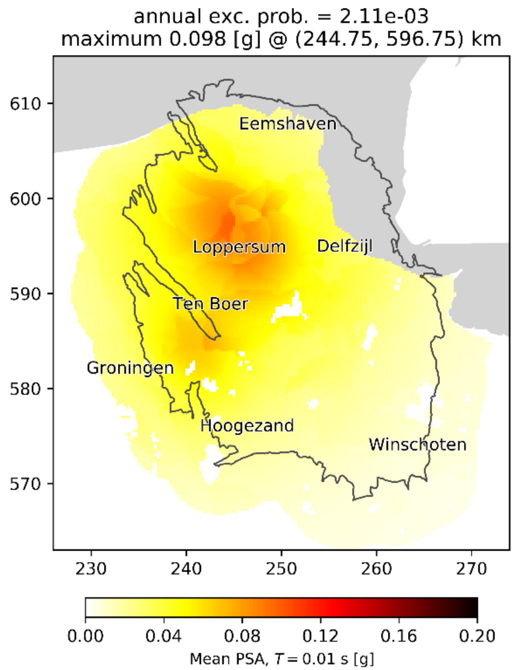

Operational Strategy 2

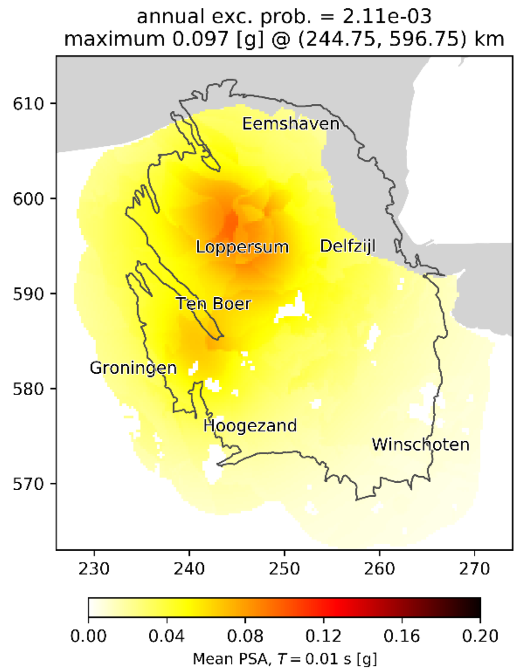

Operational Strategy 1

2024/2025

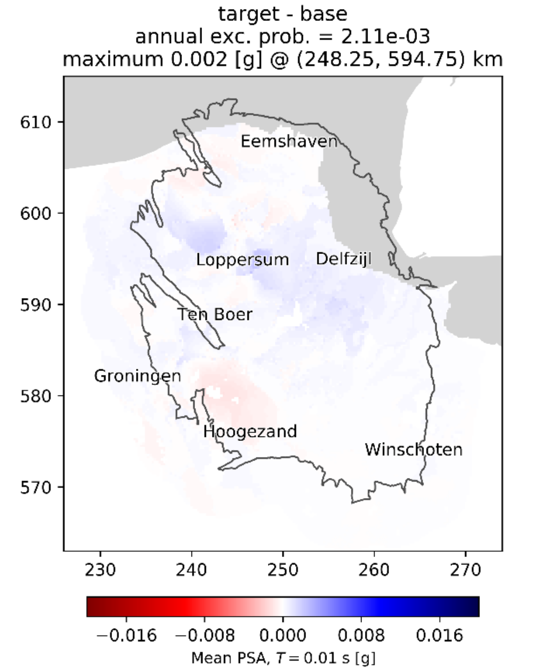

Difference

(Operational Strategy 2 – Operational Strategy 1)

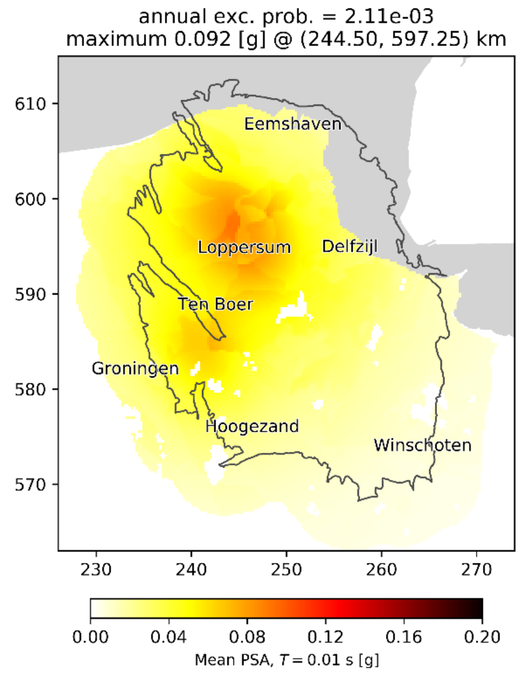

Operational Strategy 2

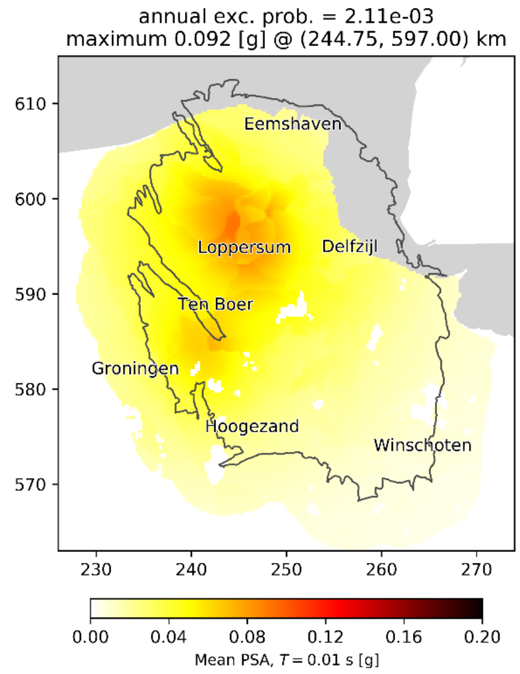

Operational Strategy 1

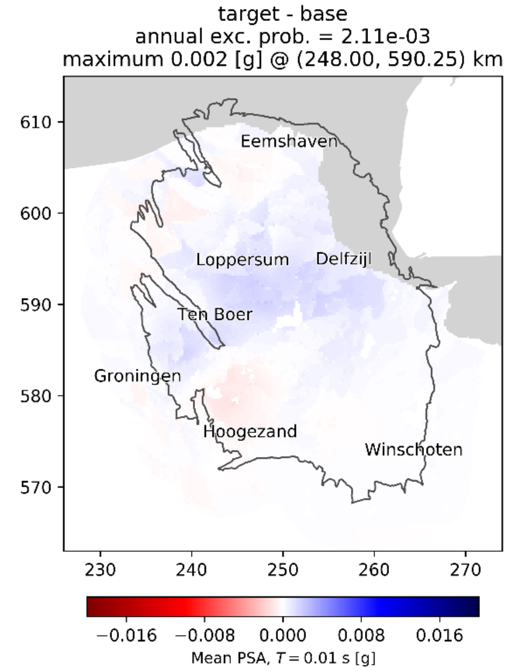

Difference

(Operational Strategy 2 – Operational Strategy 1)

2025/2026

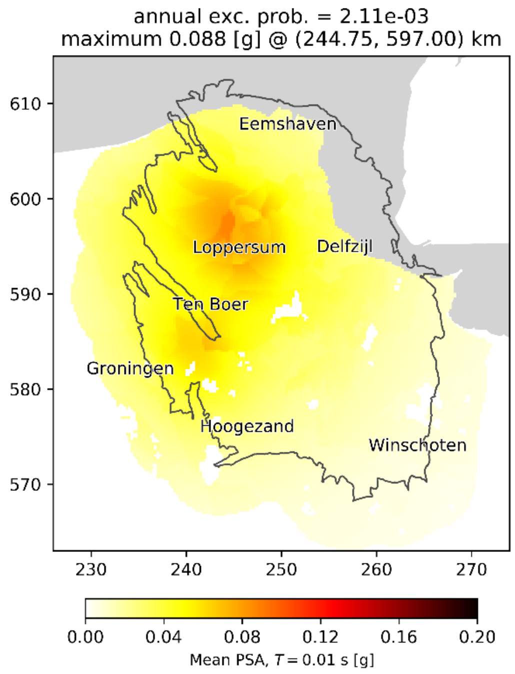

Operational Strategy 2

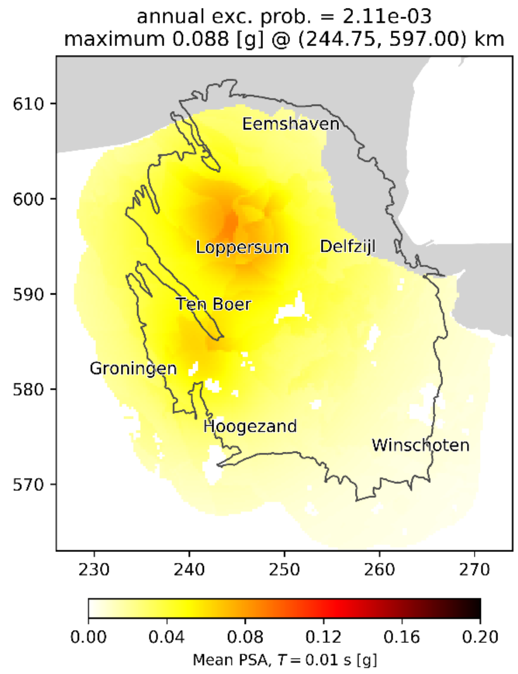

Operational Strategy 1

2026/2027

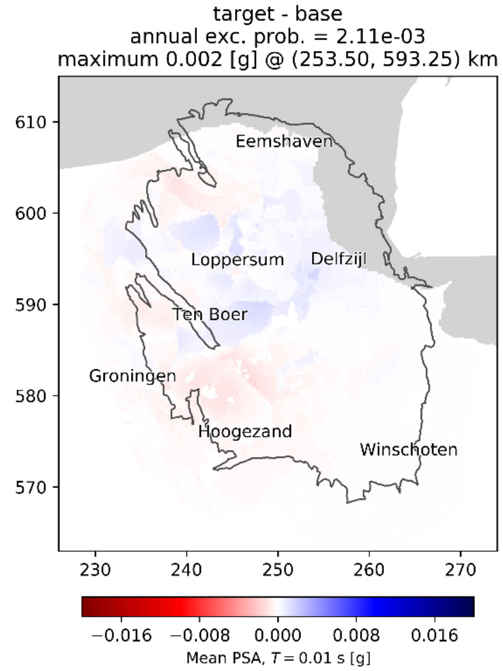

Difference

(Operational Strategy 2 – Operational Strategy 1)

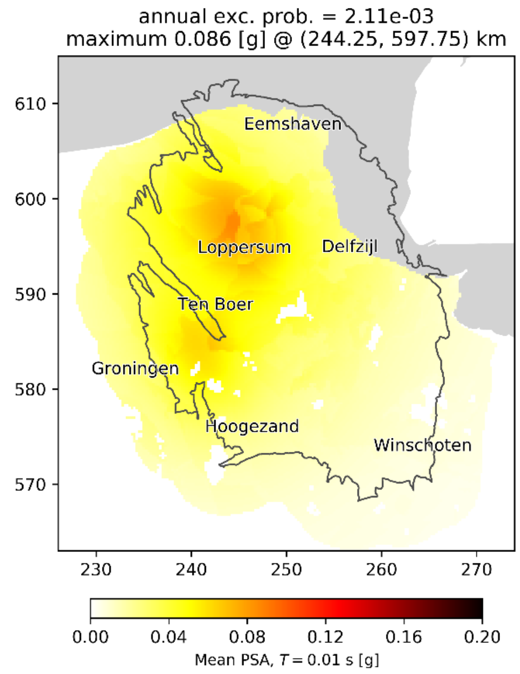

Operational Strategy 2

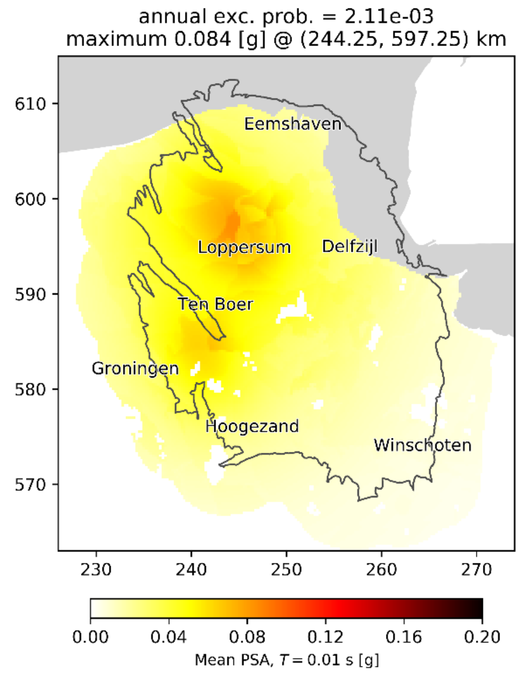

Operational Strategy 1

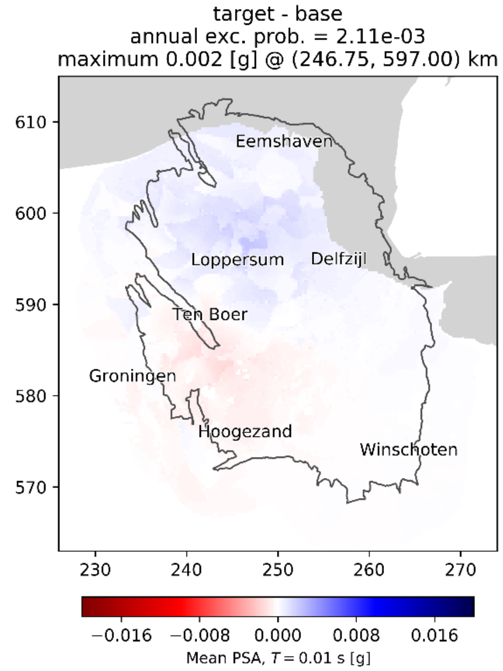

Difference

(Operational Strategy 2 – Operational Strategy 1)

2027/2028

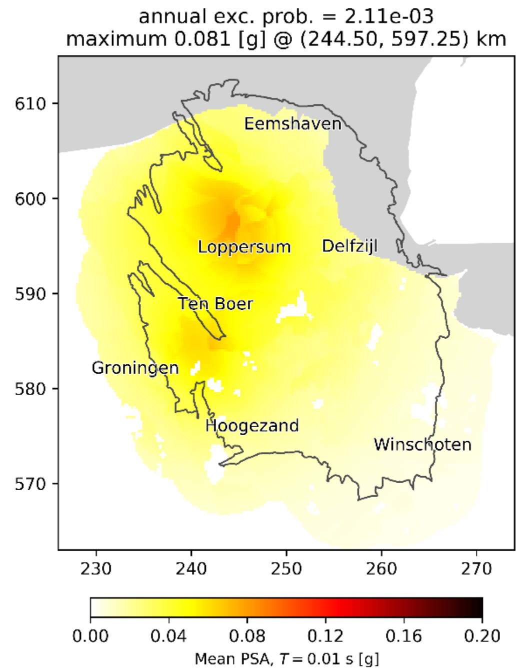

Operational Strategy 2

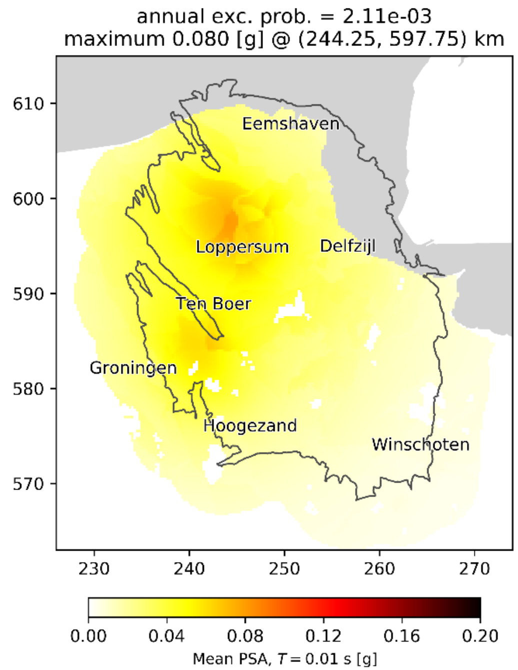

Operational Strategy 1

2028/2029

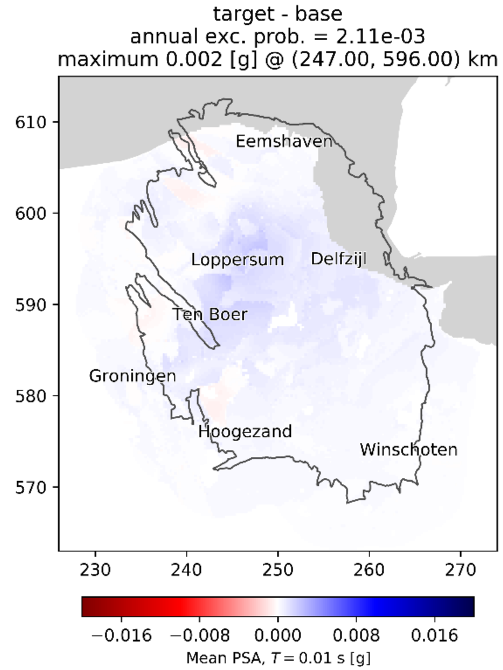

Difference

(Operational Strategy 2 – Operational Strategy 1)

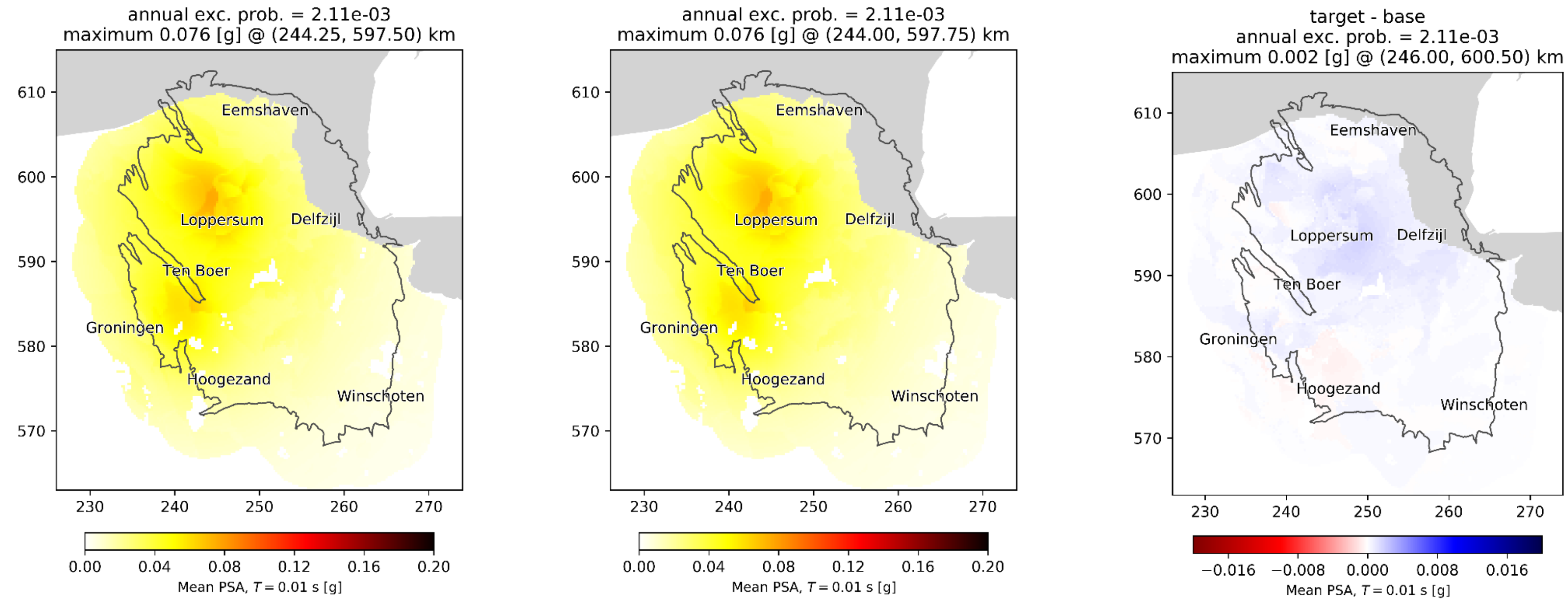

Operational Strategy 2 | **Operational Strategy 1** | **Difference** (Operational Strategy 2 – Operational Strategy 1)

2029/2030

Figure 6.7 Annual hazard maps for the two optimised Operational Strategies compared. These maps are based on the production profile "GTS-raming 2020" for an average temperature year.

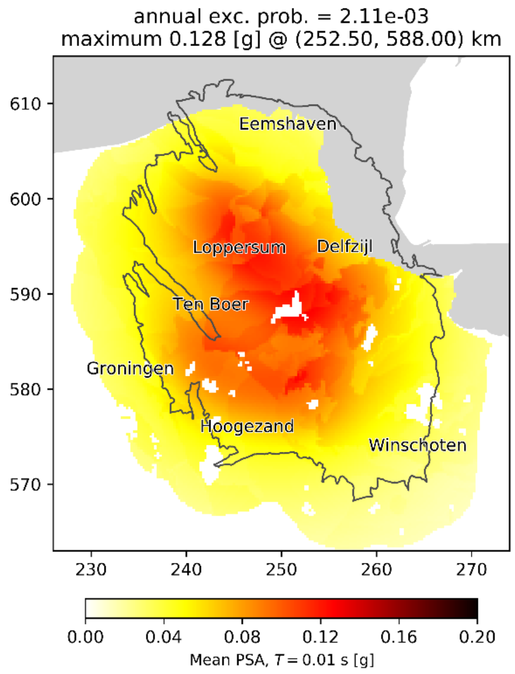

Cold Temperature

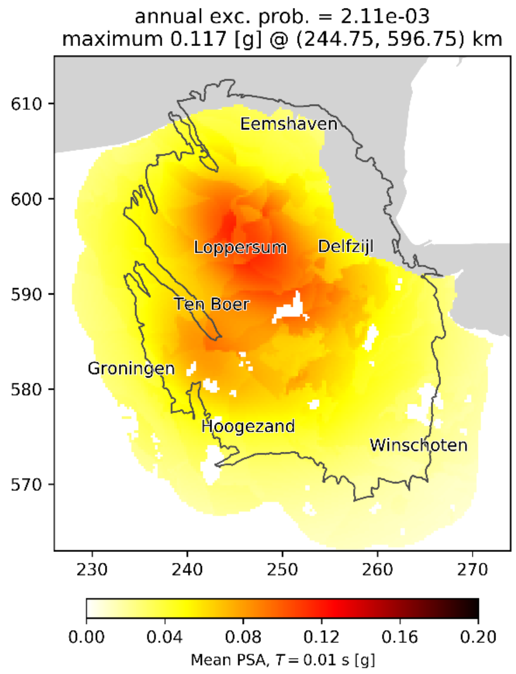

Average Temperature 2020/2021

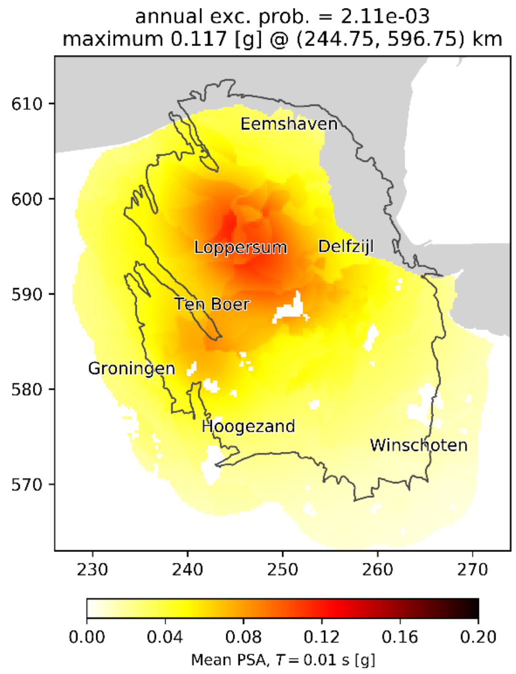

Warm Temperature

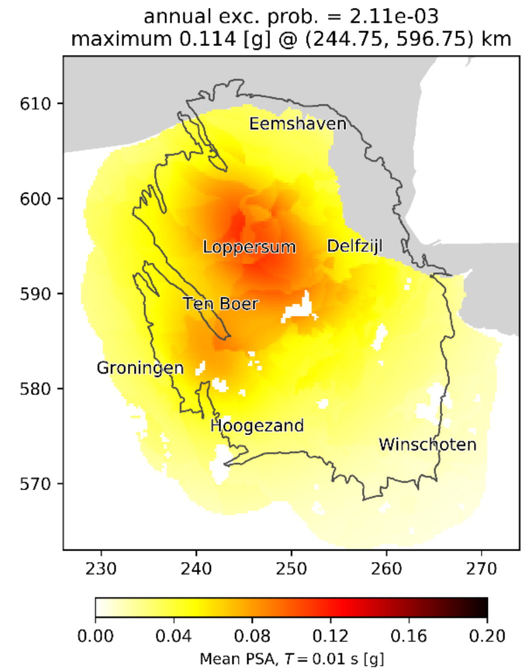

Cold Temperature

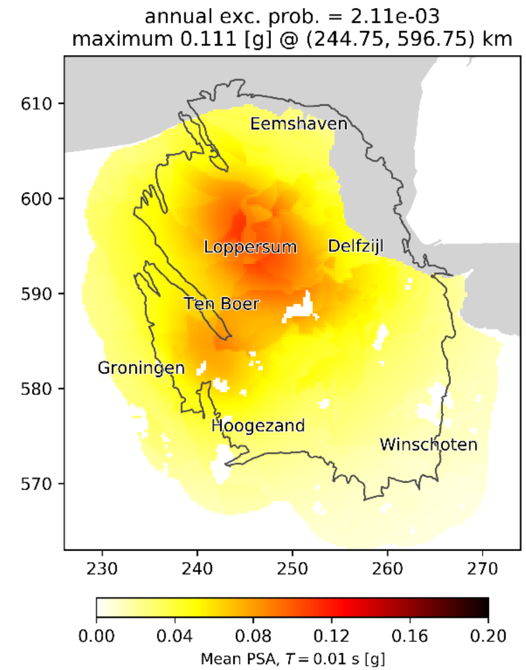

Average Temperature 2021/2022

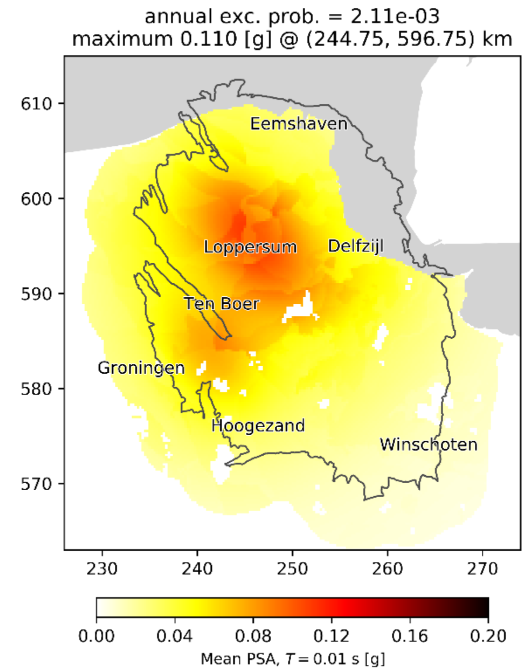

Warm Temperature

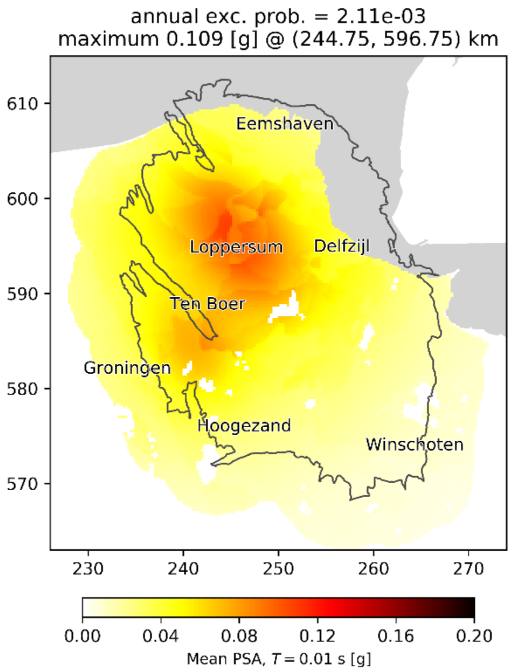

Cold Temperature

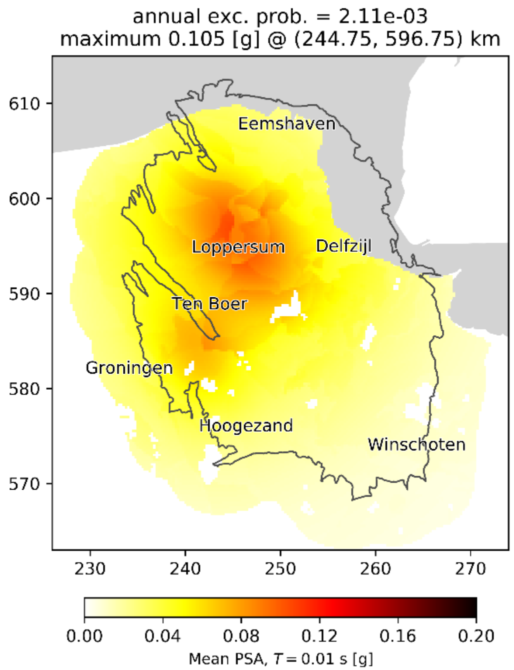

Average Temperature 2022/2023

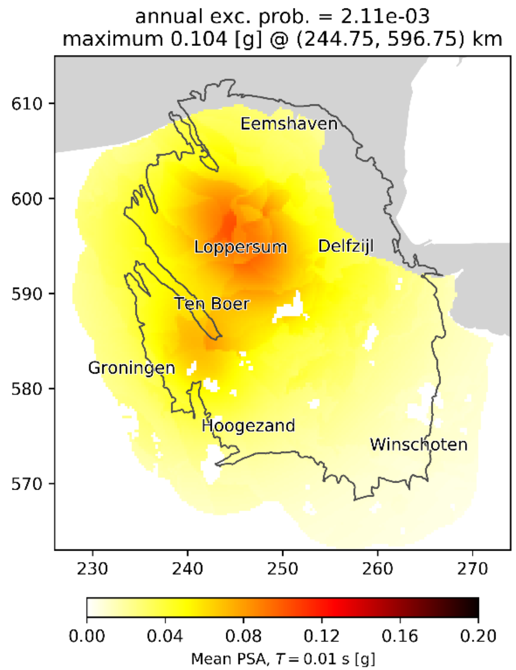

Warm Temperature

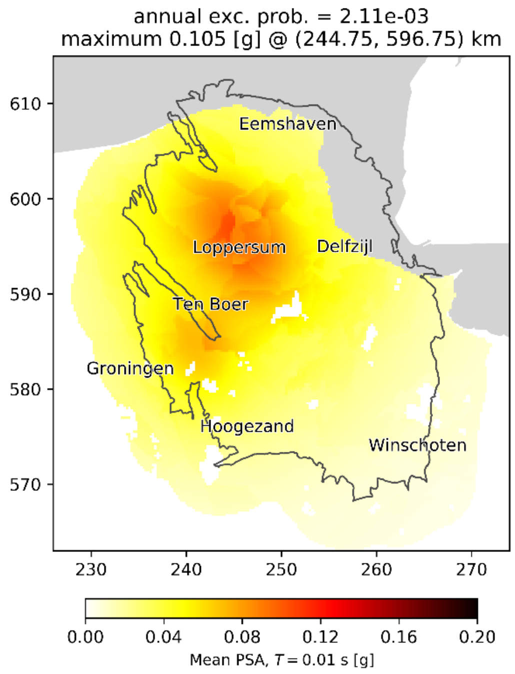

Cold Temperature

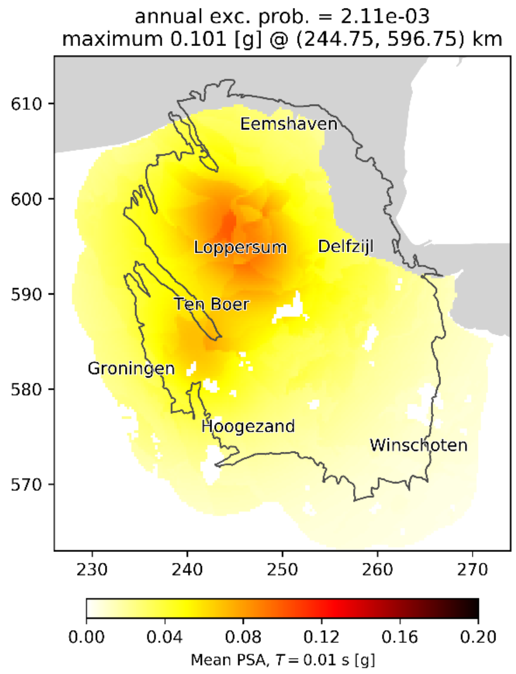

Average Temperature 2023/2024

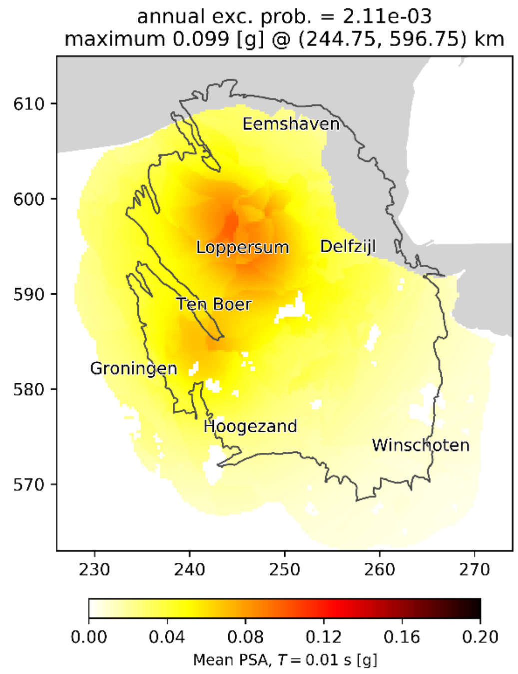

Warm Temperature

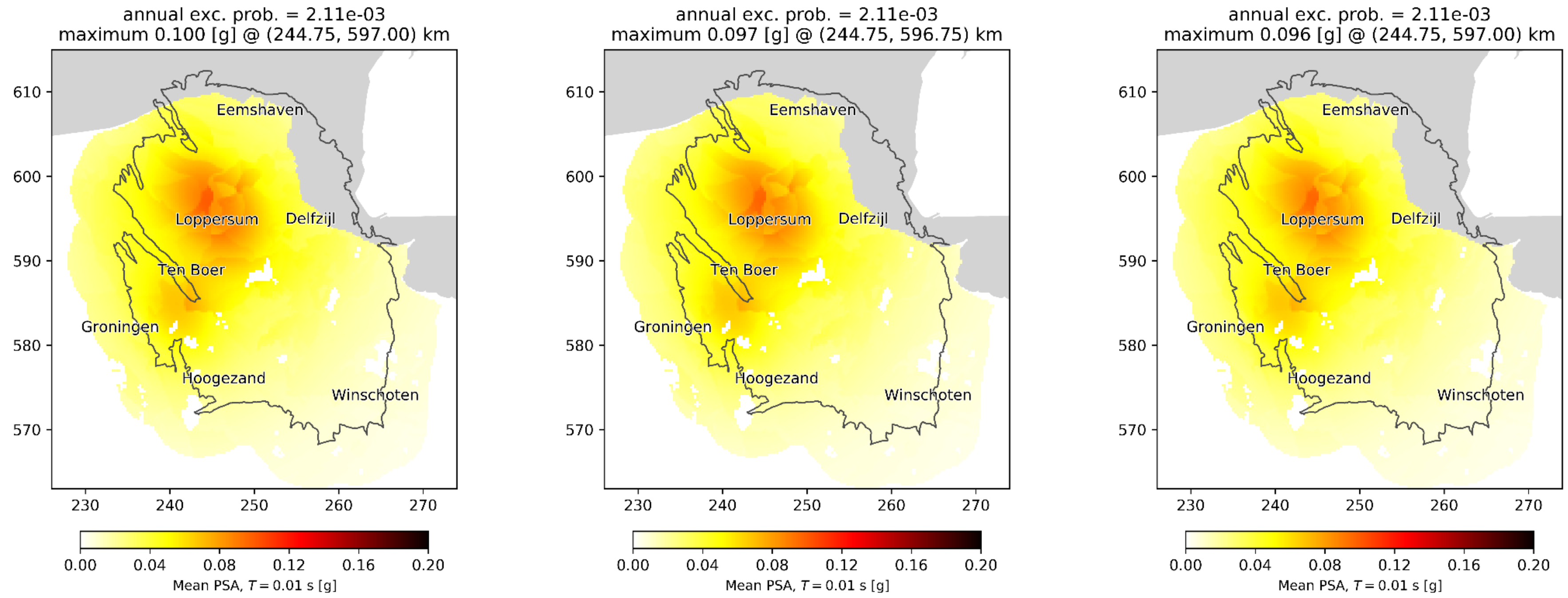

Cold Temperature

Average Temperature 2024/2025

Warm Temperature

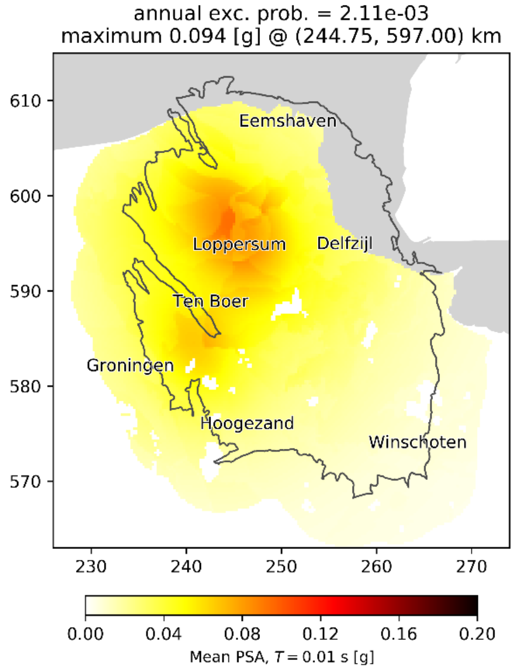

Cold Temperature

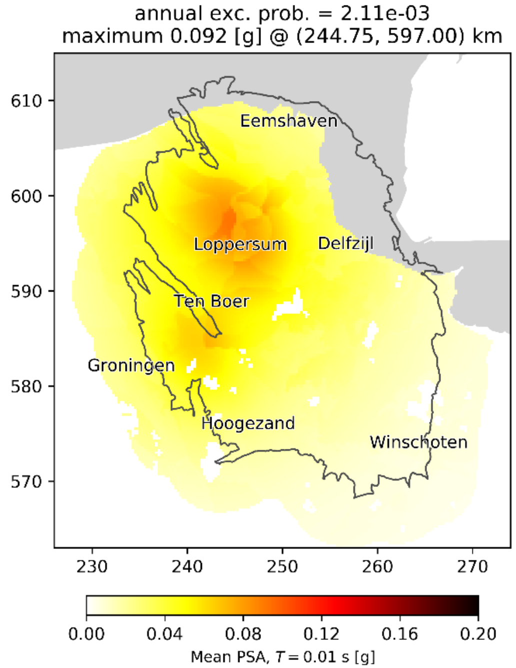

Average Temperature 2025/2026

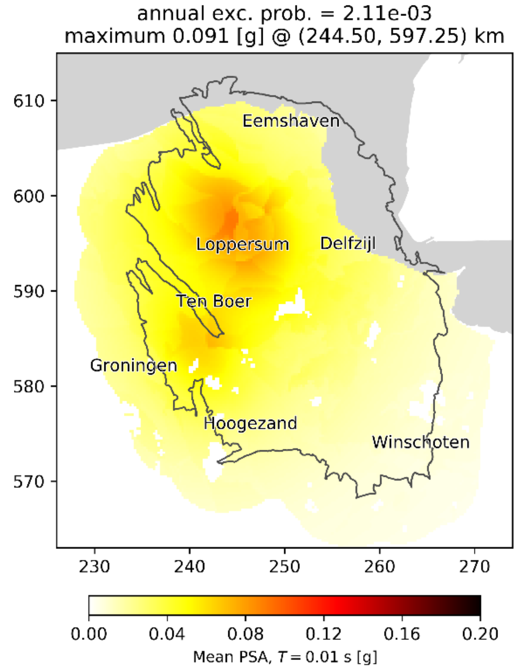

Warm Temperature

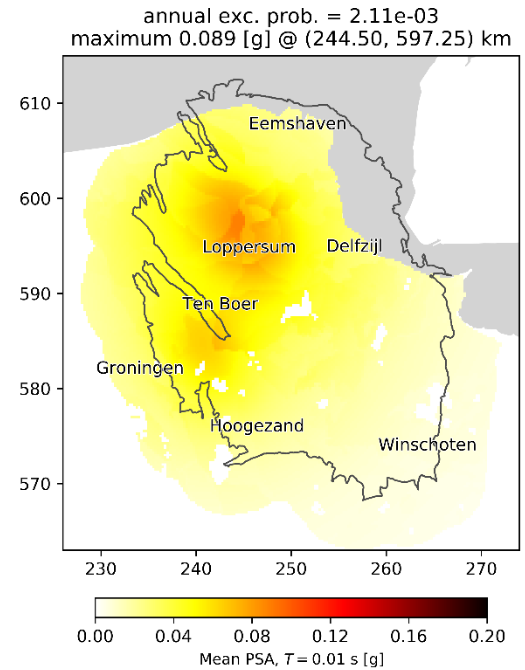

Cold Temperature

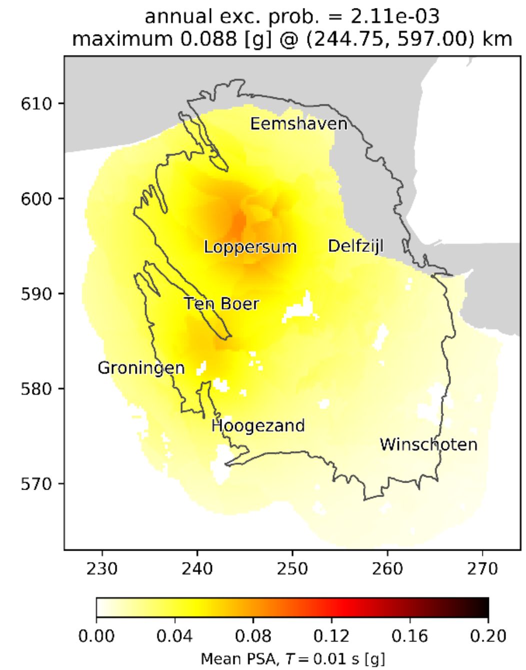

Average Temperature 2026/2027

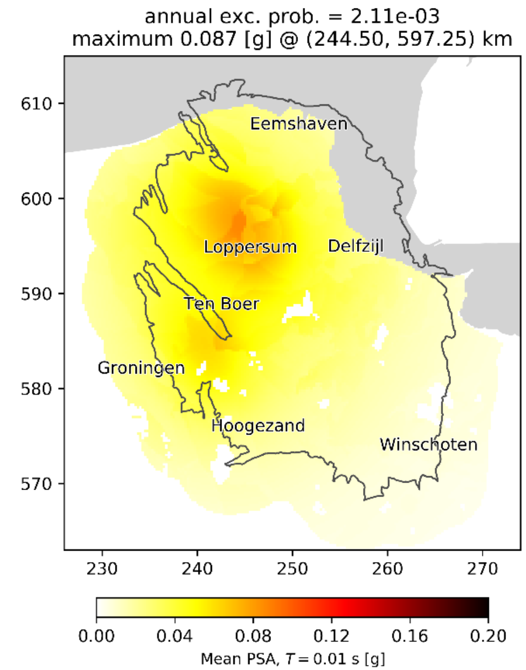

Warm Temperature

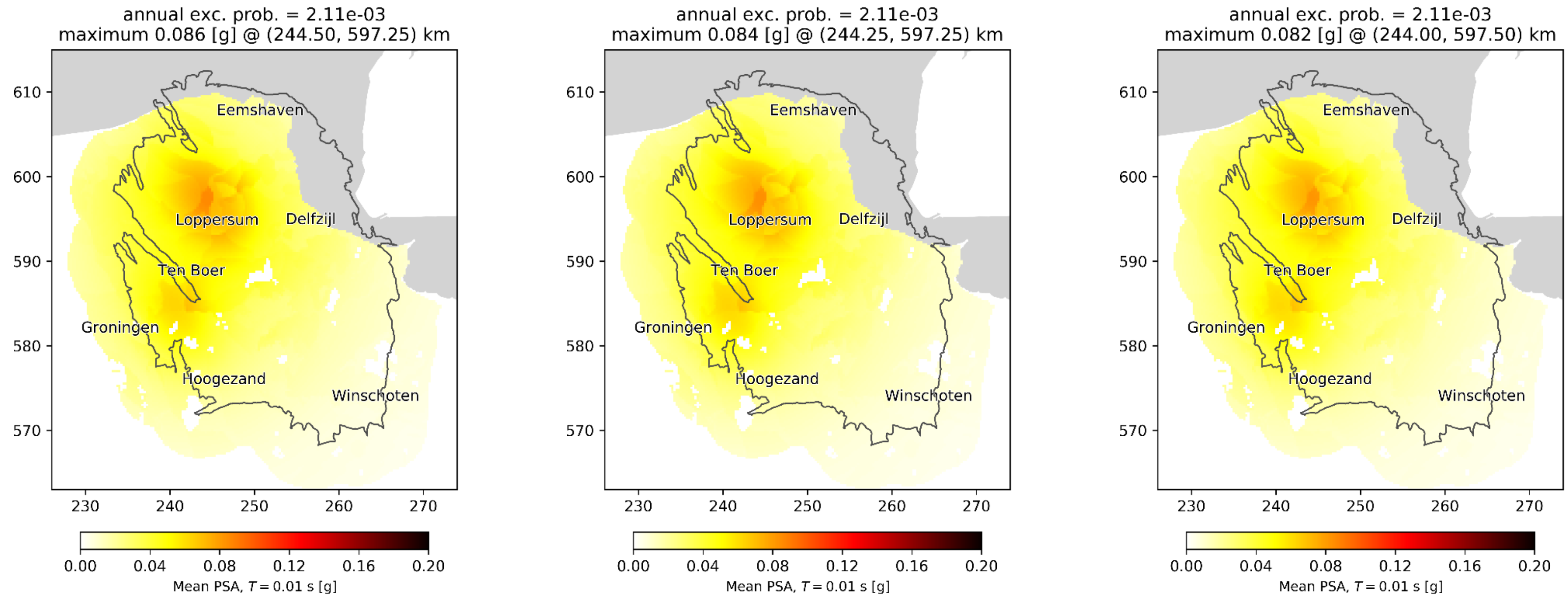

Cold Temperature

Average Temperature 2027/2028

Warm Temperature

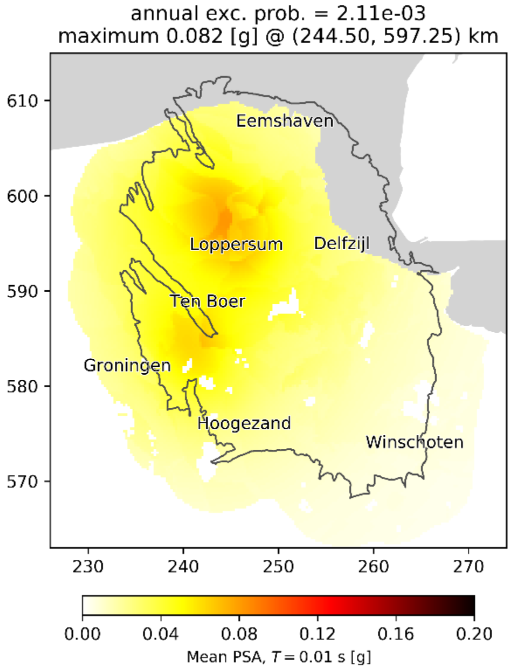

Cold Temperature

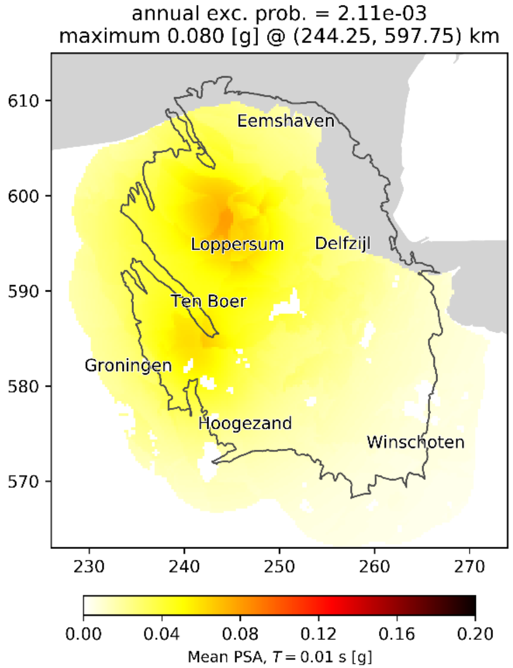

Average Temperature 2028/2029

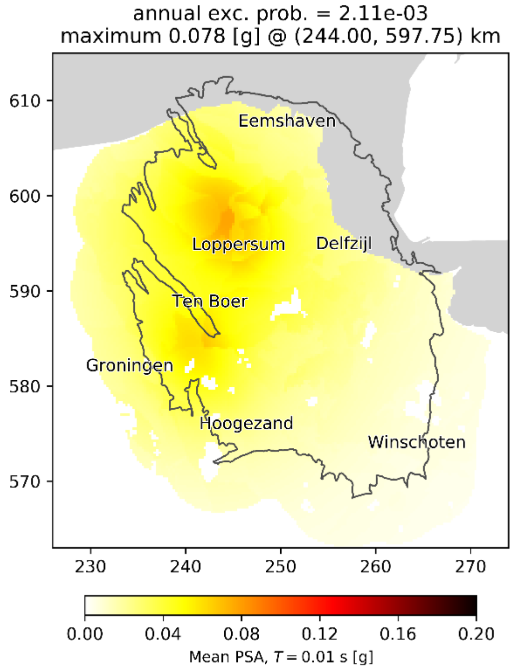

Warm Temperature

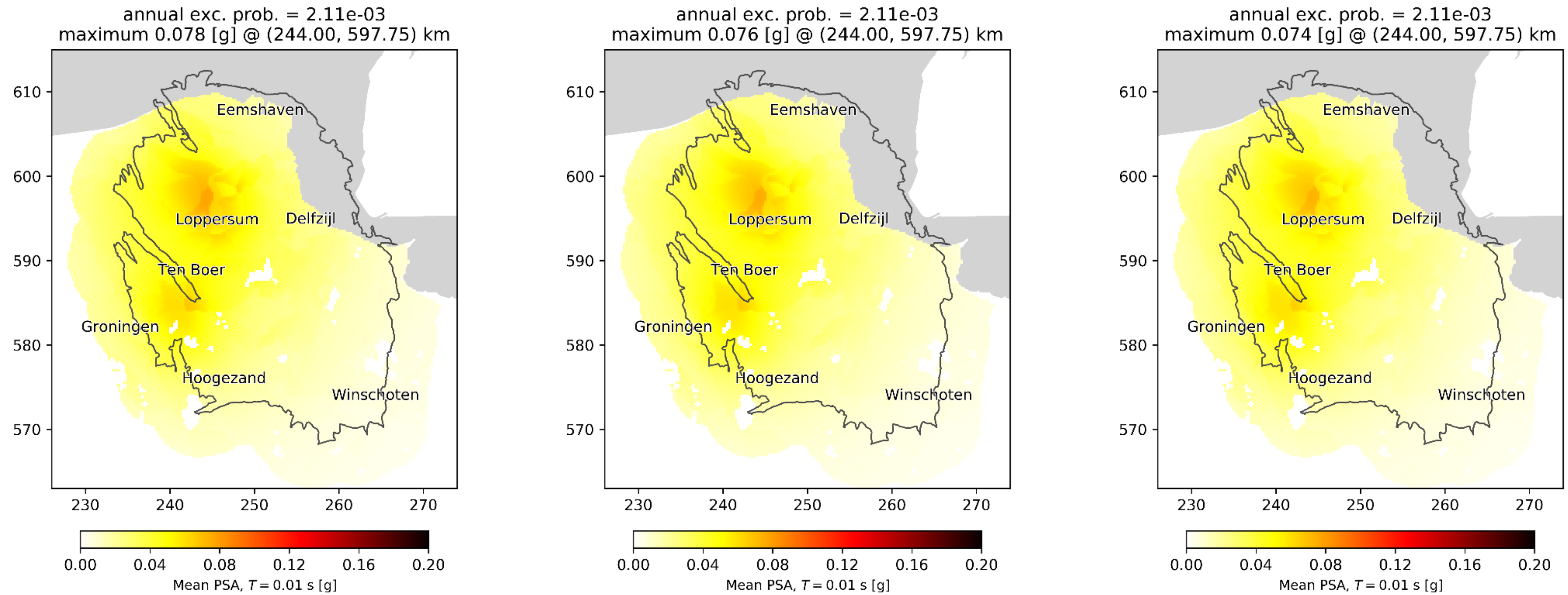

Cold Temperature | **Average Temperature 2029/2030** | **Warm Temperature**

Figure 6.8 Gas-year annual hazard maps for the three temperature cases compared. These maps are based on the production profile "GTS-raming 2020", Operational Strategy 1

6.3 Disaggregation of Seismic Hazard

The probabilistic seismic hazard assessment for the Groningen region depends on contributions from both aleatory variabilities and epistemic uncertainties. We include aleatory variabilities by Monte Carlo (MC) sampling of the joint probability distributions governing the number, location, origin time, magnitude, rupture extent, rupture strike and rupture directivity of induced earthquakes and the base rock spectral accelerations, and near surface amplifications of the associated seismic ground motions. We include epistemic uncertainties by extending the MC sampling procedures to include an ensemble of mutually independent and collectively exhaustive alternative hazard models within the hierarchical structure of a logic tree. This logic tree comprises the full factorial combination of 4 factors: the frequency-magnitude model (2 levels), the maximum possible magnitude model (7 levels), the ground-motion phi-model (2 levels), and the ground motion tau-model (4 levels). This results in a logic tree with 112 independent branches that are evaluated by independent MC simulations. These logic tree results describe a detailed discrete sampling of the joint seismic hazard probability distribution over the aleatory and epistemic variables.

Seismic hazard maps summarise the pseudo spectral accelerations (PSA) with a given exceedance probability as the mean of the joint seismic hazard probability distribution. Through disaggregation we also characterize the marginal hazard distributions for many of the key aleatory and epistemic variables. Due to practical digital storage and RAM limits we choose not to retain every MC sample of the joint hazard distribution. Instead, we store discrete joint distributions of PSA and selected aleatory variables for every spectral period and surface location. The top row of Figure 6.9 shows examples of these binned joint distribution sampled across the entire logic tree and represented as the mean annual occurrence rate. Each individual pixel in these plots represents an individual sample bin. The large number of small pixels within each plot shows the high-resolution of discrete sampling achieved for each joint distribution. We show these occurrence rates using a logarithmic colour bar spanning 6 decades from 10^{-3}/year down to 10^{-9}/year deep into the tails of these occurrence rate distributions. Grey pixels denote bins with no sampled occurrences, presumably because their occurrence rates are smaller than 10^{-9}/year. The joint PSA-magnitude distribution (Figure 6.9, top row, left column) shows that the largest occurrence rates correspond to the smallest magnitudes that we include in the hazard analysis (M=3.5). The positive correlation between PSA and magnitude shows how higher magnitude events typically yield higher PSA events. Looking along a horizontal line across this joint distribution, we observe a general increase in occurrence rate with increasing magnitude up to some peak rate corresponding to an intermediate modal magnitude, and beyond that the occurrence rates decrease. Below this modal magnitude the PSA occurrence rate is limited by the earthquake size whilst above this modal magnitude the PSA occurrence rate is limited by the earthquake occurrence rate. This modal magnitude depends on which horizontal line we select, selecting a larger PSA value yields a larger modal magnitude as expected. We also observe vertical edges in this distribution due to the imprint of the discrete M_{max} distribution, where occurrence rates step down since fewer logic tree branches permit magnitudes above this value.

As we measure seismic hazard according to exceedance rates and *not* occurrence rates, we obtain the marginal hazard distribution for magnitudes (Figure 6.9, bottom row, left column) by summing the pixels values on and above a given mean PSA value. Doing this for the PSA value with a mean annual exceedance probability of 0.2105%/year and normalizing the distribution yields relative contribution of each magnitude bin to the local seismic hazard at that location, spectral period, and exceedance probability (Figure 6.9, bottom row, left column). In this example, (Loppersum, 0.01s, 0.2105%/year), the modal hazard contribution corresponds to magnitude, M=4. In comparison the contributions of M=3.5 and M=5.0 are about 10 times smaller. This supports our MC simulation choice to truncate seismic hazard sampling for M < 3.5 events as these make a negligibly small contributions to this mean hazard metric. We also note that 5 of the 7 M_{max} logic tree levels (M_{max} = 5.0, 5.5, 6.0, 6.5, 7.0) do not significantly contribute to this mean seismic hazard as they are all too far above the modal hazard contribution (M = 4.0).

We repeat this sampling of joint distributions for PSA and the distance, R_{rup}, between the rupture plane and the surface location (Figure 6.9, middle column), and for PSA and the total ground motion variability, ε_{GM}, about the median ground motion model. These marginal hazard contributions (bottom row) indicate modal contributions from earthquakes located directly below Loppersum (R_{rup} = 3 km), and 1.5 standard deviations of the log-normal ground motion distribution above its median (ε_{GM} = 1).

Moving from the Loppersum location to the Groningen city location (Figure 6.10), changes the marginal hazard contributions (Figure 6.10, bottom row) which now exhibit a modal magnitude M = 4.5, a modal distance R_{rup} = 7 km and a modal ground motion variability ε_{GM} = 1. This increase in modal magnitude and distance indicates that the centre of seismicity that contributes most to this seismic hazard is not directly below the city of Groningen but instead offset by about 6 km. This likely corresponds to the secondary centre of event rates located east of Groningen city and south of the primary Loppersum centre of seismicity. The Loppersum seismicity region contributes as a secondary mode in the marginal hazard distribution, R_{rup} = 17 km, (Figure 6.10, bottom row, middle column).

Figure 6.11 shows maps to summarize how these modal contributions vary over the entire region of seismic hazard analysis. In summary, for seismic hazard with a 0.21%/year chance of exceedance, the modal hazard contributions throughout the hazard analysis region are due to 3.9 < M < 4.5 magnitudes, 3 km < R_{rup} < 15 km distances, and 0.5 < ε < 1.5 ground motion variability. Spatial variations in the modal distance contribution reflect the distance to the closest centre of seismicity. Within central regions located above a higher areal density of reservoir seismicity the modal distance corresponds to the reservoir depth (3 km) indicating the local seismic hazard is governed by the local underlying seismicity. Outside this central region, the local underlying seismicity is insufficient to be the primary cause of seismic hazard, which instead is driven by seismicity occurring in the central region with seismic ground motions that are diminished by distance. Likewise, modal magnitude is typically M = 3.9 – 4.2 in places located directly above regions with a higher areal density of reservoir seismicity such as Loppersum. Elsewhere this increases to M = 4.5 in regions where the higher reservoir seismicity densities are at least 5 km away. In Groningen city, Delfzijl and Eemshaven, the largest contribution comes from M = 4.2 – 4.5 earthquakes. The small region of M = 3.5 north of Winschoten is characterize by low seismic hazard and we interpret this feature as a likely finite sample artefact of the seismic disaggregation process that converges more slowly for lower seismic hazards.

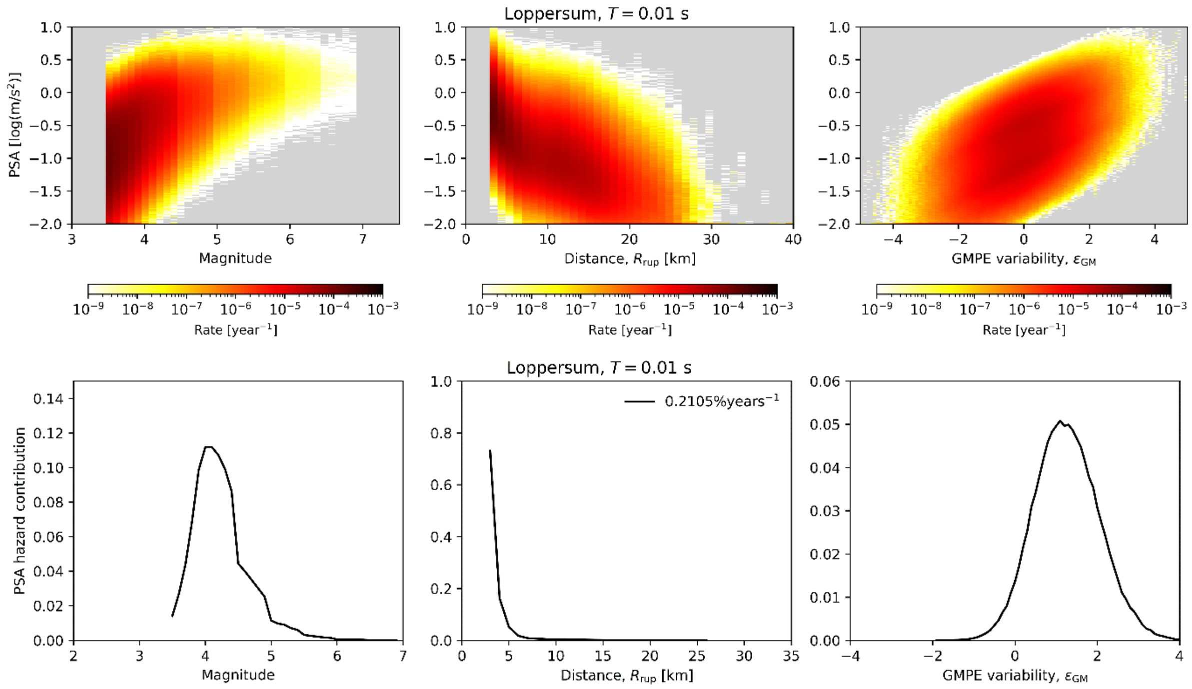

Figure 6.9 *(a) Occurrence rates for peak spectral acceleration at a spectral period of 0.01 s as a function of magnitude, distance, and GMPE epsilon, ε, for a single surface location directly above the region of maximum reservoir compaction. Grey denotes no occurrence in any of the simulations. (b) The fractional contribution to the ground motion with a 0.2% annual probability of exceedance for gas-year 2020/2021 using the production profile GTS-raming 2020 for the average temperature weather and operational strategy 1.*

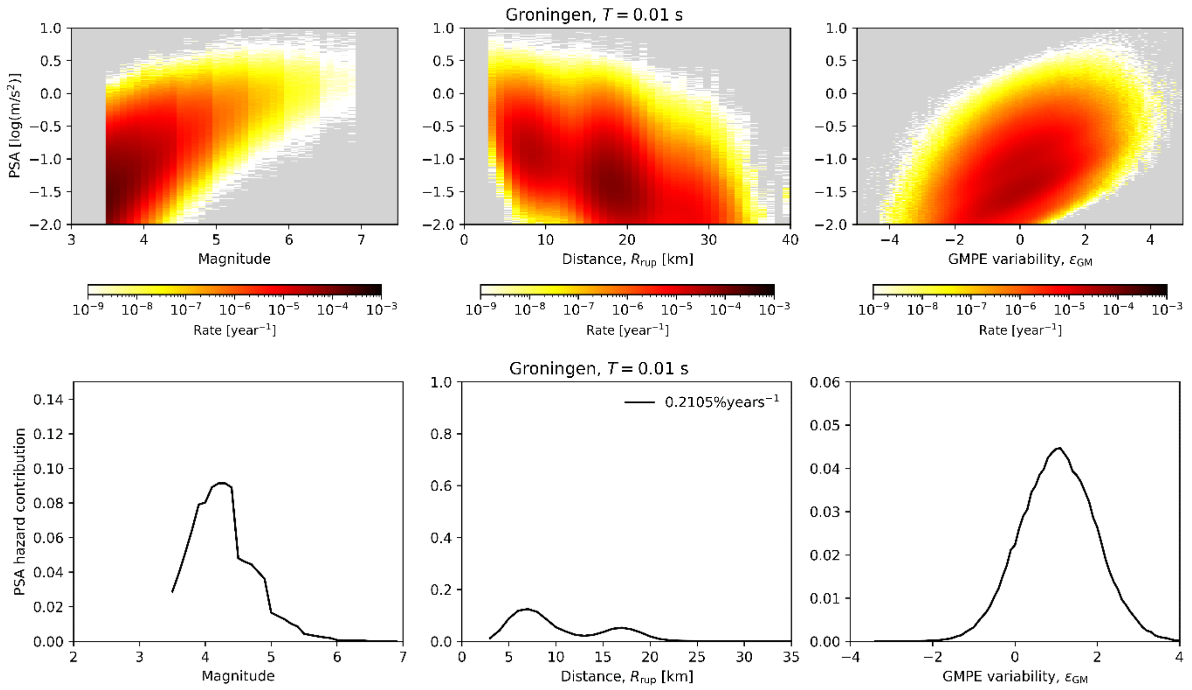

Figure 6.10 *As previous figure, except for a surface location in the centre of Groningen city.*

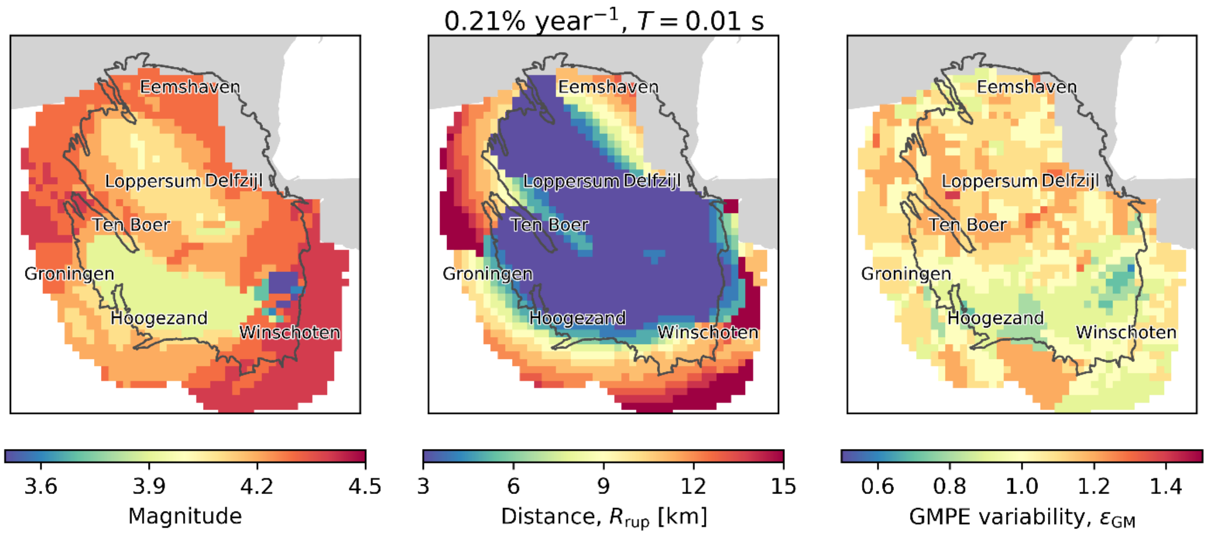

Figure 6.11: *Maps of the magnitude, M, distance, R_{rup}, ground motion variability, ε_{GM} that contribute most to the mean PSA (T=0.01s) hazard with a 0.21% annual chance of exceedance.*

7 Seismic Risk Assessment

7.1 Risk Metrics

The results from the probabilistic seismic Hazard and Risk Assessment (HRA) are summarised via risk metrics, which are related to the annualised probability of fatality for an individual person or for groups of people, taken as an average across the forecast period of the Hazard and Risk Assessment.

When assessing risk, it is important to select a risk metric that is appropriate given the purpose of the risk assessment. In many cases there is more than one option available as to which metric to use. An advisory committee, Commissie Meijdam, was established in early 2015 to advise the Minister of Economic Affairs and Climate Policy on risk policy related to Groningen earthquakes, including the selection and definition of the appropriate risk metrics. In December 2015, the Commissie Meijdam shared its third and final advice with the Minister of Economic Affairs and Climate Policy (Ref. 28 to Ref. 30). The selection of risk metrics for this Hazard and Risk Assessment is based on the final advice published by Commissie Meijdam. The Meijdam-norm was adopted by the Minister (Ref. 62) and first implemented in the HRA for Winningsplan 2016 (Ref. 8 to Ref. 14).

7.1.1 Individual Risk Metrics

7.1.1.1 Object-related Individual Risk and Individual Risk

The Commissie Meijdam introduced two individual risk metrics: Individual Risk (IR) and Object-related Individual Risk (OIA). Table 7.1 lists the definitions of the individual risk metrics used in the assessment of risk for induced seismicity in the Groningen field area. The fundamental principle of the advice of the Commission is that living and working in Groningen must be as safe as elsewhere in the Netherlands. In Groningen the same safety standards must apply as elsewhere in the Netherlands. Based on this principle the Committee Meijdam established the norm that Individual Earthquake Risk (IR) should be below 10^{-5}/year.

For buildings with an OIA above 10^{-4}/year, immediate action is required. In principle these buildings need to be strengthened immediately or vacated. Buildings with an OIA between 10^{-4}/year and 10^{-5}/year need to be strengthened within a reasonable period. The involvement of the Minister of EZK over the past years with the structural upgrading has been formally implemented in the Mining law in December 2019.

7.1.1.2 Inside and Outside Local Personal Risk

To perform the calculations, NAM uses as an intermediary result, the individual risk metric LPR (Local Person Risk) consisting of two components: Inside Local Personal Risk (ILPR) and Outside Local Personal Risk (OLPR). The use of LPR is analogous to safety assessment domains like those used for industrial activities and pipelines. "Local Personal Risk" (LPR) is generally defined as the annual probability of fatality for a fictional person, who is continuously present, without protection, at a specific at-risk location. For Groningen earthquakes, LPR is defined as follows: *"the probability of death of a fictional person who is permanently in or near a building"* (Ref. 30). The location of the person within the building is uniformly and randomly distributed inside the building. The relationship between the percentage of collapse (floor percentage covered in debris) and chance of a fatality in the building is described by the consequence model (Ref. 55 and 80).

Risk Metric	Dutch Name	Definition	Purpose(s)
Object-related Individual Risk	Objectgebonden Individueel Aardbevingsrisico (OIA)	The Objectgebonden individual earthquake risk is the risk that an individual dies in a year due to collapse or falling objects (as a result of an earthquake) of a building in which or in the direct vicinity of which this person is present. The residence time in/around that building is therefore taken into consideration.	Local individual risk metric to measure fatality risk due to structural and non-structural collapse (LPR, see below), weighted by the average residence times of the individuals in/around the building (OIA), relative to norm of 10^{-5}/year overall individual risk. Check if any buildings have occupants with an average OIA above 10^{-4}/year (high priority for immediate action).
Individual Earthquake Risk	Individueel Aardbevingsrisico (IAR)	The individual earthquake risk is the annual risk that an individual is exposed to in the various structures in or near which this individual is present.	Individual risk metric that is not considered at present (as requires knowledge of the presence of all members of the Groningen community throughout the day, in order to sum up all their object-bound individual risks over a 24-hour period).
Inside Local Personal Risk (ILPR)	Plaatsgebonden Persoonlijk Risico Binnen	The probability of death of a fictional unprotected person who is permanently present in a building.	Local risk metric to measure fatality risk due to collapse of a given building and its non-structural elements both inside (ILPR) and outside (OLPR) the building, relative to the norm of 10^{-5}/year overall individual risk. Check if any buildings have Local Personal Risk above 10^{-4}/year (high priority for immediate action).
Outside Local Personal Risk (OLPR)	Plaatsgebonden Persoonlijk Risico Buiten	The probability of death of a fictional unprotected person who is permanently present near a building.	
Local Personal Risk (LPR)	Plaatsgebonden Persoonlijk Risico	The probability of death of a fictional unprotected person who is permanently present in or near a building. This person is thought to be inside the building 99% of the time and outside near the building 1 % of the time.	

Table 7.1 Overview of the individual risk metrics used in the assessment of risk for induced seismicity in the Groningen field area.

Inside Local Personal Risk is the probability of fatality for an individual continuously present in a building. It is associated with partial or full collapse of the building. Outside Local Personal Risk is the probability of fatality for an individual continuously present in the direct vicinity of a building. It is primarily associated with failure of non-structural elements, the so-called falling objects[3] (chimneys, balconies, parapets, etc.). In this context the vicinity of a building is taken as within 5 m from the building.

The Inside Local Personal Risk and Outside Local Personal Risk are aggregated to Local Personal Risk (LPR) assuming a *fictional person* is 99% of the time inside a building and 1% of the time outside the building, but in the direct vicinity of the building. The definition of these risk metrics is also listed in table 7.1.

As Local Personal Risk applies to a fictional unprotected person who is permanently present (everywhere) in a building, it is a property of this building. It is independent of the actual occupancy of the building; how many people are present in the building and the duration of their presence are not taken into account when assessing the LPR of a building. LPR is presented as a cumulative distribution (of buildings versus risk level), which provides an estimate of the number of buildings that do not comply with the norm.

7.1.1.3 Current Practice in Risk Assessments

However, the Meijdam-norm applies to Individual Risk. To assess Individual Risk for a person in a rigorous manner knowledge of the buildings the person visits during the day and the duration the person is present in these building is required. The Individual Risk of a person is the duration weighted sum of the LPR of the buildings visited during the day. The time a person spends away from buildings does not contribute to individual risk.

NAM uses a practical and conservative approach, whereby the number of buildings with a mean LPR is evaluated and compared to the threshold safety levels of the Meijdam-norm. The underlying principle was that if all buildings have a mean LPR below the norm, no persons can be exposed to an IR above the norm. The LPR inherently assumes a full-time (100%) residency of the building. In the Hazard and Risk Assessment, the mean LPR is the primary metric used to compare against the 10^{-5}/year individual risk norm (as recommended by Commissie Meijdam, which requires the individual risk for a person to be less than 10^{-5} per year). Note that individual risk metrics that account for the proportion of time a person spends in the building will yield a lower calculated individual risk (IR) than LPR (particularly for buildings occupied a small proportion of the time).

Mid-2018, the Minister sought the advice of a panel of professors on the implementation of the life safety norm in the HRA methodology. This panel of professors pointed out that the methodology implemented in the HRA is a conservative approach (Ref. 63 to Ref. 67), which inherently assumes that for each building individuals spend their full time there. In the HRA for GTS-raming 2019 (Ref. 19) the difficulties of implementing a method based on AOI is discussed and estimates for residence times provided based on a study by the Social Plan Bureau (Ref. 68). Table 7.2 shows the mean residence time fractions for the different building usage categories. In an advice to the Minister, SodM (Ref. 69) recommended the practice of estimating and reporting LPR should be continued. In this current report, we will use the conservative LPR metric for risk, but also report the Object-related Individual Risk (OIA).

[3] Falling Objects are sometimes also referred to as High Risk Building Elements (HRBE) or Potential High Risk Building Elements (PRBE).

Building Use	Residence Time Fraction
Woonfunctie	75%
Logiesfunctie	50%
Industriefunctie	24%
Winkelfunctie	24%
Kantoorfunctie	24%
Bijeenkomstfunctie	24%
Overige gebruiksfunctie	24%
Sportfunctie	24%
Onderwijsfunctie	24%
Celfunctie	100%
Gezondheidszorgfunctie	100%
<blank> -- anything unknown is assumed to be Residential	75%

Table 7.2 Residence times for the building usage categories.

Buildings with both a primary and secondary building use (e.g. a building with a shop (commercial business) at the ground floor and apartments on the first and higher floors (residential)) will be assigned the larger of the residence times of the primary and the secondary use.

7.1.2 Group Risk and Maatschappelijk Veiligheidsrisico

Aggregated risk metrics (Tab. 7.3) are commonly applied for the evaluation and management of both technical risks (e.g. chemical plant explosions) and natural risks (e.g. flooding) (Ref. 70). These group risk (GR) metrics were developed based on the concept that society has lower tolerance to accidents involving multiple fatalities in a single event than to multiple events involving single fatalities.

The third and final advisory report from Commissie-Meijdam (Eindadvies Handelingsperspectief voor Groningen Adviescommissie ‘Omgaan met risico’s van geïnduceerde aardbevingen’) (Ref. 30) introduced the new aggregated risk metric of Maatschappelijk Veiligheidsrisico (MVR). Maatschappelijk Veiligheidsrisico is an assessment of the frequency (f) with which defined numbers of fatalities (N) occur due to earthquakes, with an offset for “basic safety” (assuming everyone exposed to the earthquake risk is at uncorrelated 10^{-5}/year individual risk). The calculation procedure for Maatschappelijk Veiligheidsrisico is fully described in the final Commissie Meijdam advice, appendix 2 (Ref. 30).

For Winningsplan 2016, for the first time Maatschappelijk Veiligheidsrisico was calculated for seven selected communities. The definition of the communities was based on the wijk- en buurten definition by CBS (Ref. 71).

Risk Metric	Dutch Name	Definition	Purpose(s)
Group Risk	Groepsrisico	Frequency (f) with which defined numbers of fatalities (N) occur due to earthquakes.	Input towards prioritisation of buildings/non-structural elements (which don't comply with individual risk norm) within structural upgrading program. Provide risk insights for prioritisation of communities. Consider additional measures (where “reasonable”) beyond reducing individual risk to below 10^{-5}/year
Maatschappelijk Risico	Maatschappelijk Risico	Frequency (f) with which defined numbers of fatalities (N) occur due to earthquakes, with an offset for “basic safety” (assuming everyone exposed to the earthquake risk is at uncorrelated 10^{-5}/year risk). The calculation procedure for Maatschappelijk Veiligheidsrisico is fully described in the final Commissie Meijdam advice, appendix 2 (Ref. 30).	

Table 7.3 Overview of the aggregate risk metrics used in the assessment of risk for induced seismicity in the Groningen field area.

7.2 Number of buildings compared to the safety norm

In this section of the report, the number of houses where the risk exceeds one of the two risk safety levels of the Meijdam safety-norm is discussed. Risk for individual building, is not addressed as such is the domain of the government and its advisor, who currently directs the structural upgrading effort. Both mean LPR and mean OIA of a building have been calculated and reported (Tab. 7.3a to f). The mean OIA is calculated as the product of the LPR and the residence time fraction. These fractions are treated as fixed.

7.2.1 Assessment of Local Personal Risk (LPR)

Figures 7.1a and 7.1b show the number of buildings exceeding an annual mean Local Personal Risk (LPR) for each gas-year of the 10-year period 2020/2021 to 2029/2030, based on the average temperature year and Operational Strategy 1. Figure 7.1c shows the number of buildings exceeding an annual mean LPR for gas-year 2020/2021, based on average temperature year for both operational strategies. The grey bands in these LPR-graphs indicate the uncertainty range. The impact of the buildings already strengthened to date has not been incorporated in this assessment, as this data is not available to NAM.

The development of the mean LPR for the Groningen building stock over the period gas-year 2020/2021 to 2029/2030 is shown in figure 7.2. The number of buildings exceeding the Meijdam-norm of mean LPR 10^{-5}/year shows a declining trend. This is particularly evident for the gas-years 2020/2021 to 2023/2024, where the number of buildings exceeding the norm declines noticeably. For each year in the period 2020/2021 to 2029/2030, tables 7.3a to 7.3f, show the number of buildings for different probabilistic assessments:

- The number of buildings with mean LPR exceeding the 10^{-4}/year level
- The number of buildings with mean LPR exceeding the 10^{-5}/year level
- The number of buildings with mean OIA exceeding the 10^{-4}/year level
- The number of buildings with mean OIA exceeding the 10^{-5}/year level
- The number of buildings with P90 LPR exceeding the 10^{-4}/year level
- The number of buildings with P90 LPR exceeding the 10^{-5}/year level
- The number of buildings with P90 OIA exceeding the 10^{-4}/year level
- The number of buildings with P90 OIA exceeding the 10^{-5}/year level

For the average and warm gas-years (for both operations strategies) all buildings are assessed to meet the 10^{-5}/year life safety norm. For the cold gas-year 2020/2021 two agricultural barns are assessed to have a risk above this norm. At the same time the house part of these farmhouses does meet this norm.

During the period of gas-year 2020/2021 to 2022/2023, the number of buildings with a 10% chance that the 10^{-5}/year norm is not met, is assessed to decrease from 162 in gas-year 2020/2021 to 72 in gas-year 2021/2022 and to 21 in gas-year 2022/2023, for production profile "GTS-raming 2020" for an average temperature profile and operational strategy 1. For operational strategy 2 the number of buildings with a 10% chance that these are above the norm is lower. In gas-year 2020/2021, this number is 82 and decreases to 54 in gas-year 2021/2022and 23 in gas-year 2022/2023. All buildings assessed to have a 10%

chance to be above the 10^{-5}/year Meijdam life safety norm belong to a single typology, i.e. agricultural barns[4].

The data captured in tables 7.3a to 7.3f is illustrated in figure 7.4, which shows number of buildings where the mean LPR and the P90 LPR exceed the 10^{-4}/year and 10^{-5}/year, for the different cases (temperature and operational strategy). The LPR results can be disaggregated to show the separate contributions of the different building typologies (Fig. 7.5).

[4] It should be noted that for all but few of these this relates to part of the building; the house part was found to have P90 LPR < 10^{-5}/year whereas the barn has P90 LPR >10^{-5}/year.

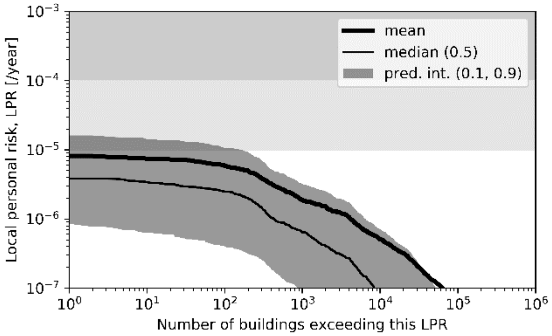

2020/2021

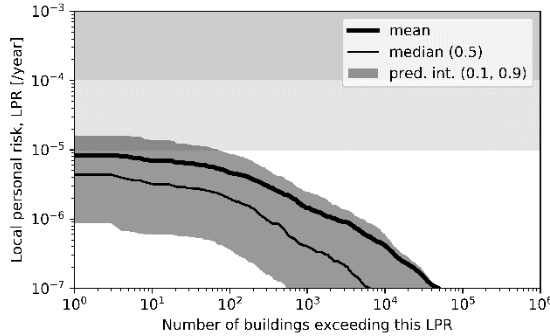

2021/2022

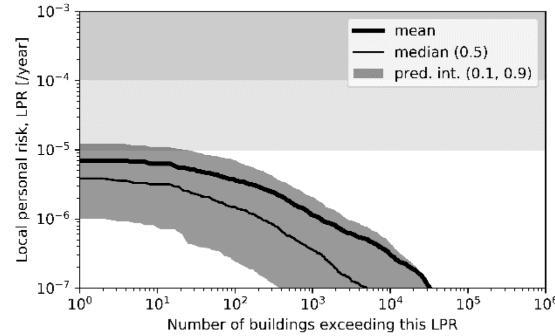

2022/2023

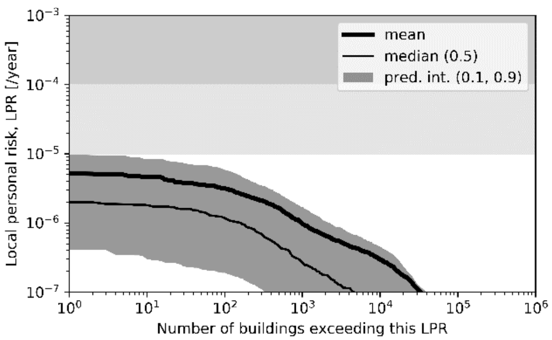

2023/2024

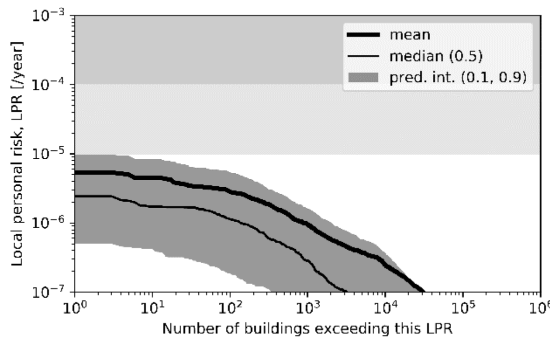

2024/2025

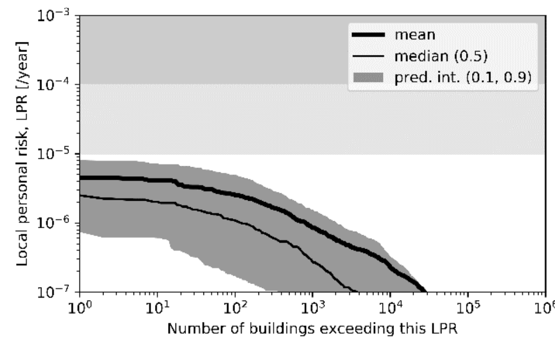

2025/2026

Figure 7.1a Local Personal Risk graphs for the gas-years 2020/2021 to 2025/2026. These show the number of houses that are exposed to a LPR. The thick black lines denote the mean and the dark grey areas the uncertainty bands. The two horizontal bands in light grey denote the LPR levels of the Meijdam-norm.

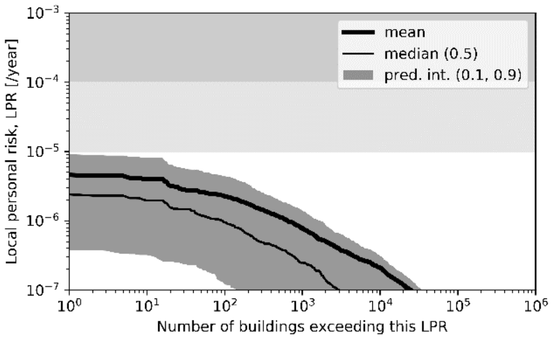

2026/2027

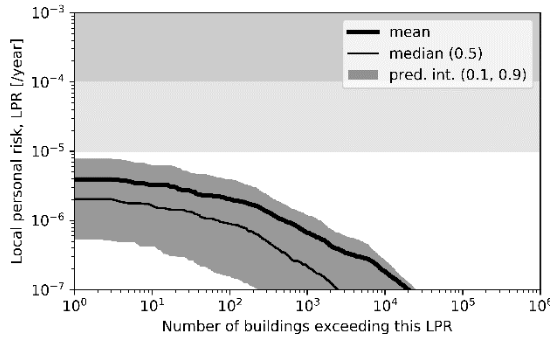

2027/2028

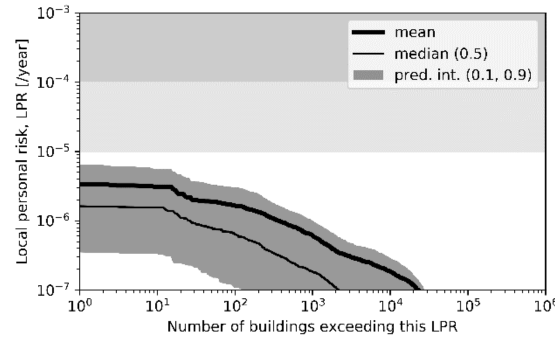

2028/2029

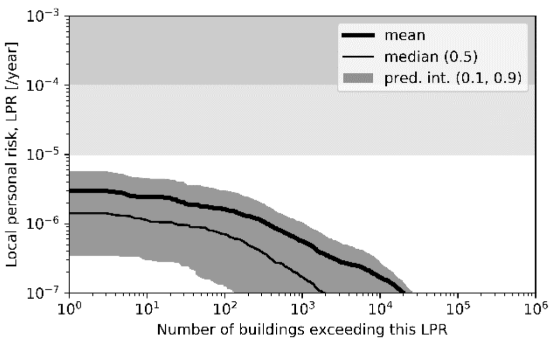

2029/2030

Figure 7.1b Local Personal Risk graphs for the gas-years 2026/2027 to 2029/2030. These show the number of houses exceeding a certain LPR. The thick black lines denote the mean and the dark grey areas the uncertainty bands. The two horizontal bands in light grey denote the LPR levels of the Meijdam-norm. The assessment is based on production profile “GTS-raming 2019” for an average temperature year and Operational Strategy 1.

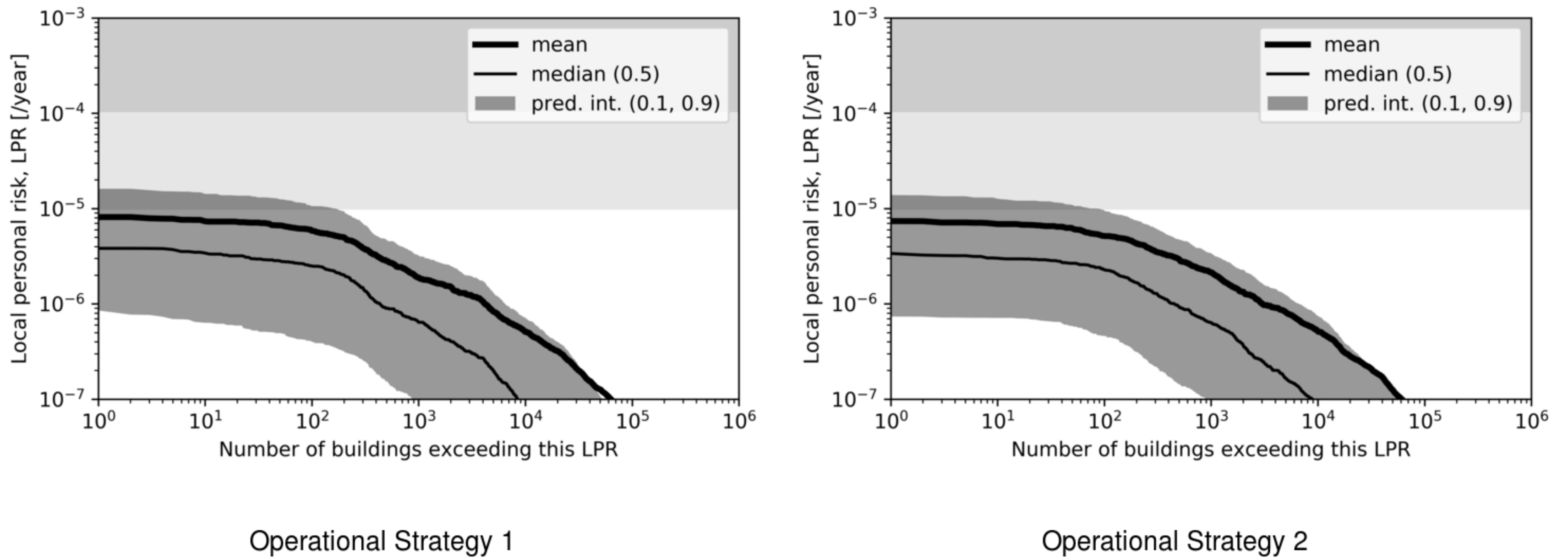

Figure 7.1c *Local Personal Risk graphs for the gas-year 2020/2021 for an average temperature year shown for both operational strategies. These show the number of houses exceeding a certain LPR. The thick black lines denote the mean and the dark grey areas the uncertainty bands. The two horizontal bands in light grey denote the LPR levels of the Meijdam-norm.*

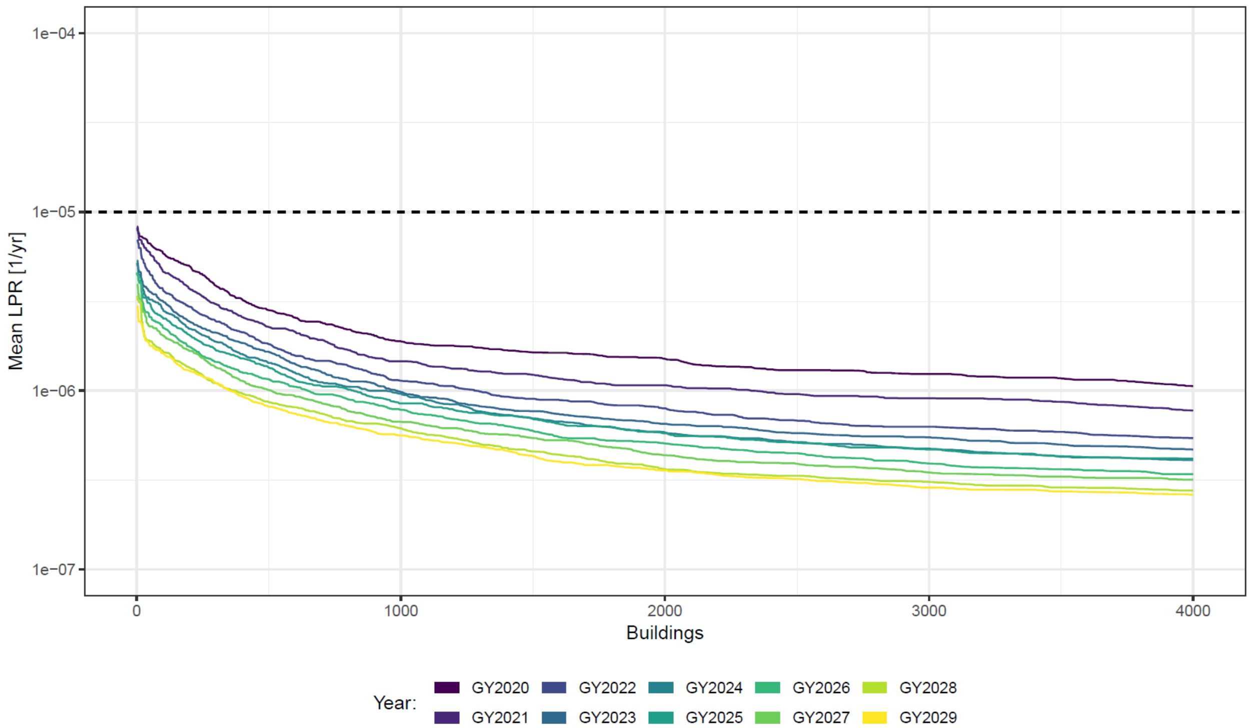

Figure 7.2 *Mean Local Personal Risk graphs for the gas-years 2020/2021 to 2029/2030. These show the number of buildings exceeding a certain LPR. The uncertainty bands have been left out of this graph but are shown in figures 7.1a and 7.1b. The years are colour coded. The assessment is based on production profile "GTS-raming 2020" for an average temperature year and Operational Strategy 1.*
Note that there are zero buildings exceeding the mean LPR norm of 10^{-5}/year.

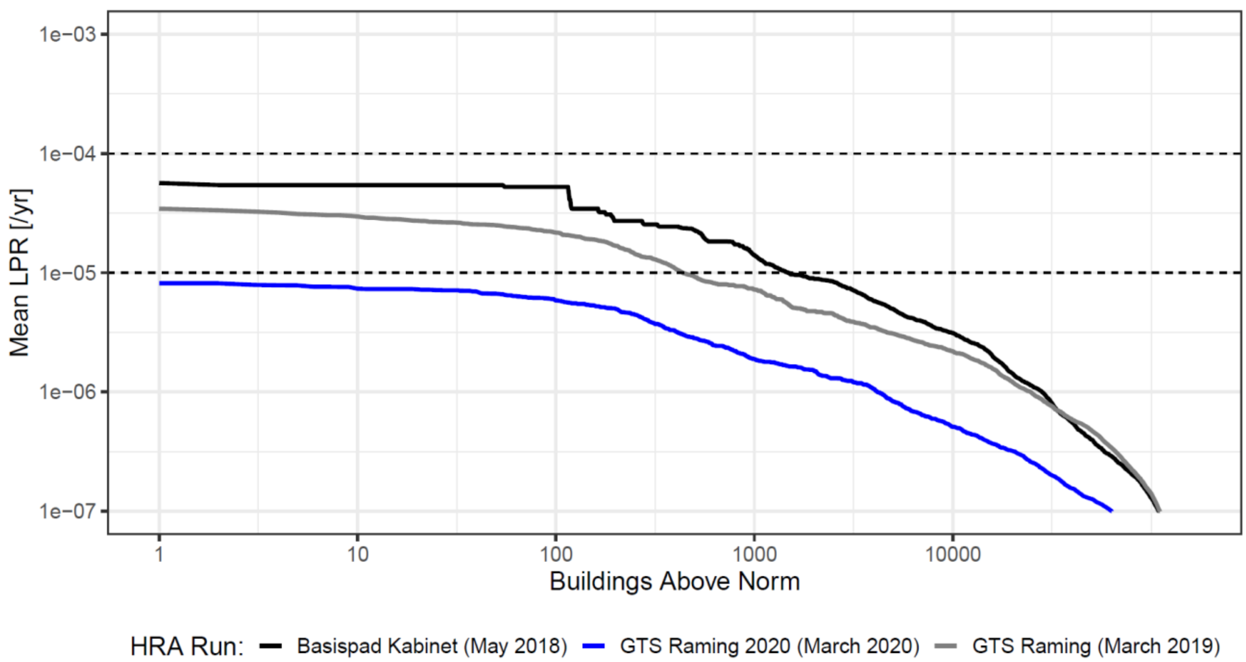

Figure 7.3 *Comparison of the mean Local Personal Risk graphs of previous HRA reports. The following is shown:*
Production profile “Basispad Kabinet” for Average Temperature and Calendar-year 2019,
Production profile “GTS-raming 2019” for Average Temperature and gas-year 2019/2020
Production profile “GTS-raming 2020” for Operational Strategy 1, Average Temperature and gas-year 2020/2021.

Gas-year	Mean LPR 10^{-4}/year	Mean LPR 10^{-5}/year	Mean OIA 10^{-4}/year	Mean OIA 10^{-5}/year	P90 LPR 10^{-4}/year	P90 LPR 10^{-5}/year	P90 OIA 10^{-4}/year	P90 OIA 10^{-5}/year
2020/2021	0	0	0	0	0	162	0	23
2021/2022	0	0	0	0	0	72	0	15
2022/2023	0	0	0	0	0	21	0	0
2023/2024	0	0	0	0	0	0	0	0
2024/2025	0	0	0	0	0	0	0	0
2025/2026	0	0	0	0	0	0	0	0
2026/2027	0	0	0	0	0	0	0	0
2027/2028	0	0	0	0	0	0	0	0
2028/2029	0	0	0	0	0	0	0	0
2029/2030	0	0	0	0	0	0	0	0

Table 7.3a *Number of buildings with mean LPR exceeding 10^{-5}/year and 10^{-4}/year, for production profile GTS-raming 2020, Operational Strategy 1 and average temperature year. See main text for further explanation. These are shown for each year of the period 2020/2021 to 2029/2030 for the production profile "GTS-raming 2020", operational strategy 1 for an average weather year.*

Gas-year	Mean LPR 10^{-4}/year	Mean LPR 10^{-5}/year	Mean OIA 10^{-4}/year	Mean OIA 10^{-5}/year	P90 LPR 10^{-4}/year	P90 LPR 10^{-5}/year	P90 OIA 10^{-4}/year	P90 OIA 10^{-5}/year
2020/2021	0	2	0	0	0	245	0	75
2021/2022	0	0	0	0	0	69	0	2
2022/2023	0	0	0	0	0	35	0	0
2023/2024	0	0	0	0	0	16	0	0
2024/2025	0	0	0	0	0	0	0	0
2025/2026	0	0	0	0	0	0	0	0
2026/2027	0	0	0	0	0	0	0	0
2027/2028	0	0	0	0	0	0	0	0
2028/2029	0	0	0	0	0	0	0	0
2029/2030	0	0	0	0	0	0	0	0

Table 7.3b *Number of buildings with mean LPR exceeding 10^{-5}/year and 10^{-4}/year, for production profile GTS-raming 2020, Operational Strategy 1 and cold temperature year. See main text for further explanation. These are shown for each year of the period 2020/2021 to 2029/2030 for the production profile "GTS-raming 2020" operational strategy 1 for a cold weather year.*

Gas-year	Mean LPR 10^{-4}/year	Mean LPR 10^{-5}/year	Mean OIA 10^{-4}/year	Mean OIA 10^{-5}/year	P90 LPR 10^{-4}/year	P90 LPR 10^{-5}/year	P90 OIA 10^{-4}/year	P90 OIA 10^{-5}/year
2020/2021	0	0	0	0	0	87	0	9
2021/2022	0	0	0	0	0	54	0	2
2022/2023	0	0	0	0	0	23	0	0
2023/2024	0	0	0	0	0	0	0	0
2024/2025	0	0	0	0	0	3	0	0
2025/2026	0	0	0	0	0	0	0	0
2026/2027	0	0	0	0	0	0	0	0
2027/2028	0	0	0	0	0	0	0	0
2028/2029	0	0	0	0	0	0	0	0
2029/2030	0	0	0	0	0	0	0	0

Table 7.3c Number of buildings with mean LPR exceeding 10^{-5}/year and 10^{-4}/year, for production profile GTS-raming 2020, Operational Strategy 1 and warm temperature year. See main text for further explanation. These are shown for each year of the period 2020/2021 to 2029/2030 for the production profile “GTS-raming 2020” operational strategy 1 for a warm weather year.

Gas-year	Mean LPR 10^{-4}/year	Mean LPR 10^{-5}/year	Mean OIA 10^{-4}/year	Mean OIA 10^{-5}/year	P90 LPR 10^{-4}/year	P90 LPR 10^{-5}/year	P90 OIA 10^{-4}/year	P90 OIA 10^{-5}/year
2020/2021	0	0	0	0	0	82	0	4
2021/2022	0	0	0	0	0	47	0	0
2022/2023	0	0	0	0	0	10	0	0
2023/2024	0	0	0	0	0	0	0	0
2024/2025	0	0	0	0	0	5	0	0
2025/2026	0	0	0	0	0	0	0	0
2026/2027	0	0	0	0	0	0	0	0
2027/2028	0	0	0	0	0	0	0	0
2028/2029	0	0	0	0	0	0	0	0
2029/2030	0	0	0	0	0	0	0	0

Table 7.3d Number of buildings with mean LPR exceeding 10^{-5}/year and 10^{-4}/year, for production profile GTS-raming 2020, Operational Strategy 2 and average temperature year. See main text for further explanation. These are shown for each year of the period 2020/2021 to 2029/2030 for the production profile “GTS-raming 2020” operational strategy 2 for an average weather year.

Gas-year	Mean LPR 10^{-4}/year	Mean LPR 10^{-5}/year	Mean OIA 10^{-4}/year	Mean OIA 10^{-5}/year	P90 LPR 10^{-4}/year	P90 LPR 10^{-5}/year	P90 OIA 10^{-4}/year	P90 OIA 10^{-5}/year
2020/2021	0	1	0	0	0	220	0	76
2021/2022	0	0	0	0	0	72	0	6
2022/2023	0	0	0	0	0	27	0	0
2023/2024	0	0	0	0	0	30	0	0
2024/2025	0	0	0	0	0	0	0	0
2025/2026	0	0	0	0	0	3	0	0
2026/2027	0	0	0	0	0	0	0	0
2027/2028	0	0	0	0	0	0	0	0
2028/2029	0	0	0	0	0	0	0	0
2029/2030	0	0	0	0	0	0	0	0

Table 7.3e Number of buildings with mean LPR exceeding 10^{-5}/year and 10^{-4}/year, for production profile GTS-raming 2020, Operational Strategy 2 and cold temperature year. See main text for further explanation. These are shown for each year of the period 2020/2021 to 2029/2030 for the production profile “GTS-raming 2020” operational strategy 2 for a cold weather year.

Gas-year	Mean LPR 10^{-4}/year	Mean LPR 10^{-5}/year	Mean OIA 10^{-4}/year	Mean OIA 10^{-5}/year	P90 LPR 10^{-4}/year	P90 LPR 10^{-5}/year	P90 OIA 10^{-4}/year	P90 OIA 10^{-5}/year
2020/2021	0	0	0	0	0	62	0	0
2021/2022	0	0	0	0	0	62	0	3
2022/2023	0	0	0	0	0	15	0	0
2023/2024	0	0	0	0	0	0	0	0
2024/2025	0	0	0	0	0	0	0	0
2025/2026	0	0	0	0	0	0	0	0
2026/2027	0	0	0	0	0	0	0	0
2027/2028	0	0	0	0	0	0	0	0
2028/2029	0	0	0	0	0	0	0	0
2029/2030	0	0	0	0	0	0	0	0

Table 7.3f Number of buildings with mean LPR exceeding 10^{-5}/year and 10^{-4}/year, for production profile GTS-raming 2020, Operational Strategy 2 and warm temperature year. See main text for further explanation. These are shown for each year of the period 2020/2021 to 2029/2030 for the production profile “GTS-raming 2020” operational strategy 2 for a warm weather year.

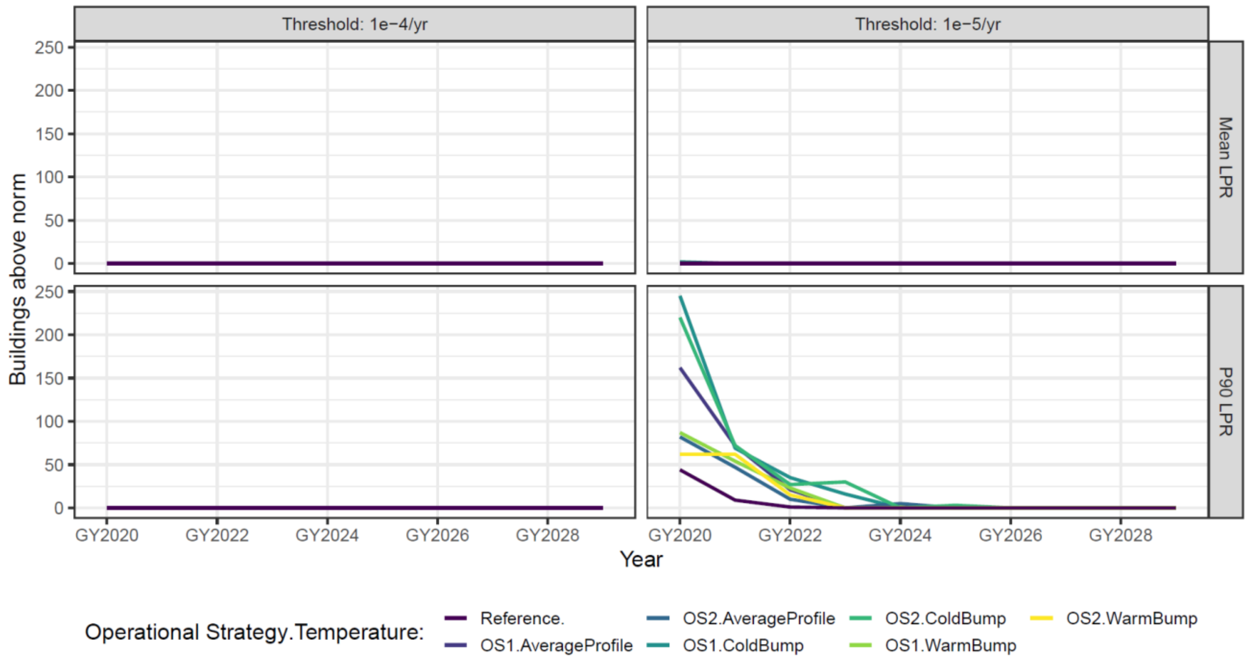

Figure 7.4 Graphs show the Local Personal Risk associated with the production profile "GTS-raming 2020" for average, cold weather and warm weather gas-years for the period 2020/2021 to 2029/2030.

Right graphs: number of buildings exceeding the norm LPR larger than 10^{-5}/year

Left graphs: number of buildings exceeding the norm LPR larger than 10^{-4}/year

Top graphs: number of buildings exceeding the norm for mean LPR

Bottom graphs: number of buildings exceeding the norm for P90 LPR

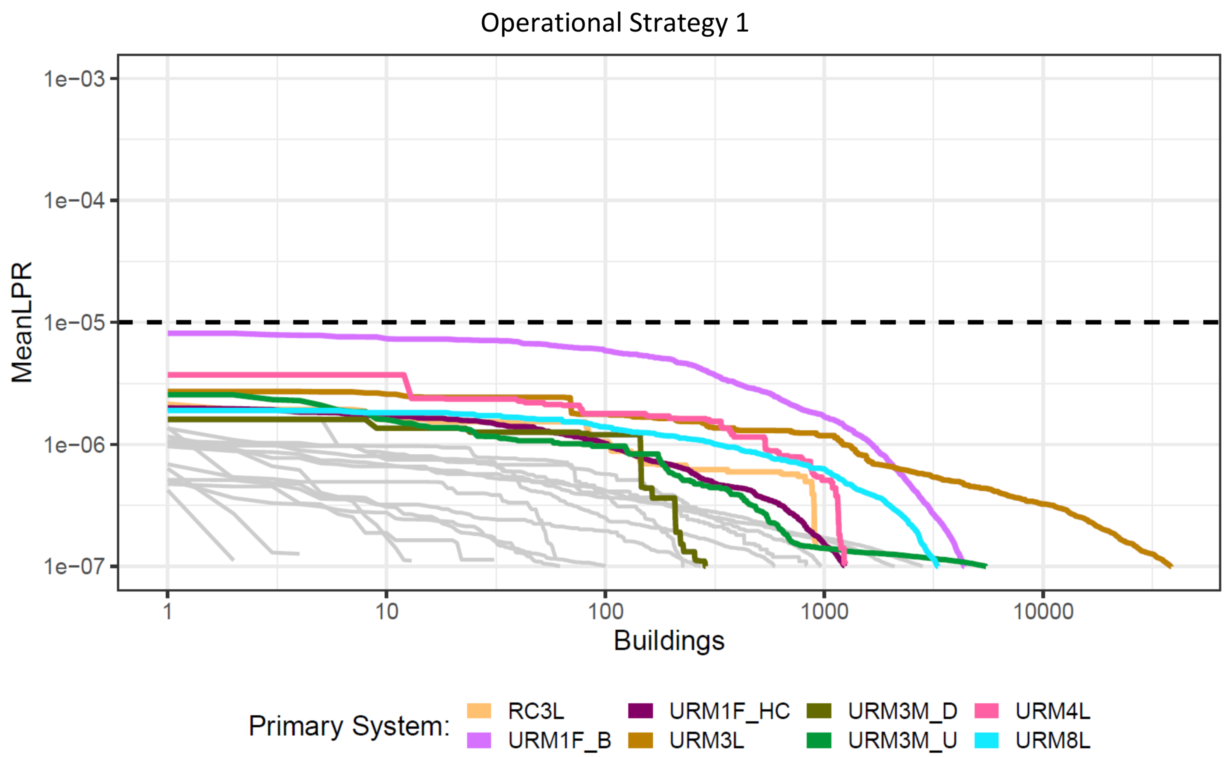

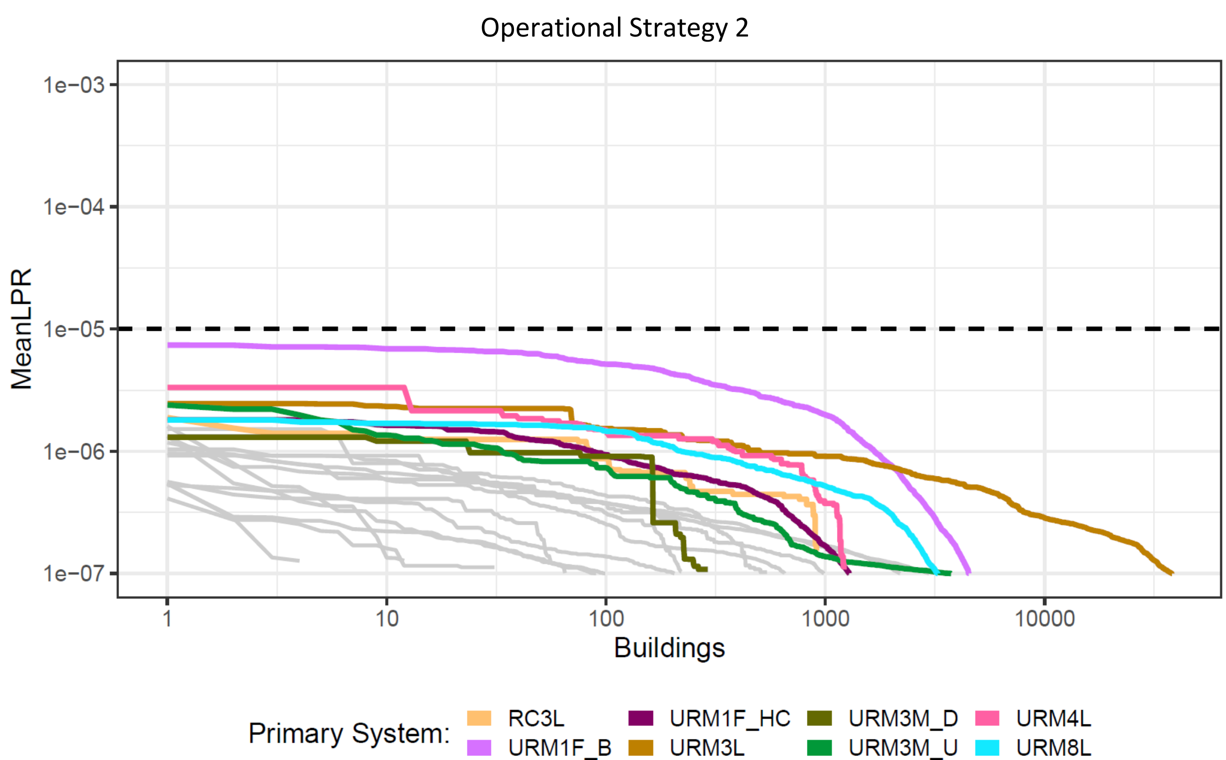

Figure 7.5 *Mean Local Personal Risk graphs shown per primary typology for gas-year 2020-2021 with average temperature demand.*

7.2.2 Number of years P90 LPR > 10^{-5}/year

Figure 7.6 gives, for buildings with P90 LPR > 10^{-5}/year in gas-year 2020/2021, an overview of the duration that these buildings remain above P90. For about half of them this duration is 1 year. All buildings will drop below P90 within 3 to 4 years. It should be noticed that the barn of the farmhouse (URM1F_B) is most fragile and shown here. The house parts of these farmhouses all remain below P90.

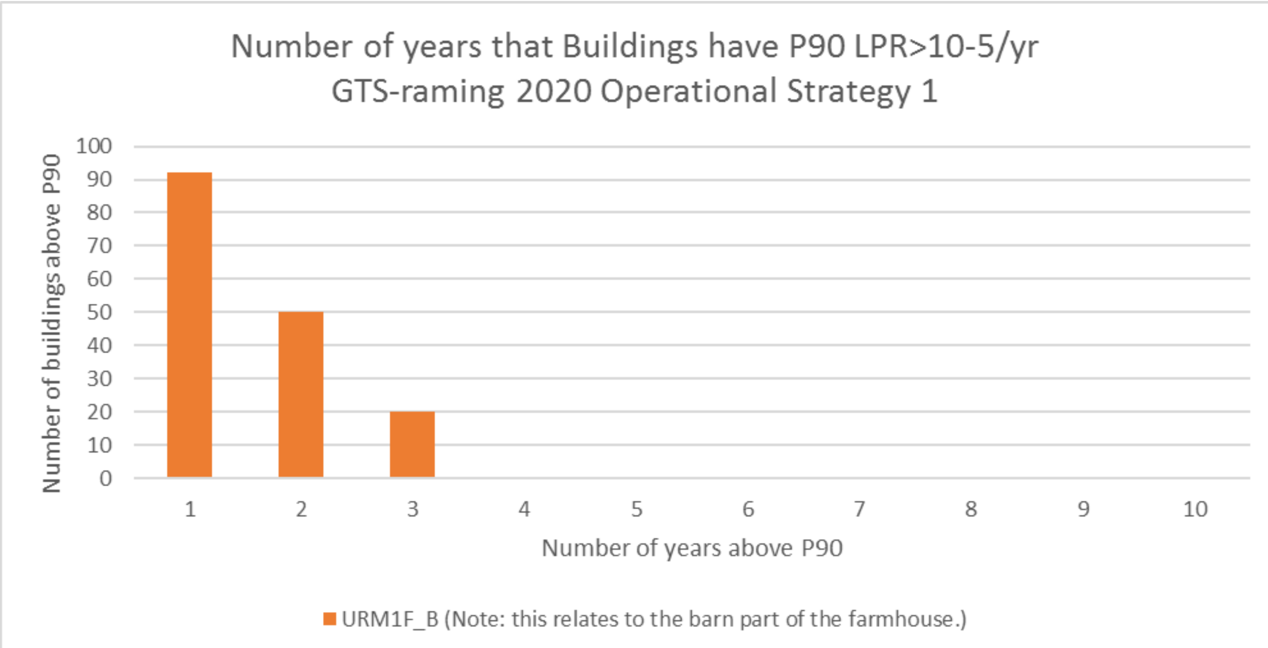

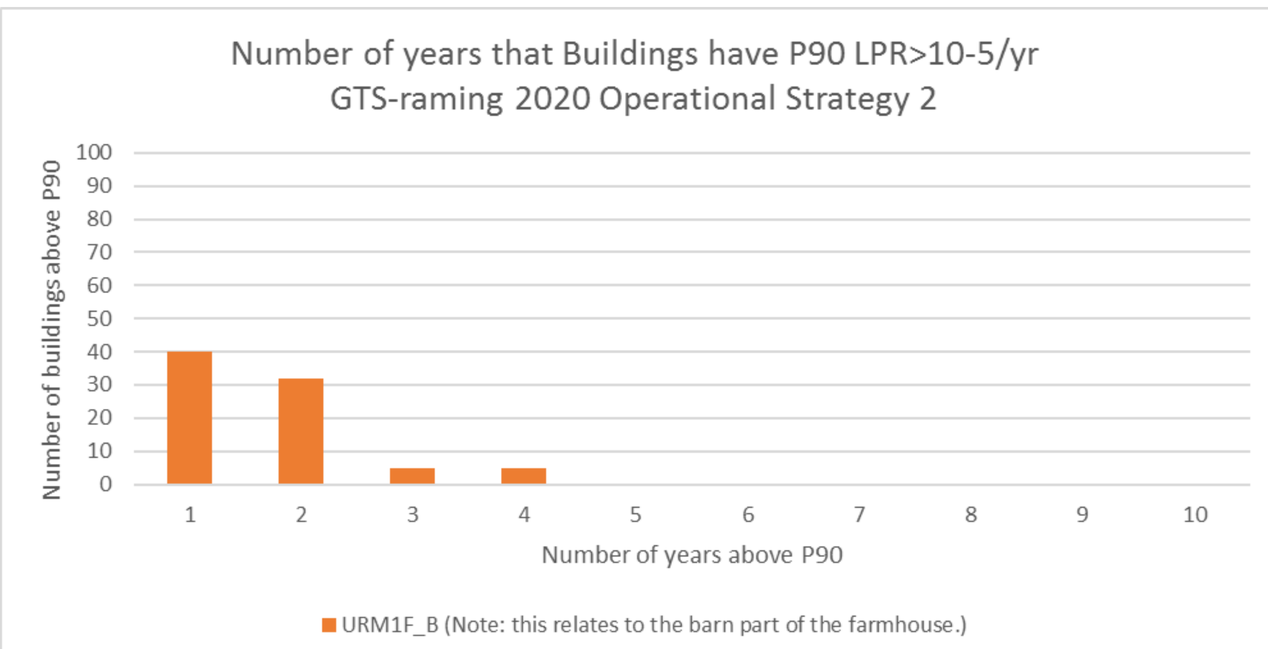

Figure 7.6 Overview of the duration that these buildings remain above the norm for buildings above the norm in 2019, shown for Operational Strategy 1 above and Operational Strategy 2 below.

7.3 Maps of Buildings compared to the Meijdam-norm Risk Levels

The maps of figure 7.7 show all buildings exceeding mean LPR>10^{-5}/year in gas-year 2020/2021 for both operational strategies. As these maps show no buildings above this norm, figure 7.7 shows the buildings that have a 10% chance of exceeding mean LPR>10^{-5}/year for the gas-year 2020/2021 to 2024/2025. The maps in figures 7.7 and 7.8 are shown for the production profile “GTS-raming 2020” with the average temperature profile for both Operational Strategies.

For the purpose of this risk assessment, the Groningen building stock has not been adjusted for the ongoing structural upgrading operations, as the list of strengthened buildings is not available to NAM.

2020/2021

Figure 7.7 *Map of all buildings exceeding mean LPR>10^{-5}/year for the gas-year 2020/2021, for the production profile “GTS-raming 2020” for an average temperature. The top maps show Operational Strategy 1, and the bottom maps show Operational Strategy 2.*

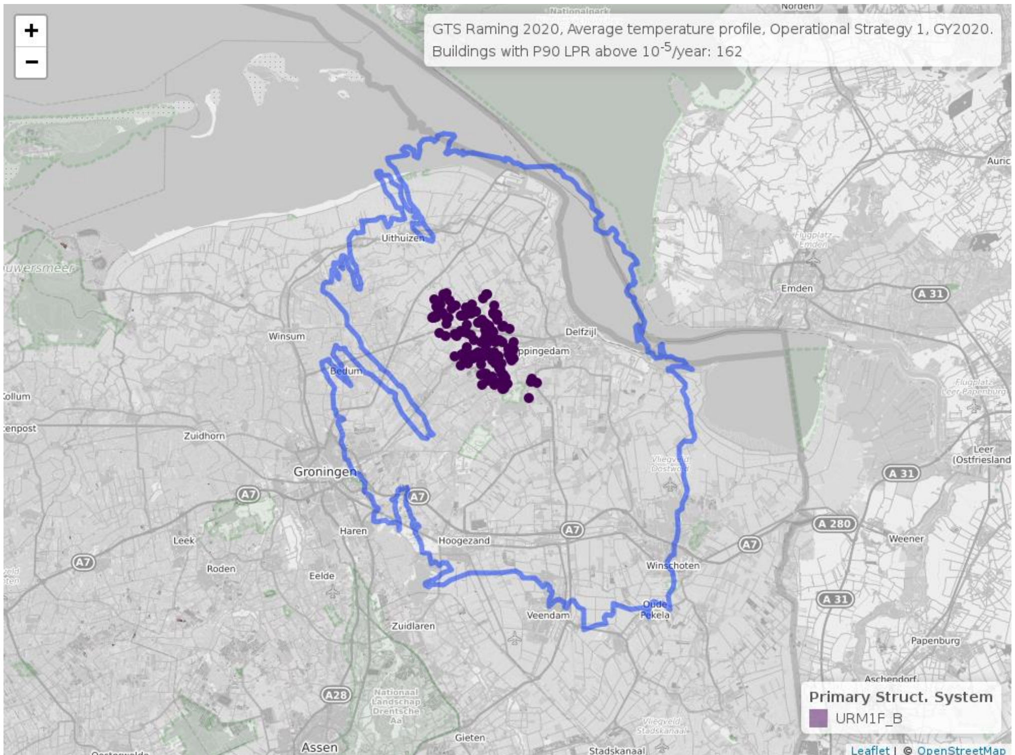

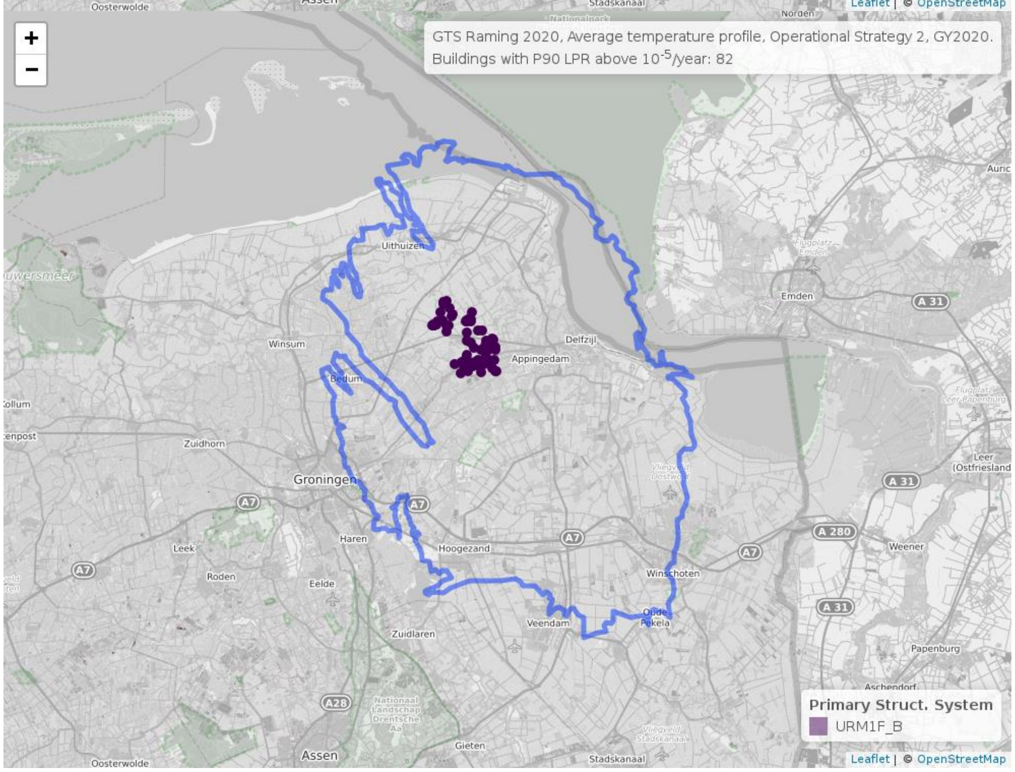

2020/2021, P90

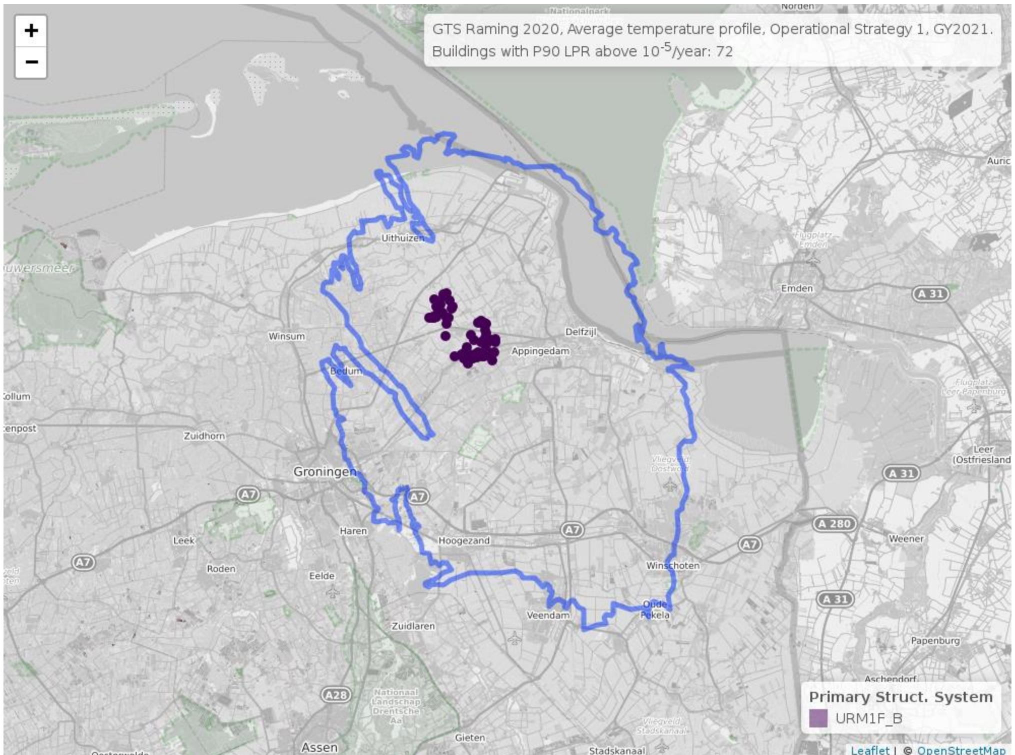

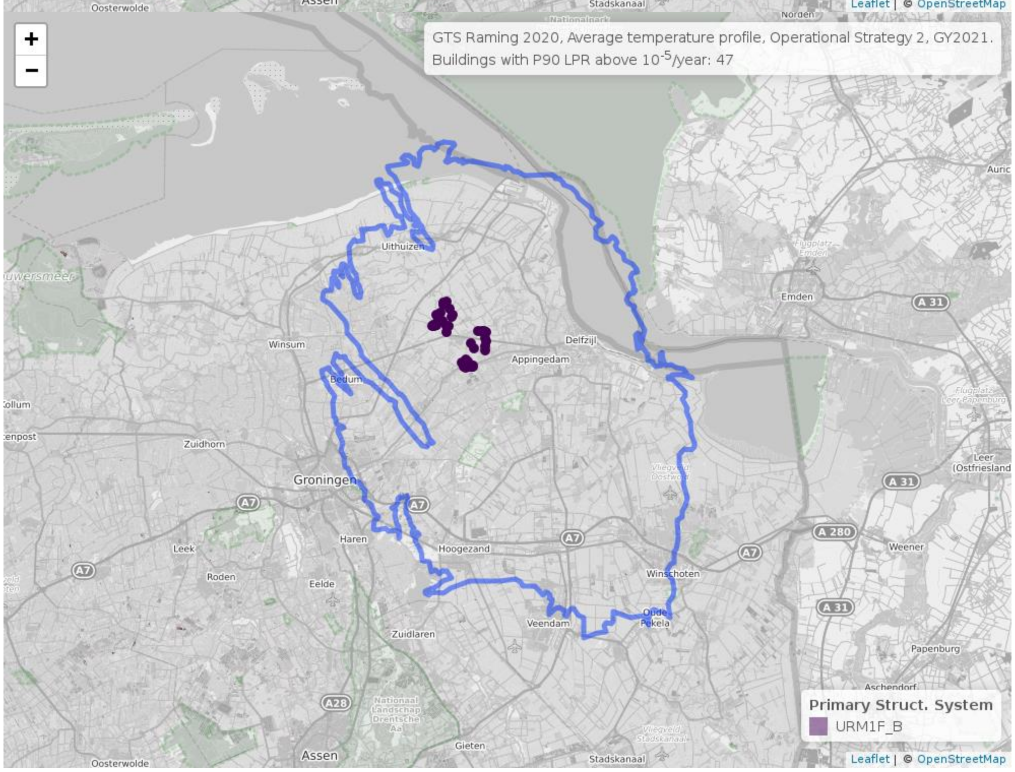

2021/2022, P90

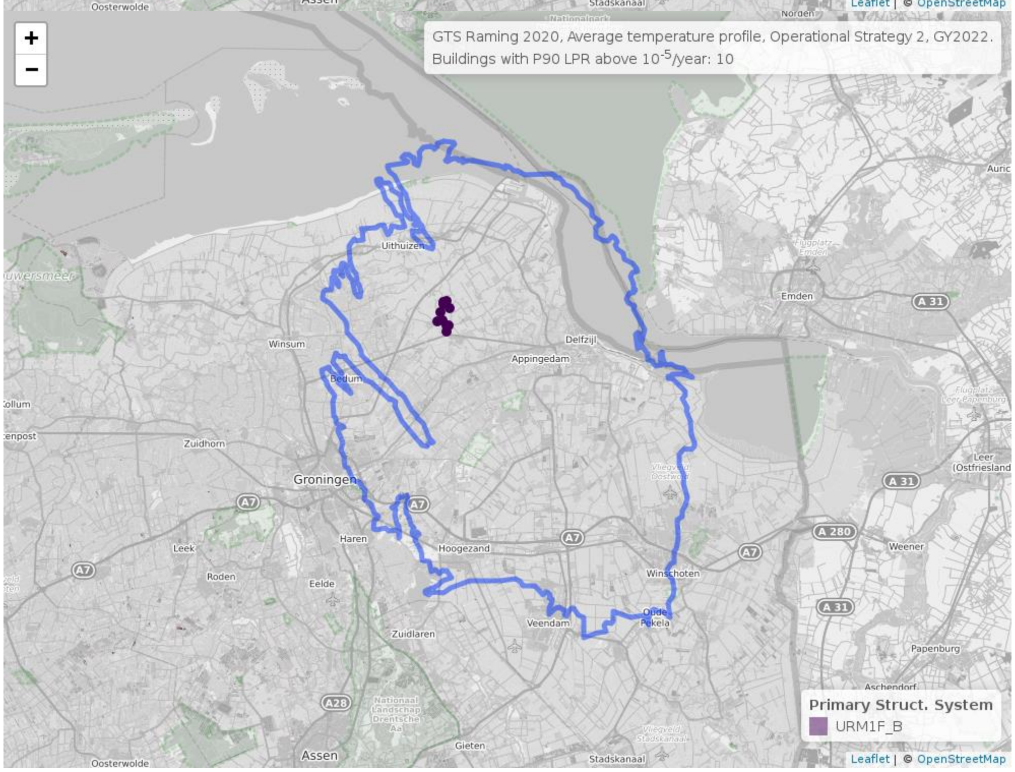

2022/2023, P90

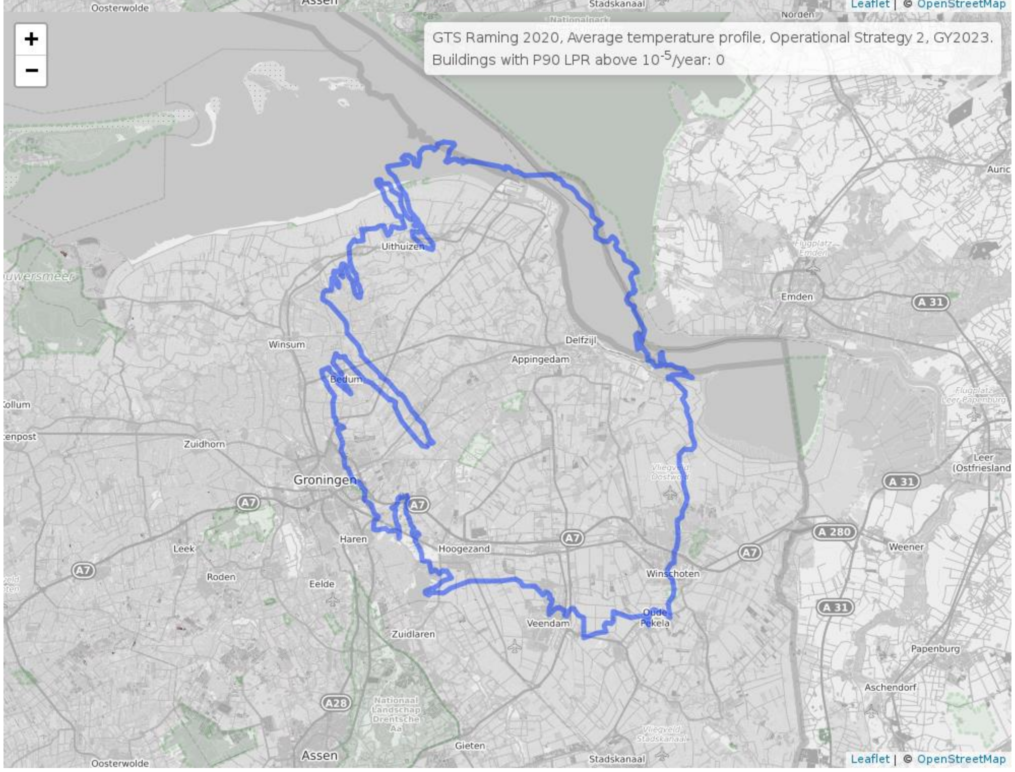

2023/2024, P90

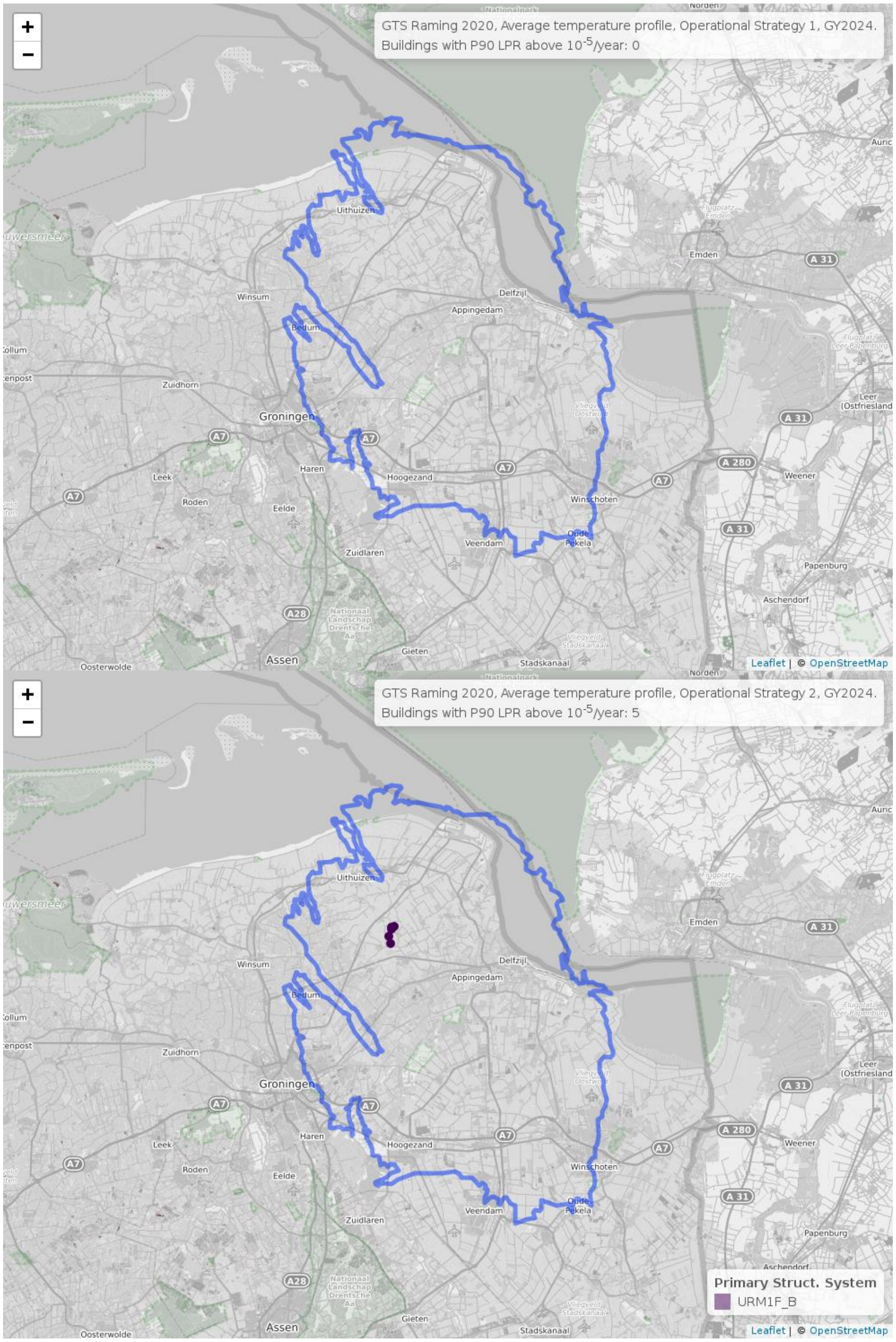

2024/2025, P90

Figure 7.8 *Map of all buildings exceeding mean LPR>10^{-5}/year for the gas-year 2020/2021, and maps of all buildings exceeding P90 LPR>10^{-5}/year for the gas-years 2020/2021 to 2024/2025, shown for the production profile "GTS-raming 2020" for an average temperature. The top maps show Operational Strategy 1, and the bottom maps show Operational Strategy 2.*

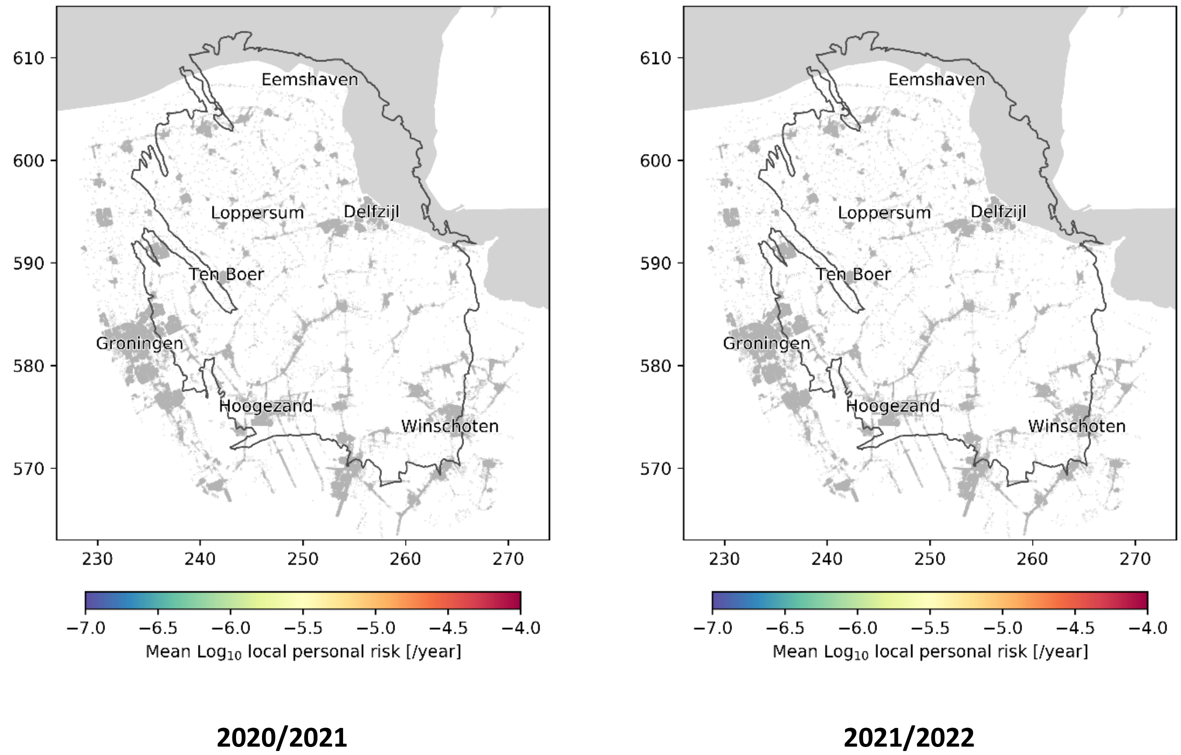

Figure 7.9 Map indicating individual building with Local Personal Risk exceeding 10^{-5}/year for the gas-years 2020/2021 to 2022/2023 and production profile "GTS-raming 2020" (average temperature).

Figure 7.10 shows a reconciliation of the buildings with a P90 LPR above 10^{-5}/year for the average temperature profile in gas-year 2020/2021, 2021/2022 and 2022/2023 between the two operational strategies. Moving from operational strategy 1 to operational strategy 2 adds 1 building near Loppersum (middle panel in figure 7.10a) and removes 81 buildings near Loppersum (right-hand panel of figure 7.9a) for gas-year 2020/2021. For gas-year 2021/2022, operational strategy 1 adds 25 buildings above the norm compared to operational strategy 2 (figure 7.9b).

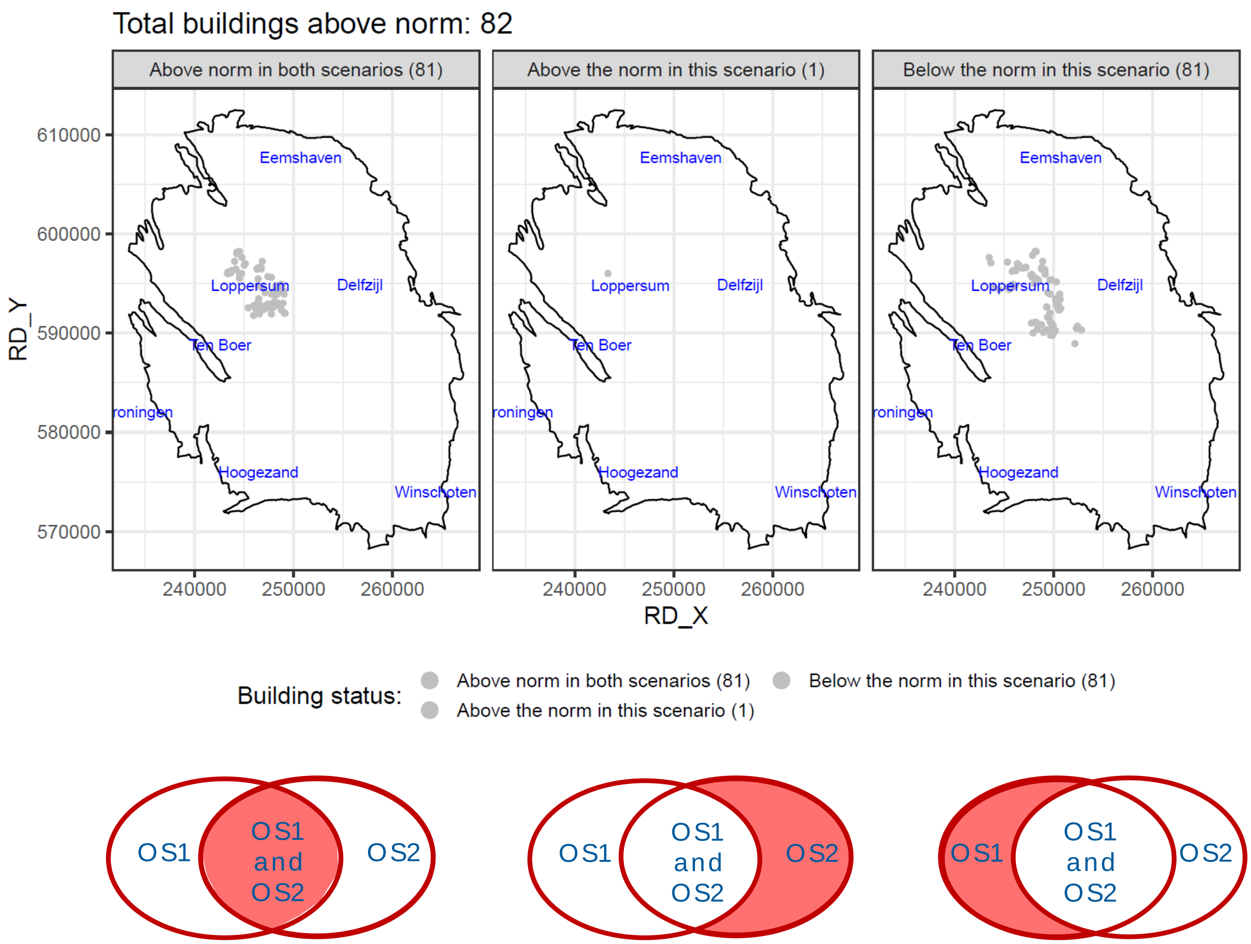

Figure 7.10a *The left figure shows the buildings with a P90 LPR above 10^{-5}/year in both operational strategies for the average temperature profile for gas-year 2020/2021. Base is operational strategy 1 and the target is operational strategy 2. The middle figure shows the buildings additionally with a P90 LPR above 10^{-5}/year for operational strategy 2, while the right figure shows the buildings additionally with a P90 LPR above 10^{-5}/year for operational strategy 1. This means that the full set of buildings in operational strategy 2 are the buildings indicated in the left and middle figure together. The buildings associated with operational strategy 1 are the buildings indicated in the left and right figure together.*

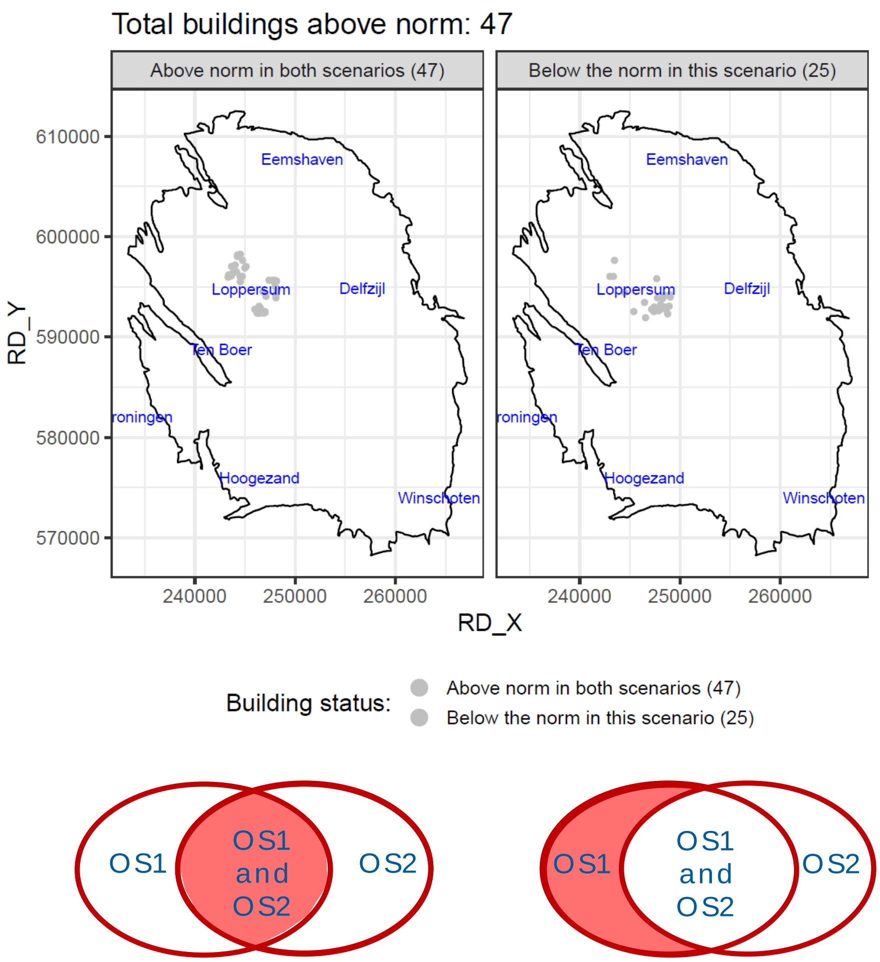

Figure 7.10b *The left figure shows the buildings with a P90 LPR above 10^{-5}/year in both operational strategies for the average temperature profile for gas-year 2021/2022. The left figure shows the buildings with a P90 LPR above 10^{-5}/year in operational strategy 2. The right figure shows the buildings additionally with a P90 LPR above 10^{-5}/year for operational strategy 1. The buildings with a P90 LPR above 10^{-5}/year in operational strategy 1 are the buildings indicated in the left and right figure together.*

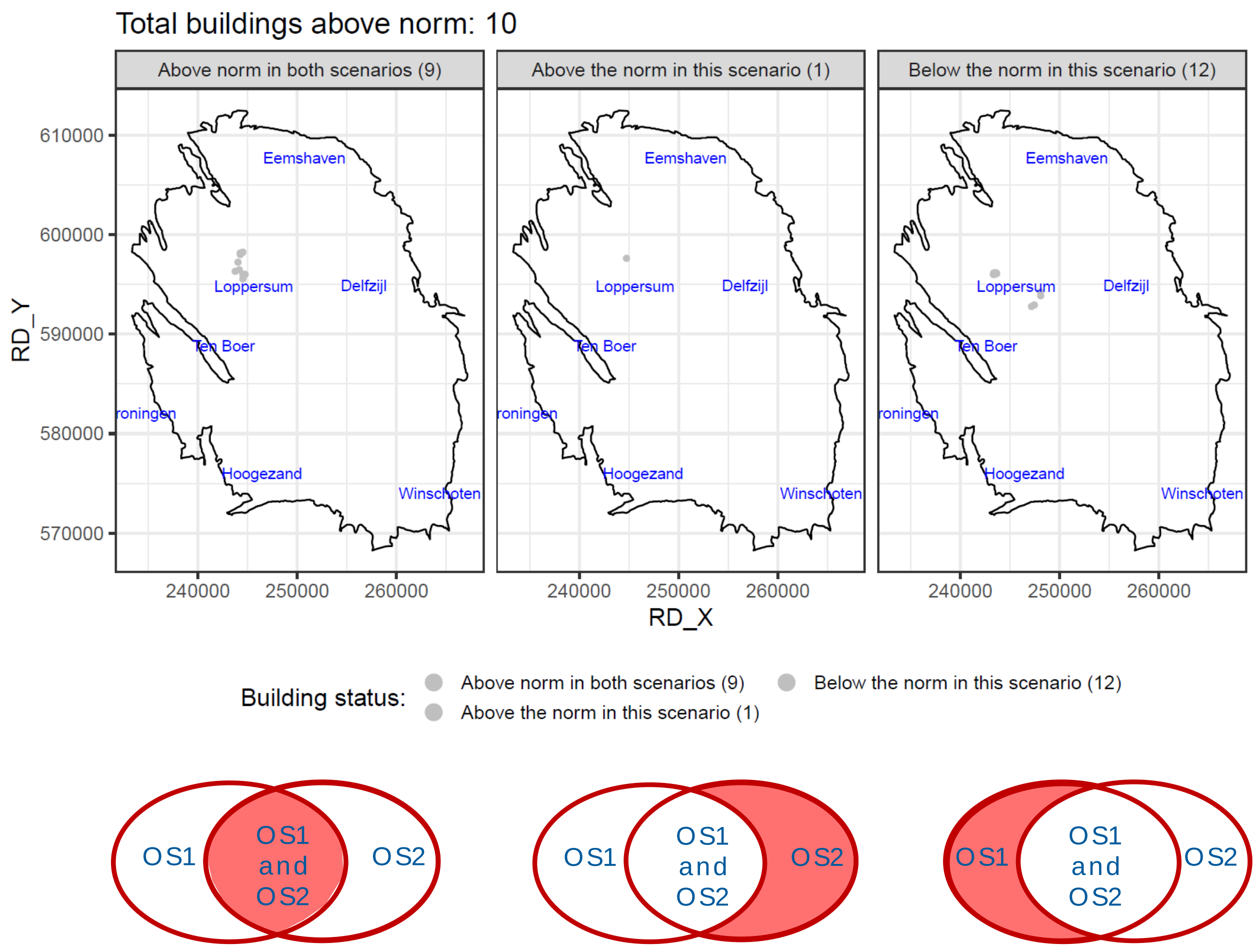

Figure 7.10c The left figure shows the buildings with a P90 LPR above 10^{-5}/year in both operational strategies for the average temperature profile for gas-year 2022/2023. Base is operational strategy 1 and the target is operational strategy 2. The middle figure shows the buildings additionally with a P90 LPR above 10^{-5}/year for operational strategy 2, while the right figure shows the buildings additionally with a P90 LPR above 10^{-5}/year for operational strategy 1. This means that the full set of buildings in operational strategy 2 are the buildings indicated in the left and middle figure together. The buildings associated with operational strategy 1 are the buildings indicated in the left and right figure together.

Figure 7.11 shows the same for the cold temperature production profile for gas-years 2020/2021 to 2022/2023. Moving from operational strategy 1 to operational strategy 2 for gas-year 2020/2021 adds 20 in the area of Loppersum and towards Hoogezand (middle panel in the figure 7.11a) and removes 45 buildings in the area of Loppersum (right-hand panel of the same figure).

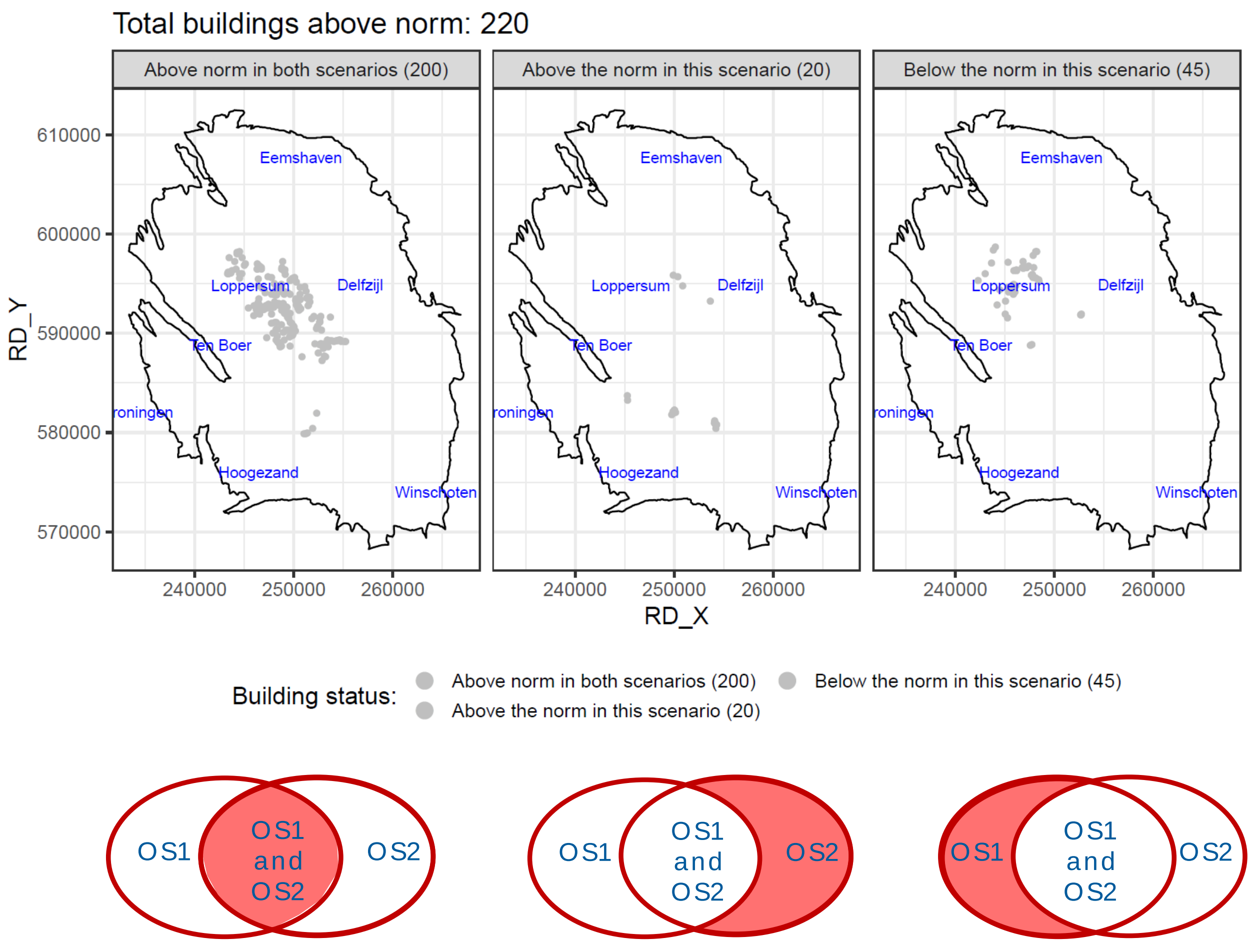

Figure 7.11a *The left figure shows the buildings with a P90 LPR above 10^{-5}/year in both operational strategies for the cold temperature profile for gas-year 2020/2021. Base is operational strategy 1 and the target is operational strategy 2. The middle figure shows the buildings additionally with a P90 LPR above 10^{-5}/year for operational strategy 2, while the right figure shows the buildings additionally with a P90 LPR above 10^{-5}/year for operational strategy 1. This means that the buildings with a P90 LPR above 10^{-5}/year in operational strategy 2 are the buildings indicated in the left and middle figure together. The buildings above the norm in operational strategy 1 are the buildings indicated in the left and right figure together.*

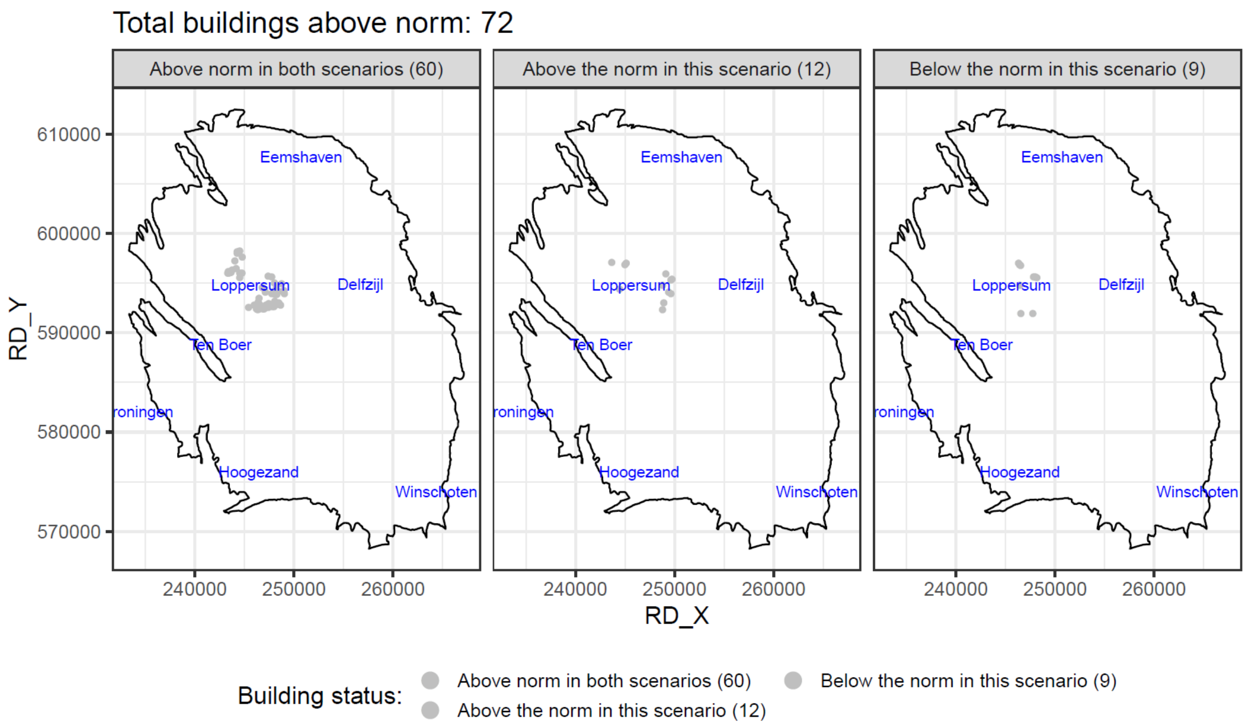

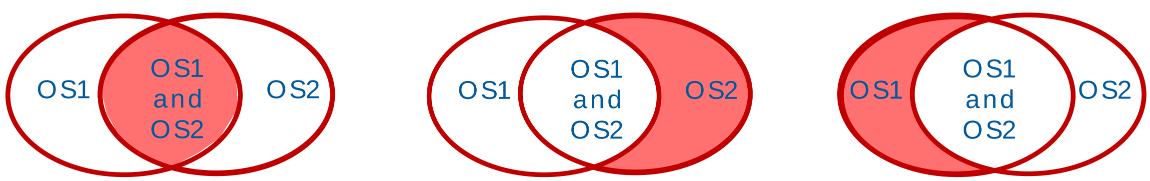

Figure 7.11b *The left figure shows the buildings with a P90 LPR above 10^{-5}/year in both operational strategies for the cold temperature profile for gas-year 2021/2022. Base is operational strategy 1 and the target is operational strategy 2. The middle figure shows the buildings additionally with a P90 LPR above 10^{-5}/year for operational strategy 2, while the right figure shows the buildings additionally with a P90 LPR above 10^{-5}/year for operational strategy 1. This means that the buildings with a P90 LPR above 10^{-5}/year in operational strategy 2 are the buildings indicated in the left and middle figure together. The buildings above the norm in operational strategy 1 are the buildings indicated in the left and right figure together.*

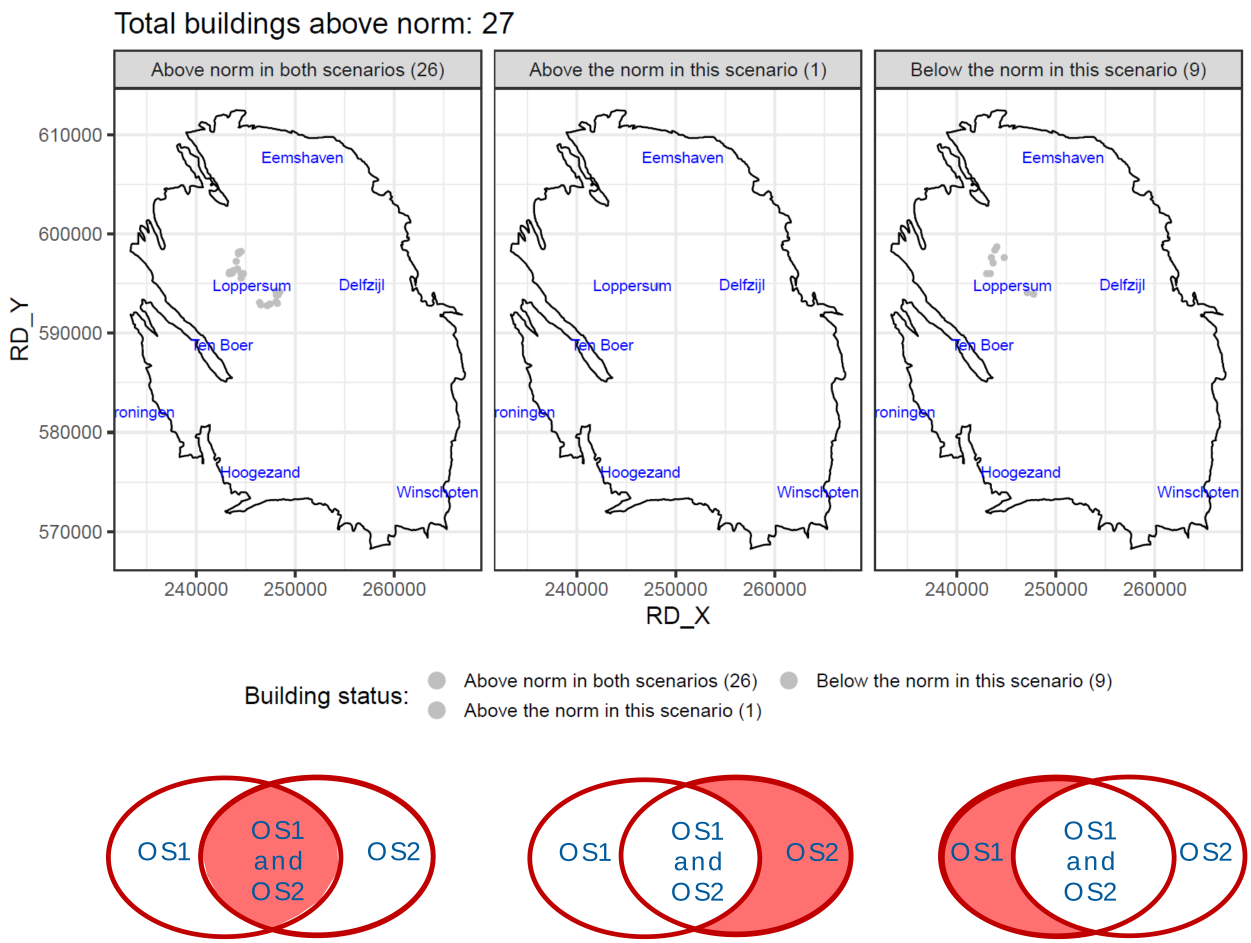

Figure 7.11c *The left figure shows the buildings with a P90 LPR above 10^{-5}/year in both operational strategies for the cold temperature profile for gas-year 2022/2023. Base is operational strategy 1 and the target is operational strategy 2. The middle figure shows the buildings additionally with a P90 LPR above 10^{-5}/year for operational strategy 2, while the right figure shows the buildings additionally with a P90 LPR above 10^{-5}/year for operational strategy 1. This means that the buildings with a P90 LPR above 10^{-5}/year in operational strategy 2 are the buildings indicated in the left and middle figure together. The buildings above the norm in operational strategy 1 are the buildings indicated in the left and right figure together.*

7.4 Insights into the development of the buildings above the norm

7.4.1 Introduction

The Hazard and Risk Assessment also provides a prioritised list of buildings that are not expected to meet the norm and of buildings which are expected to meet this norm. In the HRA report for GTS-raming 2019 (Ref. 19) we have shown that the continued decline of production, the improvements to the HRA-model, the targeted improvements to the exposure database (describing the building stock in Groningen) and the improvements of the fragility curves (describing the response of those buildings to ground motion) have had two main effects.

1. Firstly, the overall assessment of risk has decreased and consequently also the assessment of the number of buildings not meeting the norm has decreased.
2. Secondly, the assessment has increased the focus on specific typologies that are most deserving of attention in the efforts to further reduce risk.

As a result, the typology representing typical farmhouses with barns dominated the stock of buildings not meeting the norm, in addition to a few terraced houses with large opening percentages in the ground floor façade walls.

7.4.2 Comparing the results of risk assessments

This section describes the evolution of the number of buildings in a risk classification between this assessment and the previous one (Ref. 19). As the basis for this comparison “GTS-raming 2019” gas-year 2019/2020 with average temperature demand and Operational Strategy 1 (i.e. the strategy selected by the Minister of Economic Affairs and Climate Policy) is presented. For the comparison we will make use of Sankey diagrams. These are a specific type of flow diagram, in which the width of the arrows is proportional to the number of buildings.

Figure 7.12 shows a Sankey diagram summarising the overall changes (occupied buildings) per risk classification group defined by the “Mijnraad”:

- Buildings with meanLPR > 10^{-5}/year – “Mijnraad 1500” Group,
- buildings with more than 10% probability of having LPR > 10^{-5}/year, but not part of the first bullet - the “P90 Group”, and
- buildings not part of above risk priority groups – in the figure labelled P10 LPR < 10^{-5}/year.

On the left the numbers of buildings in these three groups are represented as they were in the assessment of February 2019 and on the right are the numbers in the current assessment. Also buildings that were previously not in the EDB (V6) but are now, are shown (new in EDB V7). The connections between these illustrate the movement of the buildings in these categories between these two risk assessments.

The number of buildings above the norm decreased from 435 to 0, and the “P90 Group” reduced from 3,271 to 82 Buildings.

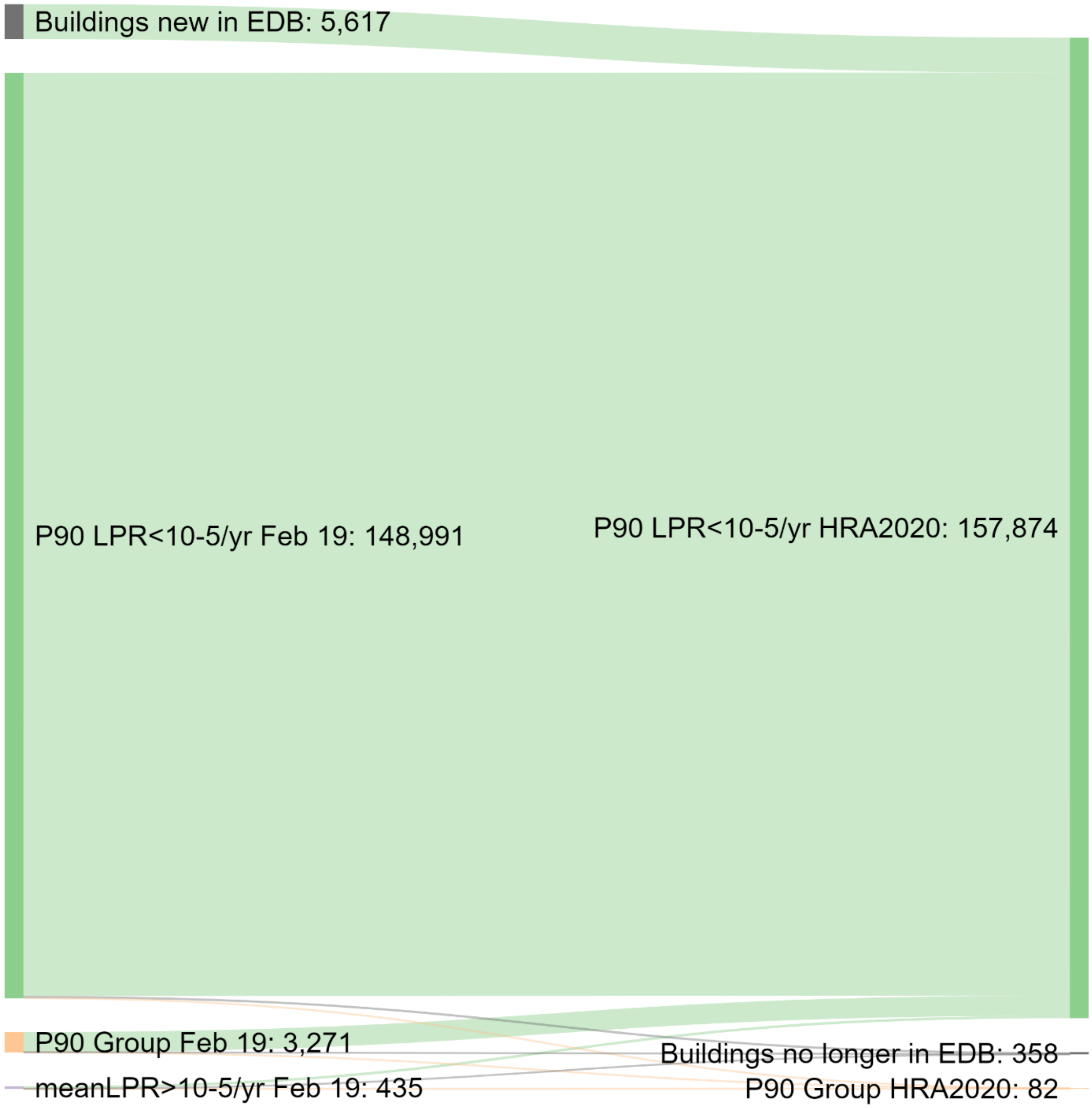

Figure 7.12 Sankey diagram summarising the changes (occupied buildings) from "GTS-raming 2019" gas-year 2019/2020 Operational Strategy 1 to "GTS raming 2020" gas-year 2020/2021 Operational Strategy 2 with average temperature demand.

Anticipating that most attention will be drawn to buildings with highest risk profile, the following paragraphs focus on buildings with mean LPR>10^{-5}/year – i.e. not meeting the Meijdam-norm.

7.4.3 Update to buildings above the norm

The total number of buildings not meeting the 10^{-5}/year norm has now further declined from 435 for GTS-raming 2019 (OS1 with average temperature demand gas-year 2019/2020) to 0 for GTS-raming 2020 (both operational strategies with average temperature demand). That reduction is caused by the following developments:

- The hazard has decreased because of further reduced production.
- The HRA-model has been updated with the latest scientific insights.
- The modelled response of buildings to ground motion as captured in the so called 'fragility curves' has changed. Fragility and consequence models were updated for several relatively more vulnerable building typologies, including farmhouses with barns.
- Improvements in Groningen building stock knowledge resulted in updates to the Exposure database EDB V7.

Of the 435 buildings that were previously assessed as not meeting the norm in gas-year 2019/2020:

- 0 buildings are still expected not to meet the Meijdam-norm (mean LPR> 10^{-5}/year).
- 4 buildings are no longer present in the EDB. This means that they are no longer registered with the Kadaster as occupied building (for example because they have been demolished in the meantime).
- The remaining 431 buildings are now all expected to meet this norm. Of those, 34 still have a small probability of not meeting the norm and are now part of the so-called 'P90 group'.

The following diagram illustrates the above:

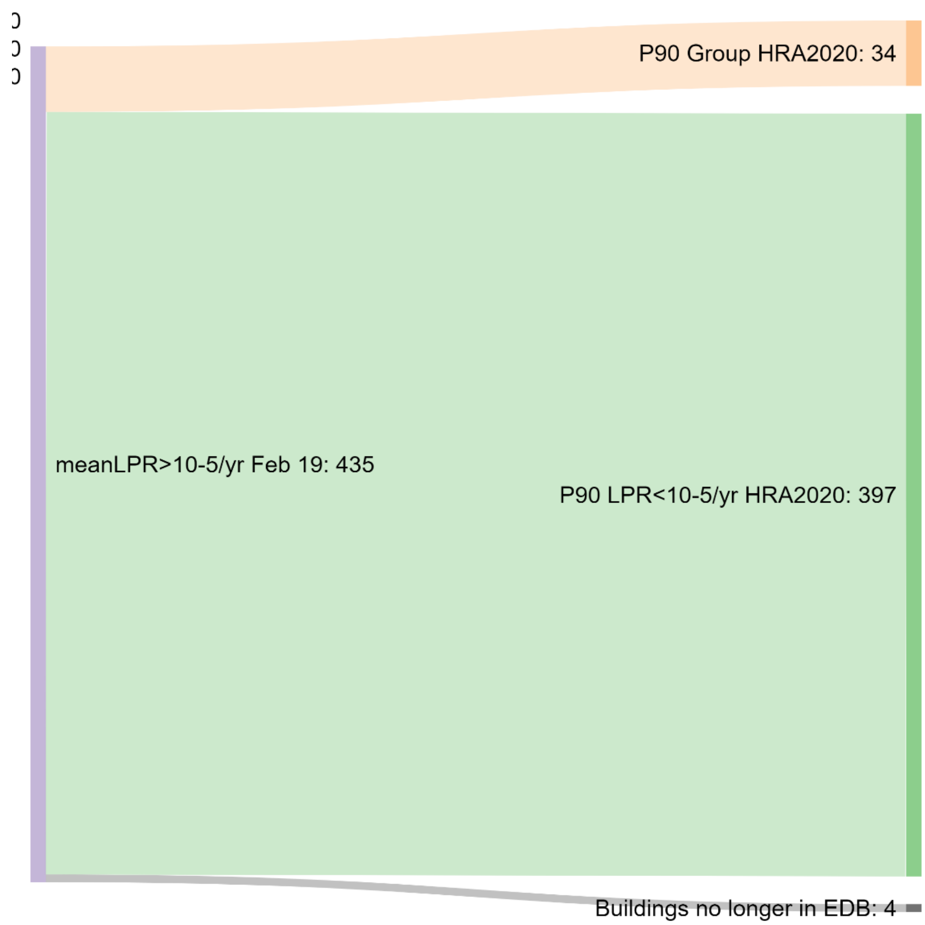

Figure 7.13 Sankey diagram showing developments between 'GTS-raming 2019" Operational Strategy 1 and "GTS-raming 2020" Operational Strategy 2 (average temperature demand) assessment for the buildings not meeting the 10^{-5}/year norm.

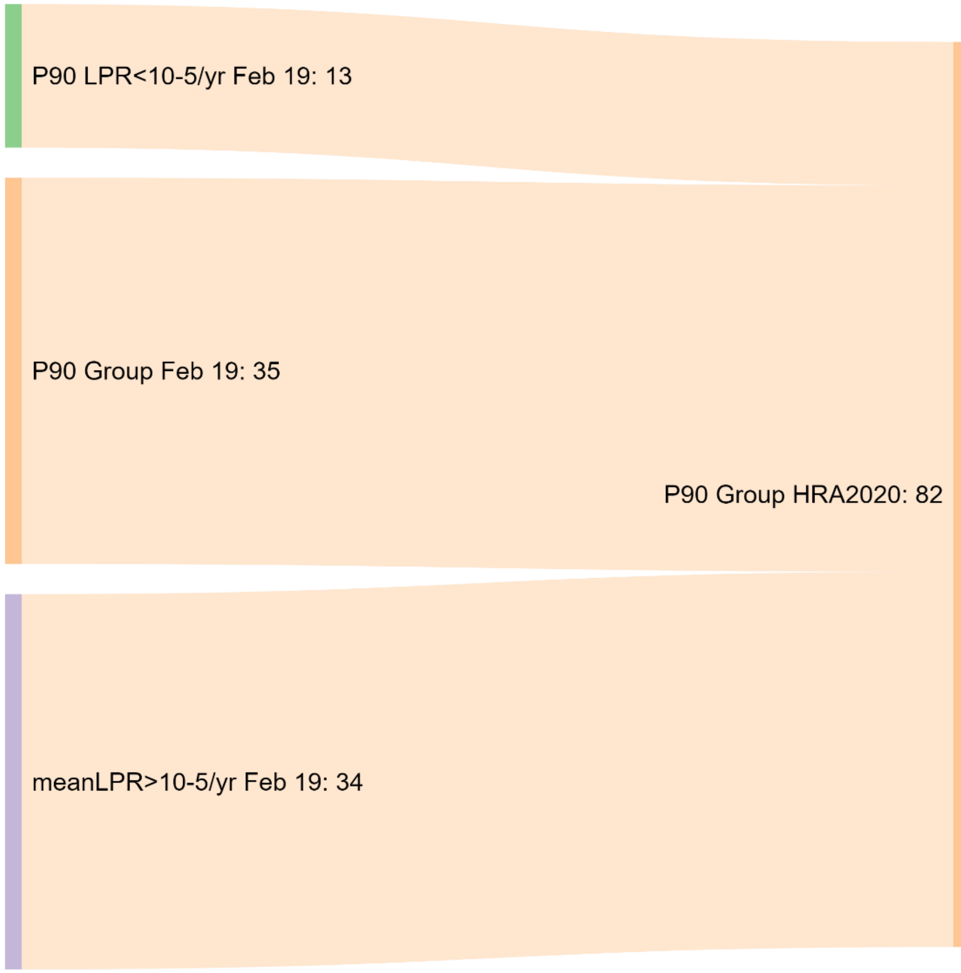

Figure 7.14 *Sankey diagram showing developments between 'GTS-raming 2019" Operational Strategy 1 and "GTS-raming 2020" Operational Strategy 2 (average temperature demand) assessment for the buildings now not meeting the P90 LPR 10^{-5}/year criterion.*

The assessment of whether individual houses are expected to meet or not meet the Meijdam-norm is one of the inputs into the risk management policy set by the Minister (Ref. 28 to Ref. 30). How this information is used to derive inspection and/or structural upgrading programmes is not described in this report and is outside the remit of NAM.

7.5 Structural upgrading program

The probabilistic assessment of the number of buildings that do not meet the Meijdam-norm does not immediately translate into an estimate of the structural structural upgrading scope. There are three main reasons why the scope of the structural upgrading plan will in general be larger than the probabilistic assessment of the number of buildings that do not meet the Meijdam norm. The involvement of the Minister of EZK over the past years with the structural upgrading has been formally implemented in the Mining law in December 2019.

- Efficiency of identifying buildings with mean LPR >10^{-5}/year (Meijdam-norm) has not yet been proven.
  The Hazard and Risk Assessment is a probabilistic assessment and does not directly identify each individual building that needs to be included in the structural upgrading plan. It identifies which buildings have the highest risk of (partial) failure based on the building features in the Exposure Database. If a risk-based approach is to be followed, verification of the building features as used in the Hazard and Risk Assessment (by inspection) would be required. This means that inspection results will either confirm the building features or otherwise, which will have implications for prioritisation (for any subsequent engineering and structural upgrading). A risk-based inspection program will be able to identify which building may need structural upgrading with reasonable efficiency and help prioritising the effort.
- Remaining uncertainty in Hazard and Risk Assessment.
  Significant progress has been made towards assessing the risk from Groningen earthquakes. However, uncertainty remains in the estimate of the number of buildings that do not meet the norm based on mean LPR > 10^{-5}/year. Further studies, experiments, modelling and building inspections can help reduce this uncertainty.
  The regulator attached therefore special relevance to the P90 estimate for risk for a building. This serves as an additional conservatism in the risk assessment.
- Differences between the Hazard and Risk Assessment and NEN-NPR building code.
  Ultimately the structural upgrading scope will be based on the NEN-NPR building code. Improvement of the Hazard and Risk Assessment and calibration of the building code with the latest technical insight from laboratory experiments and modelling in the NEN-NPR are likely to reduce the difference between the HRA assessment and the results of assessing the safety of individual buildings using the NPR building code. In the advice to the Minister of 11 February 2019 (Ref. 72), 26 June 2019 (Ref. 73) and 10 October 2019 (Ref. 74), SodM stressed the importance of using the latest scientific insights in the NEN-NPR. In the advice of 19 December 2019 (Ref. 75), SodM notes: "With regard to the NPR 9998, it appears that there is currently no prospect of introducing a new, improved version. It is therefore unclear how long it will take before the latest scientific insights are incorporated. This while there are clear signals that clear improvements are possible".

The probabilistic estimate of the number of buildings, where the Meijdam-norm safety level is exceeded, does therefore not directly translate into an estimate of the structural upgrading scope. However, the Hazard and Risk Assessment provides a useful tool for prioritisation of building inspections. Ultimately the structural upgrading scope will be based on the assessment of individual buildings based on the NEN-NPR building code.

7.6 Disaggregation of Local Personal Risk (LPR)

We analyse the contribution of aleatory variabilities to the mean logic tree Local Personal Risk outcomes for each surface location and structural system by applying the same method of disaggregation as previously described for seismic hazard. In this case the selected aleatory variables are magnitude, M, distance, R_{rup}, and the average pseudo spectral acceleration, *AvgPSA*, as defined by the building fragility model.

Figure 7.15 shows risk disaggregation results for the Loppersum location and three structural systems typically associated with the highest LPR values. In all three cases, the marginal contribution of magnitudes to mean LPR is bi-modal with the primary mode at $M = 4.7$ and the secondary mode at $M = 4.4$. We interpret this to indicate the influence of the $M_{max} = 4.5$ logic tree branch that creates a discontinuity in the distribution as previously seen within the hazard disaggregation results. Indeed, all M_{max} values within the logic tree (4.0, 4.5, 5.0, 5.5, 6.0. 6.5) appear as inflection points in all these distributions of magnitude contributions to LPR. The distributions of distance contributions to risk show much less complexity with a clear mode at $R_{rup} = 3$ km and a strong clear decline with increasing distance, all as previously seen in the hazard disaggregation results. The distributions of average PSA risk contributions all show a well-defined mode at about 0.5 g, but with significant contributions extending above 1.0 g. A small degree of jitter is visible in these distributions, which may reflect some residual stochastic variability associated with finite sample effects despite simulating 4.5×10^6 earthquake catalogues for each of the 1008 logic tree branches.

For the Groningen city location (Figure 7.16), we see the modal magnitude contribution to LPR increase to $M = 5.7$ for all three structural systems. These marginal distributions exhibit strong inflections points aligned with the choice of every discrete M_{max} value placed on the logic tree. Despite the presence of these strong secondary maxima, the primary modal value remains clear. Modal distances increase to $R_{rup} = 5$ km, as also previously observed in the hazard disaggregation results. The secondary mode seen in the hazard disaggregation at $R_{rup} = 17$ km is also discernible in these risk disaggregation results although it is much less-well sampled and may be an artefact of residual stochastic variabilities. The average PSA risk contributions show a clear mode at $AvgPSA = 0.45$ g for the URM1F_B structural system, whilst the other two structural systems show almost equal risk contributions over the interval 0.4 g < *AvgPSA* < 0.7 g. The residual stochastic jitter in these distributions means the mode cannot be reliably measured.

Figure 7.17 summarizes the variation of the largest risk contributions associated with magnitude, distance and average PSA for same three structural systems shown in Figure 7.15 and Figure 7.16. For all three structural systems, the areal distribution of modal magnitudes and distances are quite similar with magnitudes in the range $4.0 < M < 5.0$ making the largest contribution to mean LPR in the central parts of the analysis area. Outside this central region, the magnitudes that make the largest contributions to risk increase to $5.5 < M < 6.5$. As seen before in the hazard disaggregation results, most of the seismic risk is associated with local underlying seismicity in the central region and only on the edges of the analysis area does this increase up to 15 km. We observe little spatial organization in the modal values of average PSA but these do exhibit stronger variability between structural systems than seen for magnitudes and distances.

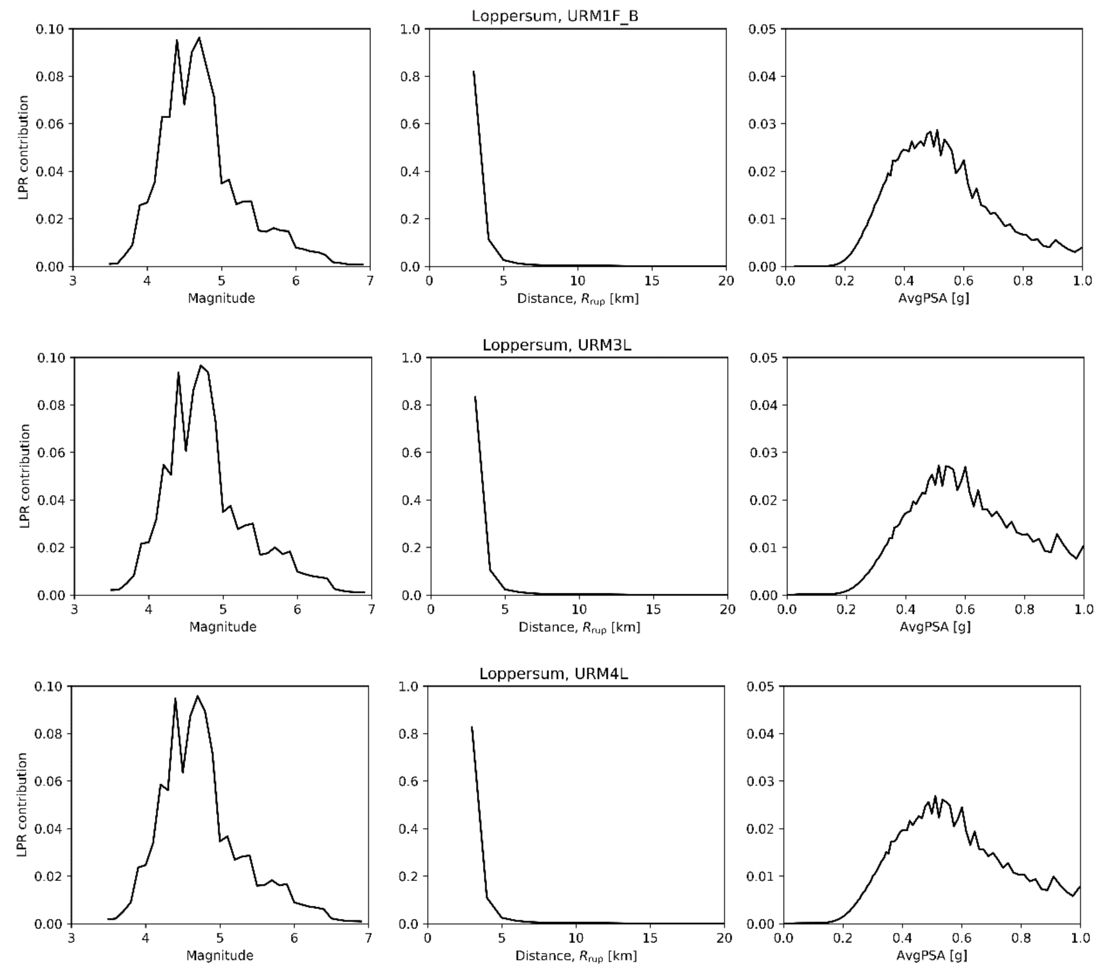

(a)

(b)

(c)

Figure 7.15 *The fractional contributions to the mean Local Personal Risk (LPR) at the Loppersum location for three structural systems (a) URM1F_B, (b) URM3L and (c) URM4L given gas-year 2020/2021 and the base case production scenario (GTS-raming 2020 for the average temperature weather and Operational Strategy 1).*

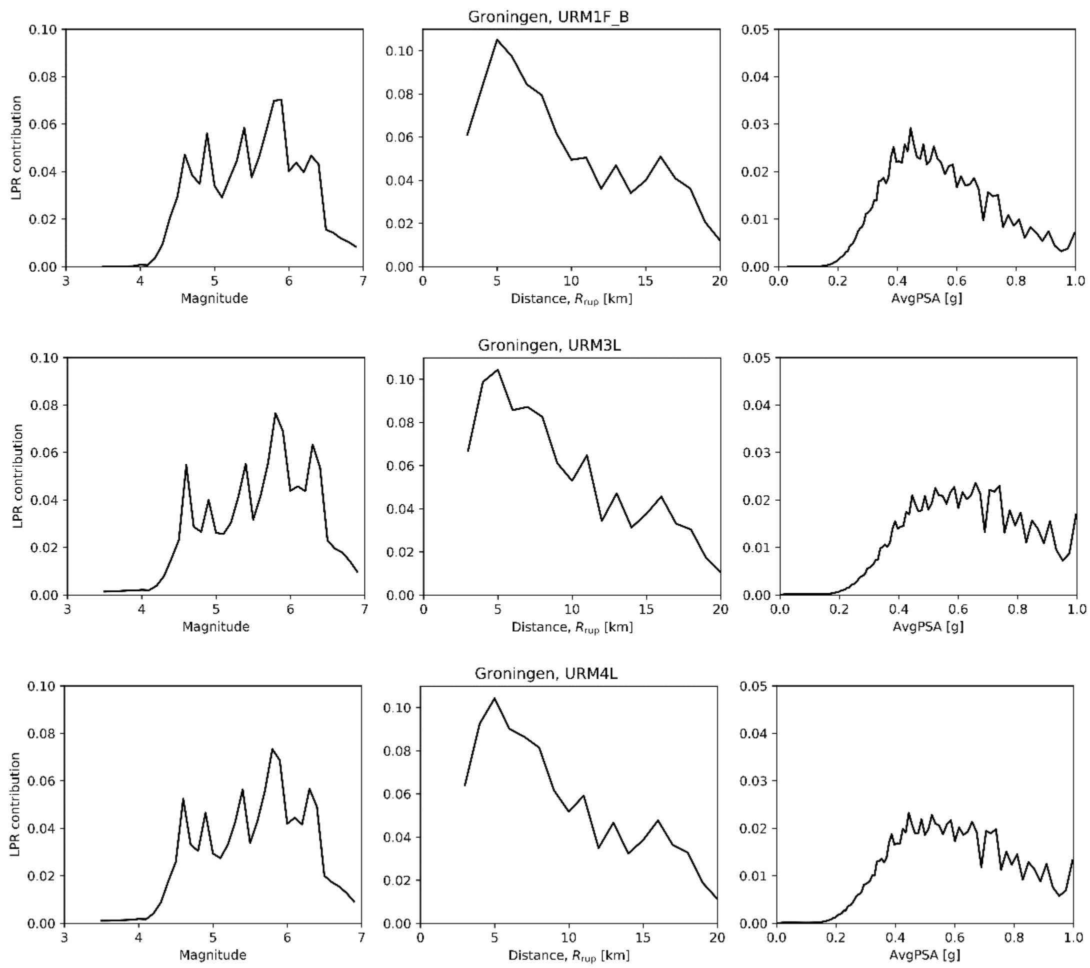

(a) (b) (c)

Figure 7.16 As Figure 7.15, except for the Groningen city location.

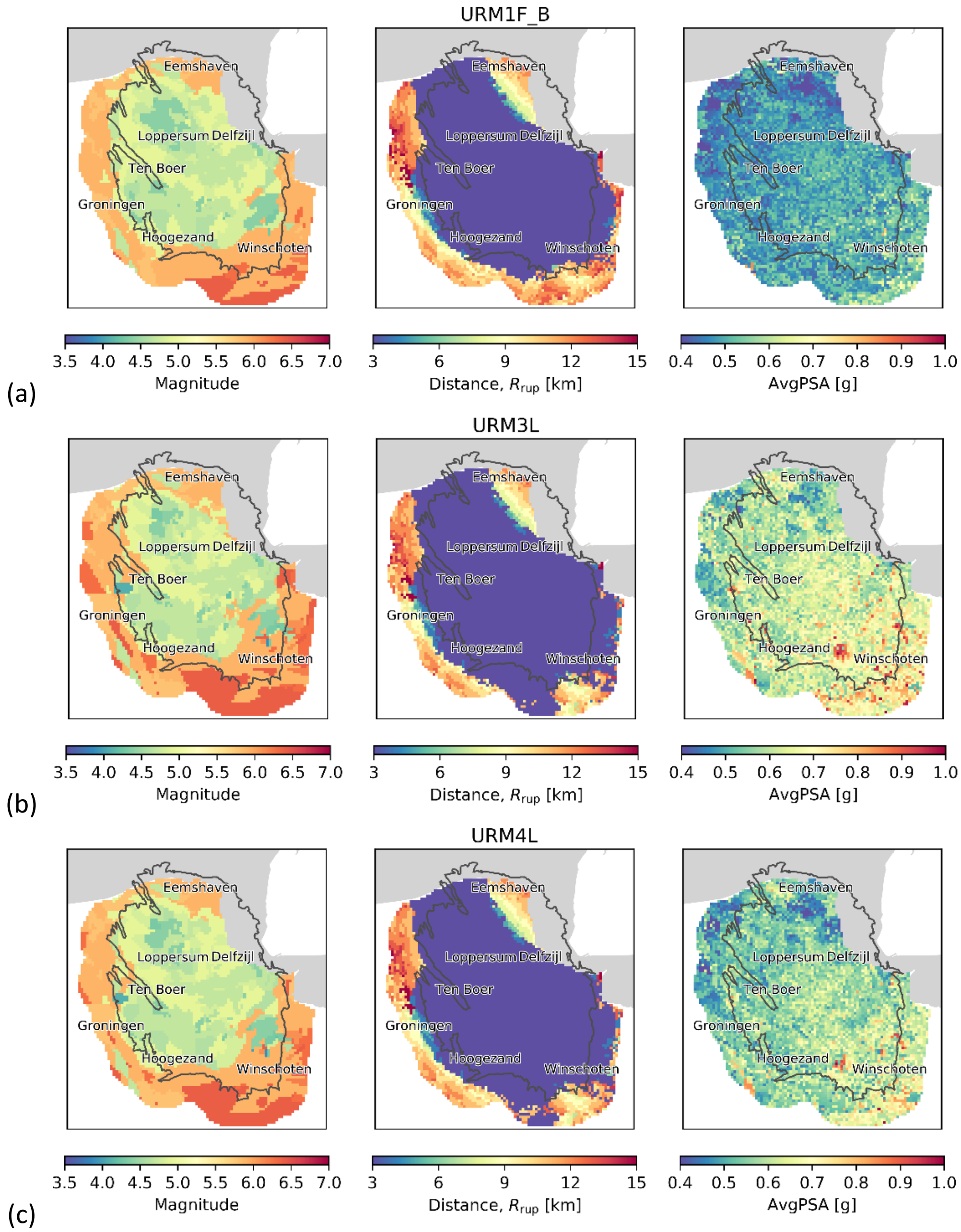

Figure 7.17 *Maps of the magnitude, M, distance, R_{rup}, and the average PSA for building fragility, AvgPSA, that contribute most to the mean Local Personal Risk metric over gas-year 2020/2021 under the base case production scenario (GTS-raming 2020 for the average temperature weather and Operational Strategy 1). Results are shown for three structural systems: (a) URM1F_B, (b) URM3L, and (c) URM4L, as previously shown in Figure 7.15.*

7.6.1 Sensitivity to epistemic uncertainties

We quantify epistemic uncertainty within our Probabilistic Seismic Hazard and Risk Analysis using the full factorial logic tree shown in Figure 7.18. This logic tree includes six key factors:

1. the earthquake magnitude-frequency model,
2. the maximum possible earthquake magnitude model,
3. the ground motion median-τ model,
4. the ground motion ϕ-model,
5. the building fragility model, and
6. the consequence model.

Each factor contains from 2 to 7 levels designed to characterise the distribution of mutually-independent alternative models that collectively span the range of epistemic uncertainties. To better understand the relative contributions of each logic tree factor to the risk prediction intervals we disaggregate the logic tree to obtain their marginal distribution for a given summary risk metric. For instance, the upper level of contributions from the magnitude-frequency model is measured as the weighted mean of all logic tree branches that include the upper level of the magnitude-frequency model re-weighted by the relative weights of these selected branches. The lower level of contributions from the magnitude-frequency model is likewise computed from all logic-tree branches that include the lower level of this factor. Repeating this procedure for all factors and levels yields a tornado plot of ranked sensitivities to epistemic uncertainties for a given risk metric. Summary risk metrics utilized for this purpose include the mean LPR for all exposed people, and the number of buildings with a mean LPR exceeding a given threshold, such as 10^{-5}/year. Figure 7.19a shows results for the mean LPR metric indicating the epistemic uncertainties recognized in the maximum possible earthquake magnitude, Mmax, are the most influential, followed by the nature of stress dependence in the frequency-magnitude model, and then the fragility model. The ranking of all 6 risk factors remains essentially unchanged for 3 other alternative risk metrics (Figure 7.19b, Figure 7.20). This indicates the most effective means of reducing the influence of epistemic uncertainties on the risk analysis is for any further data acquisition and studies to target the top-ranking risk factors shown in Figure 7.19 and Figure 7.20.

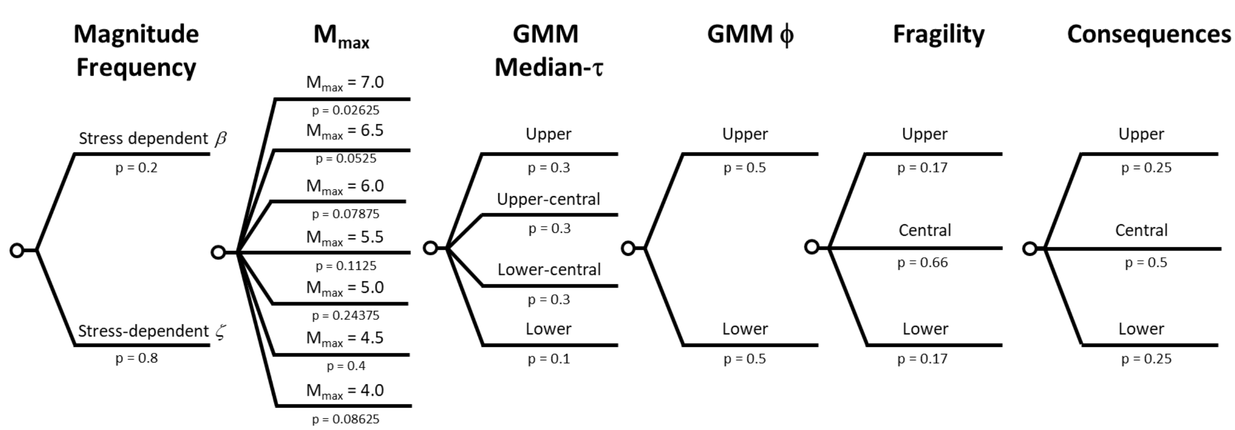

Figure 7.18 The structure and weights of the full-factorial logic tree for Probabilistic Seismic Hazard Analysis (factors 1-4) and Probabilistic Seismic Risk Analysis (factors 1-6).

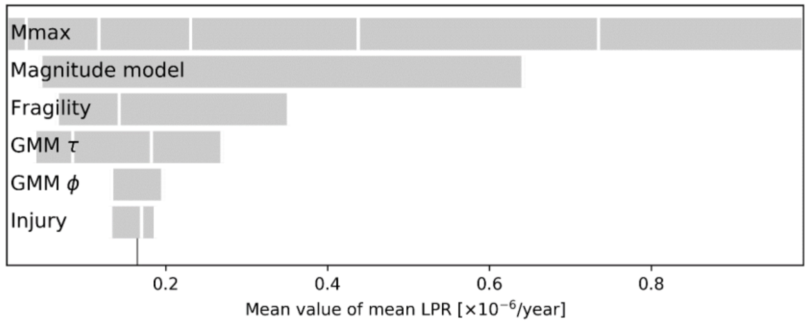

(a)

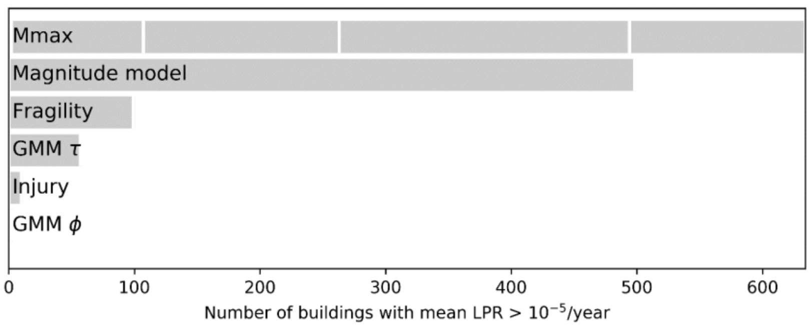

(b)

Figure 7.19 *Sensitivity of seismic risk to epistemic uncertainties as measured by (a) the mean local personal risk (LPR) per exposed individual, and (b) the total number of buildings with a mean LPR exceeding 10^{-5}/year. Grey bars denote risk intervals spanned by consecutive levels of a risk factor. The vertical black line denotes the mean of the entire logic tree. Data is shown for gas-year 2020/2021 under the base case production scenario (GTS-raming 2020 for the average temperature weather and Operational Strategy 1).*

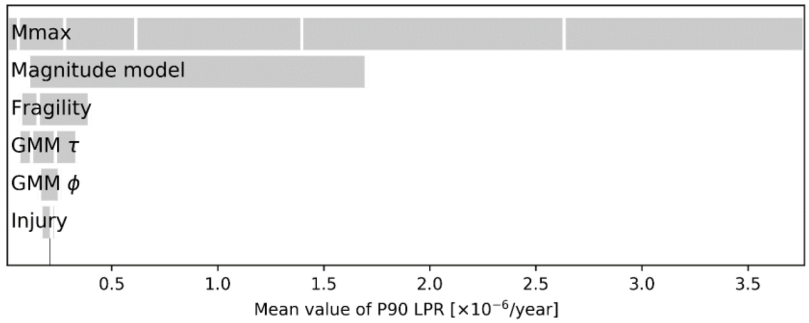

(a)

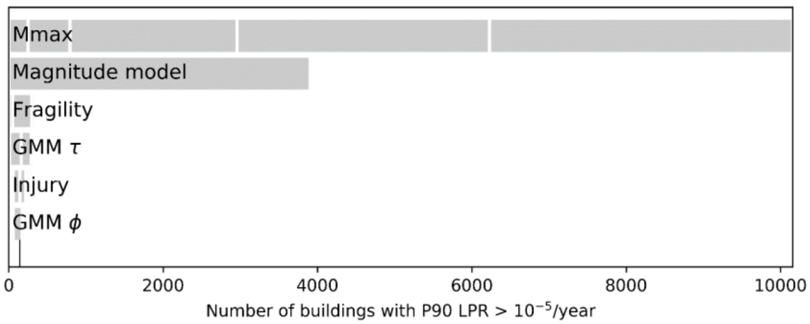

(b)

Figure 7.20 *Sensitivity of seismic risk to epistemic uncertainties as measured by (a) the mean P90 local personal risk (LPR) per exposed individual, and (b) the total number of buildings with a P90 LPR exceeding 10^{-5}/year. Data is shown for gas-year 2020/2021 under the base case production scenario (GTS-raming 2020 for the average temperature weather and Operational Strategy 1).*

7.7 Group Risk and Maatschappelijk veiligheidsrisico

The Maatschappelijk Veiligheidsrisico has been calculated for seven communities and for the area of the Groningen field (Fig. 7.21).

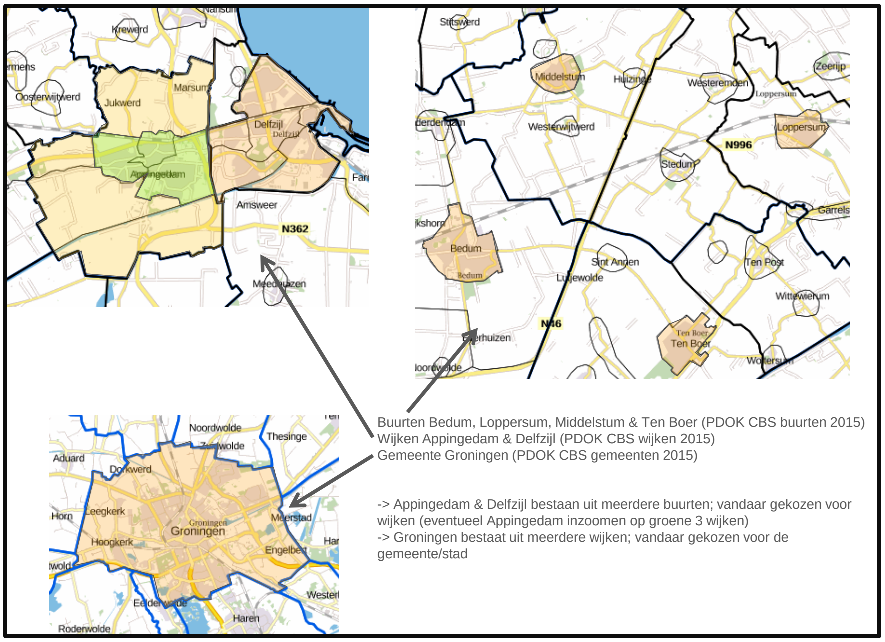

Figure 7.21 Extract from the advice by Ministry of Economic Affairs detailing the seven communities selected for calculation of Maatschappelijk Veiligheidsrisico.

This selection was based on the CBS buurtenkaart (Ref. 71). Table 7.5 shows that the seven selected communities are composed of several neighbourhoods in the CBS buurtenkaart.

Community	Attribute Value	CBS Neighborhood/District
Appingedam	Appingedam-Centrum Appingedam-West Appingedam-Oost	Appingedam-Centrum Appingedam-West Appingedam-Oost
Delfzijl	Delfzijl-Centrum Delfzijl-Farmsum Delfzijl-Noord Delfzijl-West Delfzijl-Fivelzigt Delfzijl-Tuikwerd	Delfzijl-Centrum Farmsum Delfzijl-Noord Delfzijl-West Fivelzigt Tuikwerd
Groningen	Groningen-Binnenstad Groningen-Schilders- en Zeeheldenwijk Groningen-Oranjewijk Groningen-Korrewegwijk	Wijk 00 Binnenstad Wijk 01 Schilders- en Zeeheldenwijk Wijk 02 Oranjewijk Wijk 03 Korrewegwijk
	Groningen-Oosterparkwijk Groningen-Oosterpoortwijk Groningen-Herewegwijk en Helpman Groningen-Stadsparkwijk Groningen-Hoogkerk Groningen-Noorddijk	Wijk 04 Oosterparkwijk Wijk 05 Oosterpoortwijk Wijk 06 Herewegwijk en Helpman Wijk 07 Stadsparkwijk Wijk 08 Hoogkerk Wijk 09 Noorddijk
Bedum	Bedum	Bedum
Loppersum	Loppersum	Loppersum
Ten Boer	Ten Boer	Ten Boer
Middelstum	Middelstum	Middelstum

Table 7.5 The seven identified communities consist of one of more neighbourhoods as defines in wijk- en buurten register by CBS. Community "gemeente Groningen" consists of 10 neighbourhoods.

Reliable assessment of the contribution of the collapse of groups of buildings to Maatschappelijk Veiligheidsrisico requires detailed representation of the spatial correlations in the earthquake ground motions. In the current assessment, spatial correlation is represented as strong within each near-surface amplification zone up to a distance of 3 to 5 km with no correlation beyond this distance.

The Maatschappelijk Veiligheidsrisico assessments for all seven communities are shown in figure 7.22.

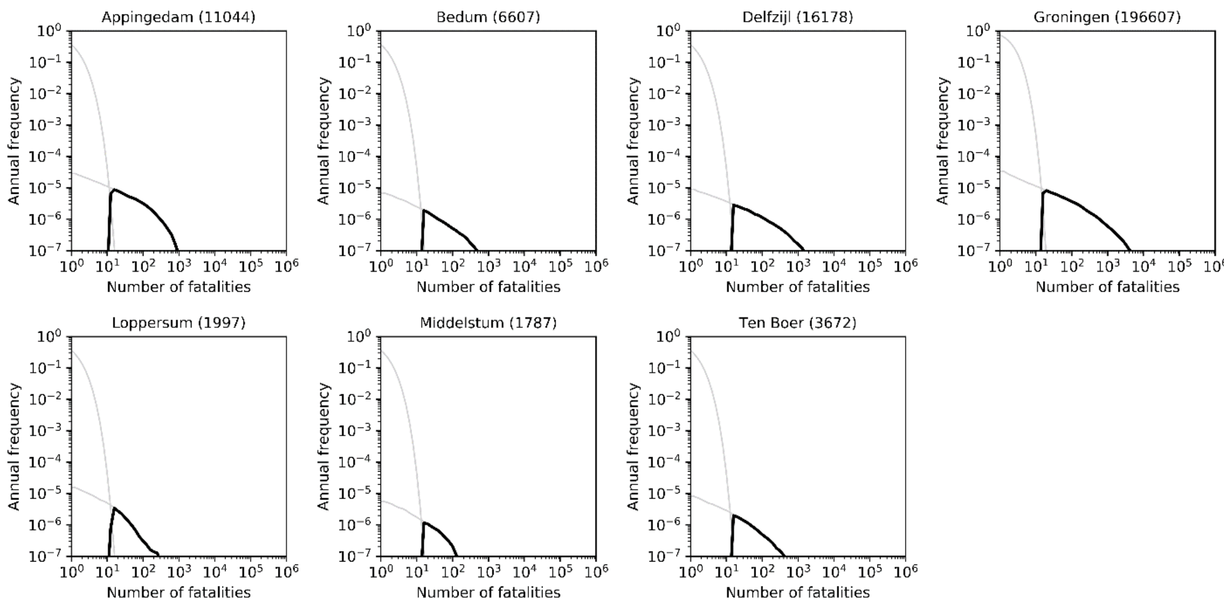

Figure 7.22 *Maatschappelijk Veiligheidsrisico based on the mean of the logic tree, for the seven communities (in alphabetical order) for Operational Strategy 1, gas-year 2020/2021, average temperature production profile. Numbers after each community name denote the average day-night inside total population for that community.*

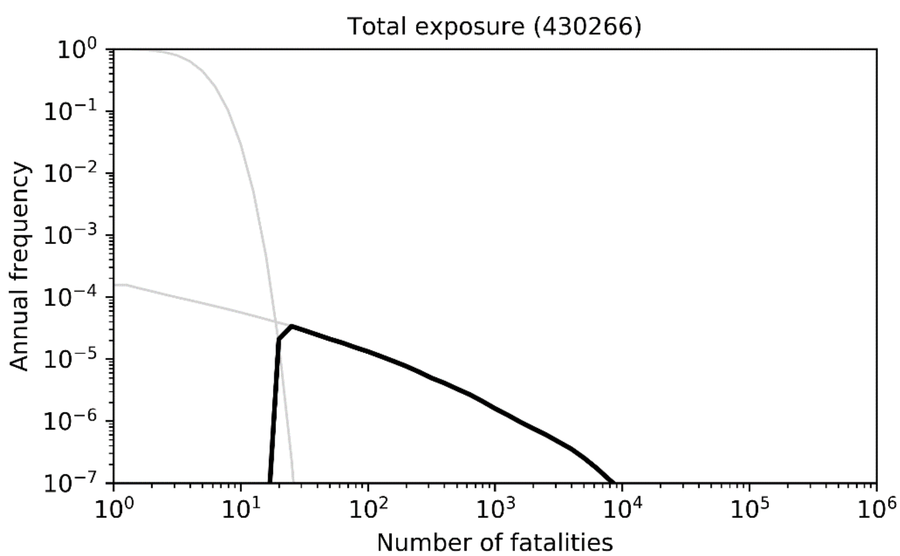

Figure 7.23 *Maatschappelijk Veiligheidsrisico based on the mean of the logic tree, for the Groningen field area for Operational Strategy 1, gas-year 2020/2021, average temperature production profile.*

For smaller number of fatalities (N) the Maatschappelijk Veiligheidsrisico is negative. The curves in fig. 7.22 show for the seven selected communities, that for *N* larger than about ten, the Maatschappelijk Veiligheidsrisico is about equivalent to Group Risk. The population (mean inside day-night population) is shown for each community. The Maatschappelijk Veiligheidsrisico clearly depends on population size. The Maatschappelijk Veiligheidsrisico for the Groningen Field area as a whole is presented in fig. 7.23.

8 Damage Assessment

8.1 Classification of Building Damage; Building Damage States

8.1.1 European Seismological Commission, EMS-1998

The EMS-98, European Seismological Commission, 1998 (Ref. 76) document provides guidelines for estimation of the intensity of an earthquake based on the damage assessment of buildings.

Damage of buildings is assessed on the basis of a damage classification. This is provided for two main categories: unreinforced masonry buildings (URM) and reinforced concrete (RC) buildings. Figure 8.2 describes the 5 distinguished damage grades for both main categories. The description of the damage states in this figure are purely qualitative. For instance, "negligible to slight damage" is termed DS1, "moderate damage" DS2, "substantial to heavy damage" DS3". The EMS scale relates DS1 to "hairline cracks in very few walls", DS2 to "cracks in many walls" and DS3 to "large and extensive cracks in most walls". The qualitative descriptions of the building damage states form a very useful, practical and generally accepted and applied classification system for building damage.

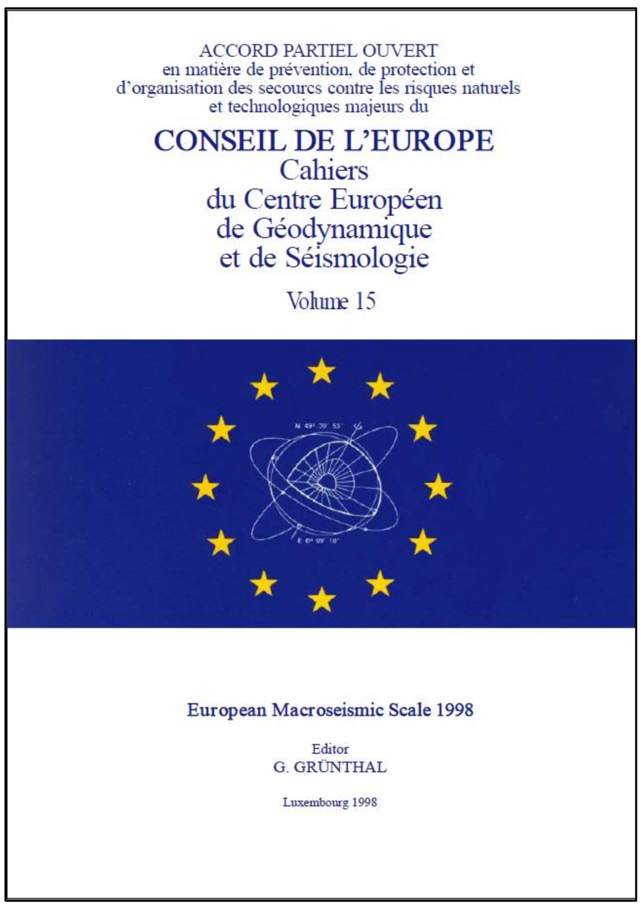

Figure 8.1 Cover of the "European Macroseismic Scale 1998, EMS-98"by the European Seismological Commission (G. Grünthal), 1998.

Classification of damage to masonry buildings	
	**Grade 1: Negligible to slight damage** **(no structural damage,** **slight non-structural damage)** Hair-line cracks in very few walls. Fall of small pieces of plaster only. Fall of loose stones from upper parts of buildings in very few cases.
	**Grade 2: Moderate damage** **(slight structural damage, moderate non-structural damage)** Cracks in many walls. Fall of fairly large pieces of plaster. Partial collapse of chimneys.
	**Grade 3: Substantial to heavy damage** **(moderate structural damage,** **heavy non-structural damage)** Large and extensive cracks in most walls. Roof tiles detach. Chimneys fracture at the roof line; failure of individual non-structural elements (partitions, gable walls).
	**Grade 4: Very heavy damage** **(heavy structural damage,** **very heavy non-structural damage)** Serious failure of walls; partial structural failure of roofs and floors.
	**Grade 5: Destruction** **(very heavy structural damage)** Total or near total collapse.

Classification of damage to buildings of reinforced concrete	
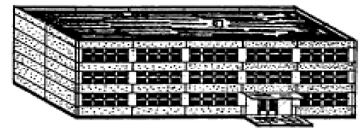	**Grade 1: Negligible to slight damage** **(no structural damage,** **slight non-structural damage)** Fine cracks in plaster over frame members or in walls at the base. Fine cracks in partitions and infills.
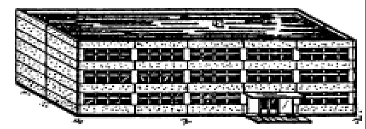	**Grade 2: Moderate damage** **(slight structural damage,** **moderate non-structural damage)** Cracks in columns and beams of frames and in structural walls. Cracks in partition and infill walls; fall of brittle cladding and plaster. Falling mortar from the joints of wall panels.
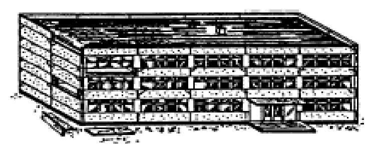	**Grade 3: Substantial to heavy damage** **(moderate structural damage,** **heavy non-structural damage)** Cracks in columns and beam column joints of frames at the base and at joints of coupled walls. Spalling of conrete cover, buckling of reinforced rods. Large cracks in partition and infill walls, failure of individual infill panels.
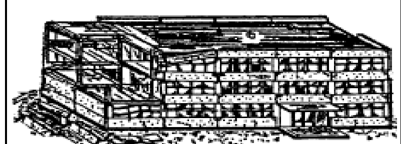	**Grade 4: Very heavy damage** **(heavy structural damage,** **very heavy non-structural damage)** Large cracks in structural elements with compression failure of concrete and fracture of rebars; bond failure of beam reinforced bars; tilting of columns. Collapse of a few columns or of a single upper floor.
	**Grade 5: Destruction** **(very heavy structural damage)** Collapse of ground floor or parts (e. g. wings) of buildings.

Figure 8.2 Classification of damage to masonry buildings (left) and classification of damage to reinforced concrete buildings (right). Illustration taken from EMS-98, European Seismological Commission, 1998 (Ref. 76).

8.2 Forecast for Damage State 1 (DS1) aesthetic damage

The report “Methodology Prognosis of Building Damage and Study and Data Acquisition Plan for Building Damage” (Ref. 77), issued February 2017, describes the studies program into building damage and the methodology for forecasting building damage. The building damage assessment of November 2017 (Ref. 15) contains an introduction into the classification of damage states and into the Monte Carlo method used for forecasting building damage and fatality risk.

This section presents the forecast of building damage level DS1 resulting from production profile “GTS-raming 2020” and is similar to the forecast provided last year for “GTS-raming 2019”. The higher damage states DS4 and DS5 are relevant for risk and have been addressed in the previous sections of this report. For the assessment of DS1 building damage, empirical methods based on analysis of historical damage data are used.

The approach to forecast DS1 based on observed damage from historical earthquakes is described in section 8 of the report “Induced Seismicity in Groningen, Assessment of Hazard, Building Damage and Risk – November 2017” (Ref. 15, pages 168-173). An update of that work has been prepared In June 2018 (Ref. 17, pages 9-11).

This section describes a further update and incorporates the latest information and knowledge available in the following areas:

- Updated empirical GMPE, following recalibration of KNMI G0 accelerometer stations (Ref. 78).
- Recalibrated DS1 fragility curves based on the updated empirical GMPE.
- Production from the Groningen field “GTS-raming 2020”
- Exposure database V7 (EDB)

8.3 Earthquake catalogue of events

For the forecast, a range of possible future realizations is needed that adequately represent the anticipated earthquake distribution, both in terms of magnitude and location in the field. These have been generated stochastically, using the hazard tool for the Operational Strategy 1 and Operational Strategy 2 based on the average temperature demand profile. These are the same profiles as used for the full Hazard and Risk Assessment. In the Monte Carlo simulation process, repeated random sampling of a set of input distributions is used to create a probabilistic distribution output. So-called ‘synthetic earthquake catalogues’ (i.e. event locations and magnitudes for the period gas-year 2020/2021 to 2029/2030) are generated from the input probability distributions of total seismic moment, number of events and event epicentres. This forecast uses events between M_L = 1.8 and 4.0.

8.4 Exposure model

The exposure database (EDB V7 Ref. 79) is an extract of a project database and consists mainly of the building typology classifications and several other building related attributes, including the population, arranged per building. In addition to its use as input into the Hazard and Risk Modelling, the EDB deliverable also provides the necessary information to assign the TNO typologies to all 263,399 Buildings (“Basisregistratie adressen en gebouwen (BAG)” from the Kadaster) in the area considered for damage forecast. The area of interest is the same for the Hazard and Risk Assessment and is based on the Groningen gas field outline. The extract boundary for the EDB V7 is a 5 km buffer around the gas field outline.

Table 8.1 shows how the different type of buildings present in the Groningen building stock have been assigned to the typologies used by TNO.

TNO typologie	EDB V7	Number of Buildings
Not categorised / Secondary "Niet gecategoriseerd"	Buildings with zero population	109,444
Farms "Boerderijen"	All buildings with system URM1F	4,001
High Rise Buildings "Hoogbouw"	Gutter height >10m	4,787
Low Rise Buildings before 1940 "Laagbouw voor 1940"	Remaining year of construction before 1940	39,154
Low Rise Buildings after 1940 "Laagbouw na 1940"	Remaining year of construction after 1940	106,013

Table 8.1 Assignment of EDB V7 typologies to the typologies used in the TNO Kalibratiestudie.

Although it has been recognized that secondary buildings representing ca. 40% of all buildings mainly consisting of sheds, garages and other small normally unoccupied buildings could also incur damage, they have been excluded from the forecast because damage data/reports are unavailable for such structures. A previous sensitivity analysis, with assumed fragility function like Low Rise buildings after 1940, shows that secondary buildings may perhaps add up to ca. 60% additional damage cases.

Due to the absence of damage observations in the earlier TNO studies, fragility function for Low Rise buildings after 1940 have also been assigned to all High-Rise buildings. This is believed to be a conservative assumption.

8.5 Results

Figure 8.3 shows results of the DS1 damage forecast in the form of an annual F/N curve for the Groningen field area, one per gas-year, shown for the period 2020-2030. The median forecast (P50 or 50%) is indicated together with the 80% confidence interval (10% to 90%). Each building in the exposure area was assigned with a relevant typology. It was assumed that any resulting building damage is repaired after the event and before the next one (instant repair). The figure shows that in gas-year 2020-2021 a forty percent chance that more than 100 buildings will be damaged with aesthetic damage (DS1) (due to all earthquakes in that year smaller than ML=4). In gas-year 2028-2029 there is a fifty percent chance that more than 10 buildings will be damaged with aesthetic damage.

Figure 8.4 shows the Mean and P50 for the DS1 damage forecast per gas-year for the period 2020-2030. Due to the skewed distribution of building damage the mean number of damaged buildings is considerably higher than the P50. The DS1 damage forecasts for both operational strategies are very similar, with a maximum difference of a few damaged buildings per year.

Operational Strategy 1

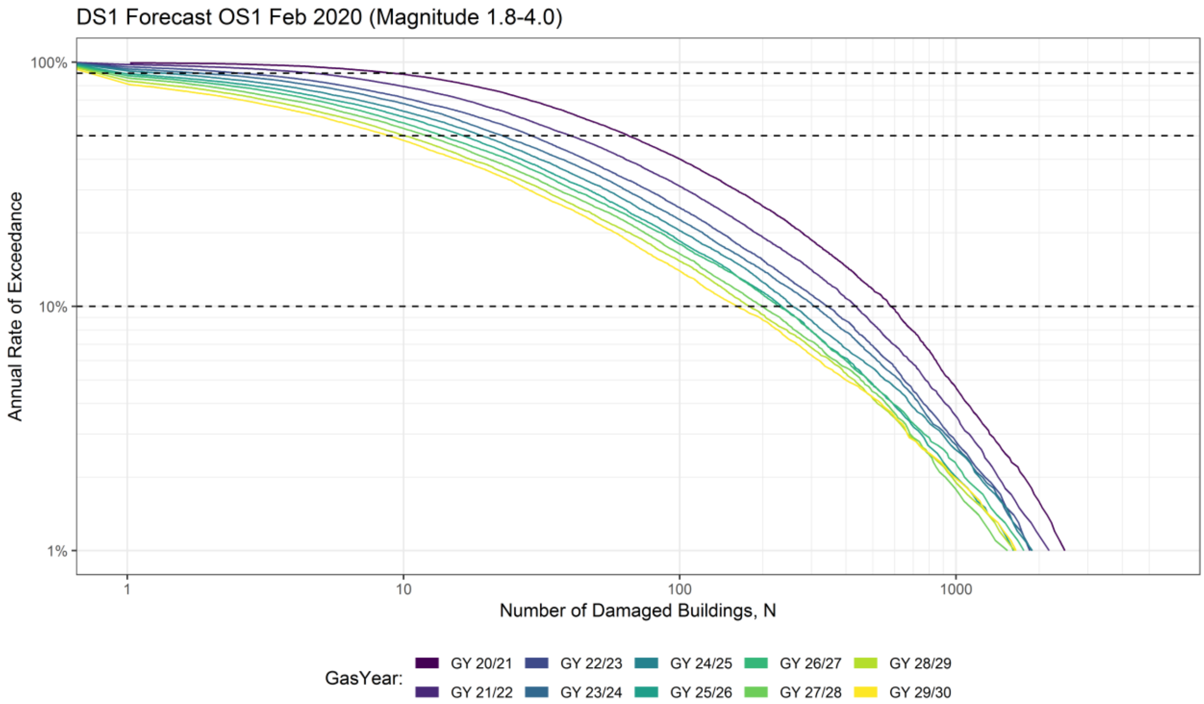

Operational Strategy 2

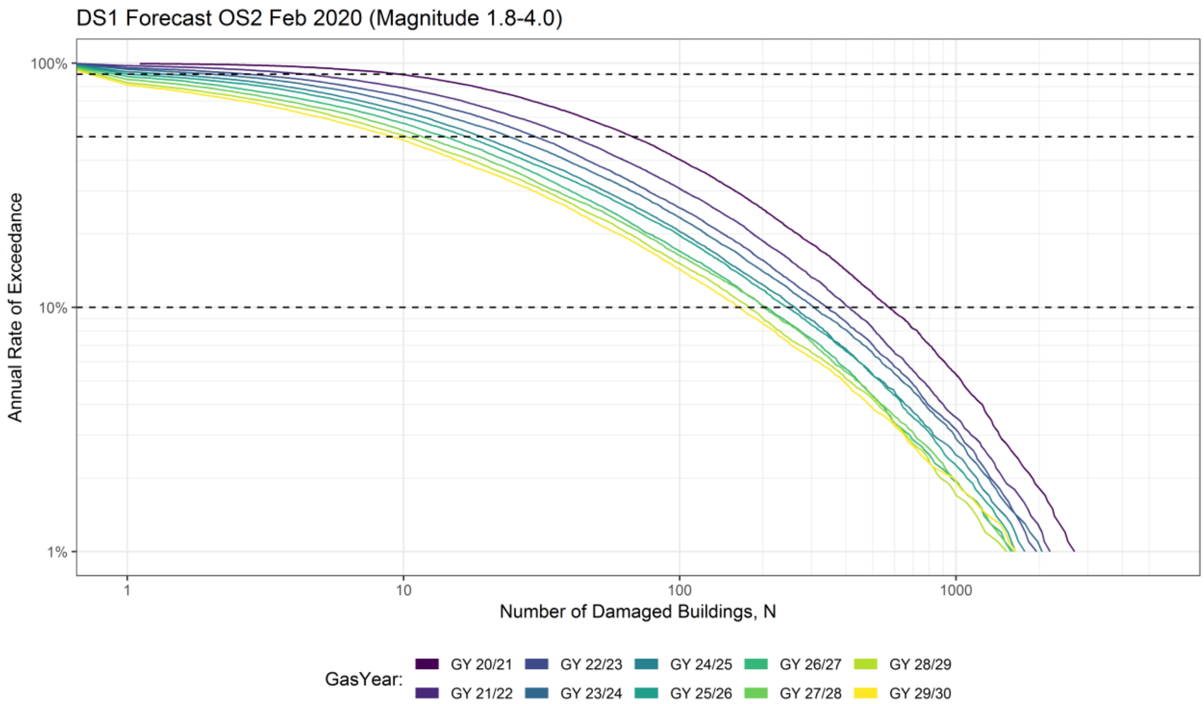

Figure 8.3 DS1 Forecast per gas-year for period 2020-2030 based on the middle branch of the M_{max} distribution, shown for "GTS-raming 2020" Operational Strategy 1 and 2 average temperature demand profile.

Operational Strategy 1 and 2 Compared

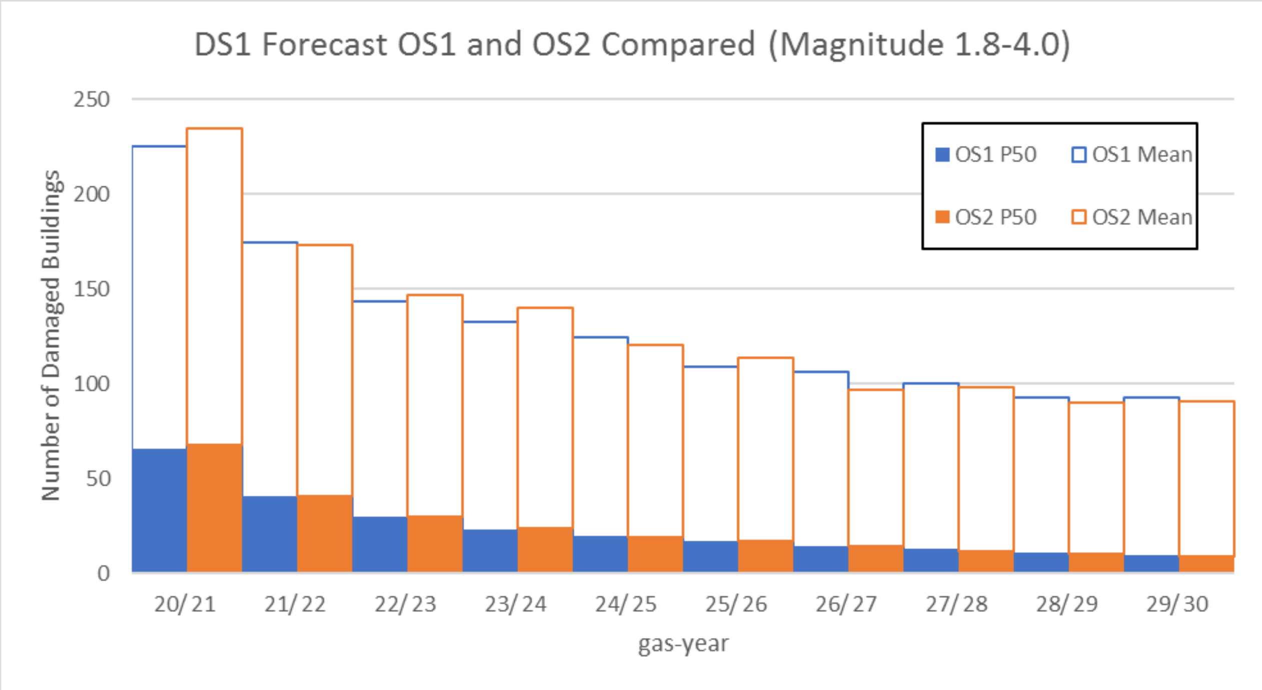

Figure 8.4 *Mean and P50 DS1 Forecast per gas-year for period 2020-2030 based on the middle branch of the M_{max} distribution, shown for "GTS-raming 2020" Operational Strategy 1 and 2 average temperature demand profile.*

8.6 Forecast for Damage State 2 (DS2) and Damage State 3 (DS3)

Fragility functions for DS2 and DS3 have been developed for each structural system identified in the exposure model using the extensive analytical modelling and experimental test campaign described in (Ref. 44). F/N curves have been calculated with the Monte Carlo risk engine which show the annual frequency of exceedance (F) of different numbers of groups of buildings (N) which simultaneously reach DS2 or DS3. Figure 8.5 shows the F/N curve for the whole field for each of the gas-years in the period 2020/2021 to 2029/2030. Figure 8.5 shows that in 2020, the annual frequency of exceedance of having anywhere 100 buildings simultaneously damaged to DS2 in a given earthquake is around 1% and the chance that 10 buildings are simultaneously damaged to DS3 in a given earthquake is a bit lower.

Figure 8.7 shows the exceedance damage count for the occurrence of the given damage state (DS). For instance, in 2020, the chance of 10 or more buildings reaching a DS2 damage state is about 3%. The chance that 100 buildings or more reach damage state DS3 is less than 0.3%. In Figure 8.8 DS2 and DS3 damage is compared for the two operational strategies. Differences are less than 1%.

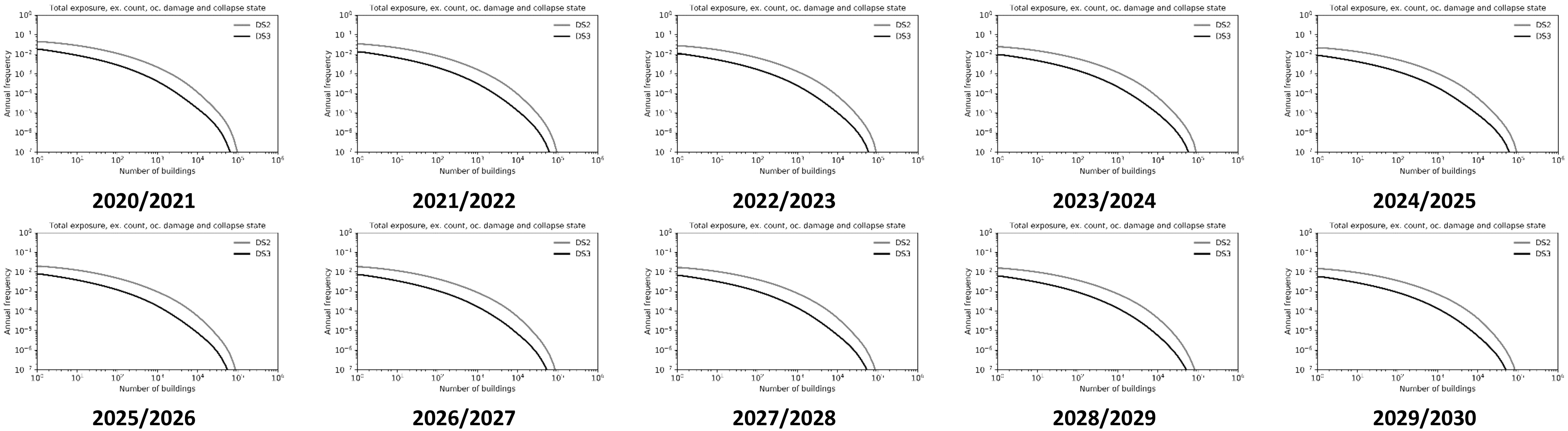

Figure 8.5 *Maatschappelijk risico for building damage DS2 and DS3 (MR(S)) for the whole field for the gas-years 2020/2021 to 2029/2030. The production is based on an average temperature year for Operational Strategy 1.*

Average Temperature Production Profile

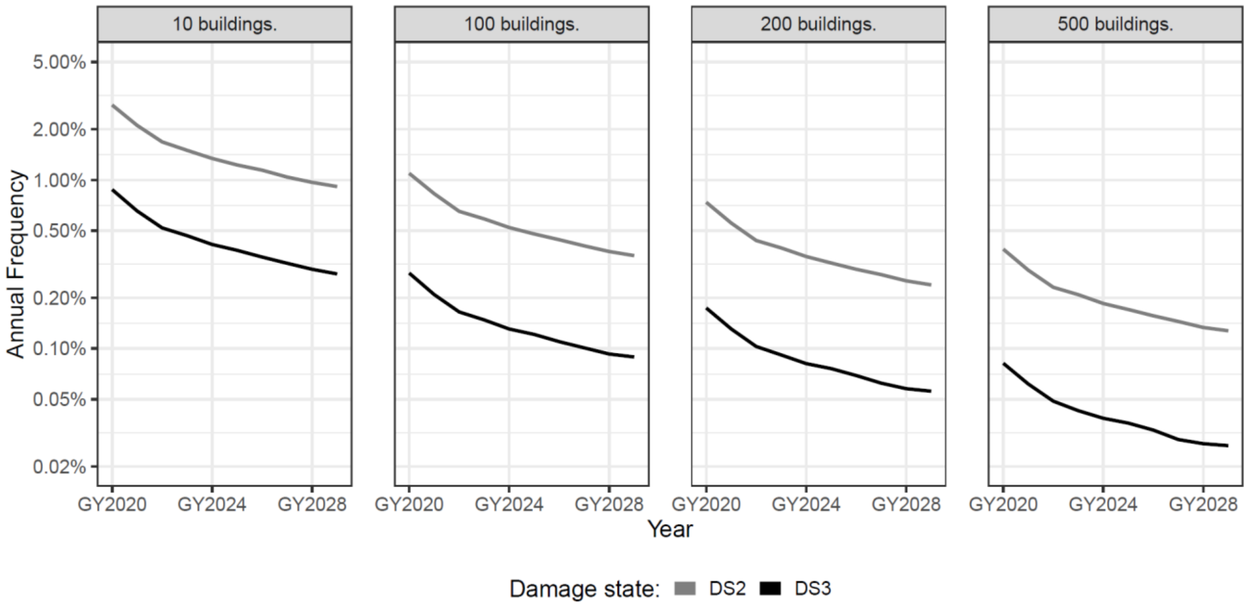

Cold Temperature Production Profile

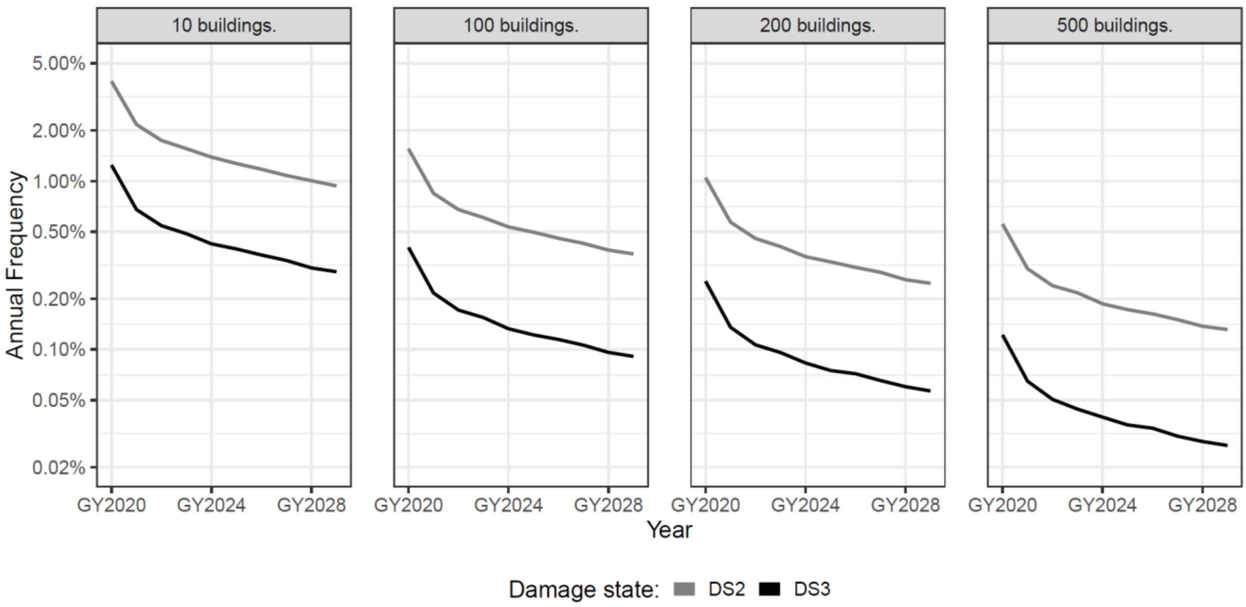

Figure 8.7a *Maatschappelijk risico for building damage DS2 and DS3 (MR(S)) for the whole field for the gas-years 2020/2021 to the gas-years 2029/2030 for operational strategy 1. Top figure is for an average temperature production profile and the bottom figure for a cold temperature production profile.*

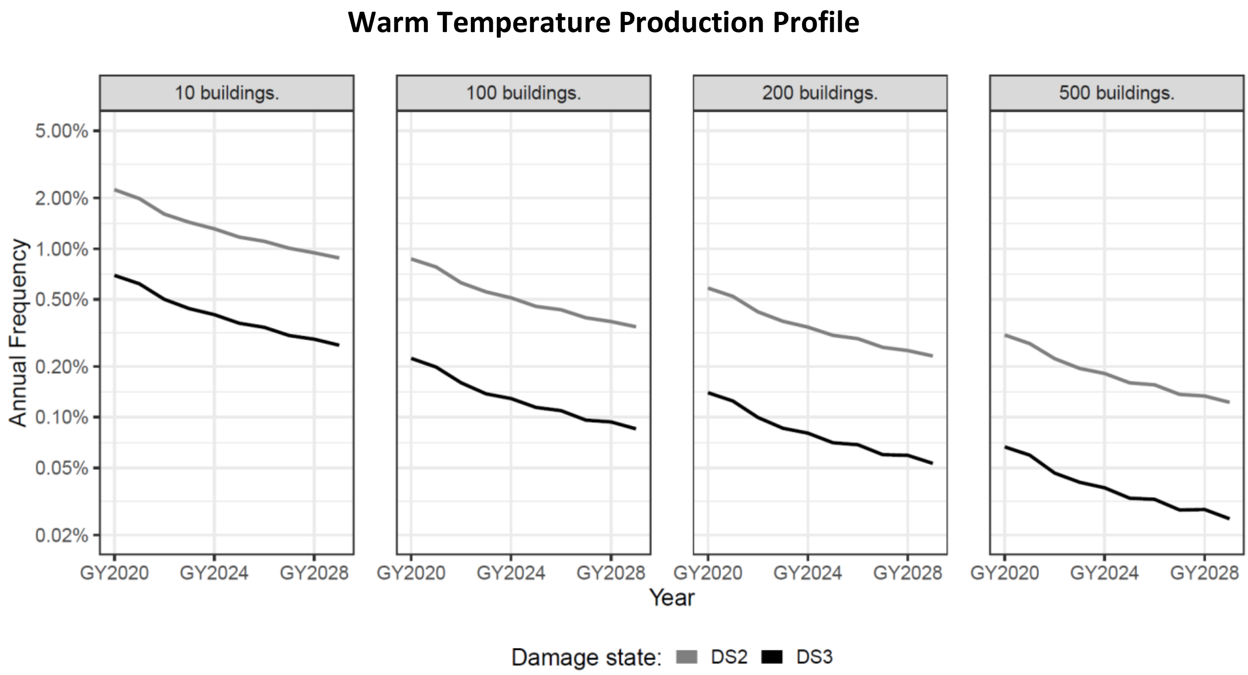

Figure 8.7b *Maatschappelijk risico for building damage DS2 and DS3 (MR(S)) for the whole field for the gas-years 2020/2021 to the gas-years 2029/2030 for operational strategy 1 for a warm temperature production profile*

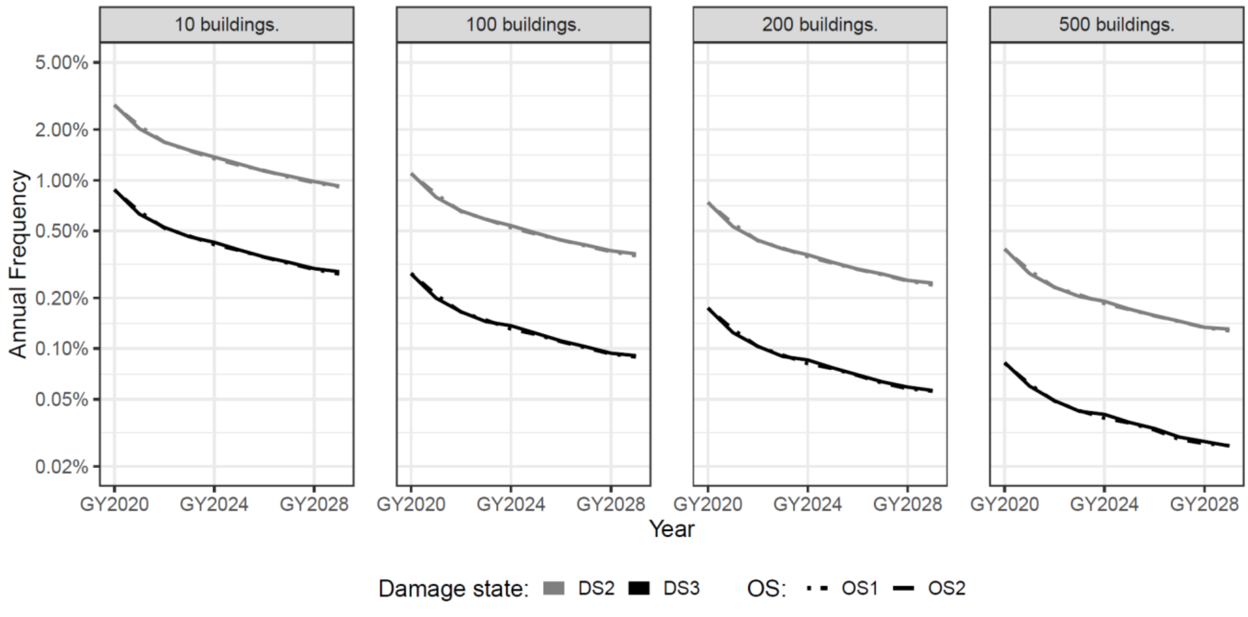

Figure 8.8 *Maatschappelijk risico for building damage DS2 and DS3 (MR(S)) for the whole field for the gas-years 2020/2021 to the gas-years 2029/2030. The results for both operational strategy 1 and 2 are shown.*

9 References

All reports referenced in this section prepared by NAM can be downloaded from the webpage "onderzoeksrapporten" on www.nam.nl.

Ref. 1 *Het Winningsplan Groningen 2013, NAM, Dec 2013.*

Ref. 2 *Technical Addendum to the Winningsplan Groningen 2013 - Subsidence, Induced Earthquakes and Seismic Hazard Analysis in the Groningen Field and Supplementary Information, Jan van Elk, Dirk Doornhof, Stephen Bourne, Steve Oates, Julian Bommer, Clemens Visser, Rob van Eijs and Peter van den Bogert, NAM, Shell and Imperial College, Dec 2013.*

Ref. 3 *Hazard Assessment for the Eemskanaal area of the Groningen field, Jan van Elk and Dirk Doornhof, NAM, Nov 2014.*

Ref. 4 Addendum to: Hazard Assessment for the Eemskanaal area of the Groningen field, Jan van Elk and Dirk *Doornhof, NAM, Nov 2014.*

Ref. 5 *Dreigings- en risicoanalyse voor geïnduceerde seismiciteit Groningen - Onderzoek 1 dreigingsanalyse, Jan van Elk and Dirk Doornhof, NAM, May 2015.*

Ref. 6 *Dreigings- en risicoanalyse voor geïnduceerde seismiciteit Groningen - Onderzoek 2 risicoanalyse, Jan van Elk and Dirk Doornhof, NAM, May 2015.*

Ref. 7 *Hazard and Risk Assessment for Induced Seismicity in Groningen, Jan van Elk and Dirk Doornhof, NAM, Nov 2015.*

Ref. 8 *Winningsplan Groningen gasveld - 2016, NAM, April 2016. EP201604259068*

Ref. 9 *Technical Addendum to the Winningsplan Groningen 2016 (chapter 1-5), Jan van Elk and Dirk Doornhof, NAM, Apr 2016.*

Ref. 10 *Technical Addendum to the Winningsplan Groningen 2016 (chapter 6), Jan van Elk and Dirk Doornhof, NAM, Apr 2016.*

Ref. 11 *Technical Addendum to the Winningsplan Groningen 2016 (chapter 7), Jan van Elk and Dirk Doornhof, NAM, Apr 2016.*

Ref. 12 *Technical Addendum to the Winningsplan Groningen 2016 (chapter 8), Jan van Elk and Dirk Doornhof, NAM, Apr 2016.*

Ref. 13 *Technical Addendum to the Winningsplan Groningen 2016 (chapter 9), Jan van Elk and Dirk Doornhof, NAM, Apr 2016.*

Ref. 14 *Supplement to the Winningsplan Groningen 2016, Jan van Elk and Dirk Doornhof, NAM, Apr 2016.*

Ref. 15 *Assessment of Hazard Building Damage and Risk for Induced Seismicity in Groningen - 2017, Jan van Elk, Dirk Doornhof, NAM, Nov 2017.*

Ref. 16 *Seismic risk assessment for a selection of seismic risk production scenarios for the Groningen field, Jan van Elk, Assaf Mar-Or, Leendert Geurtsen, Per Valvatne, Eddy Kuperus and Dirk Doornhof, NAM, Apr 2018.*

Ref. 17 *Assessment of Hazard, Building Damage and Risk based on Production Scenario Basispad Kabinet for the Groningen field, Jeroen Uilenreef, Jan van Elk and Assaf Mar-Or, NAM, July 2018.*

Ref. 18 *Assessment of Subsidence based on Production Scenario "Basispad Kabinet", Dirk Doornhof and Onno van der Wal, NAM, July 2018. EP201806209337*

Ref. 19 *Hazard and Risk Assessment - GTS raming 2019, Jan van Elk, Assaf Mar-Or, Leendert Geurtsen, Jeroen Uilenreef and Dirk Doornhof, NAM, Mar 2019.*

Ref. 20 *Letter to NAM: Mijnbouwwet instemmingsbesluit winningsplan Groningenveld; aanvullingsverzoek, Directeur Energy Markt Ministry of Economic Affairs, 20 December 2013.*

Ref. 21 *Verwachtingenbrief – Winningsplan 2016*

Ref. 22 *Wijzigingsbesluit 24th May 2017*

Ref. 23 *Letter to Parliament “Gaswinning Groningen”, 29th March 2018, Minister of Economic Affairs and Climate Policy.*

Ref. 24 *Letter to Parliament “Betreft Voortgang maatregelen gaswinningsbrief”, 6 juni 2018, Minister of Economic Affairs and Climate Policy.*

Ref. 25 *Letter “Verwachtingenbrief aanvulling winningsplan Groningenveld 2016” to NAM, 2nd May 2018, Minister of Economic Affairs and Climate Policy.*

Ref. 26 *Verwachtingenbrief “verzoek tot voorspellen van twee operationele strategieen voor het gas jaar 2019-2020”, Ministerie van Economische Zaken en Klimaat met 13 Februari 2019 met bijlage “raming benodigd Groningenvolume en capaciteit gasjaar 2019/2020 en verder”, Gasunie Transport Services, Februari 2019.*

Ref. 27 *Instemmingsbesluit Winningsplan Groningenveld, Ministry of Economic Affairs, 30th September 2016*

Ref. 28 *Eerste advies Adviescommissie ‘Omgaan met risico’s van geïnduceerde aardbevingen’ 23rd June 2015,*

Ref. 29 *Tweede advies Omgaan met hazard- en risicoberekeningen in het belang van handelingsperspectief voor Groningen Adviescommissie ‘Omgaan met risico’s van geïnduceerde aardbevingen’ 29th October 2015*

Ref. 30 *Eindadvies Handelingsperspectief voor Groningen Adviescommissie ‘Omgaan met risico’s van geïnduceerde aardbevingen’ (Commissie-Meijdam), 14th December 2015*

Ref. 31 *Verwachtingenbrief – GTS Raming 2020*

Ref. 32 *Letter Minister EZK (Wiebes) to the Voorzitter van de Tweede Kamer: Raming Gaswinning Groningen 2020/2021 en verder, 21 februari 2020 (Ons kenmerk DGKE-PGG / 20027392)*

Ref. 33 *Voorlopige beoordeling van de actualisatie van de HRA modellen, bijlage 1, SodM, 1 februari 2020*

Ref. 34 *Groningen Dynamic Model Update 2018, Quint de Zeeuw and Leendert Geurtsen, NAM, Jun 2018.*

Ref. 35 *Groningen Dynamic Model Update 2018 – V6, Quint de Zeeuw and Leendert Geurtsen, NAM, Oct 2018. EP201809202872.*

Ref. 36 *Investigation of gas presence in the aquifer of the Groningen field, Gulfiia Ishmukhametova, NAM, Sept 2018.*

Ref. 37 *Groningen Basin Model 2018, Hemmo Boscher, NAM, June 2018.*

Ref. 38 *V6 Ground-Motion Model (GMM) for Induced Seismicity in the Groningen Field - With Assurance Letter, Julian J Bommer, Benjamin Edwards, Pauline P Kruiver, Adrian Rodriguez-Marek, Peter J Stafford, Bernard Dost, Michail Ntinalexis, Elmer Ruigrok and Jesper Spetzler, , Dec 2019.*

Ref. 39 *Coefficient files for V6 Ground-Motion Model (GMM) for Induced Seismicity in the Groningen Field, Julian J Bommer, Benjamin Edwards, Pauline P Kruiver, Adrian Rodriguez-Marek, Peter J Stafford, Bernard Dost, Michail Ntinalexis, Elmer Ruigrok and Jesper Spetzler, , Dec 2019.*

Ref. 40 *Reader for the Spatial and Temporal development of induced seismicity in the Groningen field, S.J. Bourne, S.J. Oates, NAM, Nov 2017.*

Ref. 41 *Gaussian Process Optimisation of the Elastic Thin-Sheet Seismological Model for Depletion Induced Seismicity in the Groningen Gas Field, G. Joosten, J. Limbeck, G. Kaleta, S. Bourne, K. Nevenzeel, Shell Research and IBM Services, Feb 2019.*

Ref. 42 *Evolution of induced earthquake magnitude distributions with increasing stress in the Groningen gas field, S.J. Bourne, S.J. Oates, NAM, Dec 2019.*

Ref. 43 *Assurance of the report: Evolution of induced earthquake magnitude distributions with increasing stress in the Groningen gas field by Stephen Bourne and Steve Oates, S.J. Bourne, S.J. Oates, NAM, Jan 2020.*

Ref. 44 *Assurance Check on Exposure, Fragility and Fatality Models for the Groningen Building Stock, Assurance Panel Building Fragility, Typology and Exposure, Assurance Panel Building Fragility, Typology and Exposure, Dec 2019.*

Ref. 45 *Exposure Database (EDB) voor het gebied van het Groningen veld - Stand van Zaken juni 2018, NAM, June 2018*

Ref. 46 *Exposure Database (EDB) voor het gebied van het Groningen veld - Stand van Zaken september 2018, NAM, September 2018*

Ref. 47 *Exposure Database V6 - Data Documentation, Technical Report & Postprocessing to produce the v6 Exposure Model, NAM, July 2019*

Ref. 48 *Pruiksma, J.P. & Breunese, J.N. & Thienen-Visser, Karin & De Waal, Hans. (2015). Isotach formulation of the rate type compaction model for sandstone. International Journal of Rock Mechanics and Mining Sciences. 78. 127-132. 10.1016/j.ijrmms.2015.06.002.*

Ref. 49 *NAM (2017) Ensemble Based Subsidence application to the Ameland gas field – long term subsidence study part two (LTS-II) continued study.*

Ref. 50 *Van Eijs, R., & Van der Wal, O. (2017). Field-wide reservoir compressibility estimation through inversion of subsidence data above the Groningen gas field. Netherlands Journal of Geosciences, 96(5), S117-S129.*

Ref. 51 *Kole, P., Cannon, M., Tomic, J., Bierman, S. (2020) Analysis of first four years of in-situ strain data in Zeerijp-3A. EP201908210907 (Draft)*

Ref. 52 *Geertsma, J. and van Opstal, G. (1973). A Numerical Technique for Predicting Subsidence Above Compacting Reservoirs, Based on the Nucleus of Strain Concept. Verh. Kon. Ned. Geol. Mijnbouwk. Gen., 28, pp. 63-78.*

Ref. 53 *NAM (2019) Stabiliteitsanalyse van waterpaspeilmerken 2019 – Toelichting methodiek en toepassing op de meetregisters "Noord Nederland, Groningen en Waddenzee 2018" en "Zuid-Holland 2017". Nederlandse Aardolie Maatschappij, 12 juli 2019, EP20190621048*

Ref. 54 *Advies vaststellingsbesluit Groningen gasveld 2019/2020 of 7 May 2019, TNO*

Ref. 55 *Report on the v7 Fragility and Consequence Models for the Groningen Field, Helen Crowley and Rui Pinho, March, 2020*

Ref. 56 *Production Optimisation 2018, Per Valvatne, Leendert Geurtsen, Assaf Mar-Or, Gosia Kaleta, Jan Limbeck and Gerard Joosten, NAM, October 2018.*

Ref. 57 *Letter to Ministry of Economic Affairs: NAM Productie Optimalisatie Studie: Beoordeling en advies, T.F.Kockelkoren, SodM, 16 October 2018.*

Ref. 58 *Bouwstenen voor Operationele Strategie Groningenveld 2018/2019, NAM, 15/6/2018.*

Ref. 59 *Instemmingsbesluit Groningen gasveld 2018-2019, Minister of Economic Affairs and Climate Policy, 14/11/2018.*

Ref. 60 *Definitief vaststellingsbesluit Groningen gasveld 2019-2020, Minister of Economic Affairs and Climate Policy, 10/09/2019.*

Ref. 61 *SBR, Trillingsrichtlijn deel A – Schade aan Gebouwen, Stichting Bouw Research, Rotterdam, 52 pp., 2017.*

Ref. 62 *Brief Minister of Economic Affairs, Vooraankondiging veiligheidsnorm, 21 October 2015, kenmerk DGETM-EO / 15146924*

Ref. 63 *Eerste advies panel van hoogleraren over risicobeleid en veiligheidsmaatregelen geïnduceerd aardbevingsrisico, panel van hoogleraren, bestaande uit prof. dr. Eric Cator (Applied stochastics, Radboud Universiteit Nijmegen), prof. dr. Ira Helsloot (Besturen van veiligheid, Radboud Universiteit Nijmegen) en prof. dr. ir. Jan Rots (Structural mechanics, Technische Universiteit Delft), 27-6-2018.*

Ref. 64 *Eerste deel van aanvullend advies over veiligheidsrisico's van infrastructuur en cumulatie-effecten van geïnduceerde aardbevingen, panel van hoogleraren, bestaande uit prof. dr. Eric Cator (Applied stochastics,* *Radboud Universiteit Nijmegen), prof. dr. Ira Helsloot (Besturen van veiligheid, Radboud Universiteit Nijmegen) en prof. dr. ir. Jan Rots (Structural mechanics, Technische Universiteit Delft), 16 oktober 2018*

Ref. 65 *Addendum op advies panel van hoogleraren over risicobeleid en veiligheidsmaatregelen geïnduceerd aardbevingsrisico panel van hoogleraren, bestaande uit prof. dr. Eric Cator (Applied stochastics, Radboud Universiteit Nijmegen), prof. dr. Ira Helsloot (Besturen van veiligheid, Radboud Universiteit Nijmegen) en prof. dr. ir. Jan Rots (Structural mechanics, Technische Universiteit Delft)8 november 2018*

Ref. 66 *Briefadvies panel van hoogleraren over de berekening van de gemiddelde verblijfsduur in verschillende type bouwwerken, Panel van Hoogleraren (Prof. dr Eric Cator, prof. dr. Ira Helsloot en prof. dr. Jan Rots), 2nd February 2019.*

Ref. 67 *Kamerbrief "Advies hooglerarenpanel over berekening aardbevingsrisico", Ministerie van Economische Zaken en Klimaat, 7th maart 2019.*

Ref. 68 *Met het oog op de tijd - Een blik op de tijdsbesteding van Nederlanders, Sociaal en Cultureel Plan Bureau, Mariëlle Cloïn (red.), November 2013, https://www.scp.nl/Publicaties/Alle_publicaties/Publicaties_2013/Met_het_oog_op_de_tijd*

Ref. 69 *Beoordeling advies "berekening gemiddelde verblijfsduur" van het panel van hoogleraren, SodM, 11th February 2019.*

Ref. 70 *Guidelines for Developing Quantitative Safety Risk Criteria, Center for Chemical Process Safety, ISBN 978-0-470-26140-8*

Ref. 71 *Toelichting Wijk- en Buurtkaart 2013, 2014 en 2015 Respectievelijk Versie 3, 2 en 1, CBS, December 2015.*

Ref. 72 *Advies van 11 februari 2019 aan de minister van EZK over te gebruiken belasting bij de beoordelingen i.h.k.v. NPR:2018, SodM.*

Ref. 73 *Voortgangsverslag van de versterking huizen en afbouw van de gaswinning in Groningen, SodM, 26 June 2019.*

Ref. 74 *Advies van 10 oktober 2019 aan de Minister van EZK over te gebruiken tijdvak bij de beoordeling i.h.k.v. NPR:2018, SodM, 10 October 2019.*

Ref. 75 *Advies van 19 december 2019 inzake NPR 9998 en te gebruiken dreigingskaart, SodM 19 December 2019.*

Ref. 76 *European Seismological Commission (G. Grünthal), European Macroseismic Scale 1998, EMS-98, 1998*

Ref. 77 *Methodology Prognosis of Building Damage and Study and Data Acquisition Plan for Building Damage, Nederlandse Aardolie Maatschappij BV (Jan van Elk, Jeroen Uilenreef and Dirk Doornhof), 30 January 2017*

Ref. 78 *Updated Empirical GMPEs for PGV from Groningen Earthquakes – March 2019, Julian J Bommer, Peter J Stafford and Michail Ntinalexis, March 2019*

Ref. 79 *Exposure Database V7 - Data Documentation, Technical Report & Postprocessing to produce the v7 Exposure Model, NAM, March 2020*

Ref. 80 *Report on the v6 fragility and Consequence Models for the Groningen field, Helen Crowley, Rui Pinho and Francesco Cavalieri, March 2019*

Appendix A – Relevant Correspondence

Expectation Letter (Verwachtingenbrief)

Ministerie van Economische Zaken en Klimaat

> Retouradres Postbus 20401 2500 EK Den Haag

Nederlandse Aardolie Maatschappij B.V.
t.a.v. de heer drs. J. Atema, directeur
Postbus 28000
9400 HH ASSEN

Directoraat-generaal Klimaat en Energie

Bezoekadres
Bezuidenhoutseweg 73
2594 AC Den Haag

Postadres
Postbus 20401
2500 EK Den Haag

Overheidsidentificatienr
00000001003214369000

T 070 379 8911 (algemeen)
F 070 378 6100 (algemeen)
www.rijksoverheid.nl/ezk

[redacted]

Ons kenmerk
DGKE / 20018021

Uw kenmerk

Bijlage(n)
3

Datum - 0 3 FEB. 2020 -
Betreft verzoek tot voorstellen operationele strategie voor het gasjaar 2020-2021

Geachte heer Atema,

Hierbij verzoek ik u conform artikel 52c van de Mijnbouwwet twee operationele strategieën voor het gasjaar 2020-2021 voor te stellen op basis van de bijgevoegde GTS-raming voor hetzelfde gasjaar. In deze brief (inclusief bijlagen) geef ik de uitgangspunten voor de in te dienen operationele strategieën, die uiterlijk 16 maart 2020 in mijn bezit dienen te zijn.

In de Mijnbouwregeling is in artikel 1.3a.2, eerste lid, vastgelegd dat een operationele strategie omvat:

a. een beschrijving van de volgorde van de inzet van de clusters en de verdeling van het volume over de clusters per kalendermaand uitgaande van het referentiejaar voor een gemiddeld gasjaar;
b. de wijze waarop de inzet over de clusters en de verdeling van het volume over de clusters wordt verlaagd dan wel verhoogd, afhankelijk van de ontwikkeling van de actuele temperatuur gedurende het gasjaar, waarbij in ieder geval een beschrijving wordt gegeven van de volgorde van de inzet van de clusters en de verdeling van het volume over de clusters uitgaande van het referentiejaar voor een koud en voor een warm gasjaar.

Daarnaast zijn in het tweede en derde lid van artikel 1.3a.2 van de Mijnbouwregeling ter onderbouwing van de operationele strategie nadere eisen opgenomen, bijvoorbeeld over de rol van gasopslag Norg, de invloed van geplande onderhoudswerkzaamheden en over de dreigings- en risicoanalyse behorende bij een operationele strategie.

Bij het voorstellen van de operationele strategieën verzoek ik u de beschrijvingen te volgen zoals vastgelegd in artikel 52c van de Mijnbouwwet en artikel 1.3a.2 van de Mijnbouwregeling.

Voor de volledigheid merk ik op dat de GTS-raming ook informatie bevat over de benodigde capaciteit op het Groningenveld vanaf gasjaar 2022-2023, terwijl er vanaf dat moment geen volumevraag meer is uit het Groningenveld in een

Directoraat-generaal Klimaat en Energie

Ons kenmerk
DGKE / 20018021

gemiddeld jaar. In deze brief vraag ik u om nadere informatie over het in stand houden van deze capaciteit. Het vaststellingsbesluit voor gasjaar 2020-2021 kan echter los hiervan genomen worden. In deze brief geef ik expliciet aan welke informatie ik nodig heb voor de uitwerking van de operationele strategieën voor 2020-2021.

In de bijlage geef ik meer specifiek de uitgangspunten voor de beide operationele strategieën aan.

De Minister van Economische Zaken en Klimaat,
Voor deze:

[redacted]

Directeur Gastransitie Groningen

Bijlagen:
A: Uitgangspunten voor de operationele strategieën 2020-2021
B: Advies leveringszekerheid voor benodigde Groningenvolumes en -capaciteiten
C: Beschrijving en voorlopige beoordeling van de actualisatie van de HRA-deelmodellen

Directoraat-generaal Klimaat en Energie

Ons kenmerk
DGKE / 20018021

Bijlage A

Uitgangspunten voor de operationele strategieën 2020-2021
Operationele strategie 1 dient een voortzetting te zijn van de door mij vastgestelde operationele strategie van het huidige gasjaar, aangepast aan de uit de GTS-raming volgende graaddagenformule voor het gasjaar 2020-2021.

In operationele strategie 2 dient u uit te gaan van dezelfde inzetvolgorde van de clusters als bij operationele strategie 1, met dien verstande dat zowel het cluster Bierum als het cluster Eemskanaal alleen, en in deze volgorde worden ingezet, indien dit op basis van de gasvraag noodzakelijk is.

Voor beide strategieën geldt:

- De strategie voldoet aan de benodigde productiehoeveelheid van gas uit het Groningenveld om te kunnen voldoen aan het niveau van leveringszekerheid in het gasjaar 2020-2021. Deze staat, evenals de graaddagenformule die voor het gasjaar 2020-2021 van toepassing zal zijn, beschreven in de GTS-rapportage "Advies leveringszekerheid voor benodigde Groningenvolumes en -capaciteiten" van 31 januari 2020, met de aanvullende bijlagen "raming benodigde Groningenvolumes en -capaciteiten" en "uitgangspunten volumeberekeningen". Deze GTS-rapportage is als bijlage bij deze brief gevoegd.
- De strategie bevat een dreigings- en risicoanalyse waarmee een directe vergelijking mogelijk is tussen de operationele strategieën.
- De strategie wordt uitgewerkt voor een koud, gemiddeld en warm gasjaar 2020-2021.

De uitgangspunten als bedoeld hierboven zijn als volgt (in volgorde van prioriteit):

1. Produceer die hoeveelheid Groningenveldgas die jaarlijks nodig is voor de leveringszekerheid binnen de graaddagenformule;
2. Zorg voor voldoende werkvolume in de underground gas storage (hierna: UGS) Norg gedurende de hele winter ten behoeve van de leveringszekerheid;
3. Produceer het volledige werkvolume uit Norg, onder de randvoorwaarde dat de stikstofinstallaties maximaal worden gebruikt;
4. Streef binnen de graaddagenformule en de voorwaarden van het instemmingsbesluit gasopslag Norg naar het maximaal vullen van UGS Norg gedurende het injectieseizoen.

U heeft door de uitgangspunten die ik vastleg geen mogelijkheid meer om actief overschrijdingen van regionale productiefluctuaties te voorkomen. Wel vraag ik u per strategie het verwachte aantal overschrijdingen te rapporteren. Daarbij vindt een overschrijding plaats als het verschil in maandelijkse productie groter is dan 20% voor het cluster Bierum en 50% voor de overige regio's, zoals bedoeld in de Mijnbouwregeling onder artikel 1.3a.1 onder 1, die voor productie in gebruik zijn, met uitzondering van Eemskanaal. Deze percentages worden bepaald ten opzichte van de voorgaande maand en ten opzichte van de gemiddelde productie over de 12 voorgaande maanden. Voor operationele strategie 2 wordt het cluster Bierum evenals het cluster Eemskanaal alleen als capaciteitsmiddel ingezet. De overschrijdingsrapportage is daarom voor deze clusters niet van toepassing.

Uitgangpunten voor bijbehorende dreigings- en risicoanalyse bij een operationele strategie
De dreigings- en risicoanalyse dient de elementen te bevatten die in Mijnbouwregeling artikel 1.3a.2 lid 3 zijn opgenomen. Hierbij dient te worden opgemerkt:

- Bij uitwerking van artikel 1.3a.2, lid 3 sub b, dient een schadeprognose te worden gemaakt – als gevolg van geïnduceerde bevingen – voor de schadegrenstoestanden DS1, DS2 en DS3 uit het EMS-98, European Seismological Commission, 1998. Een kwalitatieve analyse van de DS1-schades evenals een verwachting van DS2- en DS3-schades dient u 16 maart 2020 te sturen. Gegeven de omvang van de berekeningen, vraag ik u de kwantitatieve prognoses van de drie genoemde schades bij het gegeven productiescenario uiterlijk 12 april 2020 bij mij in te dienen.
- Bij uitwerking van artikel 1.3a.2, lid 3 sub e, dient voor het gasjaar 2020-2021 van een koud, gemiddeld en warm scenario uitgegaan te worden, voor de jaren hierna kan een gemiddeld temperatuurprofiel worden gehanteerd.
- Als onderdeel van de verwachte bodembeweging dient een verwachting te worden gegeven van de bodemdaling voor de komende 10 jaar, waarbij de modellen gekalibreerd zijn aan de meest recente data.
- In aanvulling op deze verwachtingenbrief wil ik u nu al meegeven dat ik in het vaststellingsbesluit 2020-2021 zal gaan vragen om voor 1 oktober 2020 de lange termijn voorspelling van de bodemdaling inclusief onzekerheidsanalyse op te leveren, waarin de meest recente inzichten van langetermijneffecten op bodemdaling meegenomen zijn.

Ik heb SodM gevraagd om te beoordelen of de recent geactualiseerde versies van de verschillende deelmodellen van het dreigings- en risicoanalysemodel geschikt zijn om te gebruiken voor de uit te voeren dreigings- en risicoanalyses. SodM adviseert hierover om de meest recent geactualiseerde versies te gebruiken. Ik verzoek u dit advies (bijlage C) te volgen. Aansluitend verzoek ik u om de verbeteringen van de deelmodellen ter beschikking te stellen aan TNO zodat deze geïmplementeerd kunnen worden in de modelketen die zij in samenwerking met andere partijen op mijn verzoek ontwikkelt.

Rapportage
We vragen u bij de rapportage van bovengenoemde elementen van de beide operationele strategieën en de dreigings- en risicoanalyses in de hoofdtekst in elk geval het volgende op te nemen:

- Een tabel of figuur waarmee de inzet van de clusters als functie van de dagvraag eenduidig wordt vastgelegd.
- Een overzicht van de kans op zwaardere bevingen (M>3,5; 4,0; 4,5) per gasjaar, voor het gasjaar 2021-2022 en de 10 volgende gasjaren.

- Berekeningen van het Plaatsgebonden Persoonlijk Risico (LPR)[1] (hazard-kaarten en LPR-curves) voor het gasjaar 2020-2021 en een overzicht in een tabel van het aantal gebouwen dat niet voldoet aan de veiligheidsnorm (berekend met de verwachtingswaarde van het risico per gebouw, met P90 in een bijlage) per gasjaar, voor het gasjaar 2020-2021 en de 10 volgende gasjaren.
- Een doorkijk van de voorgestelde clusterafbouw (inclusief de productielocaties) bij de geraamde afbouw van de productie in de jaren na komend gasjaar bij voortzetting van de clusterinzetvolgorde op basis van de door GTS opgegeven dataset met volumeraming. Een overzicht van benodigde clusters en een duiding van de benodigde opstarttijd indien een cluster alleen nog nodig is voor de door GTS geadviseerde capaciteit en er dus planmatig geen volume meer nodig is uit het Groningenveld.
- Ontwikkeling van de seismische activiteit tot 10 jaar na het gasjaar 2020-2021, weergegeven in gasjaren.
- De ontwikkeling van de bodemdaling inclusief de verwachting moet weergegeven worden in:
    - Kaarten van de ruimtelijke ontwikkeling van de bodemdaling in 2018 (laatste waterpassing) tot 2030.
    - Figuren met de tijdsafhankelijke ontwikkeling van de bodemdaling op meerdere waterpaslocaties verdeeld over het gasveld.

Daarnaast vraag ik u in een bijlage in elk geval de volgende informatie aan te leveren:
- Kaarten per operationele strategie van de drukontwikkeling tot 30 jaar na het gasjaar 2020-2021.
- Ontwikkeling van de seismische activiteit per operationele strategie tot 30 jaar na het gasjaar 2020-2021, weergegeven in stappen van 5 jaar.
- Verschilkaarten van de drukverdeling tussen de verschillende operationele strategieën, per gasjaar.
- Verschilkaarten van de ruimtelijke verdeling van de seismische activiteit (mean) in de verschillende operationele strategieën, inclusief aanduiding hoeveel bevingen er meer/minder in een gebied zijn opgetreden, per gasjaar.
- Verschilkaarten van de seismische dreiging in de verschillende operationele strategieën.
- Een overzicht per operationele strategie van het aantal gebouwen dat niet voldoet aan de veiligheidsnorm (berekend met P90) per gasjaar, voor het gasjaar 2020-2021 en de 10 volgende gasjaren.
    - Daarnaast een zelfde overzicht met het aantal gebouwen berekend met zowel de verwachtingswaarde als P90 voor de kalenderjaren 2020 tot en met 2030. Deze dient uiterlijk 12 april in mijn bezit te zijn.

---

[1] Voor het vaststellingsbesluit 2020-2021 vraag ik u voor wat betreft het meenemen van de verblijfsduur in de risicoberekeningen aan te sluiten bij de eerder uitgevoerde *Hazard and Risk Assessment* van maart 2019 (in het vaststellingsbesluit Groningen gasveld 2019-2020 is hier aan gerefereerd met de term plaatsgebonden persoonlijk risico). Deze wijze, waarbij is uitgegaan een permanente aanwezigheid van personen in bouwwerken, sluit aan bij eerdere risicoberekeningen, waardoor vergelijkingen over de afgelopen jaren beter zijn in te schatten.

- Kaarten per operationele strategie met de locaties en het type van de gebouwen boven de norm op basis van de verwachtingswaarde en P90 voor het gasjaar 2020-2021.
- Verschilkaarten van de ruimtelijke verdeling van de gebouwen boven de norm voor de verwachtingswaarde en P90 voor het gasjaar 2020-2021.
- Bij het overzicht van het aantal gebouwen dat niet aan de veiligheidsnorm voldoet voor het gasjaar 2020-2021 (berekend met de verwachtingswaarde en P90) een overzicht welk percentage van deze gebouwen in het huidige gasjaar (volgens HRA 2019) eveneens niet aan de norm voldeed, uitgesplitst in verwachtingswaarde, P90 en conform norm in de HRA2019.

In aanvulling op de overzichten van de gebouwen in de hoofdtekst en bijlage, zal NAM de BAG-ID's van de betreffende gebouwen aanleveren aan de Nationaal Coördinator Groningen (NCG), conform de afspraken omtrent de uitwisseling van persoonsgegevens zodat voor de NCG gebouwen op adresniveau herleidbaar zijn.

Additioneel vraag ik u een publieksvriendelijke samenvatting bij beide operationele strategieën te leveren, waarin de relatie met de bijbehorende dreigings- en risicoanalyse wordt beschreven, en beide operationele strategieën (en hun gevolgen voor wat betreft de seismiciteit en het seismisch risico) worden samengevat.

Voorlopige beoordeling van de actualisatie van de HRA-modellen.

Staatstoezicht op de Mijnen

Ons kenmerk
ADV-434

Bijlage 1: Beschrijving en voorlopige beoordeling van de actualisatie van de HRA-deelmodellen.

Hieronder wordt voor elk van de modellen de (eventuele) actualisatie ten opzichte van het in 2019 in de HRA (verder: HRA2019) gebruikte deelmodel beschreven en de voorlopige beoordeling van SodM gegeven.

Geologisch model
Het geologisch model is ten opzichte van de HRA2019 niet gewijzigd.

Dynamisch reservoir model
Het dynamisch reservoir model heeft met het oog op de lange termijn bodemdalingsvoorspellingen enkele aanpassingen ondervonden. Deze aanpassingen richten zich met name op de onzekerheid over de wijze waarop de watervoerende reservoirdelen (de zogenaamde aquifers) met de gasvoerende delen zijn verbonden en drukdaling ondervinden.

SodM vind het belangrijk om nieuwe informatie en inzichten over de aquifers mee te nemen in het dynamisch reservoir model. SodM adviseert om deze actualisatie op te nemen in de HRA2020.

Compactie model
Het compactie model is ten opzichte van de HRA2019 niet gewijzigd.

Seismologisch model
Het seismologisch model bestaat uit twee delen: 1) een model waarmee op basis van de spanningsopbouw in de ondergrond het aantal bevingen en de locatie daarvan wordt bepaald, en 2) een model waarmee de sterkte van deze bevingen wordt bepaald. In 2019 is het tweede deelmodel verder doorontwikkeld.

In het seismologisch model wordt de sterkte van elke gemodelleerde beving willekeurig getrokken uit een kansverdeling, de zogenaamde Gutenberg-Richter (verder: GR) relatie[4]: $\log(N)=a-bM$, waar N het aantal bevingen van een bepaalde magnitude M en groter aangeeft. In deze kansverdeling zijn zwakkere bevingen meer waarschijnlijk dan zwaardere bevingen. De verhouding tussen de zwakke en zwaardere bevingen wordt bepaald door de zogenaamde b-waarde (de helling van de log-lineaire relatie). Maximale sterkte van de zwaarst mogelijke beving wordt daarnaast bepaald door de zogenaamde maximaal mogelijke magnitude (M_{max}).

Deze verhouding (b-waarde) hoeft echter niet constant te zijn. Uit de internationale wetenschappelijke literatuur is het bekend dat de b-waarde omgekeerd evenredig kan zijn met de spanningen op de breuken[5] (de

[4] Gutenberg, R. and Richter, C.F. (1944). Bulletin of the Seismological Society of America 34: 185-188.
[5] Amitrano, D. (2003). Journal Geophysical Research 108, doi: 10.1029/2001JB000680. Schorlemmer et al (2005). Nature 437, 539-542, doi: 10.1038/nature04094. Spada et al (2013). Geophysical Research Letters 40, 709-714, doi: 10.1029/2012GL054198. Scholtz (2015). Geophysical Research Letters 42, 1399-1402, doi: 10.1002/2014GL06863. Layland-Bachmann et al (2012). Geophysical Research Letters 39, doi: 10.1029/2012GL051480.

Pagina 5 van 9

zogenaamde 'differential stress'). Voor het Groningen gasveld gebruikt de NAM sinds 2015[6] een, op basis van de meetdata en berekeningen afgeleide, relatie tussen de b-waarde en de opbouw van de spanningen door de drukdaling in het veld.

In de voorliggende actualisatie van het seismologische model[7] wordt naast deze relatie tussen de b-waarde en de opgebouwde spanningen een alternatief model geïntroduceerd. In dit alternatieve model veranderd niet de b-waarde met de toenemende spanning, maar wordt de vorm van de GR-relatie mede bepaald wordt door een spanningsafhankelijke taper. Dit betekent dat de verhouding tussen kleine en grote bevingen (de b-waarde van de relatie) constant is, maar dat de kans op de zwaardere bevingen begrenst wordt door de hoeveelheid spanning die aanwezig is om in een beving vrij te kunnen komen.

Fysisch is deze relatie te verklaren vanuit het gezichtspunt dat de spanning op de breuken eerst opgebouwd moet worden tot het punt dat de breuken "kritisch" worden en kunnen gaan bewegen. In eerste instantie gebeurt dit bij kleine stukjes breuk die "optimaal" georiënteerd zijn. Voor de andere breuken is een grotere spanningsopbouw nodig voordat deze kunnen gaan bewegen. Tegelijkertijd geldt dat om grotere bevingen te krijgen grotere delen van een breuk "kritisch" of bijna "kritisch" moeten zijn. Alleen dan kan de dynamische overdracht van spanning bij de eerste slip deze delen mee laat bewegen. Als de naastliggende stukjes breuk niet "kritisch" genoeg zijn kunnen deze niet gaan bewegen en zal de beving klein blijven. Bij doorgaande spanningsopbouw worden er dus steeds meer en grotere delen van de breuken "kritisch" gespannen en kunnen ook de bevingen groter worden.

NAM stelt voor om het nieuwe model samen met het oorspronkelijke model op te nemen in de 'logic tree' van de HRA. De weging van de bijbehorende twee takken in de 'logic tree' wordt gebaseerd op basis van de mate waarin de uitkomsten van het model past op de daadwerkelijk seismiciteit[8].

NAM heeft vier onafhankelijke, wetenschappelijke experts gevraagd om hun wetenschappelijke mening over het nieuwe model[9]. Alle experts zijn van mening dat het nieuwe model ondersteunt wordt door de data en ondersteunen het voorstel van de NAM om dit model als een alternatief model op te nemen in de 'logic tree'. Wel geven drie van de vier experts aan dat gegeven de relatief beperkte hoeveelheid beschikbare data de grenzen van de mogelijkheden worden opgezocht.

SodM sluit zich aan bij de mening van de onafhankelijke, wetenschappelijke experts en adviseert om binnen het seismologische model het nieuwe model voor

---

[6] NAM (2015). An activity rate model of induced seismicity within the Groningen Field (Part 1) & An activity rate model of induced seismicity within the Groningen Field (Part 2).
[7] NAM-report (2019). Evolution of induced earthquake magnitude distributions with increasing stress in the Groningen gas field.
[8] De voorgestelde weging is 20% voor het oude model en 80% voor het nieuwe model.
[9] Prof. Dr. Ian Main, University of Edinburough; Prof. Dr. Jean-Philipe Avouac, CALTECH & UQ Foundation; Prof. Dr. Torsten Dahm, GFZ & University of Potsdam; Prof. Dr. Gert Zöller, University of Potsdam.

de bepaling van de sterkte van de bevingen samen met het oorspronkelijke model op te nemen in de 'logic tree' van de HRA. Hiermee wordt het beste de effecten van de beide modellen op de risicoschatting inzichtelijk gemaakt.

SodM wil wel opmerken dat het nog meerdere alternatieve modellen voorstelbaar zijn om de seismiciteit te modelleren. Zo hanteert het KNMI een b-waarde model waarbij de b-waarde ruimtelijk varieert. Op dit moment wordt binnen het Kennisprogramma Effecten Mijnbouw (verder: KEM) nader onderzoek gedaan naar alternatieve seismologische modellen (onderzoeksproject KEM 8). Het meenemen van de verschillende alternatieve modellen is de beste manier om de modelonzekerheid goed in te schatten. De toepasbaarheid van deze alternatieve modellen moet daarom onderzocht worden en bij een vergelijkbare of betere modelvoorspelling in de toekomst meegenomen worden in de 'logic tree'.

Ground Motion Model (GMM; 'grondbewegingsmodel')
Ten opzichte van de HRA 2019 is de GMM op een aantal punten verder doorontwikkeld[10]:

- De kalibratie dataset is met de waarnemingen van twee bevingen uitgebreid. Dit betekent dat de totale dataset met 40% is toegenomen;
- Nieuwe gegevens over de ondiepe ondergrond zijn meegenomen;
- Als uitgangspunt voor het model is nu de (gecorrigeerde) data van de G0-versnellingsmeters gebruikt waar voorheen de data van de G4-meters (op 200 m diepte) als startpunt werd gebruikt.

De NAM heeft het aangepaste model laten beoordelen door een panel van internationale, wetenschappelijke experts[11]. Naar het oordeel van de experts is het doorontwikkelde model een significante verbetering ten opzichte van het HRA2019 GMM model (v5) en geschikt om gebruikt te worden in de HRA2020.

SodM constateert dat ondanks het feit dat de dataproblemen bij de G0-versnellingsmeters zijn gecorrigeerd en deze gecorrigeerde gegevens in de GMM zijn verwerkt, de problemen die zijn geconstateerd bij de versnellingsmeters van het B-netwerk nog van invloed kunnen zijn op het GMM-model. Dit is echter het geval voor zowel de v5 als de doorontwikkelde v6 versie van het model.

Daarnaast rapporteert het ontwikkelteam nog een inconsistentie tussen de afleiding van de versnelling op het niveau van Nu_b op basis van de G0-metingen (methodiek in v6) en de afleiding van de versnelling op het niveau van Nu_b op basis van de G4-metingen (methodiek in v5).

Deze problemen waren ook bekend bij het panel van internationale, wetenschappelijke experts op het moment dat zij hun oordeel gaven. Desondanks acht het panel het doorontwikkelde model een significante verbetering ten

---

[10] NAM-report (2019). V6 Ground-Motion Model (GMM) for Induced Seismicity in the Groningen Field - With Assurance Letter.
[11] NAM Assurance team voor GMM: Gail Atkinson, Western University, Ontario, Canada; Hilmar Bungum, NORSAR, Norway; Fabrice Cotton, GFZ Potsdam, Germany; John Douglas University of Strathclyde, UK; Jonathan Stewart, UCLA, California, USA; Ivan Wong, AECOM, Oakland, USA; Bob Youngs, AMEC, Oakland, USA.

opzichte van de GMM v5. Daarbij resulteert GMM v6 voor dezelfde output van het seismologisch model in een hogere hazard en seismisch risicoinschatting dan GMM v5. Daarmee is de keuze voor GMM v6, naast een wetenschappelijk gezien betere keuze, ook een conservatieve keuze.

SodM adviseert om de doorontwikkelde GMM v6 te gebruiken in de HRA2020.

In het addendum bij het 'Study and Data Aquisition Plan - 2019' heeft NAM beschreven op welke wijze de hierboven genoemde problemen zullen worden onderzocht en de resultaten daarvan zullen worden verwerkt in een actualisatie van de GMM naar versie 7 in 2020. Dit addendum heeft SodM goedgekeurd nadat het – in het verlengde van het SodM tussenrapport omtrent de seismische metingen - op onderdelen is aangescherpt en uitgebreid.

Kwetsbaarheids- en gevolgmodel & classificatie van gebouwen
Bij de doorontwikkeling van het kwetsbaarheids-, gevolgmodel en de classificatie van de gebouwen heeft NAM zich geconcentreerd op de meest kwetsbare typologieën, met name boerderijen[12].

Voor de classificatie van de gebouwen zijn de verschillende datasets waarop de classificatie is gebaseerd geactualiseerd. Daarnaast zijn kleine aanpassingen in de gebruikte aanpak doorgevoerd. Dit heeft geresulteerd in kleine veranderingen in de verdeling van gebouwen over de verschillende typologieën.

De typologie boerderijen (URM1_F) is verder opgedeeld in 3 verschillende sub-typologieën waaronder schuren van boerderijen (URM1F_B). Voor elk van deze sub-typologieën zijn de modellen geactualiseerd of zijn nieuwe modellen gemaakt. Voor de schuren bij de boerderijen zijn vier nieuwe modellen gemaakt.

Tenslotte zijn de modellen voor de typologieën URM3L, URM3M_U, URM3M_B en URM4L geactualiseerd. Er lijken geen grote wijzigingen in de gevolgde aanpak gemaakt te zijn.

SodM vind het belangrijk om nieuwe informatie en inzichten over de sterkte van gebouwen mee te nemen in het kwetsbaarheids-, gevolgmodel en de classificatie van gebouwen. De verwachting is dat de veranderingen leiden tot een betere representatie van de gebouwen en een verbeterde risicoschatting voor de gebouwen geeft. SodM adviseert om deze actualisatie op te nemen in de HRA2020.

---

[12] Presentatie NAM (2020). Exposure Database and Building Fragility in HRA 2020; Preliminary update.

Appendix B – Glossary of Terms

This appendix contains a glossary of terms used in this report and the documents references in this report. More extensive glossaries for terms used in earthquake studies have been compiled by the USGS:

https://earthquake.usgs.gov/learn/glossary/?alpha=ALL

and at the web-site www.earthquake-report.com.

https://earthquake-report.com/2011/02/15/glossary-of-earthquake-terms-2/

Term	Explanation
Acceleration	The rate of change of velocity of a reference point. Commonly expressed as a fraction or percentage of the acceleration due to gravity (g) where g = 980 cm/s2. - (USGS)
Accelerogram	The recording of the acceleration of the ground during an earthquake.
Building Code	A building code, or building control, is a set of rules that specify the minimum acceptable level of safety for constructed objects such as buildings and non-building structures. The main purpose of building codes are to protect public health, safety and general welfare as they relate to the construction and occupancy of buildings and structures. A seismic code, refers to a building code which uses earthquake-resistant design principles. (USGS - CEDIM)
Cold temperature year	The demand for gas is dependent on the weather and especially on whether the winter will be cold. This is also reflected in the production required from the Groningen gas field to ensure security of supply. Therefore a sensitivity is performed in this hazard and risk assessment where the target year (gas-year 2020/2021) has a cold winter.
Earthquake	The expected (or probable) life loss, injury, or building damage that will happen, given the probability that some earthquake hazard occurs. Earthquake risk and earthquake hazard are occasionally used interchangeably. (USGS)
Epicenter	The point on the Earth's surface vertically above the point (focus or hypocenter) in the crust where a seismic rupture nucleates. (EQCanada)
Eurocode 8	The Eurocodes are the current technical standards for structural design in Europe, and it is now compulsory for the 28 countries in the Eurocode zone to adopt these. Eurocode 8 specifically deals with earthquake-resistant design of structures (CEN, 2006). Each country adopting Eurocode 8 must develop a National Annex to indicate how the code is implemented; the National Annex for the Netherlands is being developed. Eurocode 8 uses a standard practice to represent seismic hazard via PGA maps associated with ground motions having a 10% probability of exceedance during 50 years, equivalent to 0.2%/year for a stationary process, or a return period of 475-years.
Disaggregation	Disaggregation of a Monte-Carlo simulation result is a technique to determine the range of the factors with the largest impact on the simulation result.
Fault	A fracture along which there has been significant displacement of the two sides relative to each other parallel to the fracture. (USGS)
Fault Plane	The surface on which the earthquake movement takes place. (CEDIM)

Gas-year	Gas-years are the 12-month period starting at 1st October. The gas-year 2020/2021 is the period from 1st October 2020 up to and including 30st September 2021. Gas-years are used to avoid the high gas demand winter period to be split over two reporting periods.
Geophone	A device that converts ground movement (velocity) into voltage, which may be recorded at a recording station. The deviation of this measured voltage from the base line is called the seismic response and is analysed for structure of the earth.
Ground Motion (Shaking)	General term referring to the qualitative or quantitative aspects of movement of the Earth's surface from earthquakes or explosions. Ground motion is produced by waves that are generated by sudden slip on a fault or sudden pressure at the explosive source and travel through the Earth and along its surface. (USGS)
GTS-raming	The hazard and risk assessment is based on a production profile for the Groningen field. This is based on a prognosis of demand for Groningen gas prepared by GTS. GTS raming 2020 as made in January 2020.
Gutenberg-Richter	Earthquakes appear to follow a pattern through time in terms of no. of earthquakes vs. magnitude. This is called the Gutenberg-Richter criterion. (CEDIM)
Hazard	Any physical phenomenon associated with an earthquake that may produce adverse effects on human activities. This includes surface faulting, ground shaking, landslides, liquefaction, tectonic deformation, tsunami, and seiche and their effects on land use, manmade structures, and socioeconomic systems. A commonly used restricted definition of earthquake hazard is the probability of occurrence of a specified level of ground shaking in a specified period of time. (USGS)
Hypocenter	The point within the Earth where an earthquake rupture initiates. Also commonly termed the focus. (USGS)
Individual Earthquake Risk	The individual earthquake risk is the annual risk that an individual is exposed to in the various structures in or near which this individual is present (See also table 7.1).
Inside Local Personal Risk (ILPR)	The probability of death of a fictional unprotected person who is permanently present in a building (See also table 7.1).
Liquefaction	seismology, it refers to the loss of soil strength as a result of an increase in pore pressure due to ground motion. This effect can be caused by earthquake shaking. (IASPEI)The transformation of a granular material from a solid state into a liquefied state as a consequence of increased pore water pressures and reduced effective stress. In engineering
Local Personal Risk (LPR)	The probability of death of a fictional unprotected person who is permanently present in or near a building. This person is thought to be inside the building 99% of the time and outside near the building 1 % of the time (See also table 7.1).
Local site conditions	A qualitative or quantitative description of the topography, geology, and soil profile at a site that affect ground motions during an earthquake. (IASPEI).
Nationale Praktijk Richtlijn: NPR 9998	This document describes the structural safety of a building in case of earthquake loads. Constructors can use this guideline to calculate how strong a building must be in order to comply with the seismic safety standard for buildings used in the Netherlands.
Magnitude	A number that characterizes the relative size of an earthquake. Magnitude is based on measurement of the maximum motion recorded

	by a seismograph(sometimes for earthquake waves of a particular frequency), corrected for attenuation to a standardized distance. Several scales have been defined, but the most commonly used are (1) local magnitude (ML), commonly referred to as Richter magnitude, (2) surface-wave magnitude (Ms), (3) body-wave magnitude (Mb), and (4) moment magnitude (Mw). ML, Ms and Mb have limited range and applicability and do not satisfactorily measure the size of the largest earthquakes. The moment magnitude (Mw) scale, based on the concept of seismic moment, is uniformly applicable to all sizes of earthquakes but is more difficult to compute than the other types. In principal, all magnitude scales could be cross calibrated to yield the same value for any given earthquake, but this expectation has proven to be only approximately true, thus the need to specify the magnitude type as well as its value. An increase of one unit of magnitude (for example, from 4.6 to 5.6) represents a 10-fold increase in wave amplitude on a seismogram or approximately a 30-fold increase in the energy released. In other words, a magnitude 6.7 earthquake releases over 900 times (30 times 30) the energy of a 4.7 earthquake - or it takes about 900 magnitude 4.7 earthquakes to equal the energy released in a single 6.7 earthquake! There is no beginning nor end to this scale. However, rock mechanics seem to preclude earthquakes smaller than about -1 or larger than about 9.5. A magnitude -1.0 event releases about 900 times less energy than a magnitude 1.0 quake. Except in special circumstances, earthquakes below magnitude 2.5 are not generally not felt by humans. (USGS-IASPEI)
Mijnraad 1500 Lijst	These are the ca 1,500 buildings that in the advice of the Mijnraad of mid-2018 had a mean LPR > 10^{-5}/year.
Monte-Carlo Simulation	The Monte Carlo simulation is a simulation technique whereby a physical process is simulated not once but many times, each time with different starting conditions. The result of this collection of simulations is a distribution function that displays the entire area of possible outcomes.
Object-related Individual Risk	The Objectgebonden individual earthquake risk is the risk that an individual dies in a year due to collapse or falling objects (as a result of an earthquake) of a building in which or in the direct vicinity of which this person is present. The residence time in/around that building is therefore taken into consideration (See also table 7.1).
Outside Local Personal Risk	The probability of death of a fictional unprotected person who is permanently present near a building (See also table 7.1).
P Wave	A seismic body wave that involves particle motion (alternating compression and extension) in the direction of propagation. (USGS)
P wave	A P wave, or compressional wave, is a seismic body wave that shakes the ground back and forth in the same direction and the opposite direction as the direction the wave is moving.
Peak Acceleration	The highest acceleration in terms of value. (USGS)
PGA	The maximum acceleration amplitude measured or expected in a strong-motion accelerogram of an earthquake. (IASPEI)
Primary Wave	See P Wave (CEDIM)
Risk	The probabilistic determination of the damages a certain hazard can cause given the existing vulnerability, location and time. (UN)
Risk Assessment	Definition: A methodology to determine the nature and extent of risk by analyzing potential hazards and evaluating existing conditions of vulnerability that together could potentially harm exposed people,

	property, services, livelihoods and the environment on which they depend.Comment: Risk assessments (and associated risk mapping) include: a review of the technical characteristics of hazards such as their location, intensity, frequency and probability; the analysis of exposure and vulnerability including the physical social, health, economic and environmental dimensions; and the evaluation of the effectiveness of prevailing and alternative coping capacities in respect to likely risk scenarios. This series of activities is sometimes known as a risk analysis process. (UN/ISDR)
Rupture	The instantaneous boundary between the slipping and locked parts of a fault during an earthquake. Rupture in one direction on the fault is referred to as unilateral. Rupture may radiate outward in a circular manner or it may radiate toward the two ends of the fault from an interior point, referred to as bilateral. (USGS)
S-wave	An S wave, or shear wave, is a seismic body wave that shakes the ground back and forth perpendicular to the direction the wave is moving.
S Wave Velocity	The velocity of a secondary or S wave. Generally measured in m/s. (CEDIM)
Secondary Wave	A seismic body wave that involves a shearing motion in a direction perpendicular to the direction of propagation. When it is resolved into two orthogonal components in the plane perpendicular to the direction of propagation, SH denotes the horizontal component and SV denotes the orthogonal component. Also known as S waves and shear waves. (PDC)
Seismic hazard	Risk of a certain ground motion occurring at a location (this can be defined by scenario modeling via stochastic catalogues, DSHA, PSHA or other such methods, and can include different types of earthquake effects) (CEDIM)
Seismic Risk	See earthquake risk, also the probabilistic risk is the odds of an earthquake occurring and causing damage within a given time interval and region. (EQCanada)
Seismic Station	A ground position at which a geophysical instrument is located for an observation. (U-Milwaukee)
Seismic Waves	An elastic wave generated by an impulse such as an earthquake or an explosion. Seismic waves may propagate either along or near the Earth's surface (for example, Rayleigh and Love waves) or through the Earth's interior (P and S waves). (USGS)
Seismicity	1) The geographic and historical distribution of earthquakes. 2) A term introduced by Gutenberg and Richter to describe quantitatively the space, time, and magnitude distribution of earthquake occurrences. Seismicity within a specific source zone or region is usually quantified in terms of a Gutenberg-Richter relationship. (ICWGroup/IASPEI)
Seismogram	A record written by a seismograph in response to ground motions produced by an earthquake, explosion, or other ground-motion sources. (ICW Group)
Seismometer	A seismometer is a damped oscillating mass, such as a damped mass-spring system, used to detect seismic-wave energy. The motion of the mass is commonly transformed into an electrical voltage. The electrical voltage is recorded on paper, magnetic tape, or another recording medium. This record is proportional to the motion of the seismometer mass relative to the Earth, but it can be mathematically converted to a

	record of the absolute motion of the ground. Seismograph is a term that refers to the seismometer and its recording device as a single unit. (NASA)
Velocity	In reference to earthquake shaking, velocity is the time rate of change of ground displacement of a reference point during the passage of earthquake seismic waves commonly expressed in centimeters per second. (USGS)

Appendix C – List of Abbreviations

AHN	Actueel Hoogtebestand Nederland
ALLEA	All European Academies
AGE	TNO - adviesgroep economische zaken
ALARP	As Low As Reasonably Practicable
ARUP	Engineering Company named after founder: Ove Arup
ACVG	Adviescollege Veiligheid Groningen
BAG	Basisregistratie Adressen en Gebouwen
Bcm	N.Bcm refers to a volume of a billion normal cubic meters. Normal means the volume is measured at a standard temperature (0 degree C) and pressure (1 bar)
BGS	British Geological Survey
BOA	Begeleidingscommissie Onderzoek Aardbevingen
BZK	Ministry of Internal Affairs (Ministerie van Binnenlandse Zaken)
CBS	Centraal Bureau Statistiek
CEA	China Earthquake Administration
CEDIM	Center for Disaster Management and Risk Reduction Technology
CMI	Compaction Monitoring Instrument
CMOC	Crack Mouth Opening Displacement
CPT	Cone Penetration Test
CVW	Centrum Veilig Wonen
DAS	Distributed Acoustic Sensing
DEEP.nl	Research program led by NWO
DC	Carboniferous Formation
DIC	Digital Image Correlation
DS	Damage State
DSS	Distributed Strain Sensing
DTS	Distributed Temperature Sensing
DvhN	Dagblad van het Noorden (regional newspaper)
EBN	Energy Beheer Nederland
EDB	Exposure Database
EMS	European Macroseismic Scale
EPOS	European Plate Observatory System
ERIC	European Research Infrastructure Consortium
EVS	Extended Visual Screening
EZ	Ministerie van Economische Zaken (in English MEA)
EZK	Ministerie van Economische Zaken en Klimaat (in English MEAC)
FDSN	Federation of Digital Seismograph Networks
Frl	Friesland
GBB	Groninger Bodembeweging
GEM	Global Earthquake Model
GMPE	Ground Motion Prediction Equations
GMM	Ground Motion Model
GNSS	Global Navigation Satellite System
GPS	Global Positioning System
GR	Group Risk
GWC	Gas water contact

HRA	Hazard and Risk Assessment
HRBE	High Risk Building Element
ILPR	Inside Local Personal Risk
I&M	Ministerie van Infrastructuur en Milieu
InSAR	Interferometric Synthetic Aperture Radar
IR	Individual Risk
IVO	Instituut versterkingsopgave
IU	Interrogation Unit
KEM	Kenninsprogramma Effecten Mijnbouw (Knowledge program Effects of Mining)
KNAW	Koninklijk Nederlands Academie van Wetenschappen (Royal Netherlands Academy of Arts and Sciences)
KNGMG	Koninklijk Nederlands Geologisch Mijnbouwkundig Genootschap
KNMI	Koninklijk Nederlands Meteorologisch Institute
KU Leuven	Katholieke Universiteit Leuven (Catholic University Leuven)
LE	Latest Estimate
LIDAR	Laser Imaging Detection And Ranging
LPR	Local Personal Risk
LNEC	Laboratorio Nacional de Engenharia Civil (Lisbon)
M	Earthquake Magnitude
MEA	Ministry of Economic Affairs (prior to 2017)
MEAC	Ministry of Economic Affairs and Climate Policy (from 2017 onwards)
MR	Maatschappelijk Risico
MASW	Multichannel Analysis of Surface Waves
MIT	Massachusetts Institute of Technology
NAM	Nederlandse Aardolie Maatschappij B.V.
NARS	Network of Autonomously Recording Seismographs
NCG	Nationaal Coordinator Groningen
NFU	Netherlands Federation of University Medical Centres
NGO	Non-governmental Organisation
NORSAR	Norwegian Seismic Array (Norwegian independent, not-for-profit, research foundation within the field of geo-science)
NPR	Nationale Practijkrichtlijn
NTNU	Norges teknisk-naturvitenskapelige universitet (Norwegian University of Science and Technology in Trondheim)
NWO	Nederlands Organisatie voor Wetenschappelijk Onderzoek (Dutch National Science Foundation)
OECD	Organisation of Economic Cooperation and Development
OGP	Onafhankelijk Geologen Platform
OIA	Objectgebonden Individueel Aardbevingsrisico (Object related individual earthquake risk)
OIR	Object-related individual risk (same as OIA)
OVV	Onderzoeksraad voor Veiligheid (Safety Board)
PGA	Peak Ground Acceleration
PGK	Petroleum Geologie Kring
PGV	Peak Ground Velocity
PNL	Pulsed Neutron log
PRBE	Potential High Risk Building Elements
QRM	Quantitative Reservoir Management
RFT	Repeat Formation Tester

RGD	Rijksgeologische Dienst (later also TNO-NIGT)
RMSE	Roor Mean Square Estimate
RUG	Rijksuniversiteit Groningen
RVS	Rapid Visual Screening
RvS	Raad van State
RWS	Rijkswaterstaat
SAC	Scientific Advisory Committee
SCAL	Special Core Analysis Laboratory
SED	Schweizerischer Erdbebendienst (Swiss Seismological Survey)
SINTEF	Stiftelsen for industriell og teknisk forskning (Foundation for Scientific and Industrial Research)
SMS	Samenwerking Mijnbouw Schade
SodM	Staatstoezicht op de Mijnen (also SSM State Supervision of Mines)
SPE	Society of Petroleum Engineers
SPG	Static Pressure Measurement
SPTG	Static Pressure and Temperature Measurement
SSHAC	Senior Seismic Hazard Analysis Committee
Tcbb	Technische commissie bodembeweging
TCMG	Tijdelijk Commissie Mijnbouwschade Groningen
TIVO	Tijdelijke Instituut versterkingsopgave
TK	Tweede Kamer (Dutch equivalent of House of Commons)
TNO	Nederlandse Organisatie voor Toegepast Natuurwetenschappelijk Onderzoek, Netherlands Organisation for Applied Scientific Research
TNO-AGE	Nederlandse Organisatie voor Toegepast Natuurwetenschappelijk Onderzoek – Advies Groep Economische Zaken
TO2	Toegepast Onderzoek Organisaties (Federation of Applied Research Institutes); Deltares, MARIN, NLR, TNO and WR
TPA	Technische Platform Aardbevingen
TU Delft	Technische Universiteit Delft
TU/e	Technische Universiteit Eindhoven
UU	Universiteit Utrecht
UvA	Universiteit van Amsterdam
URM	Un-reinforced Masonry
USGS	United States Geological Survey
USNRC	United States Nuclear Regulatory Commission
VoVo	Voorlopige voorziening
VSNU	Vereniging samenwerkende universiteiten in Nederland (Association of Universities in the Netherlands)
V_{s800}	Shear wave velocity up to a depth of 800 m

Appendix D – Reconciliation of Request for proposal of the operational strategy for gas-year 2020/2021

The letter from the expectation letter (verwachtingenbief) from the Minister contained a list of deliverables to be included in this report. This Appendix contains a quick reference guide linking these requests to the tables and figures in this report.

Rapportage

Rapportage	Table, Map or Figure
Een tabel of figuur waarmee de inzet van de clusters als functie van de dagvraag eenduidig wordt vastgelegd.	**Operational Strategy and Summary (Samenvatting) of this report**
Een overzicht van de kans op zwaardere bevingen (M>3,5; 4,0; 4,5) per gasjaar, voor het gasjaar 2021-2022 en de 10 volgende gasjaren.	**Main text of the HRA Report** Chapter Event Rate Tables 5.2a to b.
Berekeningen van het Plaatsgebonden Persoonlijk Risico (LPR) (hazardkaarten en LPR-curves) voor het gasjaar 2020-2021 en een overzicht in een tabel van het aantal gebouwen dat niet voldoet aan de veiligheidsnorm (berekend met de verwachtingswaarde van het risico per gebouw, met P90 in een bijlage) per gasjaar, voor het gasjaar 2020-2021 en de 10 volgende gasjaren.	**Main text of the HRA Report** Chapter Hazard Assessment Hazard Maps: Fig. 6.4a to c, 6.6, 6.7 and 6.8. Chapter Risk Assessment LPR-Curves: Figure 7.1 a to c and Figure 7.2 Building Tables: Tables 7.3 a to f, Figure 7.4 and Figure 7.5 Maps: Figure 7.7, 7.8, 7.9, 7.10a to c and Fig. 11a to c. **Appendix E - Additional tables for buildings above the Meijdam-norm for calendar years.** Figures e.1a to f
Een doorkijk van de voorgestelde clusterafbouw (inclusief de productielocaties) bij de geraamde afbouw van de productie in de jaren na komend gasjaar bij voortzetting van de clusterinzetvolgorde op basis van de door GTS opgegeven dataset met volumeraming. Een overzicht van benodigde clusters en een duiding van de benodigde opstarttijd indien een cluster alleen nog nodig is voor de door GTS geadviseerde capaciteit en er dus planmatig geen volume meer nodig is uit het Groningenveld.	**Operational Strategy** Chapter Reservoir and Pressure Modelling Cluster reduction based on volume forecast (GTS -raming): Fig. 3.3. and 3.4.
Ontwikkeling van de seismische activiteit tot 10 jaar na het gasjaar 2020-2021, weergegeven in gasjaren.	**Main text of the HRA Report** Chapter Event Rate Figure 5.1, 5.2, 5.3 and 5.4. Appendix G – Seismic Event Rates Fig. g.1a and g.1b.
De ontwikkeling van de bodemdaling inclusief de verwachting moet weergegeven worden in: ▪ Kaarten van de ruimtelijke ontwikkeling van de bodemdaling in 2018 (laatste waterpassing) tot 2030. ▪ Figuren met de tijdsafhankelijke ontwikkeling van de bodemdaling op meerdere waterpaslocaties verdeeld over het gasveld.	**Main text of the HRA Report** Chapter Subsidence

Bijlage

Bijlage	**Table, Map or Figure**
Kaarten per operationele strategie van de drukontwikkeling tot 30 jaar na het gasjaar 2020-2021.	**Appendix F – Pressure Differences** Maps: Fig. f1.a to k.
Ontwikkeling van de seismische activiteit per operationele strategie tot 30 jaar na het gasjaar 2020-2021, weergegeven in stappen van 5 jaar.	**Main text of the HRA Report** Chapter Event Rate Figure 5.1 en 5.2 for gas-years up to 2034/2035 Additional years in Appendix G
Verschilkaarten van de drukverdeling tussen de verschillende operationele strategieën, per gasjaar.	**Main text of the HRA Report** Chapter Reservoir and Pressure Modelling Figure 3.7 and 3.7.
Verschilkaarten van de ruimtelijke verdeling van de seismische activiteit (mean) in de verschillende operationele strategieën, inclusief aanduiding hoeveel bevingen er meer/minder in een gebied zijn opgetreden, per gasjaar.	**Main text of the HRA Report** Chapter Seismic Event Rate Figure 5.5.
Verschilkaarten van de seismische dreiging in de verschillende operationele strategieën.	**Main text of the HRA Report** Chapter Hazard Assessment Figure 6.7
Een overzicht per operationele strategie van het aantal gebouwen dat niet voldoet aan de veiligheidsnorm (berekend met P90) per gasjaar, voor het gasjaar 2020-2021 en de 10 volgende gasjaren.	**Main text of the HRA Report** Chapter Risk Assessment LPR-Curves: Figure 7.1 a to c and Figure 7.2 Building Tables: Tables 7.3 a to f, Figure 7.4 and Figure 7.5 Maps: Figure 7.7, 7.8, 7.9, 7.10a to c and 7.11a to c. .
Daarnaast een zelfde overzicht met het aantal gebouwen berekend met zowel de verwachtingswaarde als P90 voor de kalenderjaren 2020 tot en met 2030. Deze dient uiterlijk 12 april in mijn bezit te zijn.	**Appendix E - Additional tables for buildings above the Meijdam-norm for calendar years.** Figures e.1a to f

Bijlage	Table, Map or Figure
Kaarten per operationele strategie met de locaties en het type van de gebouwen boven de norm op basis van de verwachtingswaarde en P90 voor het gas-jaar 2020-2021.	**Main text of the HRA Report** Chapter Risk Assessment Maps: Figure 7.6, 7.7 and 7.8.
Verschilkaarten van de ruimtelijke verdeling van de gebouwen boven de norm voor de verwachtingswaarde en P90 voor het gasjaar 2020-2021.	**Main text of the HRA Report** Chapter Risk Assessment Maps: Figure 7.10a to c and 7.11a to c.
Bij het overzicht van het aantal gebouwen dat niet aan de veiligheidsnorm voldoet voor het gasjaar 2020-2021 (berekend met de verwachtingswaarde en P90) een overzicht welk percentage van deze gebouwen in het huidige gasjaar (volgens HRA 2019) eveneens niet aan de norm voldeed, uitgesplitst in verwachtingswaarde, P90 en conform norm in de HRA2019.	**Main text of the HRA Report** Chapter Risk Assessment Table: 7.1a to f. Reconciliation: 7.12 7.13 and 7.14.

Appendix E – Additional tables for buildings above the Meijdam-norm for calendar years.

In the main text of this report the hazard, building damage and risk assessment for production profile GTS-raming 2020 was presented for gas-years. The choice of gas-years for the document is because the Ministerial Decision this report informs will also be based on gas-years.

However, the plan of approach (Plan van Aanpak) for the structural upgrading program prepared by the NCG is based on calendar years. In this appendix the numbers of buildings above the Meijdam-norm are provided in calendar years.

Calendar year	Mean LPR 10^{-4}/year	Mean LPR 10^{-5}/year	Mean OIA 10^{-4}/year	Mean OIA 10^{-5}/year	P90 LPR 10^{-4}/year	P90 LPR 10^{-5}/year	P90 OIA 10^{-4}/year	P90 OIA 10^{-5}/year
2020	0	0	0	0	0	137	0	35
2021	0	0	0	0	0	141	0	20
2022	0	0	0	0	0	67	0	7
2023	0	0	0	0	0	7	0	0
2024	0	0	0	0	0	5	0	0
2025	0	0	0	0	0	3	0	0
2026	0	0	0	0	0	0	0	0
2027	0	0	0	0	0	0	0	0
2028	0	0	0	0	0	0	0	0
2029	0	0	0	0	0	0	0	0

Table e.1a Number of buildings with mean LPR exceeding 10^{-5}/year and 10^{-4}/year, for production profile GTS-raming 2020, Operational Strategy 1 and average temperature year. See main text for further explanation. These are shown for each year of the period 2020 to 2029 for the production profile "GTS-raming 2020", operational strategy 1 for an average weather year.

Calendar year	Mean LPR 10^{-4}/year	Mean LPR 10^{-5}/year	Mean OIA 10^{-4}/year	Mean OIA 10^{-5}/year	P90 LPR 10^{-4}/year	P90 LPR 10^{-5}/year	P90 OIA 10^{-4}/year	P90 OIA 10^{-5}/year
2020	0	0	0	0	0	144	0	35
2021	0	0	0	0	0	220	0	71
2022	0	0	0	0	0	64	0	4
2023	0	0	0	0	0	43	0	0
2024	0	0	0	0	0	16	0	0
2025	0	0	0	0	0	0	0	0
2026	0	0	0	0	0	0	0	0
2027	0	0	0	0	0	0	0	0
2028	0	0	0	0	0	0	0	0
2029	0	0	0	0	0	0	0	0

Table e.1b Number of buildings with mean LPR exceeding 10^{-5}/year and 10^{-4}/year, for production profile GTS-raming 2020, Operational Strategy 1 and cold temperature year. See main text for further explanation. These are shown for each year of the period 2020 to 2029 for the production profile "GTS-raming 2020" operational strategy 1 for a cold weather year.

Calendar year	Mean LPR 10^{-4}/year	Mean LPR 10^{-5}/year	Mean OIA 10^{-4}/year	Mean OIA 10^{-5}/year	P90 LPR 10^{-4}/year	P90 LPR 10^{-5}/year	P90 OIA 10^{-4}/year	P90 OIA 10^{-5}/year
2020	0	0	0	0	0	159	0	43
2021	0	0	0	0	0	94	0	12
2022	0	0	0	0	0	32	0	4
2023	0	0	0	0	0	16	0	0
2024	0	0	0	0	0	0	0	0
2025	0	0	0	0	0	0	0	0
2026	0	0	0	0	0	0	0	0
2027	0	0	0	0	0	0	0	0
2028	0	0	0	0	0	0	0	0
2029	0	0	0	0	0	0	0	0

Table e.1c Number of buildings with mean LPR exceeding 10^{-5}/year and 10^{-4}/year, for production profile GTS-raming 2020, Operational Strategy 1 and warm temperature year. See main text for further explanation. These are shown for each year of the period 2020 to 2029 for the production profile "GTS-raming 2020" operational strategy 1 for a warm weather year.

Calendar year	Mean LPR 10^{-4}/year	Mean LPR 10^{-5}/year	Mean OIA 10^{-4}/year	Mean OIA 10^{-5}/year	P90 LPR 10^{-4}/year	P90 LPR 10^{-5}/year	P90 OIA 10^{-4}/year	P90 OIA 10^{-5}/year
2020	0	0	0	0	0	127	0	20
2021	0	0	0	0	0	126	0	22
2022	0	0	0	0	0	28	0	4
2023	0	0	0	0	0	6	0	0
2024	0	0	0	0	0	0	0	0
2025	0	0	0	0	0	0	0	0
2026	0	0	0	0	0	0	0	0
2027	0	0	0	0	0	0	0	0
2028	0	0	0	0	0	0	0	0
2029	0	0	0	0	0	0	0	0

Table e.1d Number of buildings with mean LPR exceeding 10^{-5}/year and 10^{-4}/year, for production profile GTS-raming 2020, Operational Strategy 2 and average temperature year. See main text for further explanation. These are shown for each year of the period 2020 to 2029 for the production profile "GTS-raming 2020" operational strategy 2 for an average weather year.

Calendar year	Mean LPR 10^{-4}/year	Mean LPR 10^{-5}/year	Mean OIA 10^{-4}/year	Mean OIA 10^{-5}/year	P90 LPR 10^{-4}/year	P90 LPR 10^{-5}/year	P90 OIA 10^{-4}/year	P90 OIA 10^{-5}/year
2020	0	0	0	0	0	116	0	13
2021	0	0	0	0	0	214	0	67
2022	0	0	0	0	0	61	0	0
2023	0	0	0	0	0	24	0	0
2024	0	0	0	0	0	5	0	0
2025	0	0	0	0	0	0	0	0
2026	0	0	0	0	0	0	0	0
2027	0	0	0	0	0	0	0	0
2028	0	0	0	0	0	0	0	0
2029	0	0	0	0	0	0	0	0

Table e.1e Number of buildings with mean LPR exceeding 10^{-5}/year and 10^{-4}/year, for production profile GTS-raming 2020, Operational Strategy 2 and cold temperature year. See main text for further explanation. These are shown for each year of the period 2020 to 2029 for the production profile “GTS-raming 2020” operational strategy 2 for a cold weather year.

Calendar year	Mean LPR 10^{-4}/year	Mean LPR 10^{-5}/year	Mean OIA 10^{-4}/year	Mean OIA 10^{-5}/year	P90 LPR 10^{-4}/year	P90 LPR 10^{-5}/year	P90 OIA 10^{-4}/year	P90 OIA 10^{-5}/year
2020	0	0	0	0	0	108	0	10
2021	0	0	0	0	0	22	0	0
2022	0	0	0	0	0	31	0	4
2023	0	0	0	0	0	7	0	0
2024	0	0	0	0	0	0	0	0
2025	0	0	0	0	0	0	0	0
2026	0	0	0	0	0	0	0	0
2027	0	0	0	0	0	0	0	0
2028	0	0	0	0	0	0	0	0
2029	0	0	0	0	0	0	0	0

Table e.1f Number of buildings with mean LPR exceeding 10^{-5}/year and 10^{-4}/year, for production profile GTS-raming 2020, Operational Strategy 2 and warm temperature year. See main text for further explanation. These are shown for each year of the period 2020 to 2029 for the production profile “GTS-raming 2020” operational strategy 2 for a warm weather year.

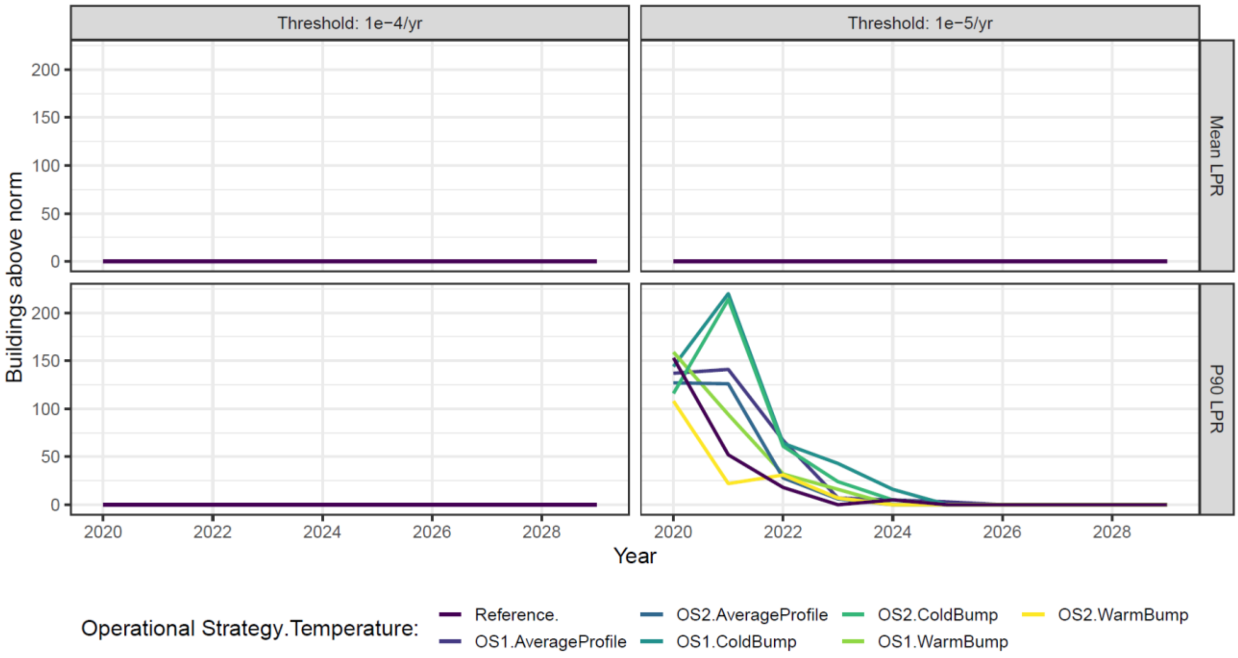

Figure e.1 *Graphs show the Local Personal Risk associated with the production profile "GTS-raming 2020" for average, cold weather and warm weather calendar-years for the period 2020 to 2029.*

Right graphs: *number of buildings exceeding the norm LPR larger than 10^{-5}/year*
Left graphs: *number of buildings exceeding the norm LPR larger than 10^{-4}/year*
Top graphs: *number of buildings exceeding the norm for mean LPR*
Bottom graphs: *number of buildings exceeding the norm for P90 LPR*

Appendix F – Pressure Differences

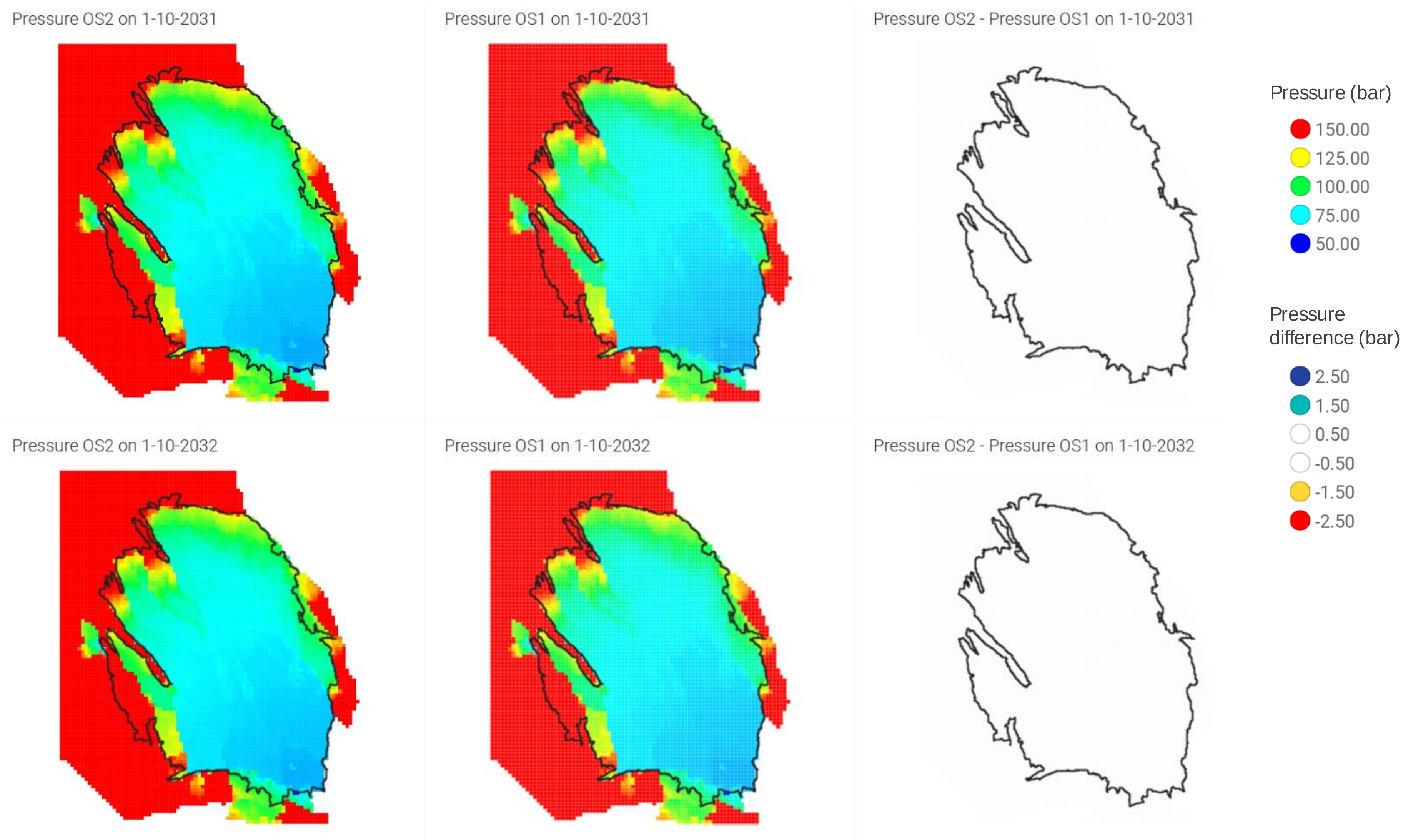

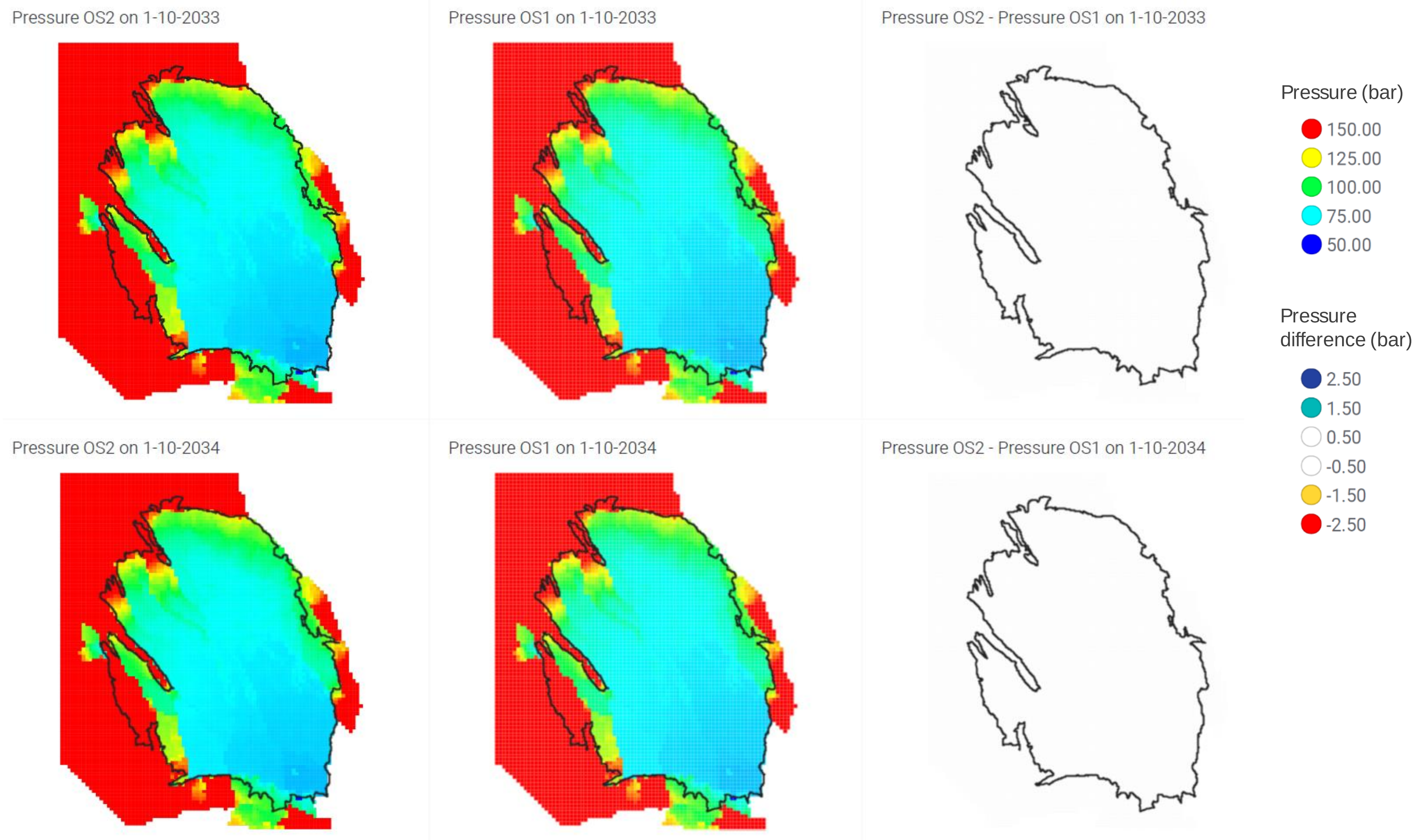
Pressure OS2 on 1-10-2033
Pressure OS1 on 1-10-2033
Pressure OS2 - Pressure OS1 on 1-10-2033
Pressure OS2 on 1-10-2034
Pressure OS1 on 1-10-2034
Pressure OS2 - Pressure OS1 on 1-10-2034
Pressure (bar)
150.00
125.00
100.00
75.00
50.00
Pressure difference (bar)
2.50
1.50
0.50
-0.50
-1.50
-2.50

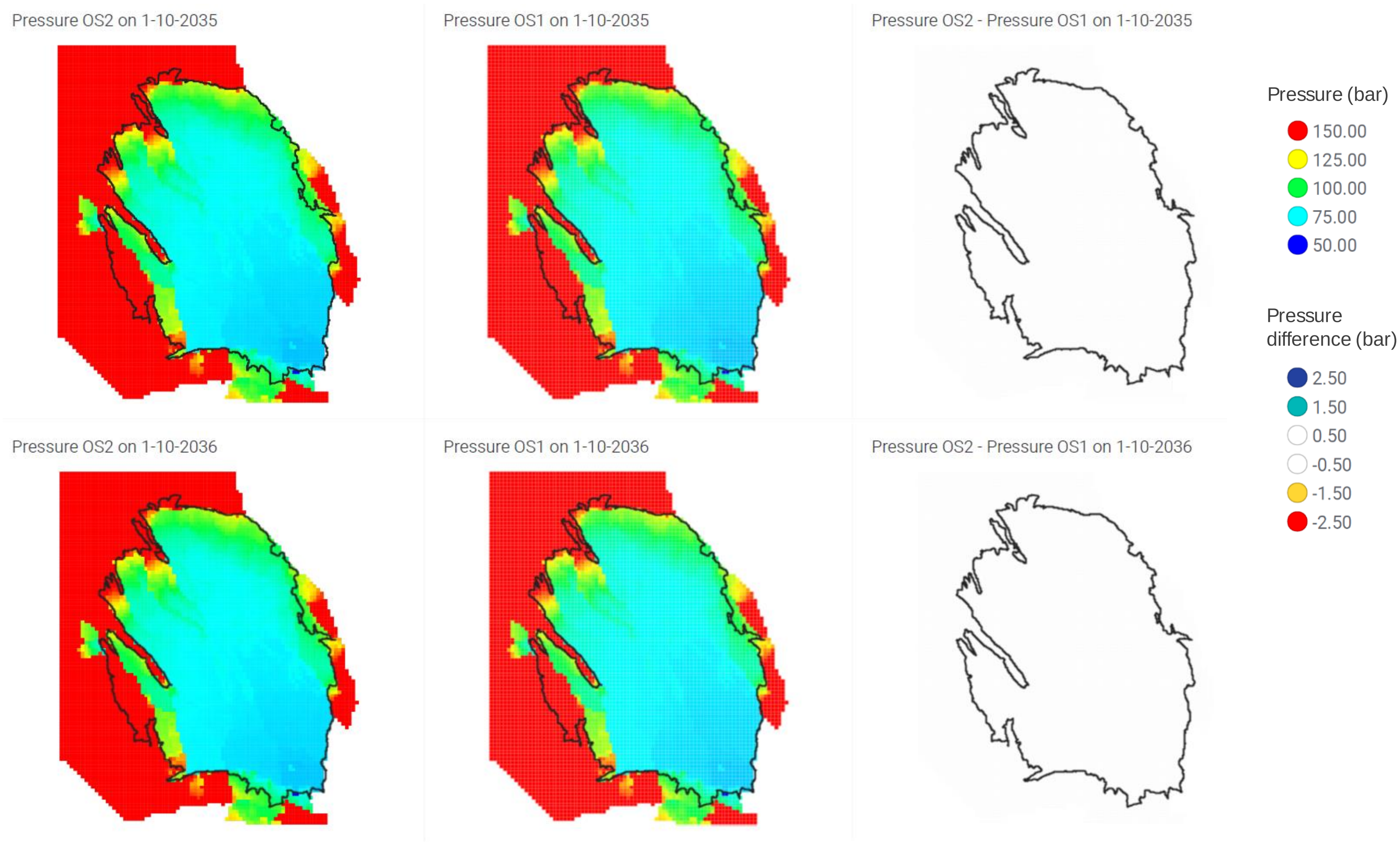
Pressure OS2 on 1-10-2035
Pressure OS1 on 1-10-2035
Pressure OS2 - Pressure OS1 on 1-10-2035
Pressure OS2 on 1-10-2036
Pressure OS1 on 1-10-2036
Pressure OS2 - Pressure OS1 on 1-10-2036
Pressure (bar)
150.00
125.00
100.00
75.00
50.00
Pressure difference (bar)
2.50
1.50
0.50
-0.50
-1.50
-2.50

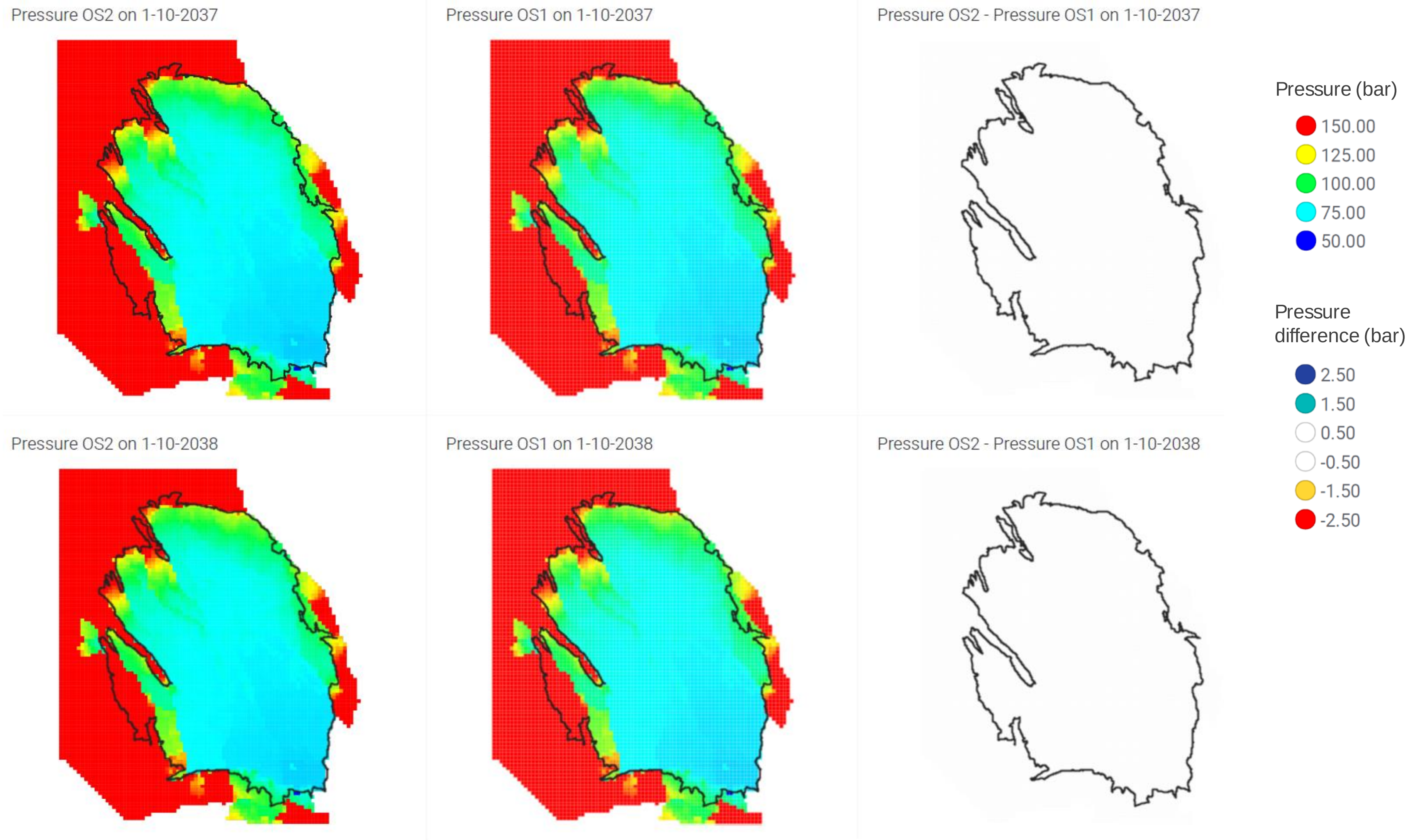
Pressure OS2 on 1-10-2037
Pressure OS1 on 1-10-2037
Pressure OS2 - Pressure OS1 on 1-10-2037
Pressure OS2 on 1-10-2038
Pressure OS1 on 1-10-2038
Pressure OS2 - Pressure OS1 on 1-10-2038
Pressure (bar)
150.00
125.00
100.00
75.00
50.00
Pressure difference (bar)
2.50
1.50
0.50
-0.50
-1.50
-2.50

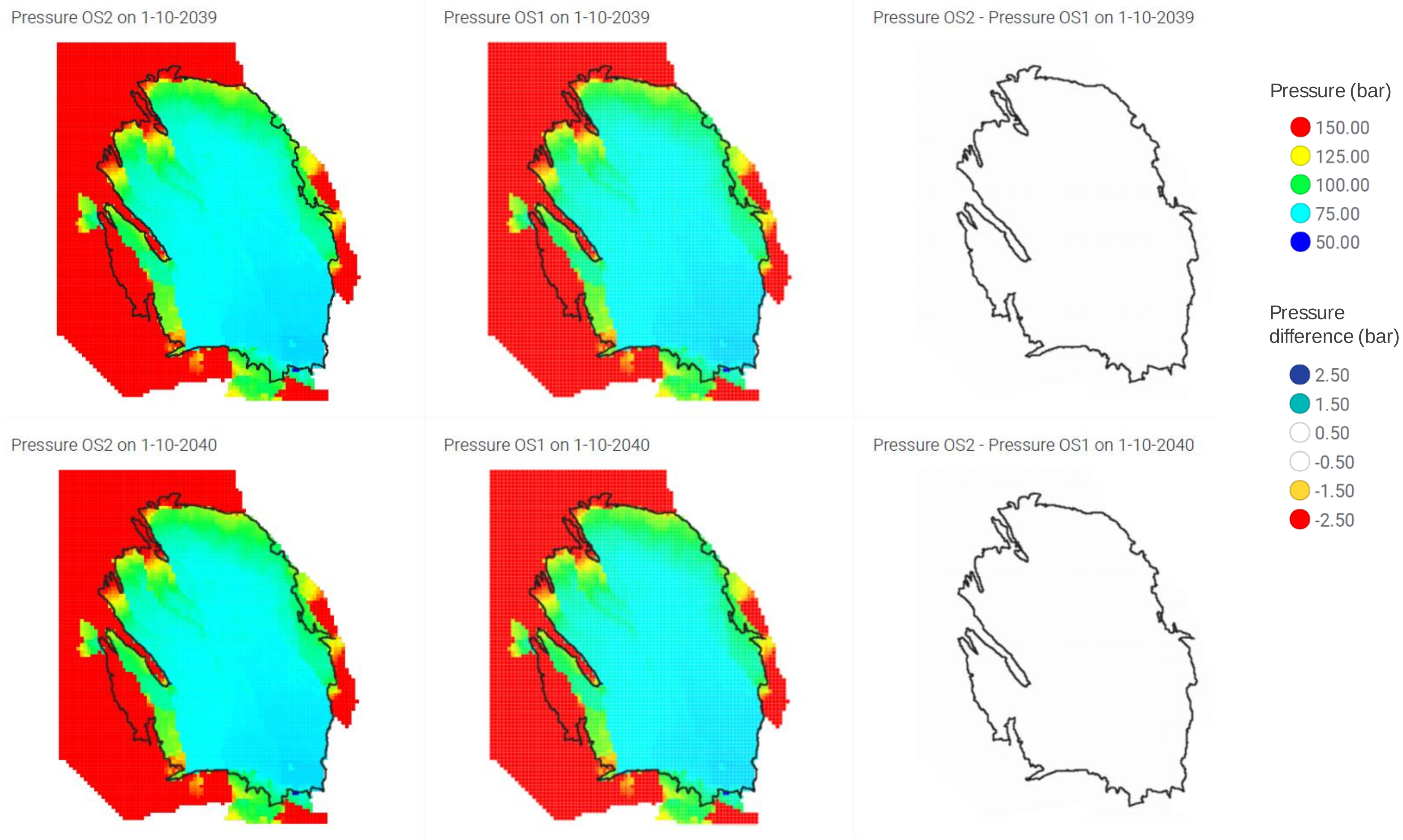
Pressure OS2 on 1-10-2039
Pressure OS1 on 1-10-2039
Pressure OS2 - Pressure OS1 on 1-10-2039
Pressure OS2 on 1-10-2040
Pressure OS1 on 1-10-2040
Pressure OS2 - Pressure OS1 on 1-10-2040
Pressure (bar)
150.00
125.00
100.00
75.00
50.00
Pressure difference (bar)
2.50
1.50
0.50
-0.50
-1.50
-2.50

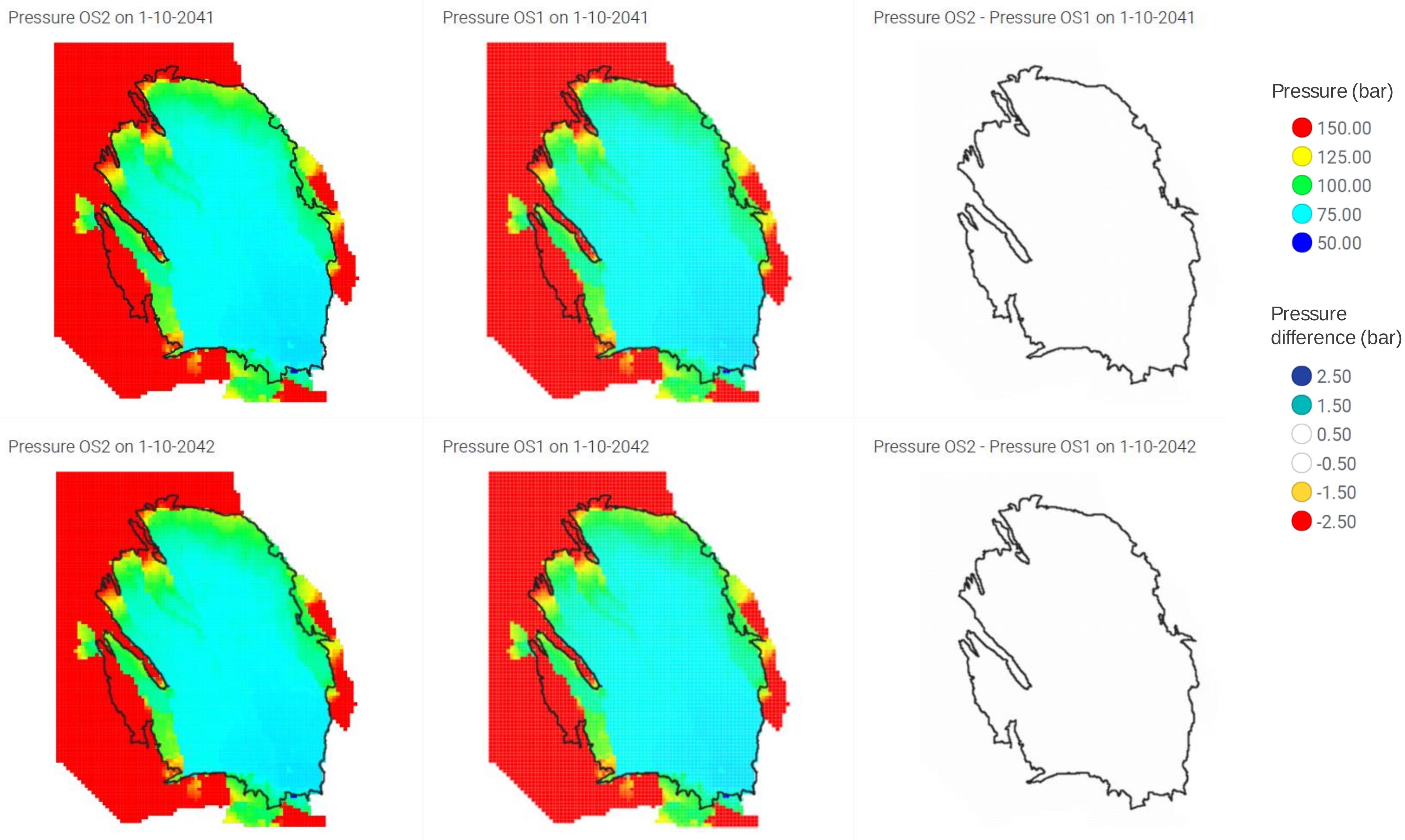
Pressure OS2 on 1-10-2041
Pressure OS1 on 1-10-2041
Pressure OS2 - Pressure OS1 on 1-10-2041
Pressure OS2 on 1-10-2042
Pressure OS1 on 1-10-2042
Pressure OS2 - Pressure OS1 on 1-10-2042
Pressure (bar)
150.00
125.00
100.00
75.00
50.00
Pressure difference (bar)
2.50
1.50
0.50
-0.50
-1.50
-2.50

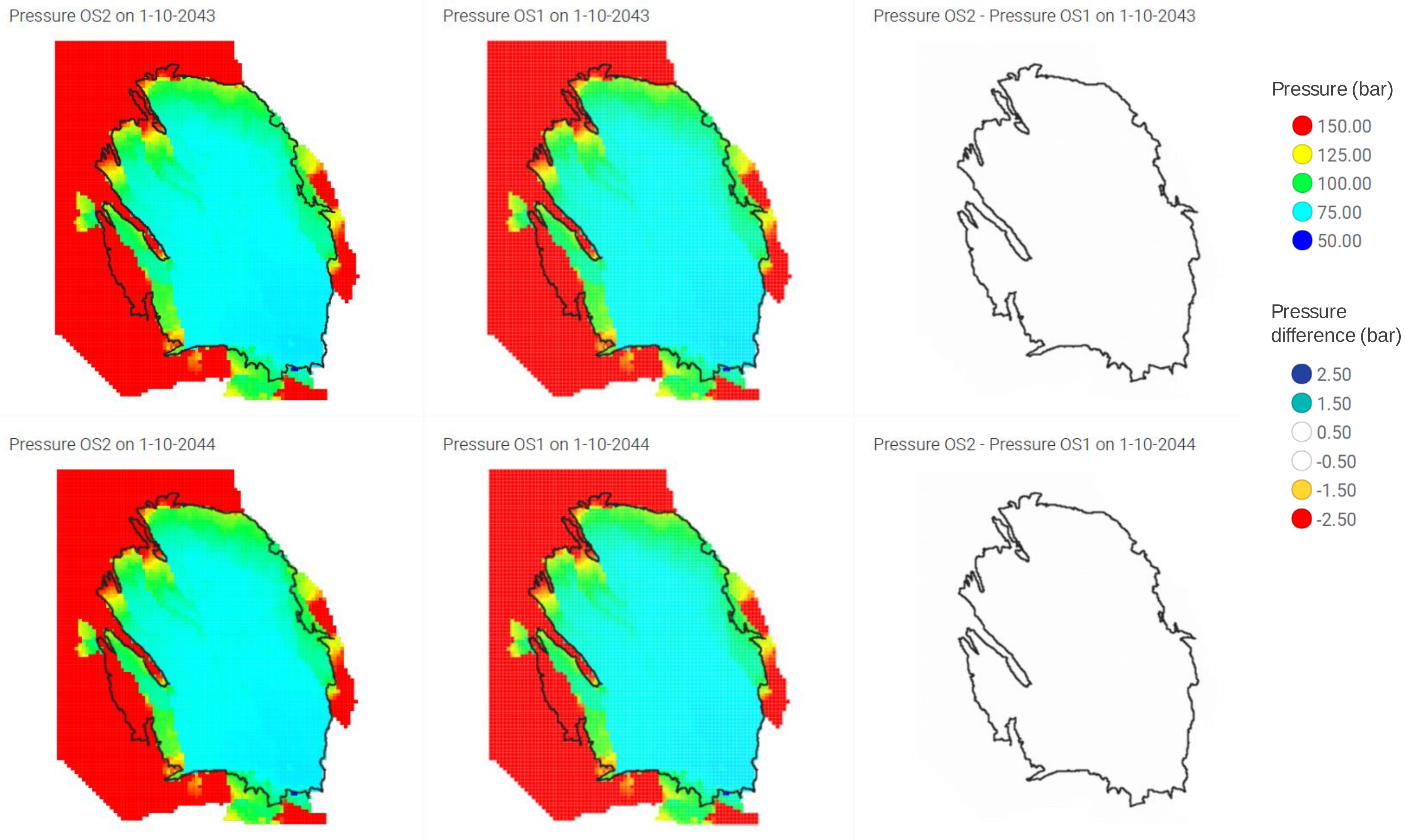
Pressure OS2 on 1-10-2043
Pressure OS1 on 1-10-2043
Pressure OS2 - Pressure OS1 on 1-10-2043
Pressure OS2 on 1-10-2044
Pressure OS1 on 1-10-2044
Pressure OS2 - Pressure OS1 on 1-10-2044
Pressure (bar)
150.00
125.00
100.00
75.00
50.00
Pressure difference (bar)
2.50
1.50
0.50
-0.50
-1.50
-2.50

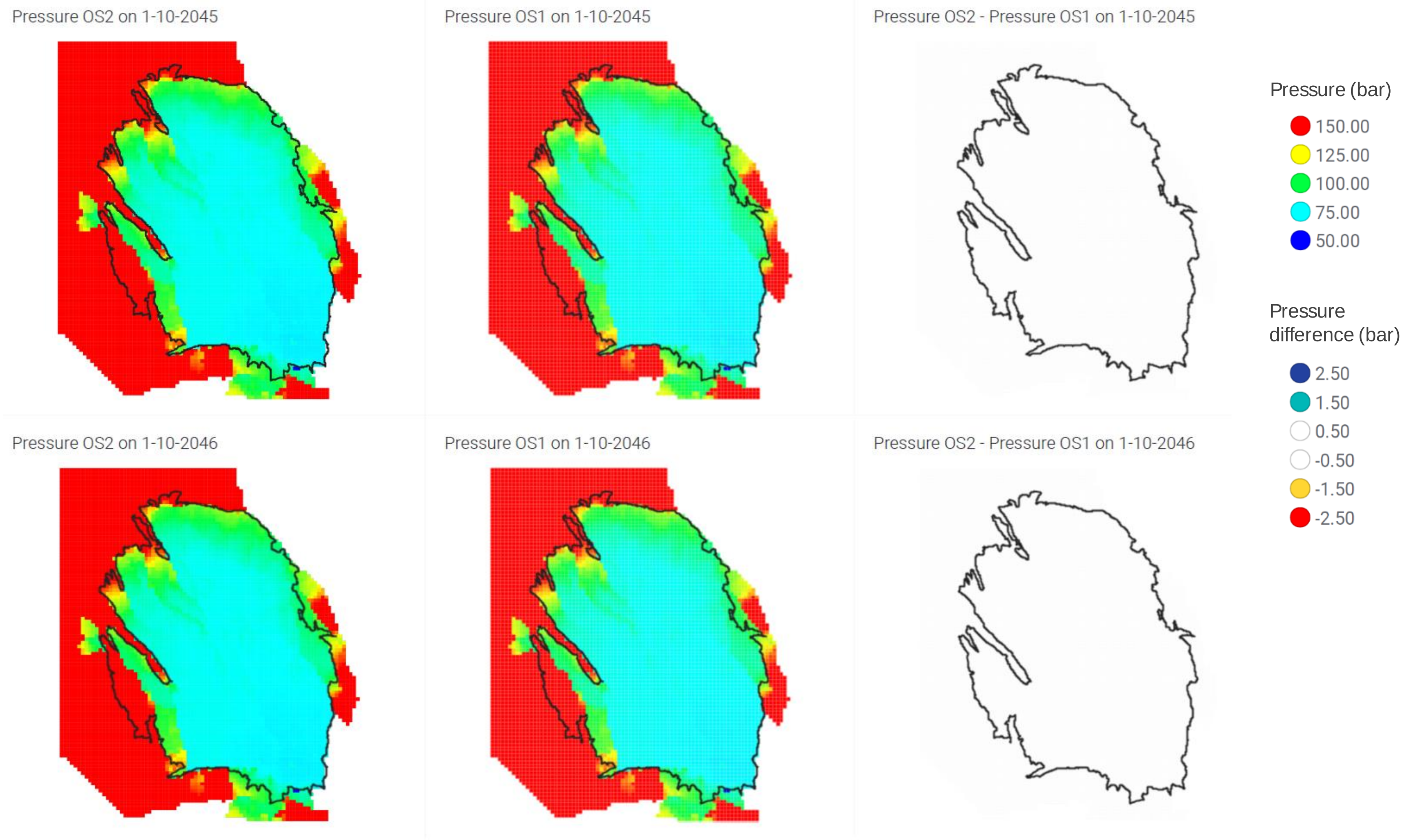
Pressure OS2 on 1-10-2045
Pressure OS1 on 1-10-2045
Pressure OS2 - Pressure OS1 on 1-10-2045
Pressure (bar)
150.00
125.00
100.00
75.00
50.00
Pressure difference (bar)
2.50
1.50
0.50
-0.50
-1.50
-2.50
Pressure OS2 on 1-10-2046
Pressure OS1 on 1-10-2046
Pressure OS2 - Pressure OS1 on 1-10-2046

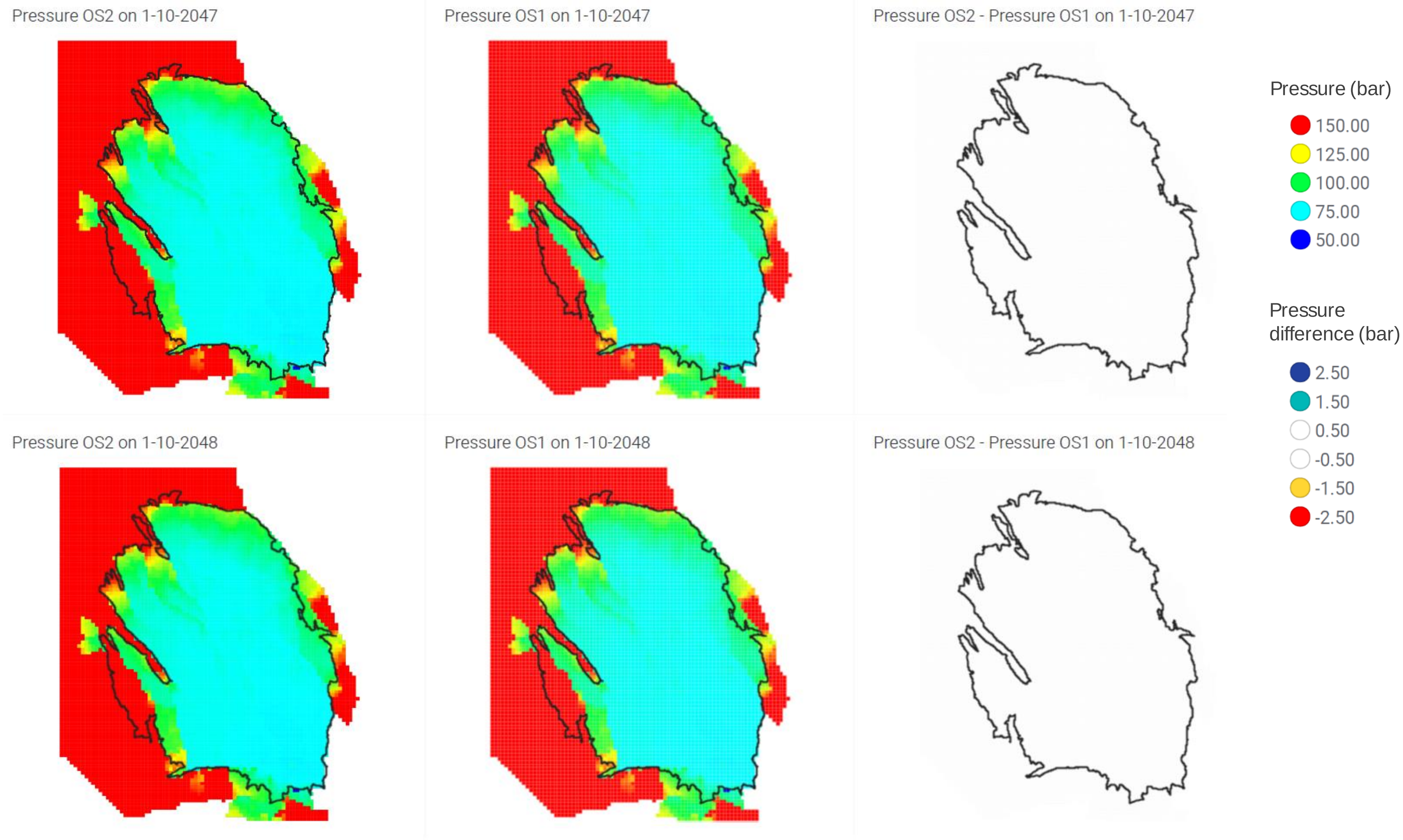
Pressure OS2 on 1-10-2047
Pressure OS1 on 1-10-2047
Pressure OS2 - Pressure OS1 on 1-10-2047
Pressure OS2 on 1-10-2048
Pressure OS1 on 1-10-2048
Pressure OS2 - Pressure OS1 on 1-10-2048
Pressure (bar)
150.00
125.00
100.00
75.00
50.00
Pressure difference (bar)
2.50
1.50
0.50
-0.50
-1.50
-2.50

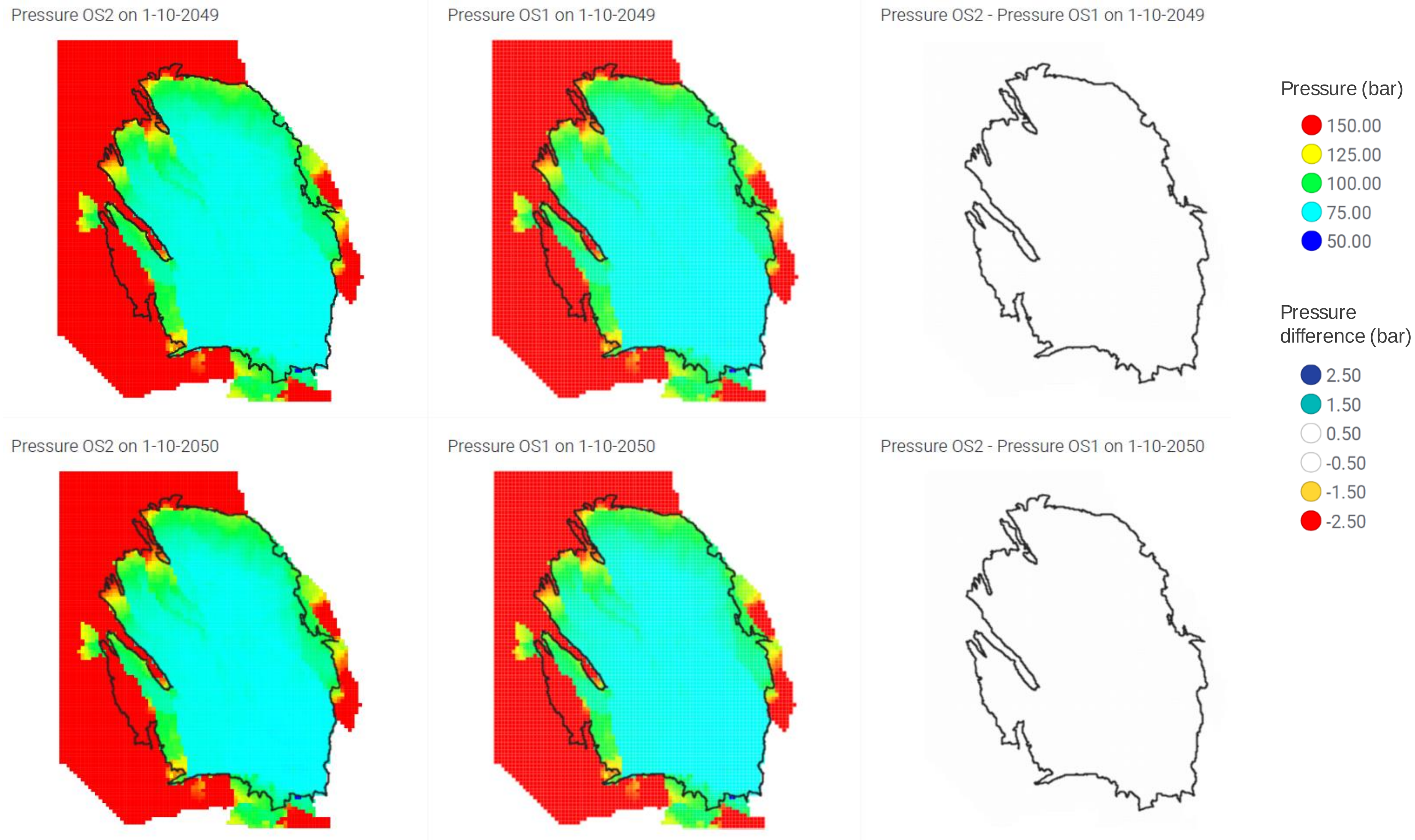
Pressure OS2 on 1-10-2049
Pressure OS1 on 1-10-2049
Pressure OS2 - Pressure OS1 on 1-10-2049
Pressure OS2 on 1-10-2050
Pressure OS1 on 1-10-2050
Pressure OS2 - Pressure OS1 on 1-10-2050
Pressure (bar)
150.00
125.00
100.00
75.00
50.00
Pressure difference (bar)
2.50
1.50
0.50
-0.50
-1.50
-2.50

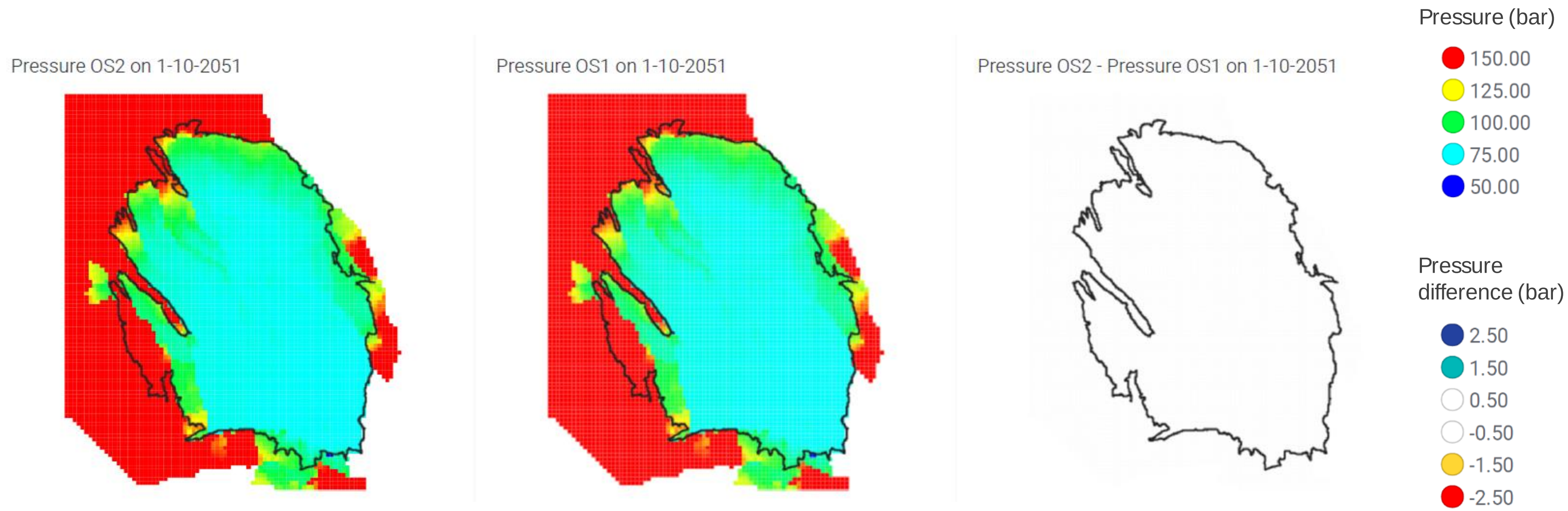

Figure f.1 Pressure and pressure difference maps for average temperature scenario for gas-years until gas-year 2050/2051.

Appendix G – Seismic Event Rate

The reservoir model has been history matched to reservoir pressure, water encroachment, gravity and compaction data stretching back to the start of production in 1963. Dynamic reservoir models have been used for many decades in the oil industry and the modelling software used to prognose future pressure development is used all over the world. Confidence in long-term pressure forecasts is therefore relatively high.

The HRA-model is bespoke for the induced seismicity in the Groningen field. The model has been developed based on the studies carried out as part of the Study and Data Acquisition Plan and data acquired in the Groningen field. It has been calibrated to the seismic catalogue of earthquakes with a magnitude larger than M=1.5, maintained by KNMI. While confidence in the seismic prognoses prepared by the HRA-model is high for the next 10 to 15 years, caution is required when using the model to forecast for longer time scales. Especially, more than 15 years in the future when seismic event rates are by comparison low, processes not incorporated in the model might play a role.

Research on the Zeerijp core has so far shown that these effects (if any) are for compaction most likely small. However, the influence of such effects cannot be excluded.

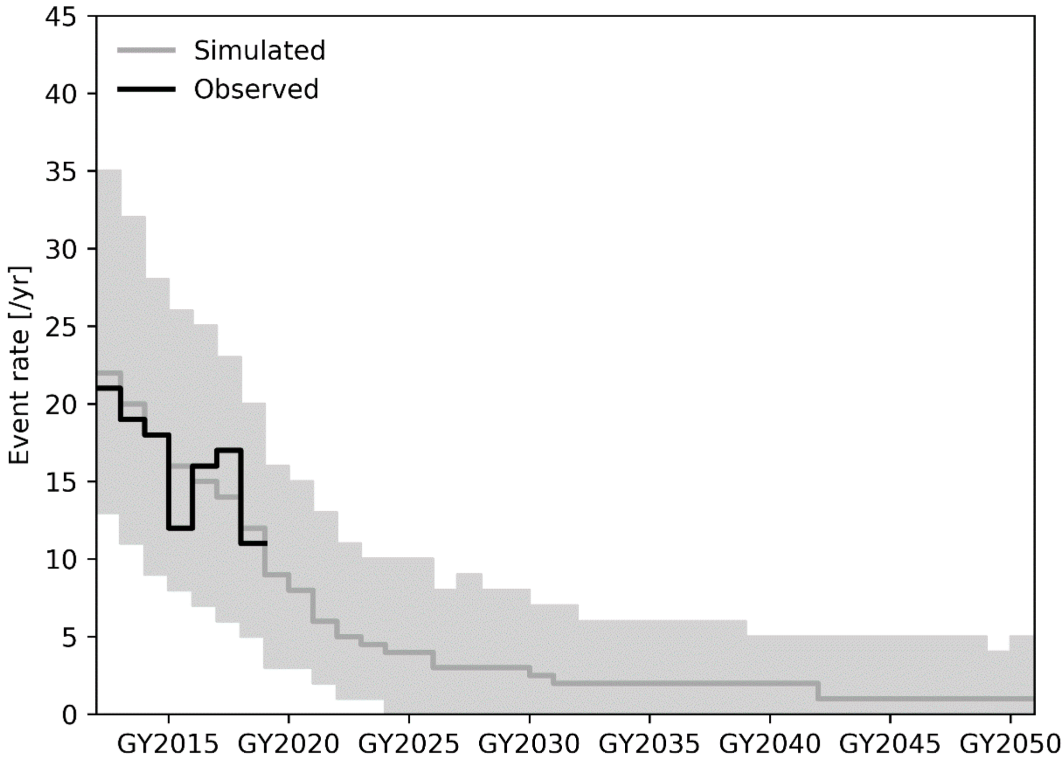

Figure g.1a *Seismic Activity Rate of earthquakes for the period gas-years 2012/2013 to 2050/2051 based on production profile GTS-raming 2020 for the average weather temperature gas-year and production profile for operational strategy 1.*

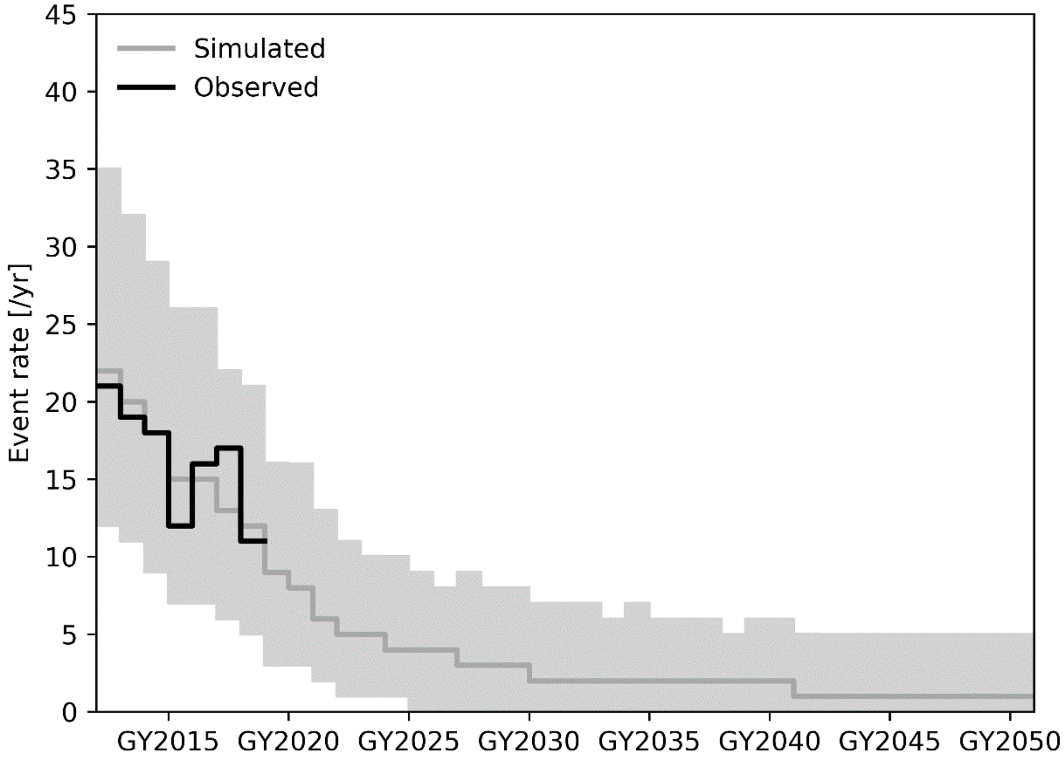

Figure g.1b *Seismic Activity Rate of earthquakes for the period gas-years 2012/2013 to 2050/2051 based on production profile GTS-raming 2020 for the average weather temperature gas-year and production profile for operational strategy 2.*

Appendix H - Exceedance Probabilities Calendar-year

The probability of an earthquake with a magnitude exceeding a given magnitude can be assessed using the seismological model (Ref. 40 to Ref. 43). In table h.1a and h.1b the annual probability of an earthquake occurring with a magnitude exceeding the specified magnitude is given. For instance, the probability of an earthquake occurring in calendar-year 2020 with a magnitude exceeding M_L=3.6 (the magnitude of the Huizinge earthquake) is equal to 4.91%. In the HRA for GTS-raming 2019, this probability was close to 9.3%. The probability of an earthquake occurring in calendar-year 2020 with a magnitude exceeding M_L=3.6 has almost halved between these two assessments (HRA GTS-raming 2019 and HRA GTS-raming 2020). For larger exceedance magnitudes the reduction between these two HRA versions is even larger.

Calendar-year	P(M>=3.6)	P(M>=4.0)	P(M>=4.5)	P(M>=5.0)
2020	4.91%	1.31%	0.17%	0.02%
2021	4.51%	1.20%	0.16%	0.02%
2022	3.57%	0.95%	0.12%	0.02%
2023	2.97%	0.77%	0.10%	0.02%
2024	2.67%	0.69%	0.09%	0.01%
2025	2.41%	0.64%	0.08%	0.01%
2026	2.20%	0.60%	0.08%	0.01%
2027	2.02%	0.54%	0.07%	0.01%
2028	1.88%	0.51%	0.07%	0.01%
2029	1.74%	0.47%	0.06%	0.01%
2030	1.59%	0.42%	0.05%	0.01%

Table h.1a Table with annual probabilities for occurrence of earthquakes exceeding a set magnitude. This table is for production profile GTS-raming 2020, average temperature calendar-year and operational strategy 1.

Calendar-year	P(M>=3.6)	P(M>=4.0)	P(M>=4.5)	P(M>=5.0)
2020	4.91%	1.30%	0.17%	0.02%
2021	4.60%	1.23%	0.16%	0.02%
2022	3.49%	0.93%	0.12%	0.02%
2023	2.94%	0.77%	0.10%	0.02%
2024	2.67%	0.71%	0.09%	0.01%
2025	2.43%	0.63%	0.08%	0.01%
2026	2.23%	0.60%	0.08%	0.01%
2027	2.06%	0.57%	0.07%	0.01%
2028	1.86%	0.48%	0.06%	0.01%
2029	1.76%	0.49%	0.06%	0.01%
2030	1.65%	0.50%	0.07%	0.01%

Table h.1b Table with annual probabilities for occurrence of earthquakes exceeding a set magnitude. This table is for production profile GTS-raming 2020, average temperature calendar-year and operational strategy 2.

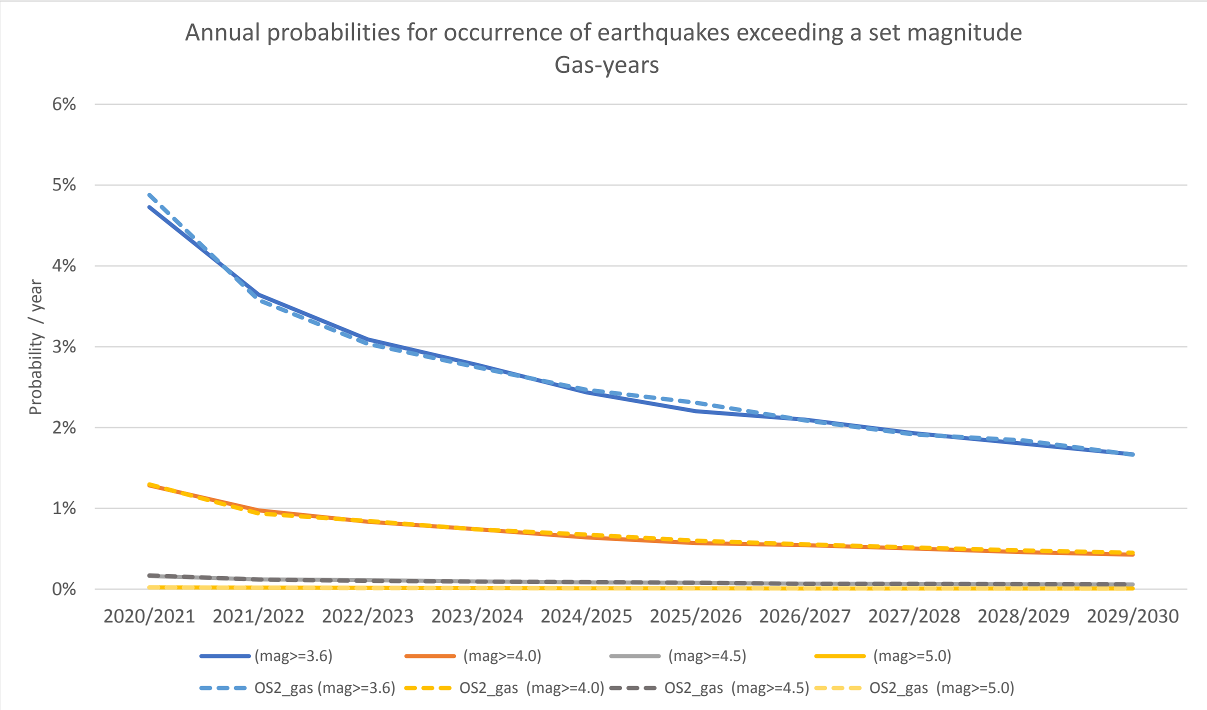

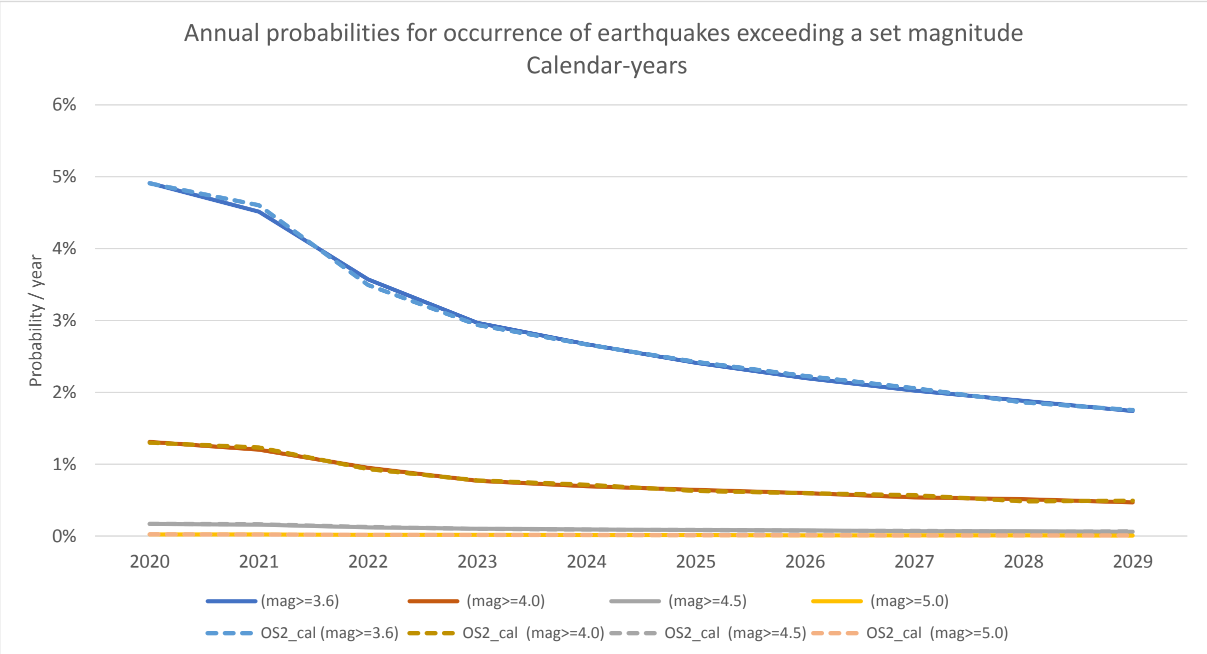

Figure h.1 *Figure with annual probabilities for occurrence of earthquakes exceeding a set magnitude. This table is for production profile GTS-raming 2020, average temperature gas-year (above) and calendar-year (below). The probabilities for operational strategy 1 are solid lines and for strategy 2 are hatched lines.*

The probabilities for gas-years appear in the graphs to be lower. However, this is due to the later start date of the gas-year (1st October) versus the calendar year (1st January).

Appendix J – Tables for comparing the results of the risk assessments

The reconciliation of buildings in different safety groups relative to the norm between HRA 2019 and HRA 2020 is in the main text of the report shown in Sanky-diagrams. In this appendix we present the reconciliation in the form of two tables.

Results for Operational Strategy 1 of (Previous) HRA 2019 compared to Operational Strategy 1 of (New) HRA 2020.

	New P90	New meanP	New others	No longer in EDB
Previous P90	60	0	3,205	6
Previous meanP	72	0	359	4
Previous others	30	0	148,613	348
New in EDB	0	0	5,617	0
Total	162	0	157,794	358

Table j.1a Table comparing the buildings in the safety groups between HRA 2019 and HRA 2020 for operational strategy 1.

Results for Operational Strategy 1 of (previous) HRA 2019 compared to Operational Strategy 2 of (New) HRA 2020.

	New P90	New meanP	New others	No longer in EDB
Previous P90	35	0	3,230	6
Previous meanP	34	0	397	4
Previous others	13	0	148,630	348
New in EDB	0	0	5,617	0
Total	82	0	157,874	358

Table j.1b Table comparing the buildings in the safety groups between HRA 2019 and HRA 2020 for operational strategy 2.